From chemistry to biological implications of polyphenols in Celiac Disease

Ricardo Jorge Correia Dias

PhD in Sustainable Chemistry
Department of Chemistry and Biochemistry,
Faculty of Sciences of the University of Porto

Supervisor: Victor Armando Pereira Freitas,
Full Professor at the Faculty of Sciences of the University of Porto

Supervisor: Nuno Filipe da Cruz Batista Mateus,
Full Professor at the Faculty of Sciences of the University of Porto

2020

“ninguém, além de ti,
sabe por onde andaste,
o que sentiste, o que superaste,
e o tanto que mereces ser feliz”

ACKNOWLEDGEMENTS

Undertaking this PhD has been one of the biggest challenges I have ever faced. A truly life-changing experience, I would say. As such, this doctoral thesis is the result of a challenging journey which it would not be possible to complete without the support and guidance that I received from so many people.

First and foremost, I would like to thank my supervisor Prof. Doctor Victor Freitas for giving me the encouragement to embark on this research, for its unfailing support, patience and trust, and for creating the intellectual space for me to explore the issues I deal with in this study. I also gratefully acknowledge the support of Prof. Doctor Nuno Mateus, Doctor Mauro Rossi and Doctor Paolo Bergamo. You have all been generous and inspirational mentors, continuously steering me in the right direction and always available to help and talk.

I would also like to thank my friends and colleagues from the FoodPhenolLab as well as those working at the Department of Chemistry and Biochemistry of the Faculty of Sciences of the University of Porto, the immunobiology group of the Institute for Research and Innovation in Health (I3S) and the *Istituto di Scienze dell'Alimentazione* of Avellino for their insights, counsel, and feedback as I progressed through the sometimes wrenching stages of computational, biophysical and biological *in vitro* and *in vivo* studies. Without them acting as sounding boards and confidantes, the findings in this thesis and their informed discussion would have suffered tremendously. I am also grateful to Dra. Helena Coelho and Doctor Eurico Cabrita from the Nova University of Lisbon and to Dra. Mariana Andrade from the Materials Centre of the University of Porto for their technical assistance and lessons regarding the analysis of proteins and peptides by NMR spectroscopy as well as to the Foundation for Science and Technology and Associated Laboratory for Green Chemistry REQUIMTE for my PhD grant and financial support, respectively. A special acknowledgement goes also to Doctors Ana Faria, Diogo Pestana Diana Teixeira, Cláudia Marques and Prof. Conceição Calhau from the NOVA Medical School of the Nova University of Lisbon and CINTESIS for receiving me so well in their group and for all the support they provided on RT-PCR analyses.

Finally, I wish to express my deepest gratitude to my family and closest friends, including Silvia, Susana, Luís, Anselmo Francisco, Carlos Eloy, Catarina, Elsa, Rui, Lia,

João, Alex and Carlos Gil who have continued to support and encourage me through this journey. Your belief in me, your encouragement when the times got tough, and your assistance through this process gave me the strength to succeed. I am also indebted to you, Rosa. After all these years together, there are no words that can describe how grateful I am for everything you have done and continue to do for me. If I am where I am, it is all thanks to you. As for you Isabel, thanks for showing me that I can love and feel myself complete again. I want you forever and ever, in a thousand worlds!

ABSTRACT

Celiac Disease is now recognized as a worldwide epidemic whose only effective treatment consists of a gluten-free diet. Despite its effectiveness in achieving clinical improvements within days of weeks, adhering to this routine is still troublesome and associated to a large number of social and financial restrictions that impair successful outcomes. For this reason, there is an unmet need for novel therapeutic approaches to supplement or supplant a gluten-free diet. Over the last years, epidemiological and population-based studies have suggested that a continuous and prolonged intake of fruits and vegetables - all rich sources of polyphenols -, may help in the prevention of several chronic and degenerative pathologies including diabetes, cancer, cardiovascular and neurodegenerative diseases, and to prevent symptoms associated to menopause and aging. If we consider the normal process of evolution of a healthy state to a disease one, we may resume that these evidences indicate an active role of dietary polyphenols in the maintenance of cellular homeostasis, delaying or even reversing the transition from healthy to pathological states. As an extremely differentiated group of natural compounds, not only in terms of their chemical structure but also in terms of their biological activities, polyphenols have been in the spotlight of extensive and ever-growing researches attempting to unravel the mechanisms behind their preventive potential and therapeutic application in the treatment of multifactorial disorders, where a multitude of cellular pathways are disrupted. One of such conditions is, invariably, Celiac Disease, even though the significance of polyphenols in this area remains largely unexplored if we consider the few studies available which, so far, provided only a glimpse of the huge potential polyphenols may have. Therefore, the main goal of the this PhD was to explore the molecular and cellular mechanisms concerning the functionality of dietary polyphenols in a Celiac Disease nutritional context, by studying, under near physiological conditions, the structural and thermodynamic basis of polyphenol interactions towards the main bioactive gluten peptide - the 32 mer. Clarification of these interactions at the molecular level is critical in order to understand the modulatory role and applicability of dietary polyphenols in a Celiac Disease framework *e.g.* in the rational design of polyphenol-rich functional foods or supplements with enhanced bioavailability's and biological effects. Greater emphasis has been placed on the green tea catechin,

EGCG, as well as on oligomeric procyanidins (*i.e.* procyanidin B3 and the trimer C2) due not only to their dietary abundance but also because their poor intestinal absorption at the gastrointestinal tract allows them to exert local effects through interaction with food matrices and/or intestinal epithelial cells.

According to our findings, polyphenol binding to the 32-mer peptide occurs primarily through an entropy-driven hydrophobic effect and is kinetically dependent on the substitution pattern and polymerization degree of polyphenol molecules. It was also found that the primarily polyphenol-binding sites correspond to leucine, tyrosine and phenylalanine-containing domains, being these located in four well-defined and almost indistinguishable hydrophobic clusters, equally spaced by non-polar proline residues. Although ITC experiments involving both EGCG and procyanidin B3 and C2 suggested the existence of one to two different, yet sequential, sets of interaction sites, by NMR spectroscopy, no specificity was observed from the peptide perspective. This was likely due to the severe signal overlap and a complex interaction mechanism in which soluble complexes co-existed with polydisperse high molecular weight aggregates with slower tumbling rates and broader signals. The high proline content of the 32-mer peptide (*i.e.* 41% of the total aminoacid residues) precipitated the occurrence of these non-specific phenomena through stacking interactions with the polyphenol's aromatic rings, strengthened by hydrogen bonding. Structural rearrangements were also detected by NMR and molecular dynamics. These arose as a result of a three-dimensional adjustment and pairing of EGCG molecules and procyanidin C2 within the 32-mer peptide-polyphenol supramolecular complexes.

Since complexation with polyphenols could potentially interfere with the 32-mer peptide bioavailability and therefore down-regulate its immunological activity at the intestinal level, *in vitro* transepithelial transport assays on Caco-2 cell monolayers were additionally performed. These experiments highlighted the ability of EGCG to efficiently scavenge the 32-mer peptide under near physiological conditions, leading to a remarkable reduction on the concentration of free peptide in the basolateral compartment (nearly not detectable by Nano-LC-MS). In a similar fashion, substoichiometric amounts of procyanidin B3 and the trimer C2 were also shown to reduce the 32-mer peptide apical-to-basolateral translocation, even though, in this case, this attenuation didn't appear to be dependent on their physical interaction. Whatever be the mechanisms involved, this multidisciplinary study provides the foundations for further explorations concerning the potential use of dietary polyphenols as a natural supportive therapy in Celiac Disease and the possibility to selectively modulate these interactions through nutrition to induce a beneficial response in patients whom a gluten-free diet is not

indicative of a better quality of life. Or at least, we hoped so … This statement arises from the fact that humans and mammals are very complex organisms in which organs achieve distinct and specific physiological functions in a highly integrated and regulated fashion. Therefore, and despite the advances that have been made on *in vitro* cellular approaches, the truth is that these techniques provide only hypothesis and models that must be tested and validated in a whole organism, otherwise they remain speculative. For this reason, in the second part of this PhD, we have decided to assess the modulatory effects of green tea catechins and grape seed procyanidins against the toxicity of gluten proteins, using a transgenic mouse model of Celiac Disease. Performed on a European Laboratory for the Investigation of Food-Induced Diseases (ELFID, Avellino, Italy) this study has provided some highly relevant breakthroughs regarding the health-promoting properties of dietary polyphenols on a Celiac Disease framework by showing that their intake contributed to the maintenance of a metabolic and redox homeostasis in the small intestine of long-term enteropathic DQ8 mice. Concomitantly with the reestablishment of the nucleophilic tone at the intestinal level, these polyphenols attenuated some of the most characteristic histological changes associated to the consumption of gliadins including villus flattening, crypt hyperplasia and infiltration of IEL. Additionally, it has been shown that the health benefits provided by EGCG supplementation don't merely depend on the dose but also on the timing and administration protocol as its co-administration with gliadin proteins in just four days was as effective on the alleviation of a gliadin-induced intestinal damage as when it was pre-administered for 2 weeks. For this reason, we speculate that the preventive potential of polyphenols against a gliadin-induced cytotoxicity relies not only on a parahormesis effect but also on their ability to physically interact and reduce the bioaccessibility and intestinal bioavailability of gliadin proteins and derived peptides. Overall, this study provides the first in vivo evidences regarding the immunomodulatory role of polyphenols in the onset of Celiac Disease and opens up new horizons concerning the applicability and valorization of polyphenol-rich functional foods and supplements as an effective nutritional strategy to manage and prevent this epidemic disorder.

Keywords: Polyphenols, Celiac Disease, Bioavailability, NMR, ITC, Bioactive peptides, Interaction, Dietary supplementation, Animal studies, Inflammation, Oxidative Stress, Cell-based assays.

INDEX

LIST OF FIGURES

LIST OF TABLES

GENERAL INTRODUCTION

1. Celiac Disease

Celiac Disease (CD) is a chronic autoimmune mediated enteropathy that develops in genetically susceptible individuals following exposure to dietary gluten proteins of wheat (gliadins and glutenins), barley (hordeins) and rye (secalins) [1]. Although CD primarily affects the proximal small intestine (duodenum and jejunum), it is now considered to be a systemic disorder with clinical symptoms that go far beyond the gastrointestinal tract [2]. When left untreated, CD is associated with severe health complications, increased morbidity and mortality, considerable burdens to health-care systems and decreased patient quality of life [3]. In the most developed lesion, there is an extensive destruction of the intestinal epithelium and remodeling of the intestinal mucosa, characterized by villous atrophy (blunting or flattening of the villi), crypt hyperplasia (elongation of the crypts) and lymphocytic infiltration [4]. CD patients typically develop IgA and IgG antibodies against gluten peptides and the endogenous enzyme transglutaminase 2 (TG2), which enables its diagnosis [5].

Before the 90's, CD was considered to be an uncommon disorder affecting mainly children and limited to individuals of European ancestry. Over the past two decades, however, it has emerged as a major public health problem with a pooled global seroprevalence in the general population as high as 1.4 % [6]. High prevalence countries (between 2.1 and 8.5%) include Algeria, Czech Republic, India, Israel, Mexico, Malaysia, Saudi Arabia, Sweden, Portugal and Turkey. In Estonia, Germany, Iceland, Libya, Poland, Republic of San Marino, Spain and Switzerland, CD is less common (0.2 - 0.8%) [7]. Of the world's top ten most populated countries, population-based data on CD prevalence are still lacking from Bangladesh, China, Indonesia, Japan, Nigeria and Pakistan. It seems, however, that in Far East Asia and sub-Saharan Africa the disease is still rare. Globally, the prevalence of CD is increasing over time: some studies report a 2-fold increase in seroprevalence over two decades (1974-89 and 1978-80 to 2000-01) and a 4 to 4.5-fold increase over approximately 50 years in the US (1948-54 to the present day) [8-10]. Despite this significant increase on CD prevalence, its diagnosis rate is growing much more slowly, thus making this disorder heavily unrecognized or misdiagnosed with other conditions [11, 12]. CD has many clinical manifestations, ranging from severe malabsorption to minimally or non-symptomatic presentations. Classic symptoms, which are becoming quite rare, include chronic diarrhea, weight loss

and failure to thrive [13]. The most common, non-classical signs, include iron deficiency, bloating, constipation, chronic fatigue, headache, abdominal pain and osteoporosis [14]. Dermatitis herpetiformis, arthritis, neurological disorders and anemia are also very frequent extra-intestinal symptoms of CD in both childhood and adulthood [15, 16]. Not surprisingly, owing to the multifaceted clinical presentation combined to a poor disease awareness among healthcare professionals, CD diagnosis still remains a challenge with diagnostic delays that can reach up to 13 years, in resource-rich countries [17].

1.1. Insights from genetics

The development of CD requires both the ingestion of gluten and genetic predisposition [18]. Of the genetic factors identified so far, the MHC locus is the single most important one. The most prominent association is with certain MHC class II alleles encoding HLA-DQ2.5 (*HLA-DQA1*05:01*, *HLA-DQB1*02:01*), HLA-DQ8 (*HLA-DQA1*03*, *HLA-DQB1*03:02*) and HLA-DQ2.2 (*HLA-DQA1*02:01*, *DQB1*02:01*). The risk for CD is particularly high for HLA-DQ2.5, especially in homozygous individuals (dosage effect). Other HLA-DQ variants that are rarely associated with CD are HLA-DQ7.5 (*HLA-DQA1*05*, *HLA-DQB1*03:01*), HLA-DQ2.3 (*HLA-DQA1*03*, *HLA-DQB1*02:01*) and HLA-DQ8.5 (*HLA-DQA1*05*, *HLA-DQB1*03:02*) [19-21]. Of note, HLA-DQ2 and HLA-DQ8 alleles are also common among healthy individuals, which suggests that HLA is necessary but not a sufficient factor for disease development. Therefore, additional genetic and/or environmental factors must be involved, supporting the idea of CD as a multigenic and stochastic autoimmune disorder requiring multiple “hits” to develop [22].

Recent genome-wide association studies have so far identified 42 non-MHC loci that contribute to CD susceptibility [23, 24]. Many of these loci harbor genes involved in thymic T cell differentiation (*Themis and Runx3*), T cell activation (*SH2B3, TAGAP, PTPN2, CD28, CTLA4, CIITA, IL2/IL21*), differentiation of inflammatory $CD4^+$ T cells (*IRAK1, IL12A, IL18RAP/IL18R1, IL1RL1/IL1RL2, STAT4*), B cell activation and differentiation (*ICOS/ICOSLG, CD28, IL21/IL2, IRF4, RGS1, BACH2, ARHGAP31, POU2AF1*), and effector cytolytic T cell migration and function (*IL21/IL2, RGS1, MAP3K7, CCR1/2/3, CCR4, UBASH3*) [25]. Interestingly, some of these genes are shared with other autoimmune diseases such as type I diabetes and rheumatoid arthritis [26, 27]. In CD, the MHC loci account for aproximatelly 40 - 50 % of the genetic variance, whereas the non-MHC variants account for another 15 % [28]. Also noteworthy is that

the prevalence for CD varies according to sex: it is more common among female individuals than males [6].

1.2. The driver antigen

CD is triggered by exposure to gluten proteins in the diet. The term gluten is frequently used to define the family of hundreds of complex and heterogeneous storage proteins found in the endosperm of cereal grains such as wheat, barley, and rye [29]. Of these, wheat (*Triticum aestivum L.*) is nowadays one of the world's major food crops being cultivated, consumed and traded worldwide (more that 770 million tons in 2017). In general, wheat kernel contains around 60 - 70 % starch, 8 - 15 % protein, 10 - 15 % moisture, 1 - 2 % lipid and 4 % ash [30]. The wheat protein content includes both water-soluble albumins and globulins (10 - 15 %) and the insoluble gluten proteins (85 - 90 %) - gliadins and glutenins. While gliadins, the wheat prolamins, are soluble in aqueous alcohols (*i.e.* 60 - 70 % ethanol), the complete solubilization of glutenins is achieved by solvent mixtures containing aqueous alcohols (*e.g.* 50% propanol), reducing agents (*e.g.* DTT), and disaggregating compounds (*e.g.* urea) [31]. Regarding their biological functions, most of the albumins and globulins are metabolic proteins, *i.e.* enzymes or enzyme inhibitors, while the main role of gliadins and glutenins is to supply the seedling with nitrogen and amino acids during germination [32].

On wheat flours, upon proper hydration and mixing, gluten proteins create a three-dimensional network with unique building properties that are usually explored and controlled in an industrial environment to create viscoelastic dough matrices. Although both gliadin and glutenin proteins are important contributors to the rheological properties and baking quality of dough, their functions are somewhat different. Hydrated gliadins are mainly responsible for dough viscosity and extensibility whereas hydrated glutenins, being more cohesive, contribute to dough strength and elasticity [33, 34]. The unusual rheological and functional properties of gluten (*e.g.* heat stability, capacity to act as a binding and extending agent), make it a widely used food addictive for improved texture, flavor, and moisture retention in packaged and processed foods. Therefore, in addition to bread and other baked products such as pasta, crackers and pastries, gluten proteins can also be found in both processed meat, reconstituted seafood and vegetarian meat substitutes as protein boosters and in packet soups, canned soups, candies, ice cream, marinades, vinegars and dressings, jams and baby foods as either thickeners, emulsifiers, and gelling agents [35]. The average daily intake of gluten in a Western diet

is thought to range between 5 to 20 g.day^{-1}, being wheat found in approximately 30 % of supermarket food products [36].

Differences in the structures of gliadin and glutenin proteins provide them with different functionalities during dough formation [37]. Although these proteins differ in terms of their amino acid sequences (due to substitutions, insertions and deletions of single amino acids and short peptides), they are all closely-related and characterized by high contents of glutamine and proline residues and by low levels of charged amino acids such as glutamic and aspartic acids [29]. Gliadins are a heterogeneous mixture of essentially monomeric proteins with molecular weights ranging from 28 to 55 kDa. These proteins can be divided into different subgroups depending on their primary structures and molecular weights into α/β-, ω5-, ω1,2- and γ-gliadins [38]. Contrary to α/β- and γ-gliadins, the ω-subtype do not contain cysteine or methionine residues and are therefore unable to form intra- and interchain disulfide crosslinks. They also occur in much lower proportions in wheat varieties when compared to the α/β- and γ-subtypes and consist almost entirely of repetitive glutamine and proline-rich sequences (*e.g.* QPQQPFP or QQQFP) [31, 39]. α/β- and γ-gliadins, on the other hand, are structurally characterized by a number of conservative motifs, a repetitive region and the ability to establish intrachain disulfide bonds responsible for their folded globular structure (*Fig. 1*) [40, 41]. These gliadins share similar structural features: a short N-terminal signal peptide, a central domain consisting in repetitive glutamine, proline, phenylalanine and tyrosine-rich sequences - unique for each type (*e.g.* QPQPFPQQPYP and QPQQPFP for α/β- and γ-gliadins respectively) - and homologous C-terminal domains containing most of the cysteine residues (if present) within non-repetitive sequences [42-44]. Studies on the secondary structure of α/β-, ω- and γ-gliadins have reported that on their N-terminal domain there is a predominance of β-turns whereas the C-terminal domain contains considerable proportions of α-helices and β-sheets [45]. The secondary structures of gliadins were found to be sensitive to environmental conditions such as solvent, hydration, and temperature [46].

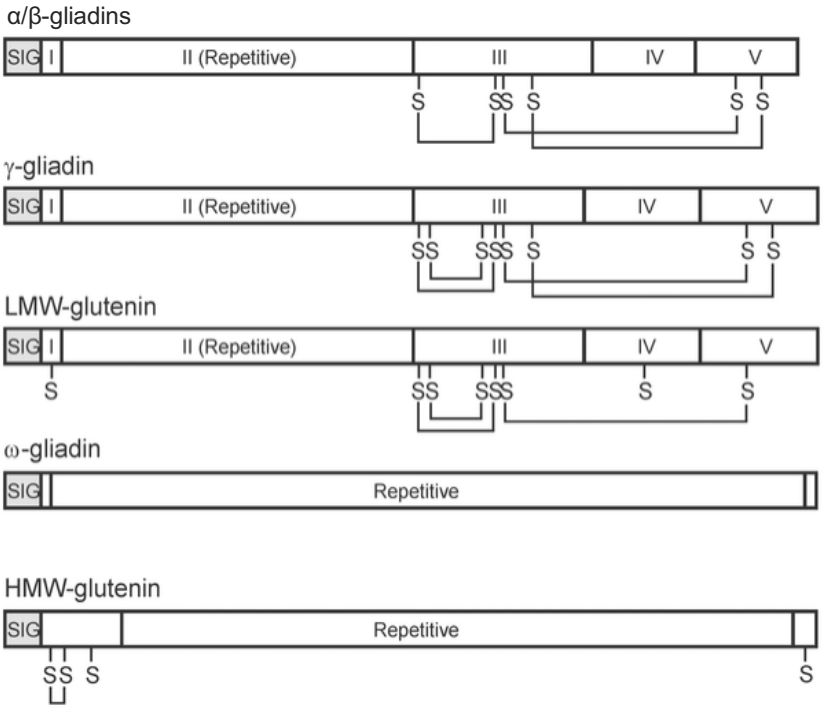

Fig. 1 - General structure of gluten proteins. Adapted from [47]

Glutenins are the polymeric proteins of gluten (*Fig. 2*). They comprise aggregated proteins linked together by interchain disulfide bonds and having molecular weights ranging up to tens of millions of kDa, a feature that makes them the largest and most complex protein polymers in the plant kingdom and one of the main determinants of dough properties and baking performance [48]. Despite being considered the alcohol insoluble components of gluten in their native/polymeric form, after reduction of disulfide bonds with reducing agents, the resulting monomeric glutenin subunits do become soluble in aqueous alcohol like gliadins. Based on their primary structure, glutenin subunits have been divided into two classes: the low-molecular-weight subunits (LMW-GS) and high-molecular-weight subunits (HMW-GS) [49]. LMW-GS have molecular weights ranging from 32 to 39 kDa and are related to α/β- and γ-gliadins in their amino acid composition and secondary structure. Their N-terminal domain consists of glutamine and proline-rich repetitive units (e.g. QQQPPFS) that fold into a regular spiral structure while the C-terminal domains are non-repetitive, more compact and have six cysteine residues involved in intramolecular disulfide bonds (*Fig. 1*). For steric reasons, two additional cysteine residues that are unique to LMW-GS are not able to form intramolecular bonds. Instead, they participate in inter-chain disulfide bonds with

cysteines of different gluten proteins (LMW-GS, modified gliadins with an odd number of cysteine residues and HMW-GS) [29].

HMW-GS can be subdivided into the x-type (82 - 90 kDa) and the y-type (60 - 80 kDa) protein subunits [50]. Both subtypes have similar structural domains: a non-repetitive N-terminal domain containing two conserved regions, a central domain dominated by repetitive sequences such as QQPGQG as a backbone with inserted sequences like YYPTSL, QQG and QPG, and a non-repetitive C-terminal domain [51]. Of note, the N- and C-terminal domains of HMW-GS are characterized by the frequent occurrence of charged amino acid residues and by the presence of most or all of cysteines (four in the x-type and seven in y-type). In their native state, HMW-GS are aggregated through interchain disulfide bonds, although intrachain bonds can also occur [52]. Predictions on the secondary structure of purified HMW-GS and synthetic or recombinant peptides indicated that the central repetitive domain adopts an unusual super-secondary structure of loose spirals consisting of regularly repeated β-reverse turns [53]. The non-repetitive N- and C-terminal domains were proposed to have globular structures rich in α-helices. The most recent glutenin model suggests a backbone formed by HMW-GS linked by end-to-end and of LMW-GS polymers branched off from HMW subunits. Accordingly, a "double unit" of glutenin polymers might consist of 2 y-type HMW-GS, 4 x-type HMW-GS and around 30 LMW-GS covalently linked by interchain disulphide bonds [48].

Different types of reactions and interactions are crucial for the formation of a gluten network upon dough mixing. In particular, disulfide bonds between the sulfhydryl groups of cysteine residues play an important role in determining the structure and properties of these storage proteins [54]. Monomeric α/β- and γ-gliadins present three and four intrachain disulfide bonds, respectively, whereas polymeric LMW- and HMW-GS include both intra- and interchain bonds. These bonds are established immediately after protein synthesis within the lumen of the endoplasmatic reticulum (ER) as an integral part of protein folding and undergo a continuous change during kernel maturation, milling, dough preparation and baking [55]. During the whole process of breadmaking, the state of large glutenin polymers (or macropolymers, GMP, *Fig. 2*) is characterized by the occurrence of three competitive redox reactions: (1) the oxidation of free SH groups which support polymerization (*e.g.* by atmospheric oxygen); (2) the presence of terminators (*e.g.* glutathione or gliadins with an odd number of cysteines) that stop polymerization and (3) SH/SS interchange reactions between glutenins and thiol compounds that depolymerize pre-existent polymers [56]. Additional covalent bonds include tyrosine-tyrosine crosslinks between gluten proteins [57]. Nevertheless, their contribution to gluten network formation appears to be negligible, since only very a low

amount of dityrosine is present in dough. Non-covalent bonds such as hydrogen bonds, ionic bonds and hydrophobic bonds are also important for the aggregation of gliadins and glutenin proteins with overall implications on the structure and physical properties of dough [29].

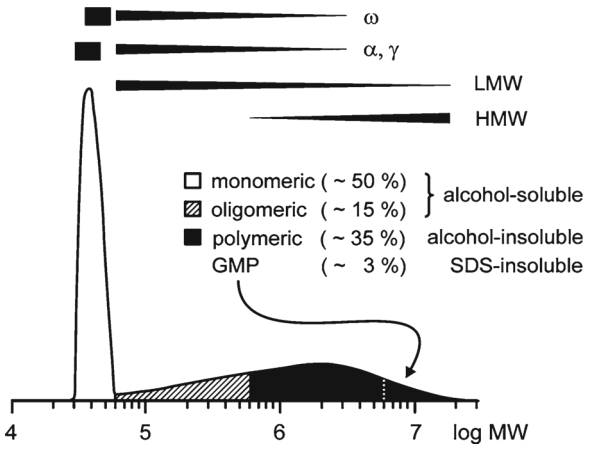

Fig. 2 - Molecular weight distribution of native wheat storage (gluten) proteins and solubility. GMP, glutenin macropolymers. Adapted from [56].

1.3. Immune mechanisms

Usually, ingested proteins undergo a complex series of degradative processes mediated by hydrolytic enzymes originating from the stomach, pancreas and small intestine. The result of this proteolytic activity is a mixture of small peptides and free amino acids that are rapidly and efficiently absorbed by small intestinal enterocytes [58, 59]. However, due to the unusually high proline content of gluten proteins and because human proteases are unable to hydrolyze amide bonds when they are adjacent to conformationally constrained proline residues, gluten proteins become fairly resistant to proteolytic processing by gastric, pancreatic and intestinal brush border membrane enzymes [60-63]. Consequently, there is an accumulation of long peptide fragments (10 - 50 residues) in the gut lumen that gain access to the lamina propria either actively by transepithelial translocation or passively by paracellular flux through a compromised epithelial barrier (*Fig. 3*) [64, 65]. In the lamina propria, immunogenic gluten peptides are selectively deaminated by TG2 (*Fig. 3*) [66-69].

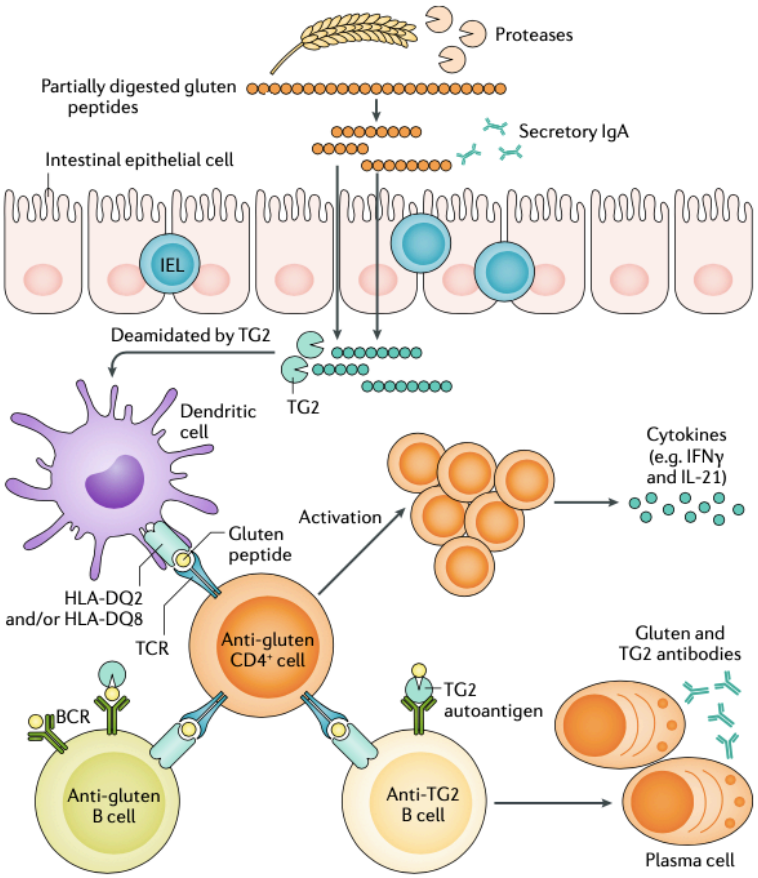

Fig. 3 - Adaptive immune response involved in CD. Adapted from [1].

TG2 is a ubiquitously expressed Ca^{2+}-dependent enzyme that is predominantly found intracellularly, bound to guanosine-5'-triphosphate (GTP), and also in the extracellular matrix. The transamidation reaction catalyzed by TG2 results in the formation of a covalent bond between the γ-carboxamide group of a peptide-bound glutamine residue and a primary amine group (*Fig. 4*). The ε-amino group of a peptide-bound lysine can act as the amine donor for the reaction; in this case a covalent crosslink is established between the γ-carboxamide group of the glutamine and the ε-amino group of lysine. TG2 can also use a water molecule as an acyl-acceptor to deaminate a peptide-bound glutamine residue occurring in specific sequence motifs such as QXP (where X is any residue and P is proline) converting it to a glutamate residue (*Fig. 4*) [70, 71].

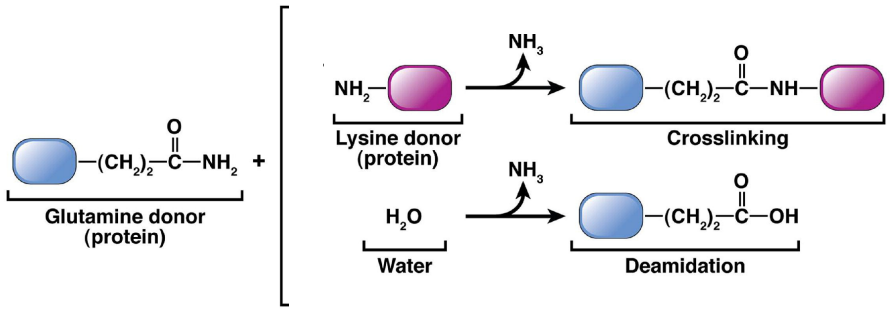

Fig. 4 - Reactions catalyzed by tissue transglutaminase (TG2). Adapted from [72].

Many gluten peptides are excellent substrates for TG2 which, through the introduction of negative charges, increases their binding affinity towards the disease-associated HLA-DQ2 or HLA-DQ8 molecules [73-75]. Under inflammatory conditions, antigen-presenting cells (APCs) including dendritic cells (DC) mature in response to tissue signals produced by stressed intestinal epithelial cells (IEC) such as interleukin-15 (IL-15) and type I interferon (IFN) and acquire the ability to support the differentiation of gluten-specific HLA-DQ2- or HLA-DQ8-restricted $CD4^+$ T cells (*Fig. 3*). When stimulated, the latter start producing pro-inflammatory cytokines including interferon-γ (IFN-γ) - a hallmark of T_H1 cells - and IL-21, but not IL-17 [76, 77]. Additionally, gluten-specific $CD4^+$ T cells provide help signals to both autoreactive TG2- and gluten-specific B cells, thereby promoting their activation and differentiation into IgA- and IgG-producing plasma cells (*Fig. 3*) [78]. These antibodies may serve as important amplifiers of the inflammatory process by engaging Fc receptors on APCs, leading to the release of pro-inflammatory mediators, or by contributing to extra-intestinal manifestations through the deposition of immune complexes in tissues outside the gastrointestinal tract [79]. Furthermore, due to an upregulation of the expression of the IgA receptor CD71 on the luminal surface of IEC, IgA antibodies are thought to increase the permeability of the intestinal epithelial barrier to harmful gluten peptides through a CD71-mediated retro-transcytosis of IgA-peptide complexes to the lamina propria [80-82].

Although activation of gluten-specific $CD4^+$ T cells is probably a prerequisite in the pathogenesis of CD, there is now evidence that these cells are not the effector cell type that mediates tissue damage in CD. Instead, $CD4^+$ T cells help to set up the necessary inflammatory environment that allows intraepithelial cytotoxic T lymphocytes (CTLs) to kill distressed IECs based on the recognition of stress-induced ligands and not cognate antigens (*Fig. 5*) [25].

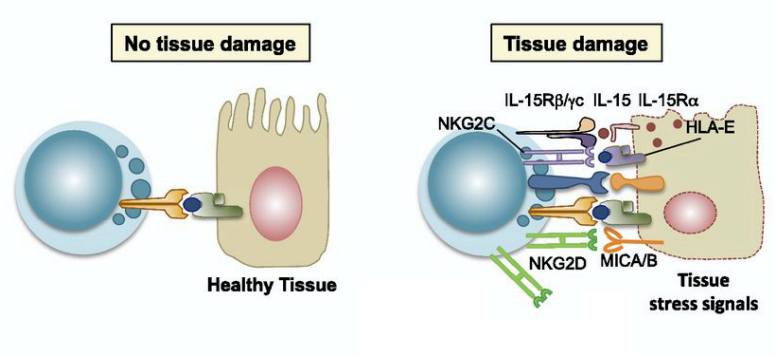

Fig. 5 - Licensing of intraepithelial cytotoxic T lymphocytes (CTLs) in CD. Adapted from [25].

Tissue-resident intraepithelial lymphocytes are derived from naive $CD8^+$ T cells that receive costimulatory signals by DC in the Peyer's patches or mesenteric lymph nodes and undergo progressive maturation during their circulation in the lymph before populating the intestinal epithelium as effector T cells. In the intestine, intraepithelial CTLs need to receive a distinct set of activating signals to unleash their effector functions as licensed killer cells. These are provided through a downregulation on the expression of the dimeric inhibitory CD94/NKG2A receptor and an upregulation of the activating natural killer receptors (NKRs) NKGD2 and CD94-NKG2C (*Fig. 5*) [83, 84]. Concomitant to the induction of these NKRs on intraepithelial CTLs, IEC upregulate unconventional stress-induced MHC class I polypeptide-related (MICA/B) and HLA-E molecules that are ligands for NKGD2 and CD94-NKG2C, respectively (*Fig. 5*) [85-87]. Under these circumstances, activated NKRs enable intraepithelial CTLs, that are gluten-unspecific, to induce epithelial cell death either directly or indirectly by lowering the T cell receptor (TCR) threshold and allowing recognition of low avidity epithelial or microbial antigens [5, 88]. Of note, when expressed, NKRs are not usually associated with ITAM-bearing adapter molecules, which ensures that proliferation and cytokine secretion remains under the control of the TCR [89]. However, it has been shown that, in CD, the intraepithelial CTLs undergo a profound genetic NK cell reprogramming characterized by the expression of DAP12 and activating NK cell receptor complexes that can promote cytokine secretion, proliferation and killing of cell targets in a TCR-independent manner [5].

Several experimental evidences provided by humanized animal models and potential CD patients strongly suggest that tissue remodeling caused by an adaptive anti-gluten CD4+ T cell response alone cannot explain villous atrophy observed in CD. Nevertheless, these cells are critical for intraepithelial CTLs to become fully operative

effector T cells [90]. Accordingly, through the production of pro-inflammatory cytokines such as IL-21 and IFN-γ, gluten-specific CD4+ T cells are reported to increase the cytolytic properties of NK cells and CTLs, for instance, by upregulating HLA-E expression on IEC and downregulating the inhibitory NKG2A receptor in intraepithelial CTLs [91, 92]. Associated to an upregulation of non-classical MHC class I molecules, there are other signals provided by the epithelium, independent of CD4+ T cells, that seem to be required for tissue destruction. In particular, IL-15 overexpression in both gut epithelium and lamina propria is known to disrupt intestinal immune homeostasis and contribute to disease development in multiple ways [93, 94]: (1) by inhibiting the regulatory effects of TGFβ (transforming growth factor β) and forkhead box P3 $(FOXP3)^+$ T_{reg} cells, thus promoting loss of oral tolerance and immune regulation [95, 96]; (2) by upregulating the transcription of NKG2D on intraepithelial CTLs, its adapter molecule DAP10 and the cytolytic signaling pathway associated to this receptor [83] and (3) by inducing, in conjunction with the activation of the NKG2D, the release of arachidonic acid (and possibly leukotrienes) by intraepithelial CTLs which in turn can promote the activation of intestinal granulocytes and non-specific inflammation in the intestinal mucosa of CD patients [97, 98].

1.4. The need for a trigger

One of the key aspects that is crucial in the effector destructive phase of CD is the upregulation of both IL-15 and non-classical MHC class I molecules by IEC. Undoubtedly, the $CD4^+$ T cell response has a role but is not sufficient alone to induce these alterations on the intestinal epithelium. Therefore, over the last years, several researchers have been trying to understand the upstream mechanisms that lead to the dysregulated production of IL-15 and expression non-classical MHC class I molecules by tissue cells in order for them to become targets of intraepithelial CTLs [28]. Accordingly, several candidates have been proposed, including gluten itself [99].

Although the literature on the innate immune properties of gluten is heterogeneous and highly controversial, several studies have reported numerous and diverse effects of gluten peptides on IECs and professional APCs. One of the peptides most studied for its immune-stimulating properties is the α-gliadin p31-43 (LGQQQPFPPQQPY) which was shown to have proinflammatory and toxic effects both *in vitro*, *i.e.* on intestinal organ cultures, primary APCs, and epithelial and monocytic cell lines, and in *in vivo* feeding studies [100]. In duodenal biopsies of CD patients, the p31-43 upregulated the

expression of stress-inducible MICs in epithelial cells and the expression of IL-15, cyclo-oxygenase 2, CD83 and phosphorylation of p38 MAP kinase in *lamina propria* cells [99, 101, 102]. It has been suggested that the p31-43 mediates these affects by interfering with endosomal trafficking, leading an intracellular stress response [103, 104]. Additionally, the p31-43 has the ability of induce proliferation of crypt enterocytes, in a process that is dependent on IL-15 and epithelial growth factor (EGF) [104-107]. Accordingly, in both celiac enterocytes and Caco-2 cells, the p31–43 localizes to the early endosomes and delays vesicular trafficking by interfering with the correct location of the growth factor regulated tyrosine kinase substrate (HRS), a key molecule regulating the maturation of endocytic vesicles [108]. By delaying the maturation of early endosomes, the p31-43 reduces the degradation of the EGF receptor (EGFR) and other receptor tyrosine kinases (RTKs), thus prolonging their activation when endocytosed in these vesicles. On the other hand, alterations on the recycling pathway direct more IL-15 receptor alpha (IL-15Rα) to the cell surface, enhancing the trans presentation of IL-15/IL15-Rα in IEC (*Fig. 5*). This results in an increased cell proliferation and permeability, alterations on cytoskeleton and cell shape and activation of an innate immune response [100].

In addition to the aforementioned mechanisms, it has been shown that the p31-43 induces an early upregulation of TG2 in both duodenal biopsy specimens from CD patients and gliadin “sensitive” epithelial cell lines (*i.e.* Caco-2 and T84 epithelial cells) [109]. This outcome results from the fact that, by staying retained at the vesicular level, the p31-43 upregulates intracellular reactive oxygen species (ROS) and ROS-mediated TG2 overexpression by decreasing TG2 degradation through the ubiquitin-proteasome system. Additionally, endosomal-trapped p31-43 causes a disturbance of Ca^{2+} homeostasis on IEC by mobilizing Ca^{2+} from the ER and mitochondria, resulting in the activation of both cytosolic and nuclear TG2 [110].

Once activated from its normally latent state, TG2 can differentially modulate cell death/survival processes by two main mechanisms: (1) through mediation of cell-to-extracellular matrix contacts, thereby triggering cell survival signaling, or (2) by controlling, directly or indirectly, the activity of several transcription factors to promote survival or facilitate demise [71]. One of the pathways known to be activated as such, and that is constitutively active in the intestinal mucosa of CD patients, is the NF-κB pathway [111]. The nuclear factor-κB (NF-κB) represents a family of inducible transcription factors that regulates a large array of genes involved in different processes of the immune and inflammatory responses [112]. It induces the expression of various pro-inflammatory genes, including those encoding cytokines and chemokines,

participates in inflammasome regulation and is critical for the survival, activation and differentiation of innate immune cells and inflammatory T cells. The current understanding of NF-κB activation by cytosolic TG2 relies on the latter's ability to polymerize the inhibitory subunit alpha of NF-κB (I-κB), through its transamidating activity [113, 114]. As a result of this polymerization, the NF-κB dissociates from the inhibitor and translocates to the nucleus where it activates transcription. The p31-43-induced TG2 also drives the cross-linking, ubiquitination and proteasome degradation of the anti-inflammatory peroxisome proliferator-activated receptor PPARγ, a negative regulator of inflammatory gene expression [109]. PPARγ downregulation leads to a derangement on the appropriate control of inflammation and the induction of an IEC pro-inflammatory phenotype, characterized by an increased tight junction permeability to luminal antigens and higher susceptibility to the toxic effects of environmental triggers [115]. Moreover, the p31-43 increases the expression of glucose-regulated protein (GRP)-78 and of CCAAT/enhancer binding protein-homologous protein (CHOP), a transcription factor that primarily mediates stress-linked apoptosis in cells with an irrecoverable level of ER-stress, thereby implicating the ER-stress pathway in CD inflammatory response [110].

Recently, the p31-43 was found to induce a stress response and subvert host mucosal defenses by inhibiting the cystic fibrosis transmembrane conductance regulator (CFTR) function at the intestinal surface [116]. CFTR is a cyclic adenosine monophosphate (cAMP)-regulated anion channel that mediates chloride/bicarbonate transport across epithelia and regulates epithelial adaptation to cell-autonomous or environmental stress [116-119]. According to this study, the p31-43 interacts with the nucleotide-binding domain 1 (NBD1) of CFTR to cause a conformational change that interferes with its ATPase activity. This inhibitory effect is sustained by the p31-43-induced activation of TG2 that covalently links p31-43 to CFTR, thus enhancing the detrimental effects of p31-43 on CFTR function. CFTR malfunction leads to an impaired endosomal trafficking, cytoskeleton disassembly, inflammasome activation, NF-κB nuclear translocation and IL-15 production that ultimately drive local inflammation and immune responses against immunodominant gliadin peptides. These effects can be prevented by potentiators of CFTR channel gating as they are able to attenuate gliadin-induced inflammation and promote a tolerogenic response in gluten-sensitive mice and cells from CD patients [120].

In conjunction with IL-15, type I IFNs could potentially be a component of an alternative pathway causing loss of oral tolerance to gluten [121, 122]. This statement is supported by the increased expression of IFN-α and myxovirus resistance protein 1 (MxA) - a downstream element of the type I IFN pathway - in the intestinal mucosa of CD patients

and by epidemiological studies suggesting that enteric viral infections such as rotavirus might trigger inflammatory or functional gastrointestinal diseases [123-127]. In this context, it has been shown that p31-43 and viral infection could act in synergy to induce innate immune responses and cause enteropathy in normal mice. The effects of the p31-43 were dependent on MyD88 and type I IFNs, but not Toll-like receptor 4 (TLR4), and were enhanced by co-administration of the TLR3 agonist polyinosinic: polycytidylic acid - a synthetic analog of dsRNA that mimics the innate response to viral infection [128]. In another study, the p31–43 activated the IFN-α pathway in small intestinal biopsies of CD patients and in the enterocyte cell line Caco-2, by delaying the TLR7 trafficking in the early endocytic compartment. Accordingly, the p31–43 cooperated with the TLR7-specific ligand loxoribine to activate the TLR7/MyD88/MAPK/NF-κB pathway suggesting that together with viral infections, dietary proteins able to mimic and potentiate the innate immune response to viruses, can trigger an autoimmune disease such as CD [129].

So far, little is known about the molecular mechanisms underlying the p31-43 cellular uptake and the possible involvement of a membrane receptor. On the basis of previous evidences demonstrating that the p31-43 is able to interact with a membrane-like environment *in vitro*, it has been hypothesized that membrane composition and organization, rather than a specific receptor protein, may have a major role in p31-43 internalization by cells and that it may behave as a cell-penetrating peptide [130]. Additionally, it is still not clear why gluten has such innate immune effects only in certain individuals and what would determine it acquiring these properties in a given individual at a certain time. All in all, it is possible that this acquired gluten sensitivity requires the encounter between a predisposing genetic background and an environmental factor that renders host cells responsive to gluten-induced activation of the mucosal immune system. Such triggers would include, for example, gut bacteria [131-135]. It is now recognized that the microbiota can affect intestinal immune homeostasis and the health of epithelial cells. In that sense, several studies report an intestinal dysbiosis in CD patients which include a decrease in butyrate-producing bacteria *Faecalibacterium prausnitzii* and representatives of the genus *Bifidobacterium* as well as an expansion of potentially pathogenic bacterial populations such as *Escherichia coli* and *Staphylococcus spp* [28].

1.5. Diagnosis and treatment

In adults, the diagnosis of CD requires a combination of serology testing and duodenal biopsy sampling during a gluten-containing diet [136]. If CD is suspected, several serological tests including endomysial-Abs (EmAbs) and TG2-Ab assays can support the diagnostic procedure in selecting patients for endoscopy, upon which duodenal biopsy samples are taken [1]. Both EmAbs and TG2-Abs have excellent sensitivities and almost 100 % specificity to CD [137, 138]. Initially regarded as the gold standard method to detect CD antibodies, the EmAbs testing has been less used due to its high cost, subjectivity and time consuming [139, 140]. These drawbacks made TG2-Ab testing the currently recommended first-line approach in clinical practice. Notably, the most accurate serological tests for CD are towards the IgA isotypes of EmAbs and TG2-Abs, and only in the case of selective IgA deficiency are IgG isotype antibody tests needed [141, 142]. If an individual proves to be seropositive for CD-specific antibodies, a duodenal biopsy-based diagnostic strategy should be implemented to ascertain the presence of histological abnormalities that include villous atrophy, intraepithelial lymphocytosis and crypt hyperplasia [143]. In children, the diagnosis can now be made without a requirement for gut biopsy examination if a high titer of serum IgA anti-TG2 Abs is present [144]. In the most challenging cases, additional non-conventional, yet reliable, diagnostic tools may be implemented to identify CD patients such as HLA typing and immunohistochemistry for IEL subsets [145, 146].

Currently, the only effective treatment for CD relies on a strict, lifelong adherence to a gluten-free diet (GFD). In practice, this means avoiding all foods based on or containing wheat, rye, barley and all cross-breeds of these cereals, which *per se* is difficult, if not impossible, to maintain [147]. When on a GFD, alleviation of symptoms is in most cases rapid and convincing although a complete recovery of the intestinal mucosal morphology can take up months or even years [148, 149]. Despite its effectiveness in achieving normalization of both serological and histological markers, the GFD has numerous difficulties and even responsive patients have expressed their wish for alternative therapies due to the restrictive nature of the diet [150, 151]. Although a wide range of gluten-free substitute products are now available, many individuals find them less palatable and substantially more expensive than their gluten-containing counterparts [152]. On the other hand, inadvertent gluten exposure as consequence of misinterpretation of food labels and cross contamination in manufacturing processes are enough to prevent gut recovery and predispose to dietary lapses [7, 147, 153]. Factors that may be associated with a poor dietary adherence to a GFD include social pressures (particularly in adolescence), lower socioeconomical status, environmental and cultural aspects, as well as eating out or travelling [154-156]. As a result of the vigilance that is

required to adhere to a GFD, the burden associated to the treatment of CD is considerably high and a source of anxiety among patients. Of note, a minority of CD patients develop the so-called refractory CD that is characterized by persistent or recurrent villous atrophy and malabsorptive symptoms despite these people best efforts to avoid dietary gluten [157]. Being at an increased risk for developing enteropathy-associated T-cell lymphoma, small bowel adenocarcinoma, and other gastrointestinal cancers, these refractory CD patients require additional therapeutic intervention in addition to a GFD [158]. Therefore, in an attempt to address the nonsatisfaction of CD patient regarding their quality of life, alternative therapies are currently under investigation to supplement or supplant a GFD [159, 160]. These are mainly focused on:

- Degradation/neutralization of gluten (e.g. by enzyme therapy, gluten-sequestering polymers);
- Barrier enhancing therapies (e.g. zonulin antagonists);
- Immune targeted therapies (e.g. glucocorticoids with low systemic bioavailability, peptide-based immunotherapy, inhibition of tTG2, blocking HLA-DQ2 or HLA-DQ8, blocking intestinal homing of inflammatory cells, cytokine therapy, etc.);
- Microbiota and nematode based therapies (e.g. probiotics for gluten proteolysis).

Despite the outcoming therapies that are being considered based on improved understanding of the disease mechanisms, successful alternatives to a GFD have yet to emerge.

1.6. What about polyphenols?

Compelling observational and interventional evidence is available on the benefits of consuming plant-based foods and beverages, with current dietary advices for optimal health and longevity suggesting a high consumption of fruit, vegetables, legumes and wholegrains [161, 162]. Plant-based foods are exclusive and rich sources of a wide variety of bioactive phytochemicals with specific groups of compounds being particularly abundant in some foods for which specific physiological effects and health implications have been attributed [163]. Among these, polyphenols have attracted considerable attention in recent years and are being actively researched for their health care potential in the prevention of several chronic diseases, such as diabetes, cardiometabolic and neurodegenerative disorders, cancer, low-grade inflammation and symptoms associated

with ageing and menopause [164-168]. This interest is being continuously stimulated by epidemiological studies and associated meta-analyses suggesting that long term consumption of polyphenol-rich fruit-, seed- and vegetable-derived food and beverages can improve, for example, endothelial function, insulin sensitivity, decrease blood pressure, modulate energy metabolism and have a protective role on the intestinal epithelium and immune homeostasis [64, 169-172]. The increasing recognition of benefits brought by polyphenols to human health has sparked a new appraisal of various plant-derived foods and beverages such as olive oil, all kinds of fruit juices, chocolate, coffee, tea, and even alcoholic beverages such as wine and cider. Their content in phenolic substances has fueled numerous investigations that, again, are unraveling the therapeutic potential of these natural products in several disease contexts, including CD, even though their bioavailability in the human body is still a fiercely debated question.

2. Polyphenols

2.1. Definition and biological relevance

In a strict chemical sense, polyphenols are plant secondary metabolites derived from the shikimate/ phenylpropanoid and/ or the polyketide pathway, featuring more than one phenolic unit and deprived of nitrogen-based functions [173]. This definition, however, would let out all monophenolic structures, as well as their naturally occurring derivatives such as phenyl esters, methyl phenyl ethers and O-phenyl glycosides. Today, the term ‘polyphenol’ is collectively used to refer to several sub-groups of natural compounds with phenolic structural features, some of which often vague even to researchers [174]. These may occur in a non-conjugated form (aglycone) or conjugated with sugars, carboxylic and organic acids, amines, lipids and other phenols. In plants, polyphenols have several functions, including protection against herbivores and microorganisms, as attractants for pollinators and seed- dispersing animals, as allelopathic agents, UV protectants, and signal molecules in the formation of nitrogen-fixing root nodules [175, 176]. In foodstuffs, polyphenols are directly related to several organoleptic characteristics such as flavor, color, aroma and oxidative stability [177]. Due to the increased demand for foods with functional and health-promoting properties, nowadays, polyphenol-rich plant extracts have been extensively studied as functional additives in diverse food systems to improve their nutritional properties and sensory attributes [178, 179].

Much of the earlier studies on polyphenols have viewed these compounds from the perspective of antioxidants [180, 181]. This was originally thought to be a panacea to explain their global mechanism of action in human disorders associated with oxidative stress. However, it has become evident over the last two decades, that polyphenols do not merely exert their beneficial effects as free radical scavengers and metal ion-chelators but may also work as modifiers of signal transduction pathways with implication in cell survival and death under both normal and pathological conditions [182-185]. These include, for example, inhibition of certain enzymes involved in ROS production like xanthine oxidase (XO), NADPH oxidase (NOX) and nitric oxide synthase (iNOS) as well as enzymes involved in arachidonic acid metabolism such as phospholipase A2 (PLA2), cyclooxygenase (COX) and lipoxygenase (LOX) [186]. The ability of polyphenols to reduce the release of arachidonic acid, prostaglandins (PGs), and leukotrienes (LTs) is considered one of their most important anti-inflammatory mechanisms [187]. Polyphenols have also been shown to modulate the NF-κB and MAPKs signaling cascades and to upregulate phase II detoxifying/antioxidant enzymes like hemeoxygenase-1 (HO-1), glutathione peroxidase (GSH-Px), glutathione-S-transferase (GST), catalase and superoxide dismutase (SOD) by targeting the common nuclear redox factor Nrf2 [187-189]. Activation of the Nrf2 transcription factor and the electrophile response element EpRE (also called the antioxidant response element or ARE) to which Nrf2 binds are key mechanisms of protection against chemically induced oxidative/electrophilic stress [190]. Of note, the health effects of polyphenols including their antioxidant and anti-inflammatory activities are highly dependent on the nature, amount consumed and on polyphenol bioavailability. In that way, not all polyphenols are absorbed with the same efficacy. Additionally, they are extensively metabolized by digestive and hepatic enzymes and by the intestinal microflora being then eliminated in urine and bile. Therefore, depending on the modifications to which dietary polyphenols are subjected during their metabolic processing, their biological activities within target tissues might be very affected [191].

2.2. Classification and main dietary sources

Polyphenols constitute one of the most numerous and widely distributed groups of natural products in the plant kingdom, with more than 8000 structural variants already identified [174]. They are usually divided into four different classes according to the number of phenolic rings that they contain and the structural elements that bind these

rings to one another. Distinctions are thus made between phenolic acids (including hydroxylbenzoic and hydroxylcinnamic acids), stilbenes, lignans and flavonoids (*Fig. 6*) [192]. Foods with high percentages of hydroxycinnamic acids include coffee, the main contributor for the intake of this subclass of phenolic acids, potatoes, loquat, pear and rye bread. Hydroxybenzoic acids, on the other hand, are mainly present in chestnut, red raspberry and cloudberry. Lignans are mostly found in fruits such as pear and apricot, in vegetables like broccoli and cauliflower and in sesame seeds [193].

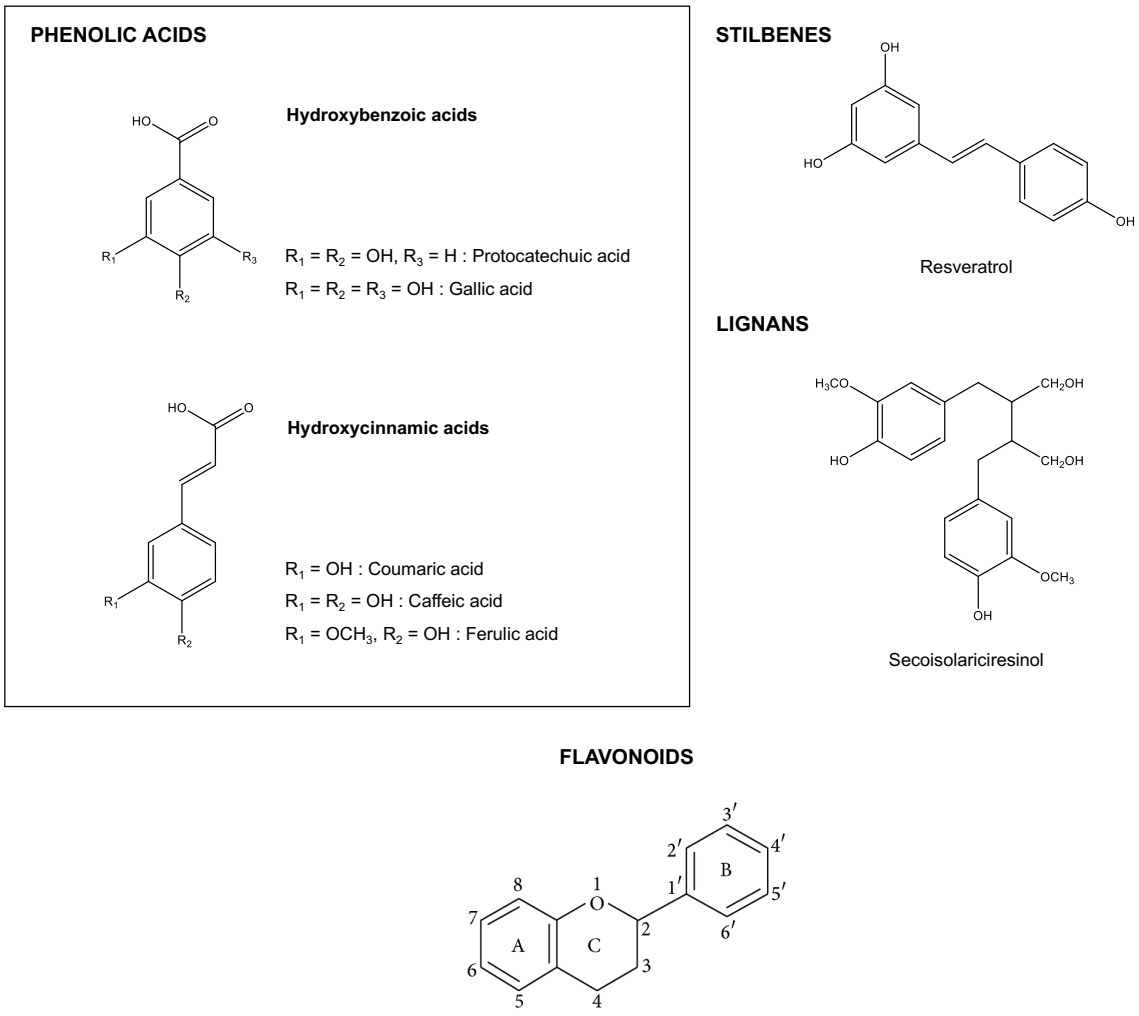

Fig. 6 - Chemical structures of the four major classes of polyphenols.

The flavonoid family constitute one of the most characteristic classes of compounds in higher plants [194]. They provide the more vibrant, brilliant colours in nature, including

most of the blue, purple and emerald green tones found in flowers, leaves, fruits and vegetables. Moreover, most of the yellow, orange and red colours that are not carotenoids belong to the flavonoid family [195]. The basic structure of flavonoids consists of a typical C_6-C_3-C_6 backbone in which two C_6 units (rings A and B) are of phenolic nature and bound together by three carbon atoms that form an oxygenated heterocycle (ring C) (*Fig. 6*). According to the type of heterocycle involved and its substitution pattern, the flavonoid group may be itself subdivided into different subclasses such as flavonols (*e.g*. kaempferol, quercetin, myricetin), flavones (*e.g*. apigenin, luteolin), isoflavones (*e.g.* daidzein, genistein), flavanones (*e.g.* naringenin, eriodictyol, hesperidin), anthocyanidins (*e.g.* pelargonidin, cyanidin, delphinidin, peonidin, malvidin), and flavanols (*e.g.* catechin, epicatechin) (*Fig. 7*) [196, 197]. Other flavonoid subclasses that are usually of minor dietary relevance include the chalcones, dihydrochalcones, dihydroflavonols, flavan-3,4-diols, coumarins, and aurones [198]. Within each subclass, the polyphenolic compounds may differ in the position and number of hydroxyl, methoxyl and glycosyl groups. They may be further substituted (*e.g.* glycosylated or acylated), sometimes resulting in very complex structures [199].

The distribution of flavonoids in plant-based foods and beverages is not uniform: flavonols are particularly abundant in red onions, spinach, asparagus and capers; flavones in celery, parsley, red peppers and chamomile; isoflavones in soybeans and other leguminous plants; flavanones in all citrus fruits such as oranges, lemons and grapes; anthocyanins in berry fruits and red wine; and flavanols in dark chocolate, cocoa powder, almonds, apples and tea [193, 200]. In most cases, plant-based food items contain complex mixtures of polyphenols [201]. Their content depends on numerous genetic, environmental (*e.g.* soil type, sun exposure, rainfall), and technologic factors (degree of ripeness at the time of harvest, processing, storage and culinary preparation) [164]. Additionally, there are significant differences on the type of polyphenols in plants at the tissue, cellular and sub cellular levels. For instance, insoluble phenolics are mainly found in cell walls, associated to polysaccharides, while the soluble ones are present within the cell vacuoles [202].

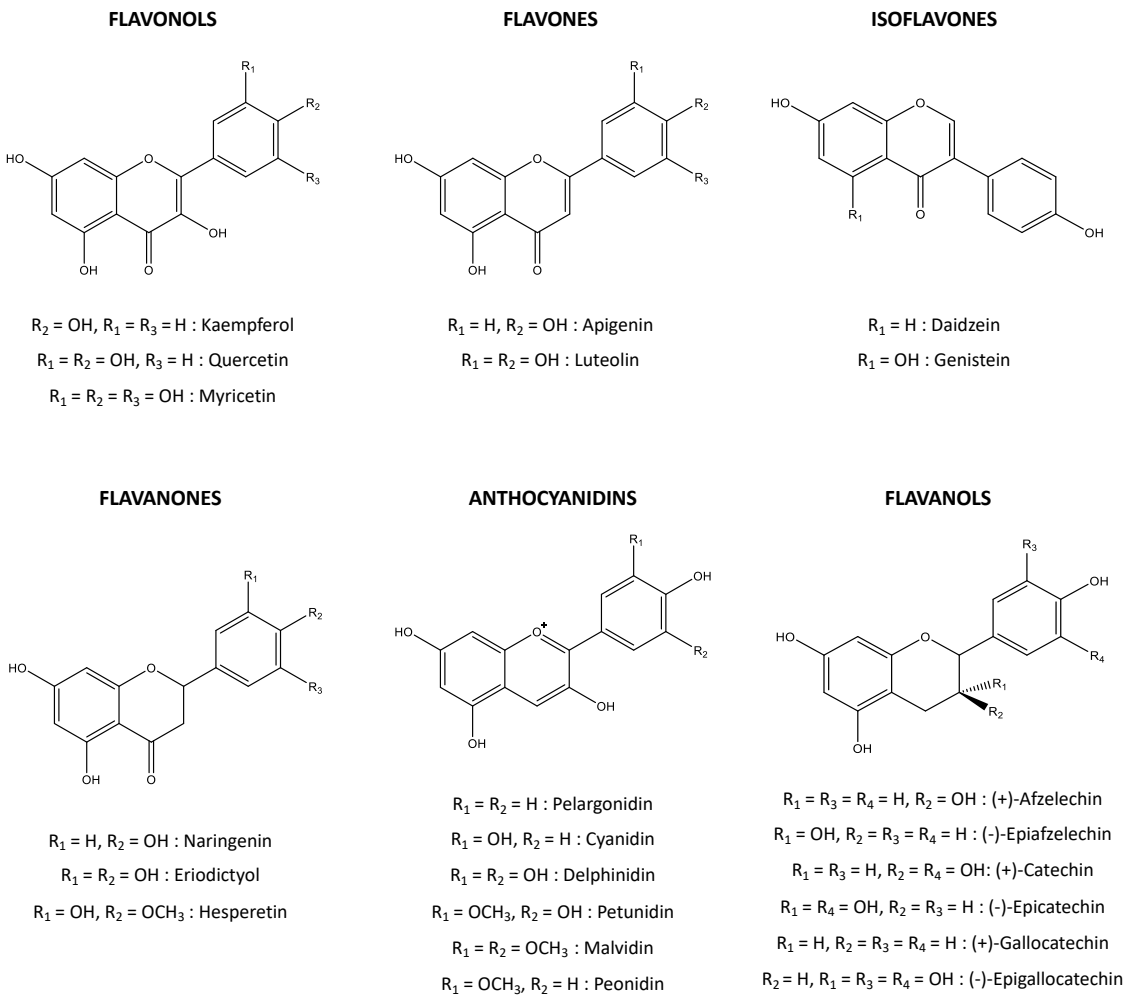

Fig. 7 - Chemical structures of the six major subclasses of flavonoids and examples of common aglycones.

2.3. Flavanols and proanthocyanidins

Flavanols are a highly diversified and complex flavonoid subgroup ranging from the simple monomers to oligomeric and polymeric proanthocyanidins (also known as condensed tannins). The two chiral centers at C2 and C3 of the monomeric flavanol produce four isomers for each level of B ring hydroxylation, two of which, (+)-catechin and (-)-epicatechin, are widespread in nature. Others, like (-)-epiafzelechin, have a more limited distribution [203, 204]. Oligomeric and polymeric proanthocyanidins have an additional chiral center at C4 in the upper and lower units [198, 205]. B-type proanthocyanidins are made from (+)-catechin and (-)-epicatechin by oxidative coupling between the C4 of the upper monomer and the C6 or C8 of the adjacent lower or extension unit to create oligomers or polymers (*Fig. 8*).

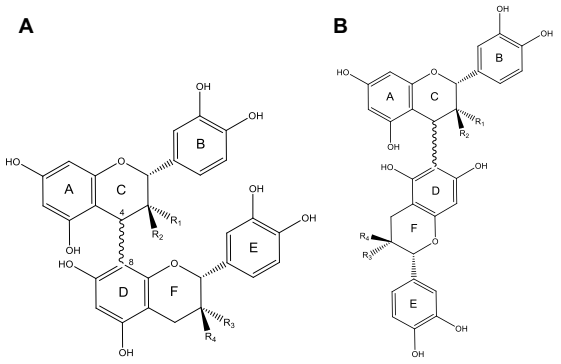

R_1	R_2	R_3	R_4	C4-C8 DIMER NAME	C4-C6 DIMER NAME
OH	H	H	OH	B1	B7
OH	H	OH	H	B2	B5
H	OH	H	OH	B3	B6
H	OH	OH	H	B4	B8

Fig. 8 - Chemical structures of type B dimeric proanthocyanidins: (A) C4-C8 and (B) C4-C6 dimers.

A-type proanthocyanidins have an additional ether bond between the C2 of one monomeric unit and the C7 of the other flavanol unit (*Fig. 9*).

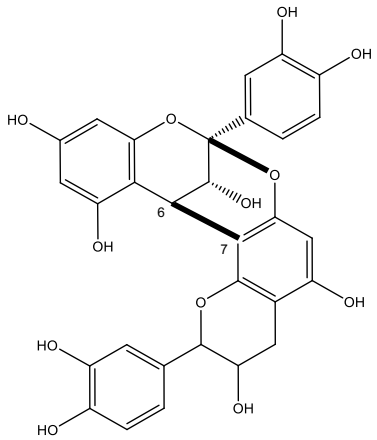

Fig. 9 - Chemical structure of procyanidin A2 dimer.

The polymerization degree of proanthocyanidins varies over a broad range of molecular forms from dimers up to about 200 monomeric flavanol units (*Fig. 10*). Proanthocyanidins that consist exclusively of (epi)catechin units are called procyanidins, and are the most abundant type of proanthocyanidins in plants. The less-common proanthocyanidins containing (epi)afzelechin or (epi)gallocatechin subunits are propelargonidins and prodelphinidins, respectively [206]. Proanthocyanidins and flavanols may sometimes be esterified by gallic acid or exceptionally with sugars, though the latter situation is quite rare.

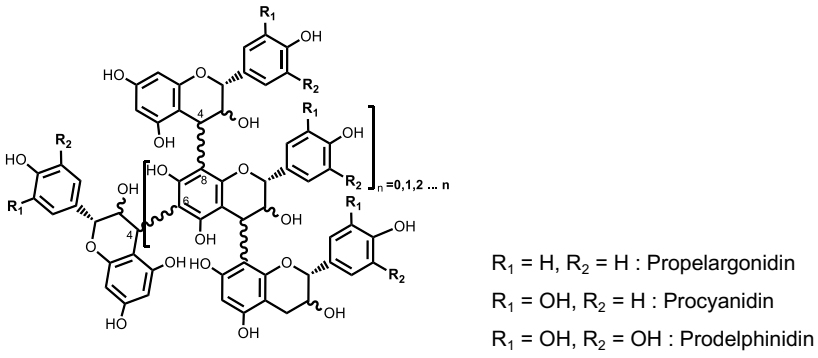

Fig. 10 - General structure of proanthocyanidins.

In general, proanthocyanidins are primarily found in fruits, especially berries, cocoa and some beverages like wine, beer and tea. Vegetables are not an important source of these tannins. Legumes, nuts and other minority cereals such as sorghum and barley also contain proanthocyanidins, but they are not detectable in staple crops such as corn, rice and wheat. Proanthocyanidins (especially the most polymerized ones) tend to concentrate in the peel of fruits or the bran of grains [207-209].

2.4. Dietary intake and bioavailability

To exert any biological effect, dietary polyphenols have to be available to some extent in the target tissues. This feature critically depends on their absorption and bioavailability [198]. In fact, phenolic compounds that are usually common in the human diet are not necessarily the most active within the body, either because they have a lower intrinsic activity or because they are poorly absorbed at the gastrointestinal tract, highly metabolized, or rapidly eliminated [210]. The total polyphenol intake for the overall population was estimated to be about 900 mg/day [211]. This value varied according to differences in target groups of subjects, including their geographic location and socio-demographics. The main food sources of polyphenols are represented by tea, coffee, red wine, fruit and vegetables [211]. Flavanols, procyanidins, flavanones, and flavonols are the more commonly consumed plant food phenols in a typical Western diet, while anthocyanidins, flavones, lignans, and isoflavones are consumed in smaller amounts [212].

To reach a conclusive evidence regarding the effectiveness of polyphenols in disease prevention and human health improvement, it is essential to determine not only the distribution of these compounds in our diet and to estimate their content in each food item but also to have a better knowledge of their bioavailability and fate of their metabolites [213]. The subject is, however, complicated because there are several factors that can affect the absorption of dietary polyphenols in humans. These include polyphenol-related factors such as the chemical structure (aglicone) and type of sugar in the glycoside as well as their interaction with food proteins, carbohydrates and fiber [210, 214]. Typically, following ingestion of polyphenols, absorption of some, but by no means all components into the circulatory system occurs in the small intestine where the glycosides are hydrolyzed as a result of the action of lactase-phloridzin hydrolase (LPH) (*Fig. 11*).

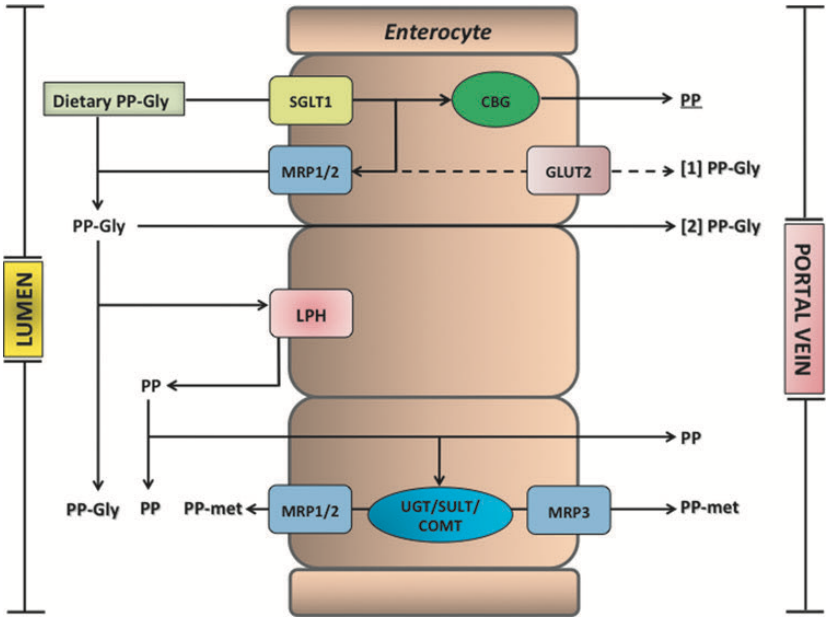

Fig. 11 - Mechanisms of absorption and metabolism of polyphenols [198]. CBG, cytosolic b- glucosidase; COMT, catechol- O-methyl transferase; GLUT2, glucose transporter; LPH, lactase-phloridzin hydrolase; MRP1-2–3, multidrug-resistant proteins; PP, polyphenol aglycone; PP-gly, polyphenol glycoside, PP-met, polyphenol sulfate/glucuronide/methyl metabolites; SGLT1, sodium- dependent glucose transporter; SULT, sulfotransferase; UGT, uridine-5¢-diphosphate glucuronosyltransferase.

LPH is a brush border membrane enzyme with a broad substrate specificity for flavonoid-O-β-D-glucosides, allowing the released aglycones to enter IEC by passive diffusion [215]. An alternative route by which glycoside conjugates may be hydrolyzed is

mediated by a cytosolic β-glucosidase (CBG). For CBG-catalyzed hydrolysis to occur, polar glucoside conjugates must be transported into IEC through the active sodium-dependent glucose transporter 1 (SGLT1) [216]. Prior to the passage into the blood stream, the absorbed aglycones undergo some degree of phase II metabolism at enterocyte level including methylation by catechol-O-methyltransferases (COMTs), sulfation by sulfotransferases (SULTs) and glucuronidation by uridine-5'-diphosphate glucuronosyltransferases (UGT). These conjugation mechanisms are highly efficient, and free aglycones are generally either absent or present in low concentrations in plasma after consumption of nutritional doses. Additionally, there is also efflux of some of the metabolites back into the lumen of the small intestine, and this is thought to involve members of the adenosine triphosphate-binding cassette (ABC) family of transporters, including multidrug resistance protein (MRP) and P-glycoprotein. MRP-3 and the glucose transporter GLUT2 have also been implicated in the efflux of metabolites from the basolateral membrane of the enterocytes. When in the portal bloodstream, these polyphenolic conjugates rapidly reach the liver where they can be subjected to further phase II metabolism. Instead of accumulating in the circulatory system, they are rapidly turned over and removed by excretion *via* the kidneys. Alternatively, enterohepatic recirculation may result in some recycling back to the small intestine through bile excretion [217, 218].

The faction of polyphenols that is not absorbed in the small intestine to any degree reach the colon where they are extensively modified by the gut microbiota [219]. These include flavonoids linked to a rhamnose moiety, polymers, hydroxycinnamic acids esterified to sugars, organic acids and lipids as well as polyphenols bound to dietary fiber and proteins (the so called non-extractable polyphenols). Upon cleavage of their conjugating moieties, the resultant aglycones are metabolized by the colonic microbiota, leading to the production of various hydroxyphenylacetic acids [198, 218]. These can be absorbed and may be subjected to metabolism in the liver before being excreted in urine in amounts that, in most instances, are well in excess of the metabolites that enter the circulatory system *via* the small intestine. Although only limited information is available on the complex pathways of catabolism by gut microbiota, this activity is of great importance for the bioavailability and biological action of polyphenols as specific bioactive metabolites are produced in such a way [220]. *In vivo*, these are slowly and continuously absorbed through the colon, leading to sustained increases of baseline concentrations rather than plasma peaks observed after antioxidant-rich foods [213]. In general, the concentrations of polyphenols post prandially are usually less than 1 μM, whereas, for gut catabolites, concentrations can well exceed this figure and are typically

>10-100-fold higher than parent compounds [221]. Therefore, the compounds that reach target cells and tissues are often chemically, biologically, and in many instances functionally different from the original dietary form. The unabsorbed metabolites are eliminated *via* faeces.

Regarding the bioavailability profile of proanthocyanidins, a study in which ileostomists consumed apple juice indicated that most pass unaltered to the large intestine, where they are catabolized by the colonic microbiota, yielding a diversity of phenolic acids and valerolactones that are absorbed into the circulatory system and excreted in the urine [222-225]. Nevertheless, because only a small percentage of metabolites are excreted in urine, it is possible for proanthocyanidins to pass through the entire gastrointestinal tract largely intact, especially for those with a high molecular weight [226, 227]. The physiological relevance of these non-absorbable compounds and related metabolites lies on their ability to counteract the activity of dietary pro-oxidants and prevent the damage caused by reactive species to IEC [205, 213].

SYNOPSIS

Alongside with the intensification of the globalization process and advances in the food industry, a pronounced increase in public health problems has been observed. Even though genetics has definitely an influence, as Hippocrates once said *"whatever be the father of a disease, the mother is always a bad diet"*. Thus, it is not surprising to see that rates of chronic disorders, most of them food pattern related, reached epidemic levels in the middle of the 21st century, being one of the most important current contributors to human morbidity and mortality. In an attempt to control such trend, a lot of effort has been devoted to the search of effective and specific chemical drugs, allegedly able to treat these modern disorders. Unsurprisingly, health-related economic and social costs have risen to represent a significant percentage of worldwide expenditure relating to medical devices, drug discovery, and other pharmacological advances that would be avoided just through lifestyle modifications. Fortunately, the times are changing and we are now witnessing the "naturals" revolution, an explosion in the niche of natural functional and fortified food products thanks to building consumer consciousness of the real value of nutrition and lifestyle patterns as important contributors to health status and long-lasting wellbeing. This global resurgence in interest and use of plant-based therapies for health-related applications has stimulated a great scientific awareness in searching potentially useful natural molecules from medicinal herbs and foods, unravel their mechanisms of action and widen the perspectives about their use not only for prophylactic but also therapeutic purposes. Additionally, the increasing demand to assess the beneficial effects of botanical functionality, natural products, and their bioactive molecules is largely driven by increasing evidence of side-effects and adverse reactions produced by pharmaceutical drugs [228-230].

Among the bioactive constituents of natural matrices, polyphenols occupy today a unique place in science as probably the major class of bioactive natural compounds that the general public has heard about as a consequence of their presence in fruit-, seed- and vegetable-derived foods and beverages and of their implication in the formulation of well-marketed cosmetic and para-pharmaceutical products. Although observational, longitudinal, and cohort studies strongly support that dietary polyphenols have a strong potential in the enhancement of human health by changing disease risk profiles through

their ability to modulate several biological pathways, their significance in a CD context remains largely unknow. This is where the starting point for this project came from. From the curiosity and novelty of exploring the potential and versatility of polyphenols in CD management. In fact, despite the outcoming therapies that are being considered based on improved understanding of the disease mechanisms, successful alternatives to a GFD have yet to emerge. For this reason, there is an urgent need for development of adjuvant therapies for CD aiming to improve the quality of life of its patients. Among the different approaches that are currently being explored, some of which still in the pre-clinical phase, the intraluminal sequestration of gluten immunogenic peptides emerged as a potentially novel therapeutic strategy to prevent the initiation of CD symptoms and associated immune response [160]. So far, much of the effort is being directed to synthetic polymeric binders such as the poly (hydroxyethyl methacrylate-co-styrene sulfonate) or P(HEMA-co-SS), a non-absorbable, high molecular weight and linear co-polymer of hydroxyethylmethacrylate (HEMA) and sodium 4-styrene sulfonate (SS) [231, 232]. *In vivo*, this polymer revealed selectivity in sequestration of gliadin proteins as compared to other nutrients, being highly effective in abrogating villous damage [233]. Promising results were also obtained by using anti-gluten antibodies and side chain fragment variable proteins to neutralize gliadins [234, 235]. At this point, a question arose: is it possible to find natural bioactive compounds with similar gliadin-binding properties and therapeutic value? What are the structural features and molecular mechanisms driving these interactions under physiological conditions?

In previous reports, the ability of grape seed procyanidins to interact with gliadin-derived peptides has been demonstrated by means of fluorescence quenching, dynamic light scattering and mass spectrometry experiments [236, 237]. At that time, the obtained results were quite encouraging and provided valuable insights regarding the potential role of polyphenols as dietary scavengers of CD bioactive peptides, a feature that would make them especially useful, at the very least, as a natural supportive therapy to a GFD. A similar outcome was accomplished by another group, showing that green tea polyphenols prevent gliadin digestion *in vitro*, through physical interactions with gliadin proteins and inhibition of digestive proteases, and reduced gliadin-mediated increases in intestinal permeability and inflammation [238]. Just as all biochemical reactions involve recognition, binding and the formation of non-covalent complexes, characterization of polyphenol binding to CD bioactive peptides is essential to understand, at the molecular level, to what extent the consumption of a polyphenol-rich diet may affect the health of CD patients, especially considering that low amounts of gluten may be present on gluten-free products which can be as harmful as lack of adherence to a GFD. Therefore, the

main purpose of this work was to unveil the structural and thermodynamic basis of polyphenol interactions with CD bioactive peptides by means of different spectroscopic and *in silico* approaches under near physiological conditions. Greater emphasis has been placed on a 32 aminoacid-long peptide from α2-gliadin (QLQPFPQPQLPYPQPQLPYPQPQLPYPQPQPF), frequently defined as the most important CD-immunogenic sequence within gluten [60]. This peptide was first described in 2002 by Shan and co-workers as being one of the main digestive products of α2-gliadin, to which they deliberately added an N-terminal leucine residue to stabilize it from the noncatalytic cyclization of the N-terminal glutamine to pyroglutamate. From that day on, even though the immunogenicity of the 32-mer version has already been proven using CD T-cell clones and intestinal T-cell lines, over time, it was forgotten, giving place to the 33-mer [239]. Recently, the stability of the 33-mer peptide to enzymatic hydrolysis by gastric and pancreatic proteases was evaluated *in vitro* [240]. In addition to the original 33-mer, the truncated forms after N-terminal removal of leucine were also identified resulting in the 32-mer and pyro-32-mer. The ratio 33-mer/32-mer/pyro-32-mer was about 12/76/12. The 32/33-mer peptide contains six partly overlapping copies of three DQ2-restricted T cell epitopes, namely PFPQPQLPY (DQ2.5-glia-α1a, one copy), PYPQPQLPY (DQ2.5-glia-α1b, two copies) and PQPQLPYPQ (DQ2.5-glia-α2, three copies) and the deamidated form was found to be an extremely potent T-cell stimulator, several-fold more potent than any other known gluten peptide [74]. As such, it plays an important role in the field of CD, *e.g.*, as a model peptide to study CD mechanisms or the efficiency of novel preventive strategies. In that sense, alongside with the characterization of polyphenol binding to the 32-mer, the second goal of this project was to assess their ability to reduce the 32-mer peptide bioaccessibility in an *in vitro* model of the small intestinal epithelium. These two topics are thoroughly explored in the first part of this document, entitled "*Physical and chemical insights on the interaction between polyphenols and CD bioactive peptides"* [241, 242].

In the second part of the present dissertation, the bar was raised. Here, the objective was to study, *in vivo*, the modulatory effect of dietary polyphenols on a gluten-induced oxidative stress and inflammatory immune response. This work was performed at the *Istituto di Scienze dell'Alimentazione* of Avellino (Italy), a *European Laboratory for Investigation of Food-Induced Diseases* (ELFID). Under the supervision and technical assistance of Dr. Mauro Rossi, Dr. Paolo Bergamo and Dr. Francesco Maurano, who monitored the whole process involving experimentation on a transgenic mice model of CD, the applicability of polyphenols from common food sources (*e.g.* catechins from

green tea) and industrial value-added by-products (*e.g.* grape seed procyanidins) was explored on a dietary supplementation basis to a gluten-containing diet. By providing an in-depth understanding regarding the benefits of dietary polyphenols in a CD framework, this cutting-edge project lays the foundations for the development of an effective nutritional intervention and alternative prevention strategy to a GFD based on innovative polyphenol-rich functional food formulations. Hopefully, the intake of polyphenols through food sources or dietary supplementation could be the simplest and safest way to manage CD in a near future.

CHAPTER I

Physical and chemical insights on the interaction between polyphenols and CD bioactive peptides

1. Introduction

Being, perhaps, the most important non-nutrient bioactive group in the human diet, it has become increasingly clear that polyphenols have many potential bioactivities within the human body. These include, for example, their interaction with other macromolecules like proteins, carbohydrates or lipids, all of which have a great impact on the bioaccessibility, bioavailability and biological effect of polyphenols [243]. Accordingly, studies conducted in recent years have shown the importance of these interactions, mainly with proteins and its relationship to the astringency perception of many foods and beverages such as unripe fruits, wines, teas and beers [244-248]. Astringency is an oral sensation that has been previously defined as puckering, rough and drying mouth-feel [249]. Although the physico-chemical mechanisms of astringency are not completely understood, it is believed to be due to the interaction and subsequent aggregation between polyphenols and salivary proteins that reduce the lubrification properties of saliva and leave an unpleasant tactile sensation in the mouth [250]. Interestingly, it has been suggested that astringency is not related to the total protein content of saliva. Instead, it correlates with the concentration of individual salivary proteins designated proline-rich proteins (PRPs) [177]. PRPs are one of the dominant classes of salivary proteins produced and secreted by the parotid and submandibular glands. They are classified as intrinsically disordered or naturally unfolded proteins, containing several repeats of short proline-rich sequences [251]. Proline accounts for about 25 to 42% of the aminoacid residues in PRPs, that, together with a high glycine content, provide an extended chain conformation with multiple contact points for polyphenols to bind [252]. Human PRPs are usually divided into glycosylated, acidic, and basic types, which, despite their structural similarities, have different functions. Accordingly, they are involved in oral lubrification, binding to hydroxyapatite (thus becoming a part of the acquired enamel pellicle on teeth), maintenance of calcium homeostasis, modulation of bacterial growth and, most importantly, protection against the detrimental effects of dietary polyphenols [253].

Although on a sensorial framework, the astringency perception ends up being a desirable quality attribute in some highly-consumed beverages such as red wine or tea, the intake of polyphenols-rich foods and drinks has been associated with adverse nutritional effects [254]. By binding to proteins, polyphenols might potentially interfere

with the availability of certain amino acids and inhibit the activity of digestive enzymes, thus affecting the functionality, digestibility and nutritional value of proteins [255]. Additionally, due to pre-absorptive interactions during digestion, it has been shown that dietary polyphenols reduce the transport of thiamin and folic acid, and change the activity of drugs through interactions that affect drug transporters or enzymes, resulting in both inhibition or increasing bioavailability depending on the case [184, 256]. They may also inhibit the nonheme iron absorption and lead to iron depletion in populations with marginal iron stores [257]. Despite these potentially harmful outcomes, the fact is that depending on the circumstances, the interaction between polyphenols and proteins may have important therapeutic implications. Epigallocatechin-3-gallate (EGCG), one of the main flavonoids found in white and green tea, has been proposed to have an anti-HIV-1 effect by preventing the binding of the HIV-1 viral envelope gp120 to the glycoprotein receptor CD4, expressed on T-cells [258]. Subsequent studies have confirmed the potential use of vegetal tannins as safe and highly effective anti-viral agents against pathogenic viruses [259]. On another report, EGCG prevented amyloid β-peptide fibrillation, redirecting Aβ aggregation into unstructured, off-pathway oligomers [260]. Regarding transthyretin (TTR)-related amyloidosis, it has been demonstrated, *in vitro* and *ex vivo*, that EGCG binds to TTR and increases its tetramer conformational stability. Furthermore, it has been shown that EGCG is able to efficiently remodel mature TTR fibrils into smaller, non-toxic unstructured protein aggregates and to lower TTR systemic deposition in a Familial Amyloidotic Polyneuropathy (FAP) mice model, particularly in the gastrointestinal tract and peripheral nervous system [261]. Interestingly, when EGCG was incubated for 15 min with HT-29 cells, 75% of radioactively labeled EGCG was found in the cytoplasmic fraction whereas membrane-associated radioactivity increased gradually with time [262]. These results provided the first evidences regarding the ability of EGCG to directly bind to cell membrane components, including proteins and lipids. More recent findings suggest several additional mechanisms of action for EGCG, beyond its antioxidant activity, including interaction with cell surface receptors, activation of second messengers and signal transduction pathways, modulation of metabolic enzymes, and autophagy [183]. For example, EGCG was shown to induce lipid-raft clustering and apoptotic cell death in multiple myeloma cells by activating protein kinase Cδ and acid sphingomyelinase [263]. These effects were mediated through the 67 kDa laminin receptor (67LR), a non-integrin cell-surface receptor conferring EGCG responsiveness to cancer cells [264].

In recent years, attention has turned to the potential use of polyphenols to aid in the treatment of symptoms associated with food allergies and intolerances [265-268].

Accordingly, many studies have sought to explore their anti-allergenic effect in different disease models and human clinical trials, some of which took advantage of the natural binding properties of polyphenols to proteins to physically block the recognition of immunostimulatory proteins by immune cells, thus resulting in the alleviation of symptoms. In addition, their endogenous antioxidant ability limits the extent of cellular injury from free radicals during the allergic insult and mediator release [269]. *Plundrich et al. (2014)*, for example, showed that fortification of peanut flour with cranberry polyphenols resulted in a hypoallergenic matrix with decreased IgE binding, degranulation capacity and allergenic response *in vivo* [270]. These effects were likely due to changes in protein secondary structure and/or epitope masking. Later, the same authors demonstrated that modification of peanut proteins with cranberry or blueberry polyphenols led to the formation of protein-polyphenol complexes with significantly reduced allergenic potential [271]. On another study, EGCG has been shown to structurally modify ovalbumin, the major allergen of egg white, by binding to the pocket that partly overlaps with the previously identified IgE-binding region [272]. Moreover, *ex vivo* studies revealed that, in the presence of EGCG, the uptake of ovalbumin by monocytes proceeds at a slower rate. On a CD background, *Perot et al. (2017)* demonstrated that polyphenol-rich extracts from artichoke leaves, cranberries, apples, and green tea leaves are efficient modulators of the immunogenicity and allergenicity of gluten proteins, based on their ability to interact with gliadins, mask epitopes and impact basophil degranulation [273]. Therefore, it is becoming increasingly evident that the interaction of polyphenols with dietary proteins may hold promise as a novel therapeutic strategy capable of influencing multiple biological pathways and immune cell functions in human immune responses by sequestration and structural modification of immunostimulatory proteins or peptides. Although the interaction between polyphenols and proline-rich peptides has been demonstrated in previous reports, the structural and thermodynamic basis of polyphenol binding to CD relevant peptides remains poorly understood [236, 237]. Therefore, the main purpose of this study was to bring light into the likely mechanisms by which some widely prevalent food phenolics may interact with the immunodominant 32-mer peptide by means of different biophysical and *in silico* approaches at the intestinal level under near physiological conditions. Greater emphasis has been placed on EGCG and oligomeric procyanidins (*i.e.* procyanidin B3 and the trimer C2) due to their dietary abundance and because their poor intestinal absorption at the gastrointestinal tract allows them to achieve luminal concentrations up to several hundred millimoles thereby exerting local effects through interaction with food matrices and/or IEC [274, 275]. From a functional perspective, structural modification of the 32-

mer *via* interaction with dietary polyphenols may provide a groundwork for developing a nutraceutical approach for alleviating CD symptoms, by masking the binding sites and epitopes capable of being recognized by TG2 or HLA-DQ2. *In vitro* transepithelial transport assays using a Caco-2 cell line model were additionally performed to assess whether the association process described herein may interfere with the 32-mer bioavailability, potentially preventing the peptide from having any effect in the in the small intestine where CD is mostly active.

2. Material and methods

2.1. Reagents

The 32-mer and WQIPEQSR peptide (>95% purity), used as an internal standard in mass spectrometry experiments, were purchased from Synpeptide Co., Ltd (Beicai Pudong New Area, Shanghai, China). Epigallocatechin (EGC) and epigallocatechin gallate (EGCG) were purchased from Biopurify Phytochemicals Ltd. (Chengdu, Sichuan, China). Catechin (CAT) was purchased from Sigma-Aldrich. All polyphenols had >98% purity.

2.2. Procyanidin B3 and Procyanidin Trimer C2 Synthesis

Procyanidin dimer B3 and the trimer C2 were obtained by hemisynthesis using (+)-taxifolin and (+)-catechin, as described in the literature [276, 277]. Briefly, taxifolin and catechin (ratio1:2) were first dissolved in ethanol under argon atmosphere followed by dropwise addition of sodium borohydride. After 15 min under magnetic stirring, the pH was adjusted to 4.5 by slowly adding acetic acid/water 50% (v/v). Then, the reaction mixture was allowed to stand under argon atmosphere for 30 minutes, after which it was extracted with ethyl acetate and passed through reversed-phase C18 gel. The resulting fraction, was subsequently separated using a TSK Toyopearl HW-40(S) gel column (300 mm x 10 mm *i.d.*, with 0.8 $mL.min^{-1}$ of methanol as eluent) coupled to a *Gilson 115* UV-Vis detector (Gilson), yielding procyanidins with varying degrees of polymerization, as revealed by LC-MS analysis (*LTQ Orbitrap XL*, ThermoFisher Scientific). The fractions

containing procyanidin B3 ($[M-H]^-$ = 577) and the trimer C2 ($[M-H]^-$ = 865) were isolated and freeze-dried (purity higher than 95%).

2.3. Nuclear Magnetic Resonance (NMR) Spectroscopy

NMR samples were prepared immediately prior to analysis by dissolving 32-mer peptide in H_2O/D_2O (90/10, v/v) or, alternatively, in D_2O alone (99.9%, Sigma-Aldrich) to achieve a final peptide concentration between 0.05 and 0.1 mM. The ligands were added at increasing concentrations (0.1 - 3.0 mM) as a lyophilized powder, allowing the same NMR tube to be used for all experiments. Prior to titration, and after the addition of more polyphenol, the pH was adjusted to 7.4 by using sodium deuteroxide (99.5%, Euriso-Top) or deuterium chloride (99%, Sigma-Aldrich). pH measurements were made in a pH-meter *WTW pH 320* (Xylem Analytics) fitted with a standard glass *Crison 5209 electrode* (Crison Instruments SA). With the exception of *Saturation Transfer Difference (STD) NMR* experiments involving EGCG (which were performed on a *Bruker Avance III 400 MHz* spectrometer, equipped with a *5 mm PABBI ^{1}H/D-BB Z-GRD Probe*), most of the NMR spectra presented herein were acquired on a *Bruker Avance III 600 HD* instrument (Bruker), operating at a ^{1}H frequency of 600.13 MHz and equipped with a 5 mm *CPPBBO BB-^{1}H/^{19}F/D Z-GRD CryoProbe Prodigy* (Bruker). All measurements were performed with standard Bruker pulse sequences at either 5, 25 or 37 °C, depending on the purpose. The ^{1}H chemical shifts are given with respect to the methyl protons of tetramethylsilyl propionate (Sigma-Aldrich), which were arbitrarily set as 0 ppm.

One dimensional ^{1}H spectra were acquired with a shaped pulse to suppress the water resonance using the following parameters: spectral width, 16 ppm; shaped pulse duration, 2 ms; relaxation delay, 2 s; 90° nutation angle duration, 12.50 µs. For each individual spectrum, 384 scans were collected *per* FID which consisted of 32768 complex data points. Two-dimensional *Total Correlation Spectroscopy* (TOCSY) and *Nuclear Overhauser Effect Spectroscopy* (NOESY) spectra were acquired with a spectral width of 15 ppm in both dimensions (F1 and F2), 256 t_1 increments, 180 scans/t_1 increment in TOCSY and 128 scans/t_1 increment in NOESY, and a relaxation delay of 1.5 s. A contact time value of 80 ms was used for TOCSY experiments while the mixing times for NOESY spectroscopy ranged between 50 and 600 ms. To confirm the NOE correlations established between EGCG and the 32-mer peptide (obtained under optimized conditions), *1D selective gradient NOESY* experiments were additionally performed. These spectra were acquired with 256-512 scans at a mixing time of 600 ms.

STD NMR spectra were acquired using 50 ms Gaussian-shaped pulses for selective saturation of the 32-mer peptide with a total saturation time of 2.5 s, a relaxation delay of 3.5 s and a receptor gain value of 2050. The *on*-resonance irradiation of the 32-mer (at 0.05 mM), when titrated with procyanidin B3 and the trimer C2, was performed at -1 ppm while the *off*-resonance irradiation was set to 20 ppm. For these two polyphenols, the number of scans at each titration point was 96 (24 interleaved acquisitions at each on/off irradiation). Later, these parameters were further optimized, always ensuring that the *on*-resonance irradiation frequency would not overlap with ligand resonances but would fully saturate the 32-mer. Therefore, the STD NMR data for EGCG were collected with 180 scans (80 interleaved acquisitions at each *on*/*off* irradiation) using an *on*-resonance irradiation at 1.4 ppm. The STD effect for epitope mapping was determined using the amplification factor (A_{STD}) according to the following equation [278]:

$$A_{STD} = \frac{I_0 - I_{SAT}}{I_0} \times \frac{[L]}{[P]} = \frac{I_{STD}}{I_0} \times \frac{[L]}{[P]} \quad (1)$$

where I_{SAT} is the signal intensity of the selectively saturated 32-mer spectrum (*on*-resonance), and I_0 is the signal intensity of the spectrum recorded without peptide saturation (*off*-resonance). [L] is the ligand concentration and [P] is the 32-mer concentration. The binding epitopes on each polyphenol molecule were identified by the presence of ^{1}H signals in the difference spectra. The importance of each individual ^{1}H in each interaction was evaluated by comparing their relative degrees of saturation. All NMR data was processed and analyzed using Topspin 3.5 from Bruker. The tentative assignment of the 32-mer peptide ^{1}H signals, performed at 5 °C, was accomplished by using the CARA (*Computer Aided Resonance Assignment*) software to support the entire process of structure determination.

2.4. Circular Dichroism

Circular dichroism (CD) spectra were measured in the far-UV region on a Jasco J-815 spectropolarimeter accessorized with a pelitier temperature controller (Jasco). CD spectra were recorded using a quartz cell of 0.1 cm path length, an acquisition time of 2 s.nm^{-1}, with a 1 nm spectral bandwidth, over a wavelength range from 190 to 330 nm.

These experiments, meant to identify changes in the secondary structure of the 32-mer peptide at 5, 25 and 37 °C, were performed in 1 mM sodium citrate, 1 mM sodium borate, 1 mM sodium phosphate buffer and 15 mM NaCl at pH 7.4. The 32-mer peptide concentration was set at 0.1 mM. All spectra were averaged from 16 scans.

2.5. Isothermal Titration Calorimetry (ITC)

ITC experiments were conducted on a *VP MicroCal* (Malvern Instruments) at pH 7.4 and two different temperatures: 25 and 37 °C. Polyphenol solutions were prepared at a concentration of 10 mM and titrated into the stirred sample cell, containing the 32-mer peptide at 0.1 mM, as a sequence of 71 injections of 4 µL each. The duration of each injection was 8 s and the time delay (to allow equilibration) between injections was 550 s. The contents of the sample cell were stirred throughout the experiment at 307 rpm. Data acquisition was achieved with *VP Viewer software*. The signals corresponding to the dilution of polyphenols in water were recorded and subtracted from each interaction raw data. By use of the *AFFINImeter* software, raw data was integrated peak-by-peak and normalized to get a plot of observed enthalpy change *per* mole of injectant (ΔH) against polyphenol/32-mer molar ratio. The experimental data was fitted to a theoretical titration curve of two sets of independent sites, each with different binding strengths, in order to obtain the binding constant (*Ka*), the number of binding sites per molecule (*n*) and the thermodynamic parameters associated with each 32-mer:polyphenol interaction.

2.6. Fluorescence Quenching

For fluorescence quenching studies, the 32-mer tyrosine and phenylalanine aminoacid residues were used as intrinsic fluorophores using a *Horiba FluoroMax-4 spectrofluorometer* (Jobin-Yvon Instruments). The excitation wavelength was fixed at 275 nm while the emission spectra were recorded from 290 to 400 nm. Fluorescence experiments were performed by combining the 32-mer peptide at 0.1mM with different concentrations of individual polyphenols (from 0.01 to 0.05 mM) in PBS (10 mM phosphate buffer, 2.7 mM potassium chloride and 137 mM sodium chloride, pH 7.4). Then, the mixtures were allowed to equilibrate for 1h in a water bath with temperature control at 37 °C before measurements. Since polyphenols absorb some energy at the

excitation wavelength, a blank was made for each polyphenol concentration in which the peptide solution was replaced by PBS. The respective spectra were then automatically subtracted from the emission spectrum of the corresponding solution.

2.7. Dynamic Light Scattering

Light scattering measurements were performed on a *Zetasizer Nano ZS* (Malvern Instruments). In this device, the size of 32-mer:polyphenol aggregates were determined by illuminating the sample solutions with a 633 nm laser and the intensity of light scattered at an angle of 173° measured by an avalanche photodiode. Different volumes of polyphenol stock solutions, prepared in PBS, were mixed with a fixed volume of 32-mer to give a final peptide concentration of 0.1 mM and polyphenol concentrations ranging from 0.05 to 0.5 mM. The mixtures were allowed to react for 1h at 37 °C before being transferred to a DLS plastic disposable cell and analyzed.

2.8. Molecular Dynamics (MD) Simulations

Nine different model systems with one 32-mer peptide and three polyphenol molecules (EGCG, procyanidin B3 and procyanidin C2) were built (MD_1, MD_2 and MD_3 for each 32-mer:$(polyphenol)_3$ system. The polyphenol molecules were randomly placed around the peptide in different positions within each simulation to increase the sampling and structural variability. The initial geometry of the 32-mer peptide was obtained by homology modeling, using the *MODELLER* program. All polyphenol molecules were optimized at *HF/6-31G(d)* level of theory, and further parameterized using the antechamber tool with the *RESP* algorithm to get the atomic charges. The *Gaussian09* software package was used to perform these quantum calculations.

The Molecular Mechanics (MM) optimizations and MD simulations were performed using *GAFF* and *ff99SB* force fields for polyphenols and peptide, respectively. The solvation environment (explicit *TIP3P* water model) was included as a rectangular box with a 15 Å distance between the box edges and any atom within each system. The geometry of each 32-mer:$(polyphenol)_3$ complex was optimized in two stages. Firstly, only the position of water molecules was optimized (steepest descent algorithm for the first 500 cycles, and conjugate gradient algorithm for the last 1500 steps), and secondly,

the whole system was optimized (steepest descent algorithm for the first 3000 cycles, and conjugate gradient algorithm for the last 5000 steps). An equilibration MD simulation of 100 ps with the *NVT* ensemble, and using periodic boundaries conditions was performed. This was followed by 50 ns of production MD simulation with the *NPT* ensemble, in which *Langevin* dynamics was used (collision frequency of 1.0 ps^{-1}) to maintain the temperature at 37 °C. All MM calculations were carried out using the *AMBER 12.0* simulations package. The *SHAKE* algorithm was employed to constrain the bond lengths involving hydrogen atoms, and the equations of motion were integrated with a 2 fs time step using the *Verlet* leapfrog algorithm. The long-range interactions were considered by the *Particle-Mesh Ewald (PME)* method, and the non-bonded interactions were truncated with a 10 Å cutoff. The MD trajectories were saved every 8 ps and were analyzed with the *PTRAJ* and *CPPTRAJ* modules of *AMBER 12.0*.

2.9. Transepithelial Transport Studies

Caco-2 cells were grown in *Minimum Essential Medium Eagle* supplemented with 15% of fetal bovine serum, 100 $U.mL^{-1}$ penicillin, 100 $mg.mL^{-1}$ streptomycin and 0.25 $mg.mL^{-1}$ amphotericin B (all from Sigma-Aldrich) at 37°C in a humidified atmosphere containing 5% CO_2. For the transepithelial transport experiments, cells were plated on 12-well transwell inserts with 0.4 µm pore size (Corning Costar, Corning). Cells were allowed to grow and differentiate to confluent monolayers for 21 days after the initial seeding, during which the culture medium was changed every two days. Twenty-four hours before the experiments, the cells were serum-deprived. Only Caco-2 monolayers with an integrity equivalent to a transepithelial electrical resistance (TEER) higher than 200 $\Omega.cm^{-2}$ were used for the transport studies. Compound solutions in *Hanks' Balanced Salt Solution* pH 7.4, including the 32-mer peptide at 0.1 mM with and without polyphenols at either 0.3 mM (for EGCG) or 0.08 mM (for procyanidin B3 and the trimer C2), were added to the apical compartment of the cell monolayers. The chamber was incubated at 37 °C for 4 hours after which basolateral aliquots were taken for Nano LC-MS analysis.

Basolateral aliquots were analyzed on an UltiMate 3000 RSLCnano LC system coupled to an LTQ-Orbitrap XL mass spectrometer equipped with an EASY-nano spray source (Thermo Fisher Scientific). Prior to mass spectrometry analysis, samples were enriched with an internal standard, the WQIPEQSR peptide at 0.01 mM, and then cleaned-up to remove salts and other contaminants on C18 spin tips according to the manufacturer's instructions (ThermoFisher Scientific). An *EASY-spray PepMap C18* (15 cm x 75 µm, 3

μm particle size) was used in these analyses. Solvent A was 0.2% (v/v) formic acid in milli-Q water and solvent B 0.2% (v/v) formic acid in acetonitrile. The injection volume was 20 μL. The 32-mer peptide was eluted with a linear gradient of solvent B in A, from 5 to 50% in 14 min, 50 to 85% in 11 min and 85 to 90% in 2 min. The flow rate was 0.3 $\mu L.min^{-1}$. Electrospray conditions were set as follows: capillary temperature 280 °C, capillary voltage 12 V, source voltage 1.9 kV and tube lens 100 V. *Thermo Xcalibur 2.2* software was used to process the MS spectra. These experiments were repeated six times (n=6) for each treatment. Results were expressed as mean values ± standard error mean.

3. Results and Discussion

3.1. NMR spectroscopy

3.1.1. 32-mer peptide assignment

For resonance assignment of the 32-mer peptide, a set of two different experiments were recorded: TOCSY and NOESY. While TOCSY spectra (*Fig. 12*) allowed to partially identify the peptide spin systems by selecting the amide proton region (at approx. 7.8 - 8.6 ppm) in *F2* and the aliphatic region (0 - 5 ppm) in *F1* dimension, NOESY experiments were performed in an attempt to obtain inter-residue connectivities and to distinguish equivalent spin systems (*data not shown*). Nevertheless, due to a severe signal overlap on TOCSY spectra and because the NOESY spectroscopy presented very little information with few contact peaks in the NH-Hα region, it was not possible to achieve a complete and unequivocal proton assignment to their sequence-specific position. In fact, the 32-mer peptide primary structure contains a cluster of repeated aminoacid sequences that, when inserted in slightly different chemical environments, contribute to a high spectral complexity and compromise the unambiguous peptide resonance assignment.

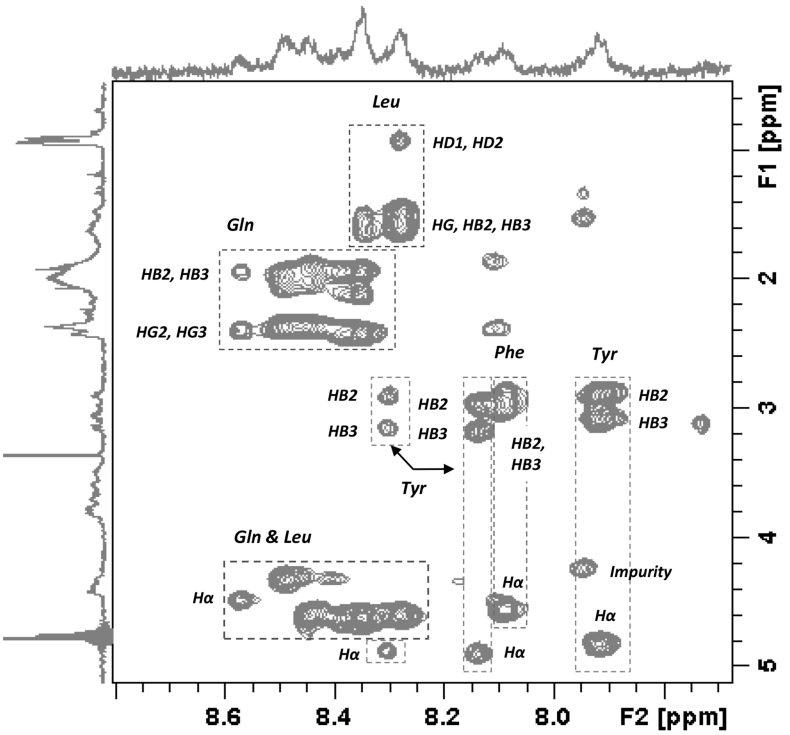

Fig. 12 - Segment of the 32-mer TOCSY spectrum (at 0.1 mM) recorded in H_2O/D_2O (90/10, v/v), pH 7.4, showing connectivities between the backbone amide resonances and α and side-chain proton resonances.

As each type of aminoacid gives a characteristic connectivity pattern in a TOCSY spectrum, coupled spin systems were extracted and readily identified as either tyrosine (Tyr), glutamine (Gln), proline (Pro), phenylalanine (Phe) and leucine (Leu) residues based on their chemical shift values and correlation patterns. Therefore, it was possible to define spectral areas within the *NH-Hα-δ* "fingerprint" region that are composed by equivalent spin systems (*Fig. 12*). For example, the glutamine residues were distinguished based on their characteristic distribution pattern for H_β and H_γ whereas the leucine spin systems had their unique δ-methyl protons at < 1 ppm. Proline has no amide protons. However, this aminoacid, which is the most represented elementary unit in the 32-mer peptide structure, displayed its characteristic pattern in the aliphatic region of the TOCSY spectrum (*Fig. 13A*). Both tyrosine and phenylalanine spin systems also had their characteristic signals in the aromatic region of the spectrum as well as the amine Hε protons corresponding to each of the glutamine side chains (*Fig. 13B*).

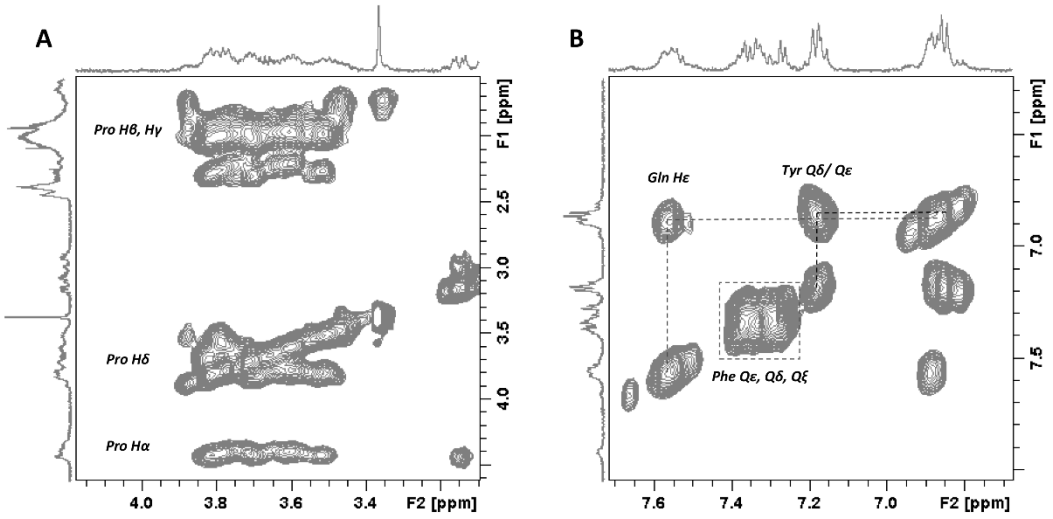

Fig. 13 - 32-mer TOCSY spectra (at 0.1 mM) recorded in H_2O/D_2O (90/10, v/v), pH 7.4; contour plot of the cross peaks region corresponding to the proline residues connectivity pattern (A) and to the aromatic Tyr, Phe and amine H_ε protons of glutamine side chains (B).

Apart from what was expected considering the primary sequence of the 32-mer peptide, a greater level of diversity was found in TOCSY spectra. Some aminoacids such as glutamines, were found to have different sets of chemical shifts, indicating that different chemical environments are experienced by these. On the other hand, three different tyrosine signals are observed, although only one environment is found in the primary sequence (-LP-Y-PQ-). The chemical shifts observed for the three tyrosine Hα were approximately 4.83, 4.88 and 4.90 ppm, respectively. Comparing these chemical shift values to the random coil values determined by *Wishart et al.* (1995) the H_α chemical shift of a tyrosine residue followed by a proline is 4.84 ppm [279]. Similarly, the Hα chemical shifts obtained for the glutamine spin systems range from 4.33 to 4.63 ppm which has to be compared with a predicted value of 4.34 ppm when followed by an alanine residue or 4.65 ppm when followed by a proline spin system. For the proline residues, their Hα showed analogous chemical shifts that range from 4.36 to 4.46 ppm. The random coil value for these nuclei, as measured in unstructured small peptides, is 4.42 ppm. For phenylalanine spin systems, the reference random coil value for the H_α is 4.90 ppm when followed by a proline. On the other hand, the experimental chemical shift obtained for the two overlapped phenylalanine residues was approximately 4.57 ppm. Even though we were not able to identify all the leucine spin systems in the 32-mer TOCSY spectra (they only appeared well differentiated when the measurements were

performed at 1 mM, 5°C), the H_α of a representative one appeared at a chemical shift of 4.61 ppm. According to the literature, the random coil value of this residue is 4.34 ppm when followed by an alanine or 4.63 ppm when followed by a proline residue. The deviation of H_α chemical shifts from random coil values provides some information concerning the peptide secondary structure [280]. Considering that almost all the aminoacid residues in the 32-mer peptide are interleaved by individual proline spin systems and considering that, in these conditions, the chemical deviations were very small, the data presented herein do not suggest any kind of local secondary structure. Therefore, it is likely that the 32-mer peptide adopts an alternative, possibly unfolded conformation at these conditions.

Early circular dichroism studies reported that the 32-mer peptide has a strong type II polyproline helical (PP II) conformation in solution [280, 281]. These structures have been shown to be important to its recognition by key receptors [282]. Experiments performed at both at 25 °C and 37°C showed that the 32-mer circular dichroic spectrum was consistent with a natively unfolded secondary structure as it presented a deep minimum in the range of 203 to 215 nm and molar ellipticity close to zero in the vicinity of 250 nm (*Fig. 14*). At these temperatures, it did not show any positive band in the region of 222-230 nm, as expected for PP II. Its absence reflects a higher extent of disorder of the 32-mer peptide compared to that of PPII structure, whose signature was only slightly observed at 4°C (*Fig. 14*).

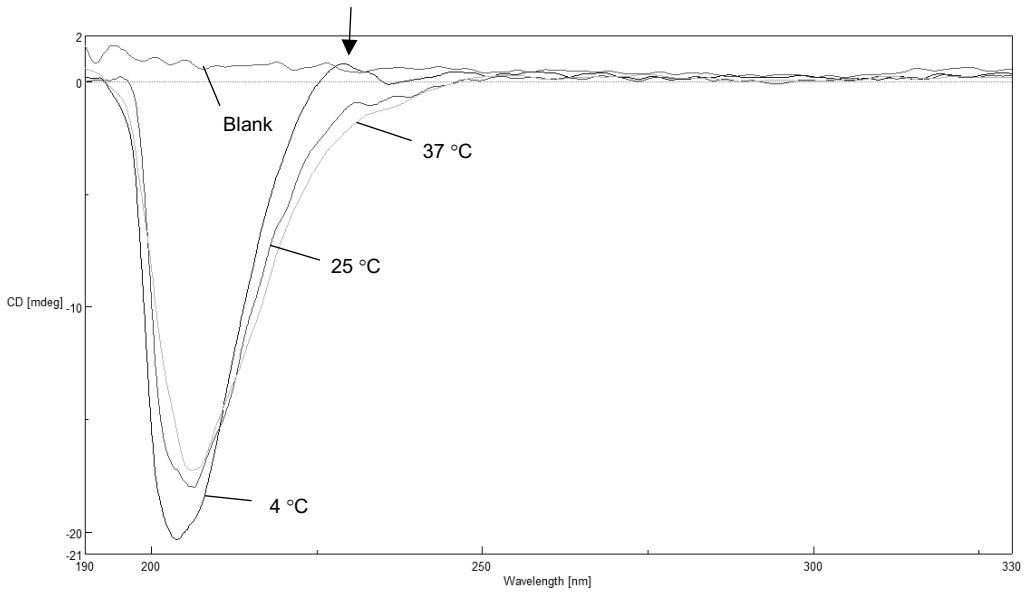

Fig. 14 - Circular dichroism spectra of 32-mer recorded at different temperatures in 1 mM sodium citrate, 1 mM sodium borate, 1 mM sodium phosphate buffer, 15 mM NaCl with pH adjusted to 7.4.

3.1.2. Titration experiments

The interaction between the 32-mer peptide and five structurally different flavanols and proanthocyanidins, including catechin, procyanidin B3, procyanidin C2, epigallocatechin (EGC) and EGCG, was monitored by following the ^{1}H chemical shift perturbations of the 32-mer when titrated with these polyphenols. As it can be seen from *Fig. 15*, concentration increments of catechin, procyanidin B3 and procyanidin C2 resulted in a progressive broadening, intensity decrease and ligand-dependent upfield chemical shift perturbations in most of the 32-mer peptide resonance signals, which suggests a non-specific, rather than specific, peptide binding dominated by either ring current effects and/or hydrogen bonding [283]. The same behavior was also observed for epigallocatechin and EGCG (*data not shown*). Of note, the physical state of both polyphenols and peptide molecules appeared to be dependent not only on their concentration ratio but also on the catechin or procyanidin involved. Accordingly, as the concentration of polyphenol increased, the 32-mer peptide solution, which on the beginning was crystal clear, became gradually more and more turbid until a point were precipitation of insoluble complexes, and consequent phase separation, occurred. This turbidity threshold, resulting from the presence in solution of numerous colloidal size peptide aggregates, was lower for both EGCG and procyanidin C2. These observations are in line with previous studies focusing on the interaction between polyphenols and proline-rich salivary proteins and peptides, most of which share structural similarities to the 32-mer peptide in terms of their natively unfolded conformation and high frequency of residues that have been implicated as preferential binding sites for polyphenolic interactions. The latter include aromatic and pyrrolidine ring structures, both of which are present in the 32-mer peptide in the form of 13 proline residues and 5 aromatic aminoacids. Therefore, approximately 56% of the 32-mer peptide aminoacids provide potential binding sites for polyphenols to attach, leading to an overall aromatic shielding effect driven by π-π stacking of polyphenolic rings onto planar hydrophobic surfaces. In general, the highest frequency shifts occurred in the *HN-H*α region. These changes are related to the higher sensitivity of the peptide backbone to the surrounding chemical environment and, in particular, on the existence of polar interactions with the solvent media or with specific functions of either the backbone or aminoacid side chains. Addition of polyphenols should interfere with this network, either by providing new hydrogen bonding acceptor and donor groups or by causing overarching conformational changes when bound.

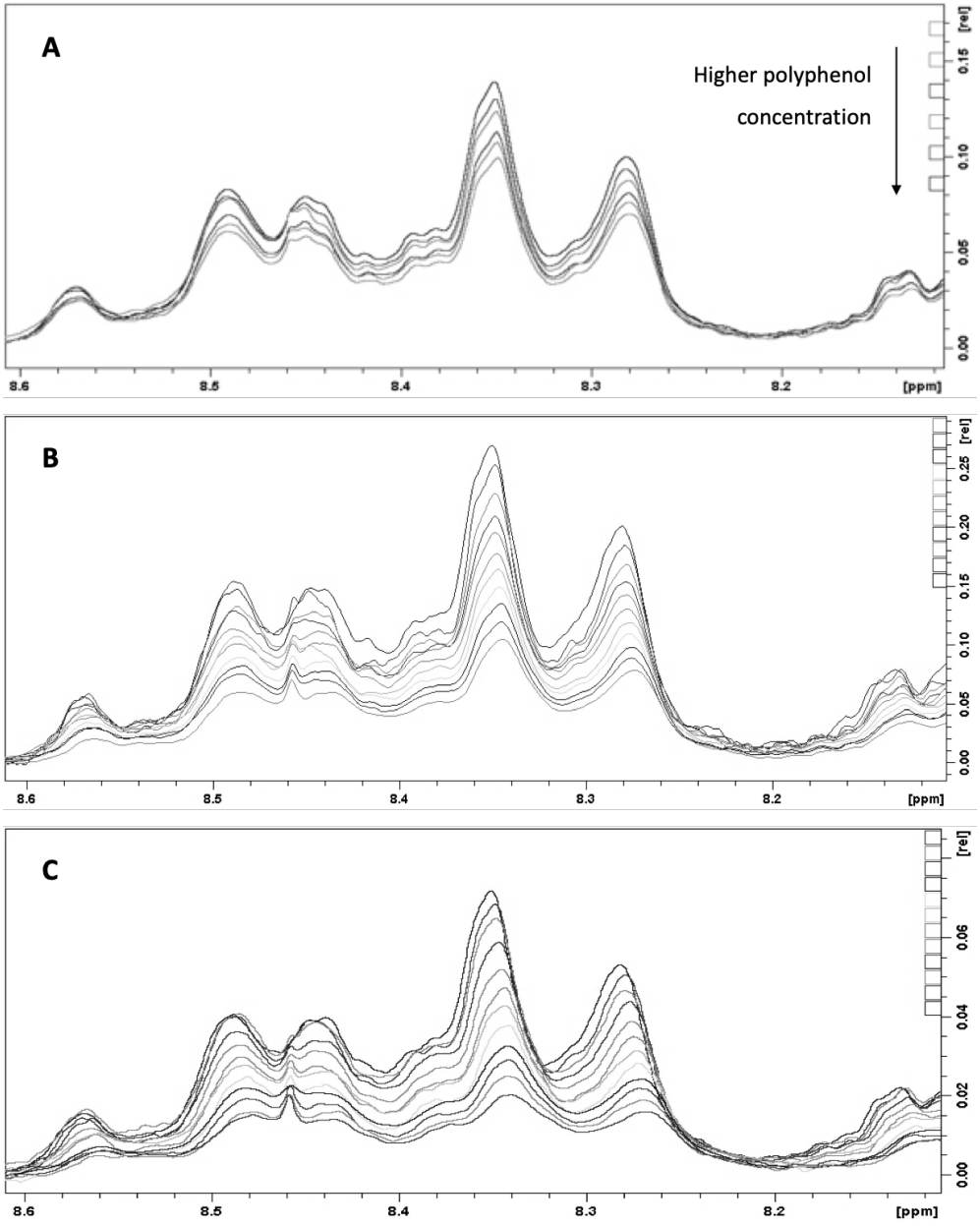

Fig. 15 - Chemical shift variations in the fingerprint region of the 32-mer peptide (at 0.1 mM) in the presence of increasing concentrations of catechin (A), procyanidin B3 (B) and procyanidin C2 (C) at 25 °C and pH 7.4.

Even though the observed chemical shift changes could not be isolated to specific aminoacid residues, they provided valuable insights regarding the areas within the 32-mer peptide that are structurally affected upon formation of polyphenol-peptide complexes. Interestingly, the most significant chemical shift perturbations involved both leucine and tyrosine ^{1}H resonances, with changes in their characteristic frequencies being noticed at substoichiometric amounts of ligand. At these polyphenol

concentrations, *i.e.* below 0.1 mM, most of the remaining peptide signals were unaffected, thus suggesting that leucine and tyrosine residues may constitute key elements of potentially hydrophobic interacting platforms to which polyphenols preferentially bind. This tendency was further confirmed by TOCSY experiments, which were extremely useful when following changes in the positions of highly overlapped signals (*Fig. 16*).

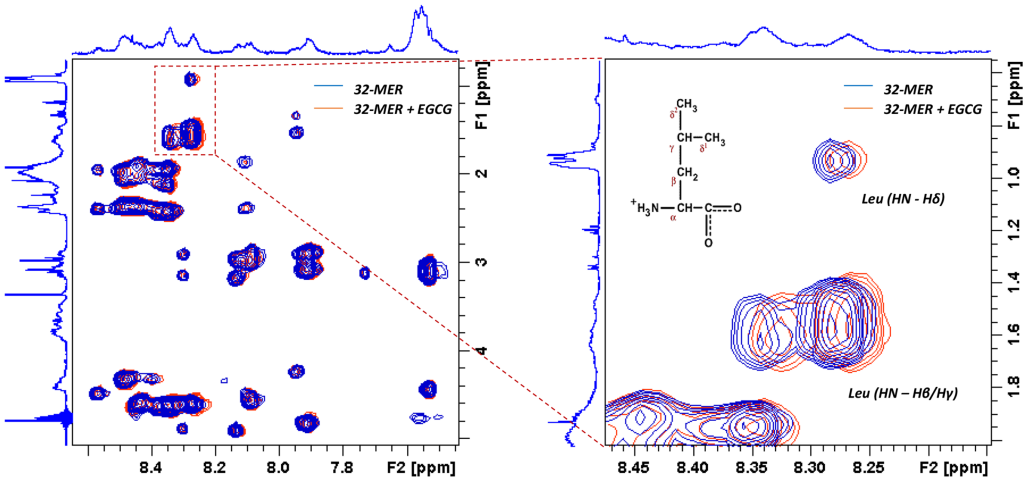

Fig. 16 - Comparison of the 32-mer TOCSY spectra (at 0.1 mM) before (in blue) and after (in orange) addition of EGCG (at 0.3 mM); contour plot of the crosspeaks region between HN and Hα, Hβ, Hδ or Hγ.

The existence of specific hydrophobic motifs within the 32-mer peptide was evaluated using *ProtoScale* tool of EXPASY. This program allows the user to compute and represent the hydrophobicity or hydrophilicity profile of any peptide or protein along its aminoacid sequence according to predefined scales that consider different chemical and physical properties. Herein the *Kyte-Doolittle* method was employed to determine the average hydropathy within a segment of predetermined length as it advances through the 32-mer peptide sequence [284]. These calculations are based on a combination of experimental observations derived from the literature and depend not only on the free energy of transfer (ΔG_{trans°) of the solute aminoacids between water and condensed vapor phase but also on the interior-exterior distribution of aminoacid side-chains determined by *Chothia et al.* in 1976 to assign the final hydropathy values that are not more than a measure of how the 32-mer aminoacid side-chains interact with water [285]. To calculate the hydropathy index of the 32-mer peptide, the individual hydropathy

values for an arbitrary number of 3 amino acids residues were averaged starting at the N-terminus. These stretches of aminoacids, or windows, shifted by one amino acid and the individual hydropathy scores continued to be averaged for each window until the end of the 32-mer peptide was reached. By plotting the normalized hydropathic index versus the position of the different amino acid residues in the 32-mer sequence it was possible to represent graphically where the hydrophobic and hydrophilic regions of the 32-mer are located (*Fig. 17*).

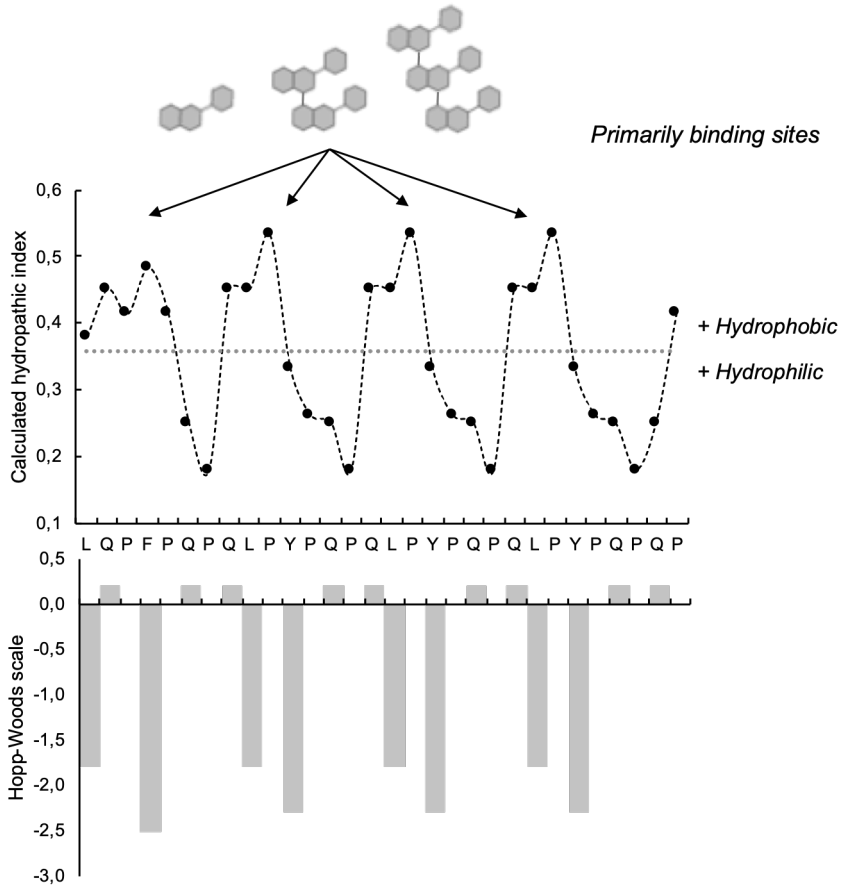

Fig. 17 - *Kyte-Doolittle* hydropathy profile of the 32-mer peptide sequence considering a window size of 3 aminoacid residues. The hydropathicity index and *Hopp-Woods* hydrophilicity scale were calculated using the *ProtoScale* tool of EXPASY. According to the 1D and 2D NMR data, the peptide domains containing both leucine, tyrosine and possibly phenylalanine aminoacid residues, and therefore of higher hydrophobicity, should be the primarily polyphenol binding sites in the 32-mer peptide.

As it can be seen from *Fig. 17*, both leucine, tyrosine and phenylalanine residues are located in four well-defined and almost indistinguishable hydrophobic clusters, equally spaced by non-polar proline residues. These sites are most likely the primary binding

surfaces to which the added polyphenols will initially bind, with more or less affinity depending on their structure and complementarity. Accordingly, when the polymerization degree increased from catechin to the procyanidin trimer C2 or even upon galloylation, these structural changes led to a proportional variation in the magnitude of the observed chemical shift perturbations (*Fig. 18*).

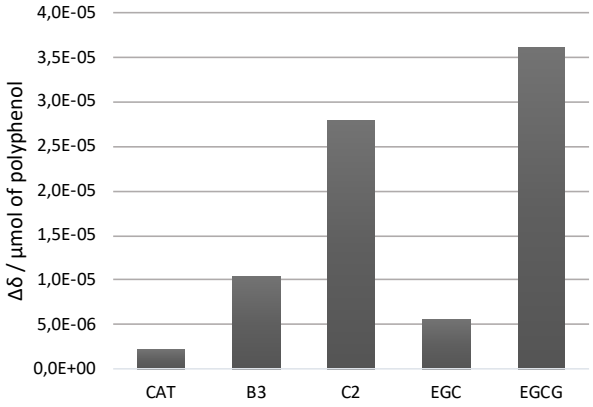

Fig. 18 - Polyphenol-induced chemical shift perturbations on a leucine ^{1}H-N signal per micromole of either catechin (CAT), procyanidin B3, procyanidin C2, epigallocatechin and EGCG at 25 °C and pH 7.4.

A similar trend was also observed when following the 32-mer peptide-polyphenol aggregation/precipitation throughout the titration experiments. To do so, the area corresponding to the H_{δ} leucine residues region was integrated while the area of the internal reference TSP was used to calibrate the intensity from one spectrum to another. Through these calculations, it was possible to determine the percentage of peptide remaining in solution at each titration point (*Fig. 19*). Again, while EGCG and the trimer C2 appeared to be the most reactive towards the 32-mer peptide in a low tannin concentration window (*Fig. 19A*), for procyanidin B3, changes in peptide solubility only started to be noticed from 1 mM onwards (*Fig. 19B*).

In the last years, many works in the literature have highlighted the strong influence of the polyphenol structure (hydroxylation degree, size, conformation, flexibility and others) on the interaction with proteins and peptides [177]. In general, the affinity of proanthocyanidins for proteins increases with their molecular weight and galloylation degree apparently because the number of aromatic moieties and hydroxyl groups available for non-covalent interactions increase with size. This behavior seems to be independent of the protein structure and may explain the differences observed during titration of the 32-mer peptide with catechin, procyanidin B3 and procyanidin C2. On the

other hand, it has been demonstrated that the tannin 3D structure has an important effect on its colloidal behavior and ability to interact and precipitate proline-rich proteins and peptides [286, 287]. It thus appears that the more the phenolic moieties are exposed and available for interaction in an extended conformation, the higher the affinity. Therefore, contrary to trimer C2 that preferentially adopt an extended conformation, that is, a conformation in which phenol rings are free of intramolecular stacking, procyanidin B3 adopts mainly a "compact" conformation meaning that the two phenol rings B and E are already involved in intramolecular π-π stacking. As a consequence, the dimer B3 has a significantly lower affinity towards the 32-mer and needs a higher tannin concentration for peptide precipitation to occur (*Fig. 19B*). In the case of EGCG, the hydroxylation pattern of ring B and the additional gallate group, when compared to epigallocatechin, appears to be critical for its distinguished kinetics (and thermodynamic) binding profile.

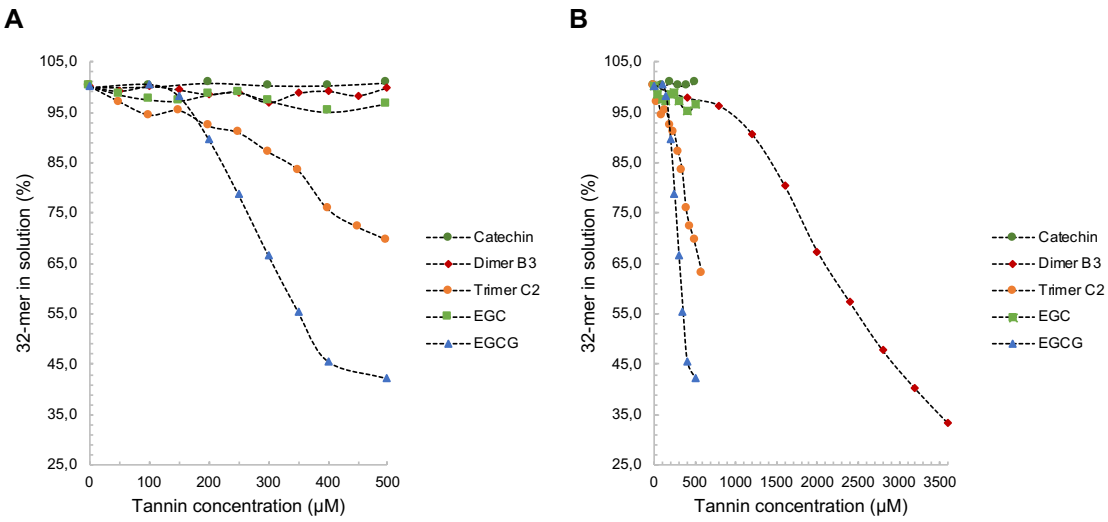

Fig. 19 - Variation of peptide solubility at 25 °C as a function of polyphenol concentration in a low (A) and high concentration range (B).

Epitope mapping by STD NMR

STD NMR is a pseudo-2D experiment in which a receptor is selectively irradiated to obtain structural information regarding the parts of the ligand that are in close contact with him (≤ 5 Å) [288]. This method allows for semi-quantitative characterization of binding epitopes on ligands through calculation of the relative degree of saturation of

each proton involved in the interaction. To assess whether it could be applied in a system composed by the 32-mer peptide as a receptor and food tannins as ligands, we have conducted some preliminary assays in which the 32-mer peptide (at 0.05 mM) was placed in the presence of different concentrations of EGCG, procyanidin B3 and procyanidin C2. To confirm that the *on*-resonance irradiation frequency did not overlap with the ^{1}H signals of polyphenols and that the 32-mer peptide was fully saturated, some additional experiments were performed at higher polyphenol concentrations. Starting on EGCG alone, for example, no ^{1}H signals were visible on the difference spectra when the *on*-resonance irradiation was performed at 1.4 ppm (*Fig. 20A*). Nevertheless, when mixed with the 32-mer peptide, irradiation at the leucine aliphatic protons resulted in a selective magnetization transfer to EGCG, thus providing a clear indication that a peptide-EGCG interaction took place.

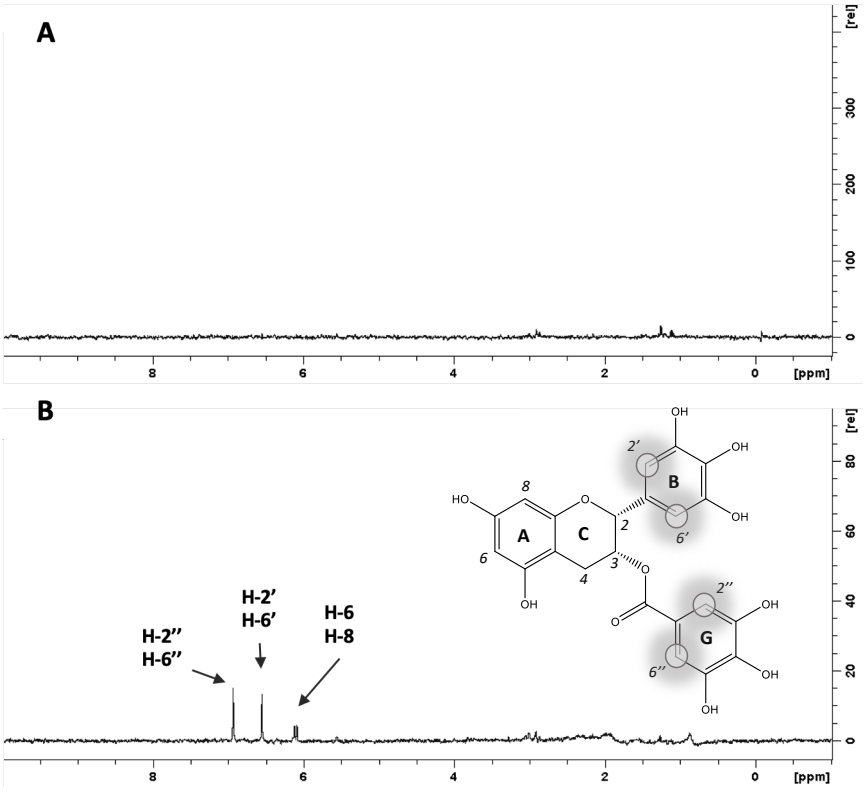

Fig. 20 - STD NMR spectra recorded in D_2O at pH 7.4 for 0.5 mM of EGCG (A) and a mixture of 0.3 mM EGCG and 0.05 mM 32-mer peptide (B). The most important binding epitopes were identified by shaded circles. These preliminary assays confirmed the occurrence of a STD effect between the 32-mer peptide and the bound EGCG molecules and that the *on*-resonance irradiation frequency does not overlap with EGCG resonances.

The localization of more intense STD signals within the structure of EGCG suggest the possibility of preferential binding or interaction specificity (Fig. 20B). By comparison of the overall saturation of each ring constituent of EGCG, the B- and G-ring ^{1}H signals showed the highest STD amplification with no significant difference between one another. On the contrary, the hydrogens on the A-ring showed a lesser degree of saturation than those of the B- and G-rings, suggesting further distance from the peptide and a lesser role in the overall interaction. No STD signal was detected on C-ring. Taken together, these results suggest the importance of the EGCG's gallate and galloyl moieties with respect to interaction with the 32-mer peptide while the A- and C-ring hydrogens are more likely to be affected by steric hindrance and play a less meaningful role on binding (*Fig. 20*). As was done for EGCG, STD NMR spectroscopy was also used to characterize the interaction between the 32-mer peptide and procyanidins B3 and C2. The selectivity of the *on*-resonance irradiation frequency was, again, confirmed by performing a couple of control experiments at high tannin concentrations (*Fig. 21*).

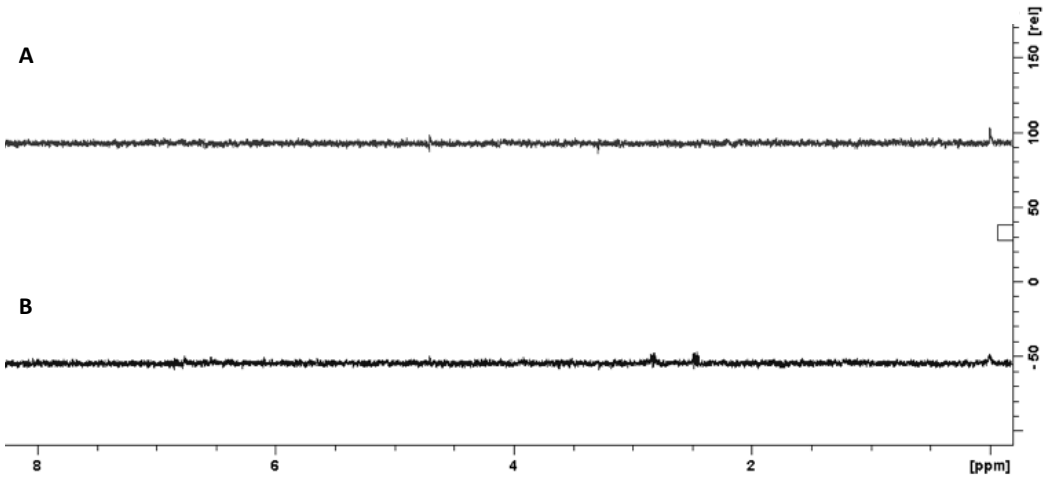

Fig. 21 - Control STD NMR spectra of 1 mM procyanidin B3 (A) and the trimer C2 (B), recorded in D_2O at pH 7.4. These preliminary assays confirmed that the *on*-resonance irradiation frequency at -1 ppm does not overlap with any of polyphenol's resonances.

The STD NMR spectra of procyanidin B3 and the trimer C2 are displayed in *Fig. 22A* and *Fig. 22B*, respectively, as well as the structural moieties that have been identified as being closer to the 32-mer peptide.

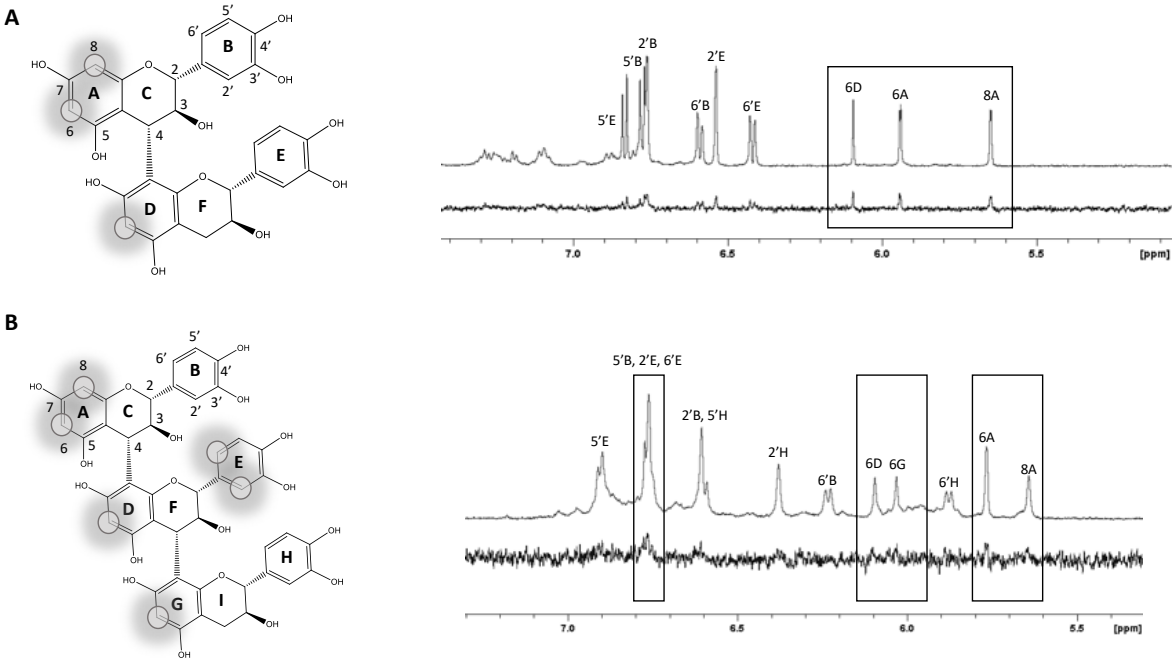

Fig. 22 - (A) Left: chemical structure of procyanidin B3 and identification of the main binding epitopes as evidenced by STD-NMR; Right: STD spectrum for the interaction of procyanidin B3 (0.6 mM) with the 32-mer peptide (0.05 mM). (B) Left: chemical structure of procyanidin C2 and identification of the most important binding epitopes as reveled by both STD (and NOESY) experiments; Right: STD spectrum for the interaction of procyanidin C2 (0.3 mM) with the 32-mer peptide (0.05 mM).

For procyanidin B3, the phloroglucinol A- and D-ring were the ones that elicited a higher STD response which indicates that they should be in close spatial proximity to the 32-mer peptide. Although to a lesser extent, the catechol protons of rings B and E were also amplified (*Fig. 22A*). For procyanidin C2, the observed STD effect was less pronounced than for procyanidin B3, probably because of its lower dissociation rate (very slow k_{off}) and higher affinity (*Fig. 22B*). This behavior leads to a less efficient non-scalar magnetization transfer from the bound to the free tannin molecules. Despite this technical limitation, the procyanidin C2 moieties involved in the interaction with the 32-mer peptide were evidenced: the STD-NMR spectra of *Fig. 22B* shows that the phloroglucinol rings A, D, G, and the catechol $H_{2'E}/H_{6'E}$ are the most important binding epitopes.

Of note, the application of STD NMR as an analytical tool to monitor small ligand binding to low molecular weight peptide receptors is not usual. Typically, due to their size, medium to high molecular weight proteins often show long correlation times (τ_c), highly efficient spin diffusion and fast cross-relaxation mechanisms. These features allow not only the *on*-resonance magnetic saturation to spread over the entire protein but also

the non-scalar magnetization transfer to bound ligands, when they are part of this high molecular weight system [289]. In fact, the larger the target, the more favorable the conditions for the STD NMR experiment. In these particular cases, however, the situation is a little bit more complex. If on the one hand it would be expected the 32-mer R_2 relaxation rate to be insufficient for the intramolecular spreading of the saturation and the intermolecular transfer to the ligand, we believe that the observed STD effect results from a peptide oligomerization induced by the presence of highly reactive polyphenols. Therefore, the dynamic cross-link of peptide units mediated by multidentate polyphenols may lead to the formation of high molecular weight complexes with slower molecular tumbling. EGCG, among other polyphenols, may also act as a viscosity enhancing reagent and therefore amplify magnetic saturation and transfer.

3.1.3. 1D and 2D NOESY

When ligand molecules bind to receptor proteins or peptides, the sign and size of the *Nuclear Overhauser Effect* (NOE) cross relaxation between protons of the ligand undergo drastic changes leading to the observation of *transferred NOEs* (*trNOEs*) [290]. These changes are the basis for a variety of experimental schemes that are designed to detect and characterize binding activity. The 2D NOESY spectrum of a mixture containing the 32-mer peptide and EGCG, at a molar ratio of 1:3, was analyzed for the presence of inter- and intra-molecular *NOEs* in an attempt to determine the orientation and bound conformation of the EGCG molecules within the 32-mer peptide binding sites. Several mixing times, ranging from 50 to 600 ms, were assayed in order to resolve and differentiate the EGCG-peptide *NOE* effect from background noise. As the best results were obtained for a mixing time of 600 ms, only the NOESY experiments acquired under this condition will be presented and discussed. In these, EGCG alone exhibited positive NOE enhancements, a feature that is consistent with low-molecular-weight molecules with short tumbling times (τ_c). Some intramolecular NOE correlations were observed for EGCG, indicating a close proximity between the $H_{2',6'}$, H_2, H_3 and H_4 protons (*Fig. 23A*).

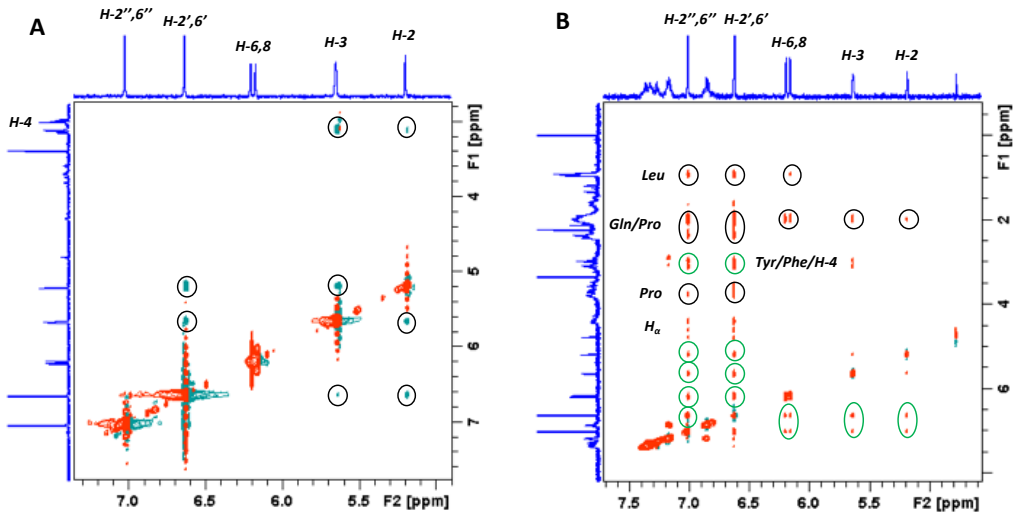

Fig. 23 - Comparison of the EGCG NOESY spectra (at 0.3 mM) before (A) and after (B) addition of the 32-mer peptide (0.1 mM). In (B), the intermolecular *NOEs* are highlighted in continuous circumferences and the intramolecular *NOEs* emphasized in dashed circumferences.

When EGCG bound to the 32-mer peptide, it behaved as a part of this bigger macromolecule and adopted the corresponding NOE, that is negative (*Fig. 23B*). In general, one can observe inter- and intramolecular *NOEs*. The establishment of new and negative intramolecular NOE cross-peaks between protons belonging to EGCG appears to indicate that when it interacts with the 32-mer peptide, some structural rearrangements or aromatic stacking may occur, leading to dipolar cross-relaxation events between protons that become spatially close to one another within the supramolecular EGCG-peptide aggregates. Intermolecular *NOEs* were also observed and involved mainly the $H_{2''}$ and $H_{6''}$ of the galloyl group as well as the $H_{2'}$ and $H_{6'}$ of B-ring. These results are in agreement with those of STD NMR, highlighting the structural relevance of both B- and G-ring of EGCG when interacting with the 32-mer peptide. On the peptide point of view, based on the established NOE correlations, it is possible to conclude that EGCG binding to the 32-mer peptide, at a 1:3 ratio, is mainly non-specific since it involves the sidechains of most aminoacid residues (*Fig. 23B*). These 2D NOESY experiments were further supported by 1D selective gradient NOESY in which several peptide and ligand proton resonances were irradiated and the corresponding NOE signals integrated.

The interaction between the procyanidin trimer C2 and the 32-mer was also studied by means of NOESY measurements. Together with EGCG, procyanidin C2 was one of the most reactive polyphenols towards the 32-mer peptide (*Fig. 18* and *Fig. 19*). Several

NOE cross-peaks between the 32-mer and procyanidin trimer C2 were detected with wide-ranging intensities; these provided qualitative deductions about relative distances (*Fig. 24A-D*).

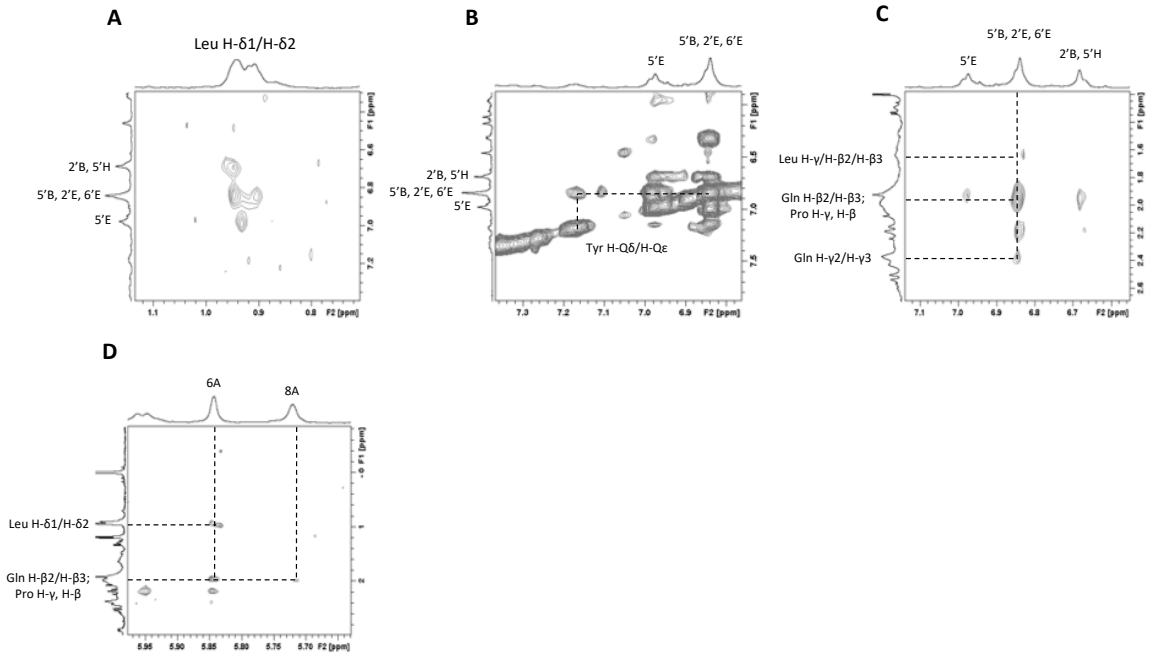

Fig. 24 - NOESY spectra relative to the interaction between procyanidin trimer C2 (at 0.3 mM) and the 32-mer peptide (at 0.1 mM). (A) Medium intensity NOE correlations between leucine's side-chains and the catechol moieties of procyanidin C2; (B) Strong intensity NOE correlation between tyrosine's side-chain and the catechol E ring of procyanidin C2; (C) Medium intensity NOE correlations between leucine, glutamine and proline side-chains with the catechol moieties of procyanidin C2; (D) Weak intensity NOE correlations between leucine, glutamine and proline side-chains with the phloroglucinol A protons of procyanidin C2.

According to *Fig. 24*, the catechol protons of B-, E- and H-rings of trimer C2 and leucine $H_{\delta1}/H_{\delta2}$ sidechain protons were in close spatial proximity (*Fig. 24A*) as well as the catechol E moiety and tyrosine $H_{Q\delta}/H_{Q\varepsilon}$ aromatic protons (*Fig. 24B*). Of note, these results corroborate the distribution profile of the chemical shift perturbations induced by procyanidin C2 on the local magnetic environment of the 32-mer backbone amides. It presupposes the establishment of thermodynamically favored hydrophobic clusters involving the aforementioned leucine and tyrosine-rich peptide domains and the catechol groups of trimer C2 through van der Waals contacts and π-π staking interactions (*Fig. 17*). The fact that the intermolecular NOEs involved these same protons suggests that the chemical shift changes were directly brought by binding interaction. Medium-to-weak

intensity NOE correlations were also observed between the catechol protons $H_{2'E}/H_{6'E}/H_{5'B}$ and the aliphatic sections of glutamine or proline side-chains (mainly the H_{δ}) (*Fig. 24C*). Rings B and H, on the other hand, produced weak NOE signals as well as the heterocyclic protons of rings C, F and I (*data not shown*). In such cases, the severe signal overlap within the 32-mer peptide sequence and the trimer itself made it difficult to distinguish the precise aminoacid residue and procyanidin moieties that are close to each other in the complex. Lastly, the phloroglucinol H_{6A} had very weak intermolecular NOE cross-peaks with the 32-mer peptide (they were almost in the background noise level) (*Fig. 24D*), while for protons H_{8A}, H_{6D} and H_{6G} no NOEs were detected.

Concerning the conformation of the procyanidin trimer C2 when complexed with the 32-mer peptide, the occurrence of some important intramolecular NOE correlations made it possible to postulate the most likely orientation of each catechin unit towards the neighboring ones (*Fig. 22B* and *Fig. 25*).

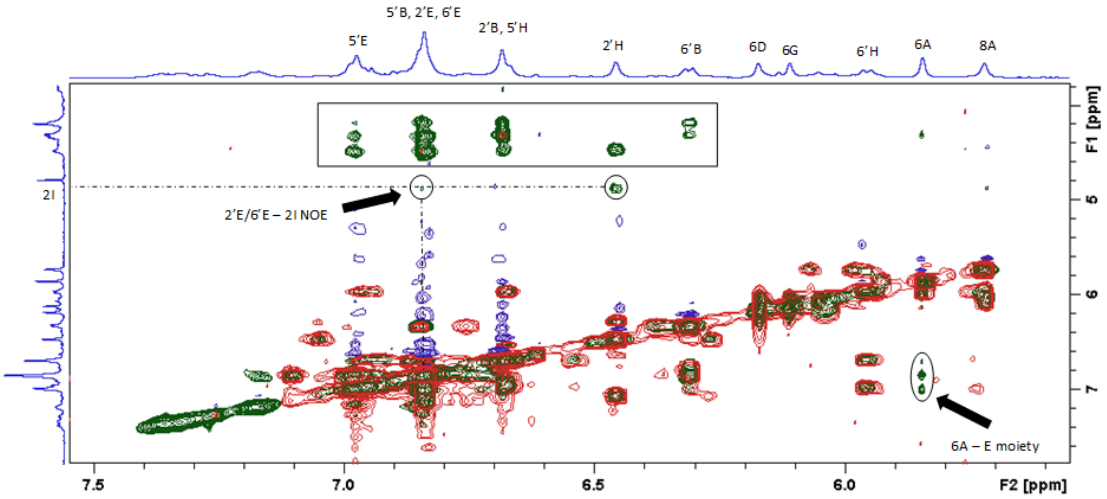

Fig. 25 - Identification of the main intramolecular NOE correlations of procyanidin C2 when complexed with the 32-mer peptide. Red: NOESY spectrum of procyanidin C2 at 0.3 mM; Green: NOESY spectrum of procyanidin C2 in the presence of 32-mer (0.05 mM).

When bound to the 32-mer, there was a strong NOE signal between H_{6A} and $H_{2'E}/H_{6'E}/H_{5'E}$, which indicated that the catechol E ring was spatially close to the phloroglucinol ring A. These moieties were, on the other hand, orientated towards the hydrophobic side-chains of tyrosine and leucine aminoacid residues and as such they experienced a considerable STD amplification (*Fig. 22B*). The last catechin unit of trimer C2 should have its catechol moiety orientated in the same direction as the middle one

due to the occurrence of two major NOE correlations: between $H_{5'E}$ and $H_{6'H}$ s well as between $H_{2'E}$/$H_{6'E}$ and H_{I2} (weak intensity) (*Fig. 25*). Overall, these NMR experiments suggested that upon binding to the 32-mer peptide, there was a conformational transition of the trimer C2 into a complex that was energetically more favorable by reducing the exposure of local hydrophobic moieties to the surrounding aqueous environment. It is important to highlight that the proposed molecule orientation is probably just one possibility among many others due to the high complexity of this kind of supramolecular systems and the fact that trimer C2 may act as a highly flexible and multivalent ligand [291]. The same for EGCG and most probably for procyanidin B3. Also, the role of proline residues on polyphenol binding should not be overlooked. Even though its involvement could not be assessed by NMR due to the severe signal overlap of its H_α protons and close proximity to water resonance, these residues are considered to be good binding sites, since they provide an open, flat, rigid, hydrophobic surface favorable for the association with other flat, hydrophobic functions, such as aromatic rings [292]. It has also been shown that the tertiary amide function, which is present in proline, has a more favorable enthalpy of binding to zwitterionic groups than do secondary amides due to the poorer solvation of the tertiary amide group [293]. Therefore, when a ligand binds to proline, it requires the breaking of fewer solvating hydrogen bonds in comparison to binding to the secondary amide functions. A smaller positive change in enthalpy will thus occur, making this binding reaction more favorable. In addition, the methylene substituents of the tertiary nitrogen function donate electrons into the peptide bond causing it to be electron-rich. The carbonyl function is thus an enhanced hydrogen-bond acceptor, further implying that the amide bond preceding proline may be expected to be important for binding. All in all, these NMR data were used in conjunction with findings from ITC to define the stochiometric characteristics of the interaction based on available interaction sites within the structures of each reactant.

3.2. ITC Experiments

The heats of interaction between the 32-mer peptide and EGCG, procyanidin B3 and the trimer C2 were determined at 25 and 37 °C using ITC. All the binding isotherms had a clear measurable change in enthalpy (ΔH) and showed evidence that the 32-mer peptide contains multiple polyphenol binding sites, resulting in a cooperative, multiphasic reaction. *Figure 26A* shows the typical titration for the interaction of EGCG with the 32-

mer peptide, performed in water at pH 7.4 and 25 °C. While the complexation between these two partners in solution appeared to be mainly exothermic (second wave of negative peaks in the ITC output), the obtained isotherm demonstrated a complex reaction of both endothermic and exothermic responses. Accordingly, for the first few EGCG injections, heat absorption (endothermic) phenomena can be attributed to EGCG dilution or stacks disruption. The subsequent heat release (exothermic peaks) arose from solvent mismatches between the syringe and the cell sample thus causing those artifact peaks to appear in the first part of the thermogram. This hypothesis was later confirmed by performing control experiments in which EGCG was injected in water with pH adjusted to 7.4 (*Fig. 26B*). Energy absorption due ECGC dissociation was also evidenced during the last injections. *Figure 27* represents the enthalpy change profile *per* mole of injectant against EGCG:peptide molar ratio. Two phases were observed during EGCG titration resulting in an "*inverted bell*" curve: at the beginning, and until the EGCG:peptide molar ratio reached a value around 5, there was a relatively sharp decrease of ΔH with each injection; then, the binding isotherm presented a sigmoid shape as if site saturation had been reached so that addition of more EGCG molecules led to a plateau. Contrary to procyanidin B3, whose interaction with the 32-mer peptide produced a sigmoidal curve (*Fig. 28*), for procyanidin C2 the behavior was very similar to the one obtained for EGCG (*Fig. 29*). The absence of an endothermic response in the latter case may be related to the higher *critical micelle concentration* "CMC" value for procyanidin C2 when compared to EGCG (15 mM vs 6 mM, respectively) [294]. The ability of polyphenols to self-associate in aqueous solution, leading to the formation of colloids, has already been shown in previous studies and is an important factor to take into account when studying polyphenol-protein interactions since they may affect the number of available polyphenol binding sites [177].

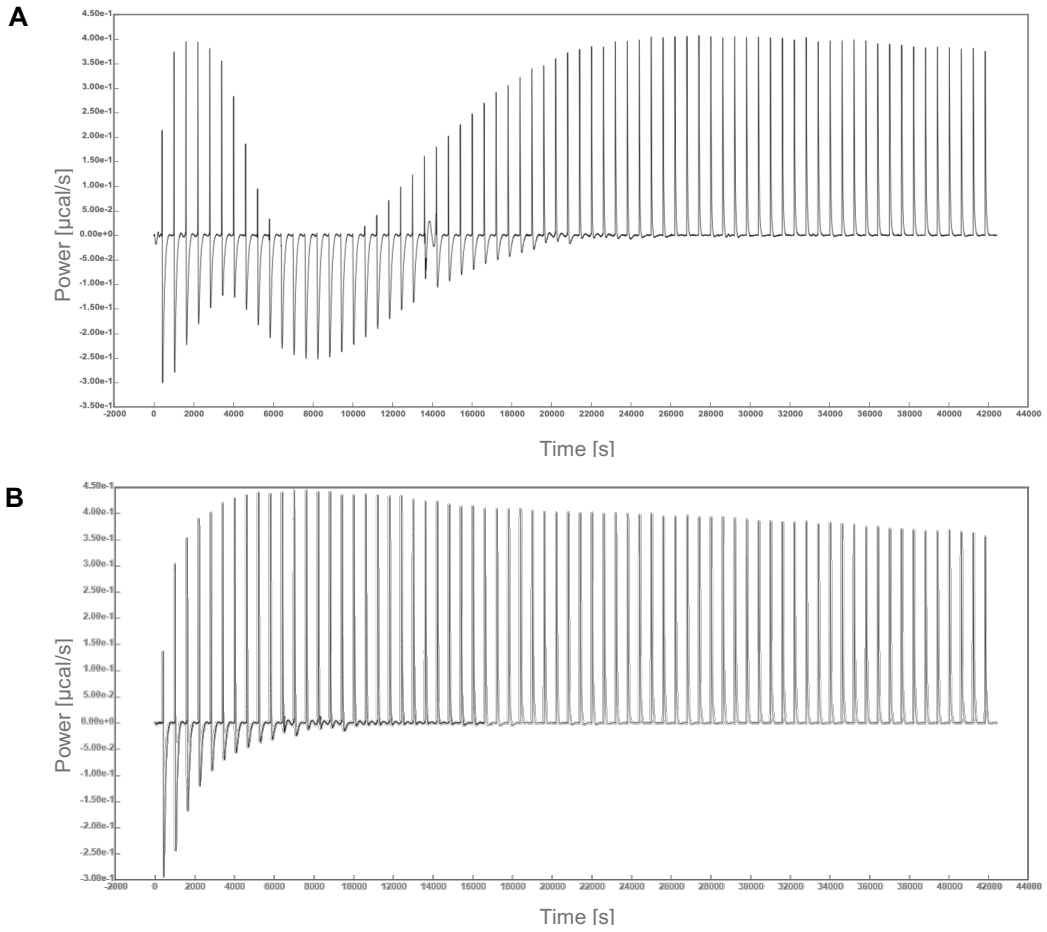

Fig. 26 - Raw data obtained over a series of injections of EGCG (at 10 mM) into 0.1 mM of 32-mer peptide in water, pH 7.4, at 25 °C (A). EGCG titration in water (B) yielded weak endothermic responses, which were later subtracted from (A).

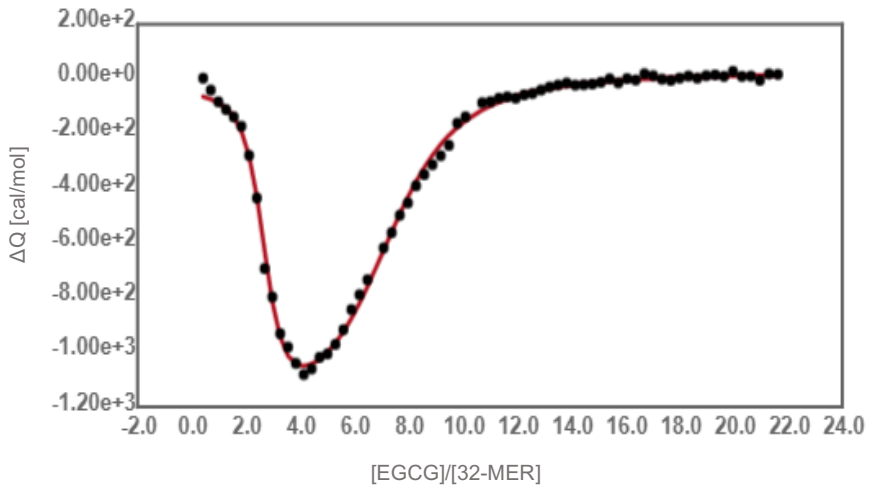

Fig. 27 - Binding isotherm created by plotting the areas under the peaks in *Fig. 26A* (after blank subtraction) against the molar ratio of EGCG injected. The best-fit curve, obtained by using a two sets of independent binding site model, is displayed as a red line.

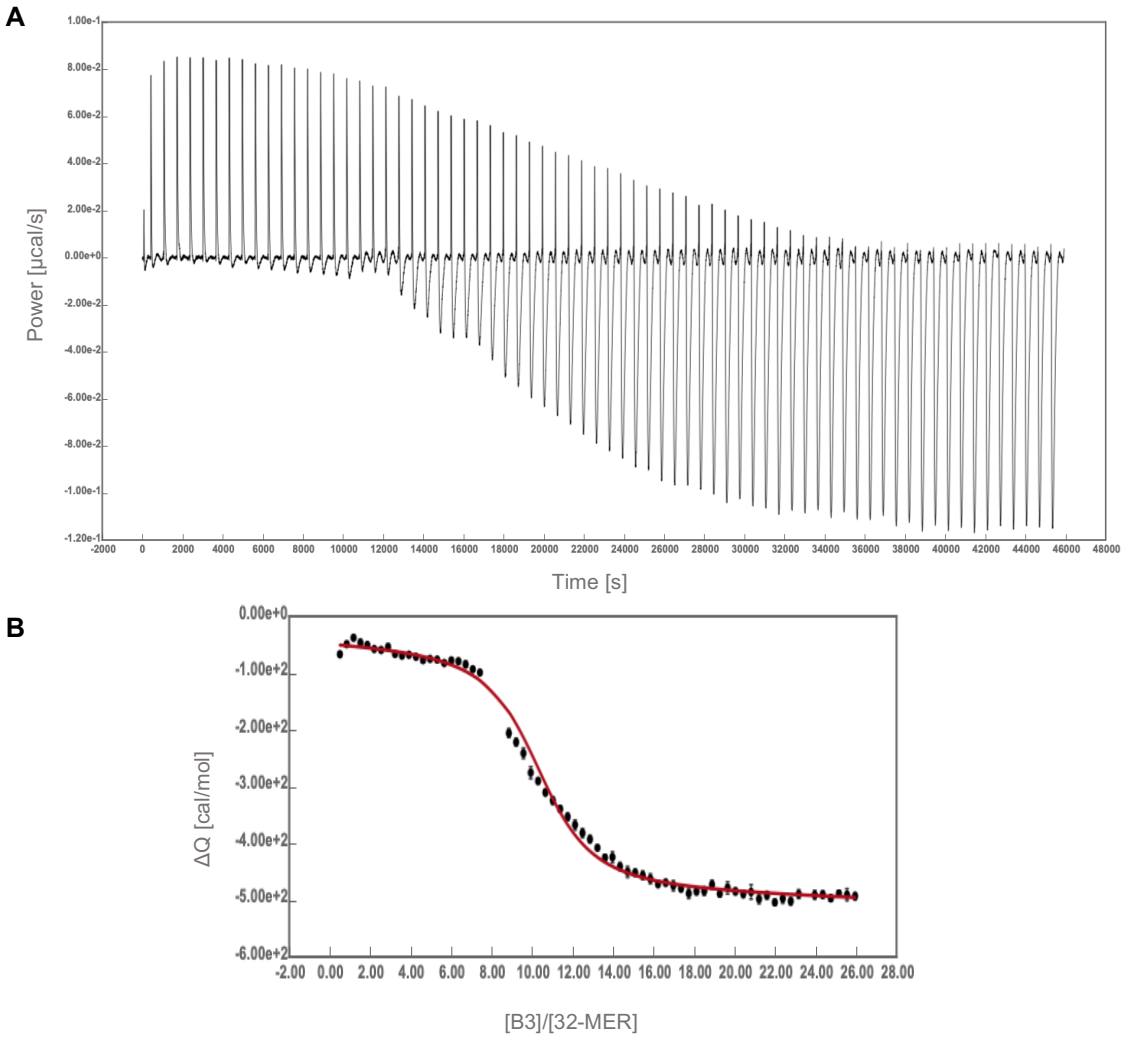

Fig. 28 - (A) Raw data obtained over a series of injections of procyanidin B3 (at 12 mM) into 0.1 mM of 32-mer peptide in water, pH 7.4, at 25 °C; (B) Binding isotherm created by plotting the areas under the peaks (after blank subtraction) against the molar ratio of procyanidin B3 injected. The best-fit curve, obtained by using a one-site binding model, is displayed as a red line.

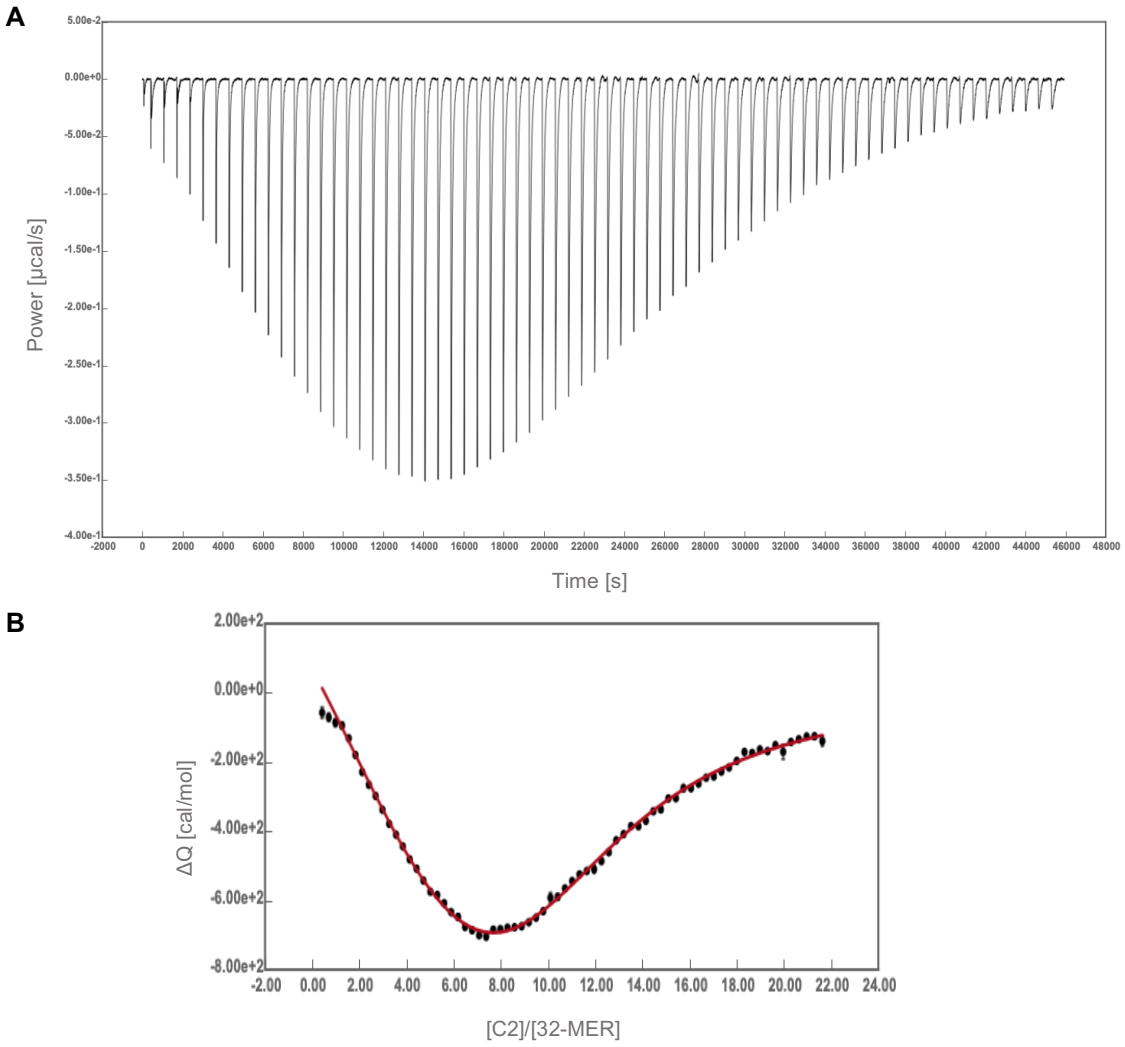

Fig. 29 - (A) Raw data obtained over a series of injections of procyanidin C2 (at 10 mM) into 0.1 mM of 32-mer peptide in water, pH 7.4, at 25 °C; (B) Binding isotherm created by plotting the areas under the peaks (after blank subtraction) against the molar ratio of procyanidin C2 injected. The best-fit curve, obtained by using a two sets of independent binding site model, is displayed as a red line.

Integrated heat data (*Fig. 27*, *Fig. 28B* and *Fig. 29B*) yielded differential thermal binding curves which could be analyzed by standard nonlinear regression methods to give estimates of the binding stoichiometry (*n*), equilibrium constant for association (K_a), and enthalpy of binding (ΔH). As in previous reports, the isotherms corresponding to EGCG and procyanidin C2 were fitted considering an independent site model with two sets of sites, each with different binding strengths. For procyanidin B3, it was only considered one set of binding sites. Hence, from the best fitting curves, thermodynamic parameters were calculated for each polyphenol at 25 and 37 °C (*Table 1*).

Table 1 - Thermodynamic values derived for polyphenols interaction with the 32-mer peptide in water at pH 7.4.

	T (°C)	Sites	n	K_A (M^{-1})	K_D (μM)[1]	ΔG (kcal.mol^{-1})	ΔG_T (kcal.mol^{-1})	ΔH (kcal.mol^{-1})	ΔH_T (kcal.mol^{-1})	-TΔS (kcal.mol^{-1})	$-T\Delta S_T$ (kcal.mol^{-1})	ΔS_T (kcal.mol^{-1})
EGCG	25.0	n (1.1)	3	2.23×10^6	0.4	-8.7	-14.7	-1.3	-1.4	-7.3	-13.3	0.044
		n (1.2)	5	2.48×10^4	40.3	-6.0		-0.1		-5.9		
	37.0	n (1.1)	3	1.31×10^5	7.6	-7.3	-12.3	0.0	-0.7	-7.3	-11.6	0.037
		n (1.2)	10	3.80×10^3	263.0	-5.1		-0.8		-4.3		
PROCYANIDIN B3[2]	25.0	n (1.1)	11	4.95×10^4	20.2	-6.4	-6.4	0.5	0.5	-6.9	-6.9	0.023
	37.0	n (1.1)	1	8.32×10^3	120.2	-5.6	-5.6	0.2	0.2	-5.7	-5.7	0.018
PROCYANIDIN C2	25.0	n (1.1)	6	1.68×10^4	59.4	-5.8	-10.8	1.0	-1.5	-6.8	-9.3	0.031
		n (1.2)	7	5.26×10^3	190.1	-5.1		-2.6		-2.5		
	37.0	n (1.1)	6	1.72×10^5	5.8	-7.4	-13.2	0.2	-0.2	-7.7	-13.0	0.042
		n (1.2)	9	1.22×10^4	82.3	-5.8		-0.5		-5.3		

[1] Dissociation constants were calculated as the inverse of the association constants (K_A) and expressed in micromolar (10^{-6} M).

[2] Contrary to EGCG and procyanidin C2, the thermodynamic parameters for procyanidin B3 were determined using a one-set of independent binding sites, all with the same binding strength.

The standard free energy of binding (∆G) was calculated from the equilibrium constant of the association (K_a), using the following expression:

$$\Delta G = -RTlnK_a \quad (2)$$

The change of entropy on binding (T∆S) was subsequently calculated from the relationship:

$$T\Delta S = \Delta H - \Delta G \quad (3)$$

where ∆H is the enthalpy change of binding.

As shown in *Table 1*, the interaction of 32-mer peptide with EGCG, procyanidin B3 and procyanidin C2 was found to be thermodynamically favorable at both 25 and 37 °C (∆G<0). There were, however, significant differences on the ∆G values depending on the polyphenolic molecule and peptide binding sets to which they bound. Interestingly, with the increase in temperature from 25 to 37 °C, there was a substantial decrease in the affinity constants of both EGCG and procyanidin B3 towards the 32-mer peptide (the obtained values were, at least, one order of magnitude lower), while for procyanidin C2, the behavior was just the opposite *i.e.* higher temperatures favored C2-peptide association due to a compensating change in the calculated T∆S. The binding stoichiometry also changed with temperature, thus suggesting that the polyphenol-peptide complexes in solution differ at different temperatures. With the exception of procyanidin B3, in which the *n* value was reduced to 1 at 37 °C, it is possible that, for EGCG and procyanidin C2, a higher, physiological, temperature leads to dissociation of weakly bound species into smaller complexes, a feature that would increase the binding stoichiometry by exposing additional binding surfaces, especially when they involve the second set of independent sites.

In general, the second set of binding sites had the lowest association constant values when compared to the first ones. According to the literature, this is exactly what we would expect for multiple binding modes: if the primary binding event has an affinity at least 10 times greater than any secondary event, then the added ligand will initially bind almost exclusively to the primary site [283]. Once most of the primary binding sites become

saturated, then the ligand will start to bind to other places, which in most cases, occurs in a weak and non-specific manner. Through these concepts, it is possible to postulate a rational and mechanistic understanding regarding the molecular basis of polyphenol interaction with the 32-mer peptide. It thus appears that as polyphenol molecules begin to occupy each of the primary available peptide binding sites - leading to the formation of what has been previously defined as a "*polyphenolic coating*"-, eventually, there comes a moment in which most of them become completely filled with polyphenols. From this point forward, their interaction with the 32-mer peptide will become increasingly unspecific so that any additional polyphenol will end up promoting the cross-linking of soluble peptide-polyphenol complexes into progressively larger and insoluble aggregates. This two-step mechanism, although simplistic and perhaps misleading depending on the multivalent nature of the species involved, may explain the multiphasic appearance of the binding isotherms for EGCG and procyanidin C2 titration as well as the turbidity of the reaction mixtures at the end of the ITC experiments.

Besides confirming direct interactions with the target of interest, thermodynamic measurements also provide insights on the nature of the noncovalent forces responsible for binding. For a binding process, the binding enthalpy (ΔH), reflects the energy change of the system when a ligand binds to a receptor protein or peptide. In a non-strict sense, ΔH is generally treated as the changes in energy resulting from the formation of non-covalent interactions including Van der Waals contacts, hydrogen bonds, ion pairs, and any other polar and apolar interactions at the binding interface. Nevertheless, the heat effect associated to a binding reaction is a global property of the entire system. As such, it arises from contributions not only from the solute, but also from the solvent, and it is almost unconceivable to form favorable interactions without disrupting any others. In fact, the change in enthalpy upon binding is a result of forming and disrupting many individual interactions, including the loss of the hydrogen bonds and van der Waals contacts between the protein (and ligands) and solvent molecules, the formation of the non-covalent interactions between the protein and ligand, and the solvent reorganization near the complex surface [295]. These individual components make either favorable or unfavorable contributions, and the net enthalpy change is a result of the combination of these different inputs. Entropy, on the other hand, could be viewed as a measure of the disorder or randomness in atoms and molecules in a system. The total entropy change associated with binding (ΔS) may be divided into three entropic terms to include the solvent entropy change arising mainly from surface burial and solvent release upon binding, the conformational entropy change reflecting the changes in the conformational freedom of both the protein and ligand upon binding and the loss of translational and

rotational degrees of freedom of the protein and ligand upon complex formation. The above three entropic terms determine the net entropy change, that can be positive or negative thus making the interaction either favorable or unfavorable, respectively. An unfavorable enthalpy change and large positive entropies associated with biomolecular complex formation is characteristic of hydrophobic interactions. In the case of polar interactions such as hydrogen bonding, salt bridge formation, and other electrostatic effects, the unfavorable enthalpy change results from a net loss of such bonds, in forming the complex itself, or between ordered solvent molecules on the biomolecular surface. An unfavorable enthalpy change in hydrophobic interactions is due to the burial of hydrophobic groups, which also requires disruption of an ordered solvation network. In most hydrophobic interactions, the net enthalpy change is low and the entropy change is high [296]. However, in both polar and hydrophobic interactions, most of the entropy gain is related to the release of water molecules from a binding interface in the course of complex formation, outweighing the loss of entropy associated with the formation of the complex itself. Therefore, while polar interactions such as hydrogen and Van der Waals bonding within the complex tend to contribute favorably to the enthalpic component (ΔH), entropically (ΔS) favored interactions tend to be more hydrophobic in character compared to an enthalpy-driven one. The values obtained for the binding enthalpy and entropy factor (-TΔS) in each of the 32-mer binding sets (*Table 1*) reveal that, in general, the interaction between the 32-mer peptide and both EGCG, procyanidin B3 and the trimer C2 is entropy-driven. As a matter of fact, in most of these peptide-polyphenol interacting systems, the enthalpic contribution over ΔG, which in the end determines the stability of any existent complex, is residual when compared to the dominant contribution of ΔS. Interestingly, with exception of EGCG interaction at 25 °C, the enthalpic factor ΔH tends to be a little bit more favorable when it involves the second set of independent binding sites (*Table 1*). Therefore, according to these results, it is expected that hydrophobic interactions, which are relatively long-range, should drive the binding process between the 32-mer peptide and polyphenols due to the high solvation entropy and water release from the aliphatic and aromatic sidechains of Leu, Tyr and Phe (they occupy a much more higher volume than the apolar Pro) while the establishment of hydrogen bonds between polyphenol hydroxyl groups and the peptide H-acceptor sites (short-range and highly directional) along with Van der Waals interactions may strengthen and stabilize the resulting complexes and subsequent aggregates. Although in most cases an increasing temperature leads to a general destabilization of the peptide-polyphenol complexes by interfering with both enthalpic and entropic phenomena, for procyanidin C2, however, there is an apparent

compensatory effect of ΔS to the overall free energy of binding. Probably, when procyanidin C2 binds to the 32-mer peptide at 37 °C, there is some sort of positive change in the degrees of freedom of the complex in comparison with the non-bound state where the binding partners exist separately.

When ITC experiments are performed at varying temperatures, the heat capacity change (ΔC_p) of a binding reaction can be obtained. ΔC_p provides thermodynamic information regarding the change in hydration upon protein-ligand binding, as hydrated water (particularly those interacting with hydrophobic surfaces) and the bulk water have different behaviors and properties [297, 298]. This will lead to a change in heat capacity due to the release of water molecules upon complex formation, with the magnitude of ΔCp being proportional to the amount of surface area involved. The ΔCp value for each polyphenol-peptide interaction was derived from the temperature-dependent ΔH curve with linear regression analysis, using the standard thermodynamic relationship:

$$\Delta C_p = d\Delta H / dT \quad (4)$$

All polyphenol-peptide complexes showed a small, yet significant, temperature dependence of ΔH. Accordingly, it was found that complexation of procyanidin B3 with the 32-mer peptide became less endothermic as the temperature rose (ΔC_p = - 0.289 kcal.mol^{-1}.K^{-1}). For EGCG and procyanidin C2, however, the obtained ΔC_p values (0.674 kcal.mol^{-1}.K^{-1} and 1.299 kcal.mol^{-1}.K^{-1}, respectively) indicate that their complexation becomes less exothermic at higher temperatures. Although controversial, it has been postulated that desolvation of both protein and ligand molecules upon binding can make positive or negative contribution to ΔC_p, depending on the burial of the apolar (leading to negative ΔC_p) or polar (positive ΔC_p) surface areas. Therefore, while a negative ΔC_p is usually interpreted as an indication that water is being displaced from apolar groups during hydrophobic interactions, a positive ΔC_p is consistent with an extensive additional hydration upon binding. It is now becoming clear that large ΔC_p effects, together with associated entropy–enthalpy compensations, are a much more general phenomenon to be anticipated in any system comprising a multiplicity of weak interactions, and this has been quantitatively demonstrated in some systems.

3.3. MD Simulations

3.3.1. EGCG: a case study

The intermolecular interactions between EGCG and the 32-mer peptide in aqueous solution were also studied by a computational approach. Three MD simulations of 50 ns each were performed. *Figure 30* illustrates structures extracted from each simulation, in which the maximum number of EGCG molecules interact with the residues from the 32-mer peptide. *Table 2* summarizes different average and maximum time indicators considering the formation peptide-$EGCG_n$ complexes for each MD simulation.

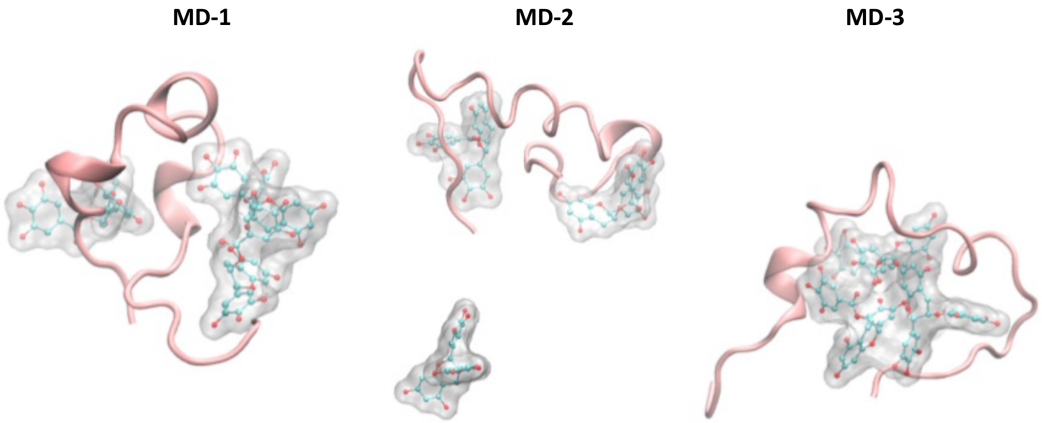

Fig. 30 - Representation of geometries of three 32-mer:$(EGCG)_3$ complexes extracted from each MD simulation. The peptides are depicted with cartoon and are colored pink, whilst the EGCG molecules are depicted with surface and balls-and-sticks and are colored by atom type.

Table 2 - The binding of three EGCG molecules to the 32-mer peptide was analyzed by: i) time of binding of one, two and third polyphenols, ii) time of binding of the first EGCG, iii) time of binding of the maximum number of EGCG molecules in simultaneous. The average total binding time of peptide-polyphenol interactions is also shown.

SYSTEM	1 EGCG	2 EGCG	3 EGCG	TIME OF BINDING OF THE 1ST EGCG	TIME OF BINDING OF THE MAXIMUM NUMBER OF EGCG
MD 1	22.0	10.1	3.1	13.9	43.9
MD 2	39.4	1.3	0.0	1.5	10.5
MD 3	5.6	7.9	30.6	5.9	16.6
Average	22.3	6.4	11.3	7.1	23.7
Sum	67.0	19.3	33.8	---	---

Analyzing the times of binding for the first MD simulation, one can see that the first EGCG molecule binds after 13.9 ns, and two additional molecules bind after 43.9 ns of simulation. For the second MD, one EGCG binds at 1.5 ns, followed by another at 10.5 ns. However, after few picoseconds, one of these molecules ceases to interact with the peptide and starts to interact with the third EGCG molecule in solution, and the assembly of these two EGCG molecules was maintained throughout the remaining simulation. As for the third MD simulation, a cooperative and sequential binding of EGCG molecules was observed. One, two and three EGCG's bound at 5.6 ns, 7.9 ns and 30.6 ns, respectively, being the latter structural rearrangement maintained until the end of simulation. Overall, the average binding times of one, two and three EGCG molecules to the 32-mer peptide, in simultaneous, are 22.3 ns, 6.4 ns and 11.3 ns, which indicates a higher stability of the interactions between these two partners.

As mentioned, the interaction of polyphenols with proteins occurs mainly by hydrogen bonding and hydrophobic contacts. *Supplementary Table 1* shows the specific hydrogen bonds involving EGCG molecules along each MD simulation. As observed, EGCG interacts with a frequency higher than 5% with the backbone NH and/or CO groups of Pro4, Phe5, Pro6, Leu10, Leu17, Pro20, Leu24, Pro29, Pro31 and Phe32 residues, as well as with the side chains of Gln9, Gln14, Gln16, Gln21, Gln23, Gln28 residues of the 32-mer peptide. It was found that EGCG molecules do not bind to the 32-mer peptide in a specific region, although the first interactions are directed towards nonpolar residues. In general, EGCG interact with different parts of the peptide, in particular with regions populated by Leu, Pro and Gln residues. In addition, hydrophobic π-π stacking and van

der Waals interactions were also observed due to the small proximity between the EGCG aromatic rings and nonpolar residues, such as Phe32 and Leu24. Some π-π stacking interactions are also established between rings of different EGCG molecules. All these interactions contribute to a higher stability of the global peptide-$EGCG_n$ complex. The average distances between the different rings of EGCG to 32-mer peptidewere also determined. The ranking of proximity to peptide is B ring > G moiety ≈ AC rings, a result that is close to the one obtained by STD NMR epitope mapping (*Fig. 20*). Of note, this small proximity is not directly related with a higher effect on binding, but instead, is the overall geometry adopted by all rings of each polyphenol during the interaction with the other partner.

The initial 3D conformation of the 32-mer peptide included a helix (composed by residues Phe5-Gln23) surrounded by unfolded extremities. However, throughout the simulations, the binding of EGCG molecules caused conformational rearrangements and the peptide adopted a more coiled conformation that encapsulated the polyphenols (*Fig. 30*). The determination of head-to-head distance of the 32-mer peptide revealed that it changes from an average of ca. 23 Å to 13 Å, indicating a 41% decrease in length. Some conformational changes were also proposed previously in the study of the interaction between tannins and proline-rich proteins [299]. We also determined the Solvent-Accessible Surface Area (SASA) values for the 32-mer during each MD simulation. It was observed that the SASA value of the peptide decreases from an average of 3466 ± 187 $Å^2$ (first 5 ns) to 3000 ± 80 $Å^2$ in the last 5 ns with the presence of polyphenols. This represents a decrease of 13% on the surface area of the peptide that is accessible to solvent. It occurs due to EGCG binding, which subsequently influences the conformational rearrangements of the 32-mer peptide.

3.3.2. Procyanidin B3 vs Procyanidin C2

MD simulations were also used to evaluate the intermolecular interactions between the 32-mer peptide and procyanidins B3 and C2. *Figure 31* illustrates the time of simulation in which one, two or three polyphenol molecules (B3 or C2) interacted in simultaneous with the 32-mer peptide. *Figure 32* displays the extracted structures at 30 ns and 50 ns of the third MD simulations of 32-mer:$(B3)_3$ and 32-mer:$(C2)_3$. As the binding mode between both procyanidins and the 32-mer peptide was quite similar in the three simulations, only structures from MD-3 were chosen because in these simulations all the three polyphenols interacted with the peptide.

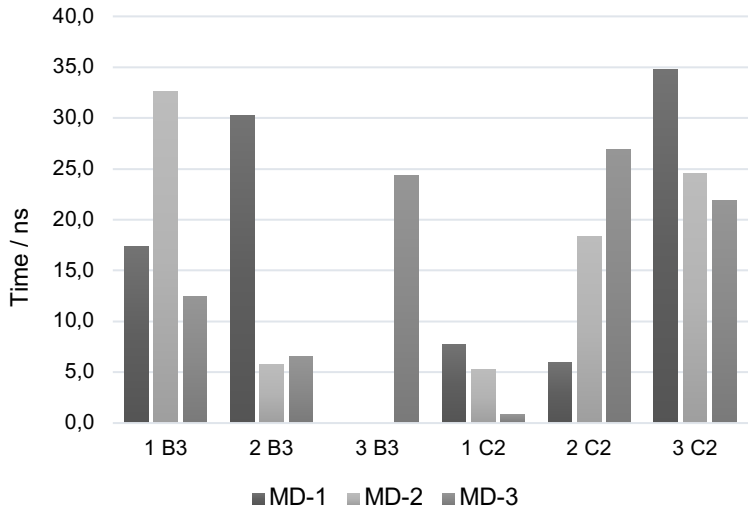

Fig. 31 - Schematic representation of the time of simulation in which one, two or three polyphenol molecules (B3 or C2) were bound in simultaneous to the 32-mer peptide, in each MD simulation.

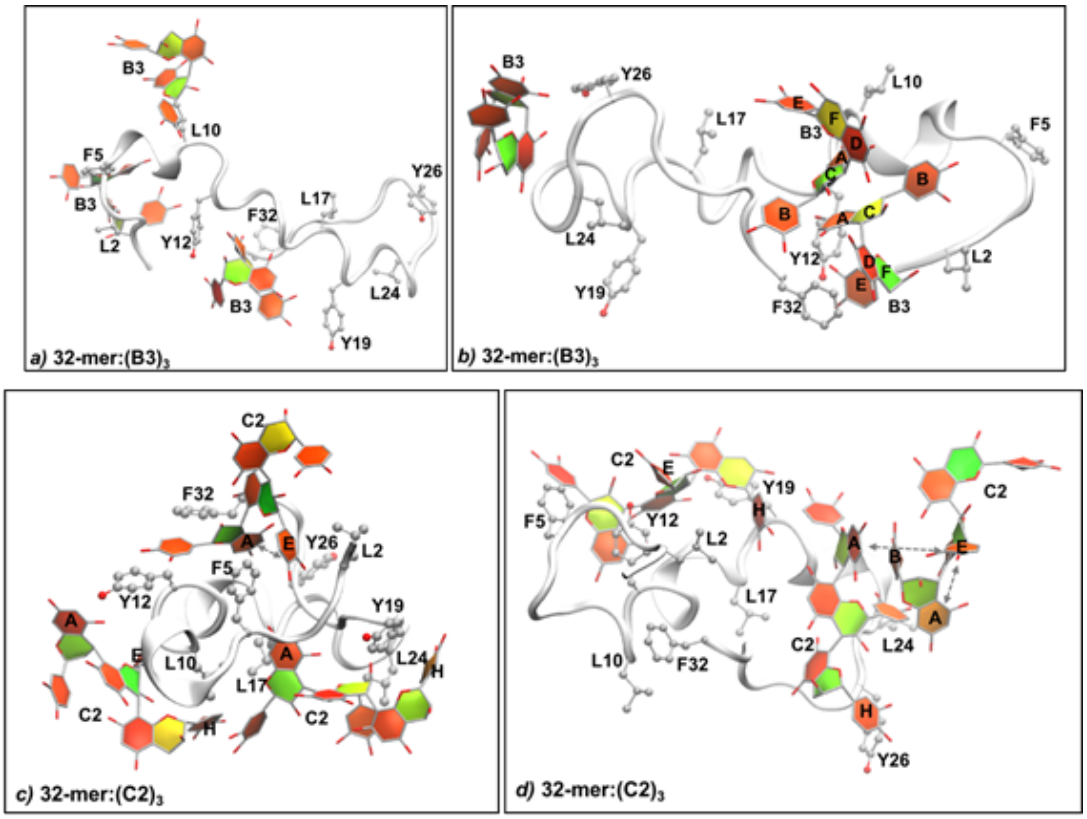

Fig. 32 - Representation of geometries extracted from MD-3 simulations of the 32-mer:$(B3)_3$ complex at 30 ns (A) and at 50 ns (B) as well as of the 32-mer:$(C2)_3$ complex at 30 ns (C) and 50 ns (D). The 32-mer peptide is depicted with cartoon and is coloured grey (tyrosine, leucine and phenylalanine residues are highlighted with the balls-and-sticks representation), whilst the B3 and C2 molecules are depicted with sticks and are coloured by atom type. The rings of B3 and C2 are coloured by pucker, using the Cremer-Pople pucker amplitude.

Supplementary Tables 2-7 show the hydrogen bonds and hydrophobic interactions established between procyanidins B3 and C2 and the 32-mer peptide with a frequency higher than 5% in each MD simulation.

A cooperative and sequential binding of B3 or C2 molecules to the 32-mer peptide was observed in all MD simulations. For example, in the MD-1 of 32-mer:$(C2)_3$, one, two and three C2 molecules were bound at 1.4 ns, 7.9 ns and 15.2 ns, respectively, being the three polyphenols bound throughout the remaining simulation time. All MD simulations of 32-mer:$(C2)_3$ system revealed that the three C2 molecules interact in simultaneous with the 32-mer peptide (*Fig. 31*). On the contrary, in MD-1 and MD-2 of the 32-mer:$(B3)_3$ system, only two B3 molecules interacted with the 32-mer peptide. In general, procyanidin C2 molecules established a higher number of interactions with the 32-mer peptide than B3. It thus appears that procyanidin C2 has a higher binding ability than the dimer B3, which is probably due to their distinct sizes and molecular structures. Indeed, the dimeric geometry of B3 allows the formation of stable intramolecular π-π interactions (perpendicular stacking between the AC - DF nucleus and/or planar stacking between the AC - E nucleus) (*Fig. 32*) that restricts the conformation and flexibility of these molecules. Similar interactions can also occur between rings from different B3 molecules. Regarding the trimeric C2 molecule, it has a more lengthened geometry that weakens the intramolecular stacking, thus having higher conformational degrees of freedom that may increase its ability to interact with other molecular partners such as the 32-mer peptide. Additionally, these molecules are able to form clusters that may encapsulate some peptide regions (as seen in *Fig. 32C* and *D*).

Both polyphenol molecules bound to the 32-mer peptide by hydrogen bonds and hydrophobic contacts (π-π stacking and van der Waals interactions). As observed in all MD simulations, both polyphenols established more hydrophobic contacts than hydrophilic interactions. This fact is particularly notorious in the first polyphenol-peptide complexes. During the first 2 ns of all 32-mer:$(C2)_3$ simulations, the C2 molecules established hydrophobic contacts with fourteen residues of the 32-mer peptide without any hydrogen bond. Regarding the first 12 ns of all 32-mer:$(B3)_3$ simulations, the B3 molecules made hydrophobic contacts with fifteen residues of the peptide and twelve hydrogen bonds (only five involve polar sidechains). This fact suggests that the molecular mechanism of binding between the C2 and B3 to the 32-mer occurs firstly by hydrophobic driving forces that are followed by hydrophilic contacts. This observation agrees with the previous experimental data that suggests a dominant entropic phenomenon over the enthalpic ones. Both polyphenols interacted more with leucine (Leu2, Leu10, Leu17 and Leu24), tyrosine (Tyr12, Tyr19 and Tyr26) and phenylalanine

(Phe5 and Phe32) residues. The fact that their large aliphatic and/or aromatic sidechains can establish van der Waals interactions and π-π stacking with the large planar surfaces of polyphenols may explain their highly relevant contribution in peptide-polyphenol binding. Tyrosine residues, in particular, have a key role in molecular recognition and binding mode because of their dual ability to establish hydrophobic and hydrophilic interactions. The hydrophobic effect of the formers favors the peptide-polyphenol binding and the creation of higher ordered clusters (strong π-π interactions may cause the occlusion from solvent molecules), while the hydrogen bonds are specific driving forces that optimize the number of interactions and the stability of the 32-mer:$(polyphenol)_3$ complexes. At this point, it is important to highlight that procyanidin B3 and C2 also interact with proline residues. However, their contribution for the binding driving force should be small due to their little non-polar sidechains. Their specific localization between bigger residues along the peptide suggest that their main role is to help the conformational rearrangements on the peptide structure (from an α-helix to coiled and unfolded states) observed upon binding of polyphenols. Although the hydrophobic contacts are the major contributors to the interaction between procyanidins B3 and C2 to the 32-mer peptide, this process could also be strengthened by hydrogen bonds involving the polar glutamine residues.

The large size and complex structure of all molecules involved, allows a huge number of possible 32-mer:$(polyphenol)_3$ complex structures that are difficult to characterize [300]. However, we determined the nearest regions of the polyphenol molecules to the 32-mer peptide by calculating the average distances between the different rings of B3 and C2 molecules to 32-mer. The ranking of proximity of B3 rings to peptide is AC > B ≈ DF ≈ E. The ranking of proximity of C2 rings to peptide is AC > H > GI > E ≈ DF ≈ B. The proximity of AC, H and E rings to leucine and tyrosine residues is highlighted in *Fig. 32C* and *D*. *Figure 32* also shows the interaction between the AC and E rings of one (intramolecular) or two (intermolecular) C2 molecules, which agrees with the small proximity between these two groups as observed in the aforementioned NMR results.

3.4. Fluorescence Quenching

To complement the previous NMR and ITC data and to provide molecular level insights into the mechanism of interaction between EGCG, procyanidins B3 and trimer C2 towards the 32-mer peptide in a substoichiometric concentration range, fluorescence quenching experiments were performed at intestinal physiological pH and temperature.

Accordingly, it has been seen that micromolar increments of these polyphenols lead to a gradual decrease in the fluorescence intensity of the peptide phenylalanine and tyrosine residues by a quenching process without any significant shift in the emission wavelength (*Fig. 33*).

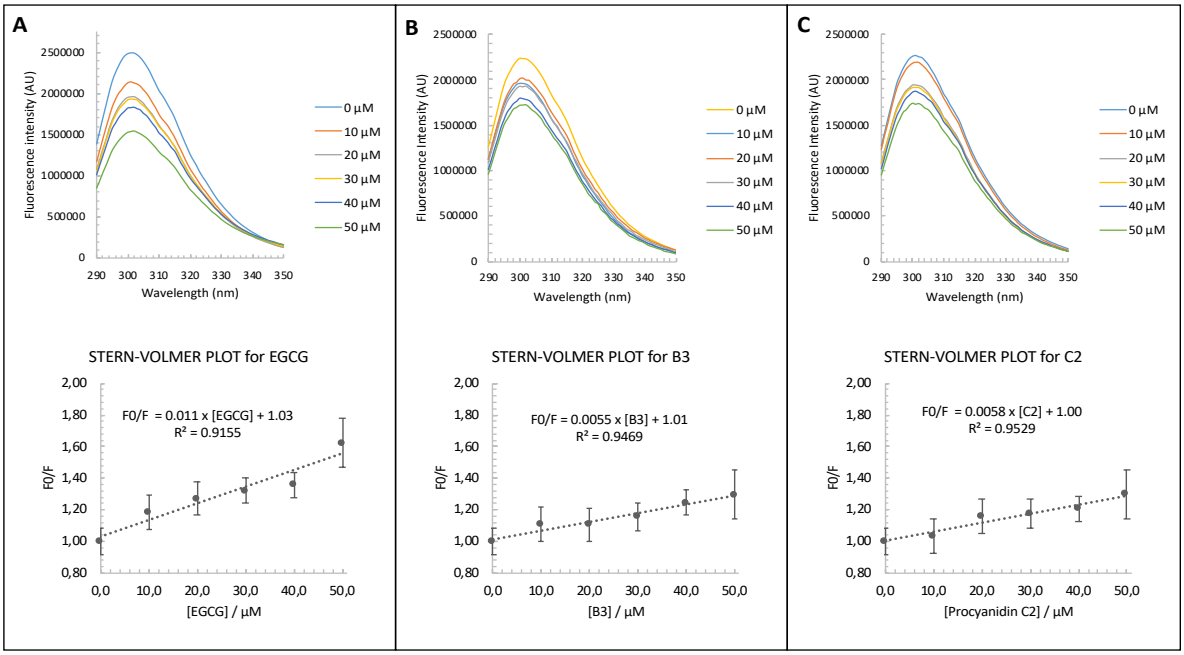

Fig. 33 - Fluorescence emission spectra and corresponding Stern-Volmer plots of the 32-mer peptide (λ_{ex} = 275 nm) in the presence of increasing concentrations of EGCG (A), procyanidin B3 (B) and procyanidin C2 (C) in PBS at 37 °C.

Through determination of the corresponding Stern-Volmer quenching constants (K_{sv}), determined as the slope of the F_0/F = f([Polyphenol]) plot (F_0 and F are the fluorescence intensities in the absence and presence of the quencher, respectively), it can be seen that EGCG stands out to procyanidin B3 and C2 with a Stern-Volmer constant of 11000 M^{-1} (*Table 2*). At these experimental conditions, procyanidin dimer B3 and trimer C2 had statistically similar Stern-Volmer quenching constants and as such they have the same ability to interact with the 32-mer peptide in solution and reduce its intrinsic fluorescence. As the Stern-Volmer plot for each of these polyphenols was mainly linear and their constants were considerably high, these results point out to static mechanism of fluorescence quenching [301]. Accordingly, the binding constant (K_A) and the number of binding sites (n) can be determined by plotting the double logarithm regression curve of the fluorescence data with the modified Stern-Volmer equation (5):

$$Log\ \frac{F_0-F}{F} = Log\ K_A + n\ Log\ [Polyphenol] \quad (5)$$

The association constants K_A and *n* values were obtained from the intercept and slope of the Log [(F_0-F)/F] = f(Log [Polyphenol]) plot, respectively. The obtained parameters are summarized in *Table 3*.

Table 3 - Stern-Volmer quenching constants and binding parameters of the interaction between the 32-mer peptide and EGCG, procyanidin B3 and procyanidin C2 in PBS at 37 °C.

	STERN-VOLMER QUENCHING CONSTANTS	BINDING PARAMETERS	
POLYPHENOL	K_{SV} (μM^{-1})	Log K_A (μM^{-1})	*n*
EGCG	0.011 ± 0.002	-1.4 ± 0.2	0.7 ± 0.1
Procyanidin B3	0.0055 ± 0.0007	-2.5 ± 0.1	1.15 ± 0.09
Procyanidin C2	0.0058 ± 0.0006	-2.6 ± 0.3	1.2 ± 0.2

With the exception of EGCG, the remaining *n* values were approximately equal to one, indicating that only a single low-affinity binding site in the 32-mer peptide was involved. For EGCG, the binding ratio was close to 1:2 (*n* = 0.5, 2 peptides: 1 ligand) highlighting the ability of EGCG to promote peptide oligomerization under near physiological conditions. Moreover, EGCG exhibited a relatively high affinity towards the 32-mer peptide according to the K_A value of approximately 4.0 x 10^4 M^{-1}. Oppositely to what was obtained by NMR spectroscopy and ITC, procyanidin B3 and the trimer C2 had a similar binding constant that was an order of magnitude lower to that of EGCG (*Table 3*). Therefore, it might be concluded that at an intestinal environment, the interaction between both procyanidins and the 32-mer peptide is not as strong as in the presence of EGCG, at lower concentrations.

3.5. Dynamic Light Scattering

Light scattering measurement were performed to determine the size distribution of the supramolecular complexes between EGCG, procyanidin B3 and trimer C2 and the 32-mer peptide at near physiological conditions. These results are summarized in *Fig. 34*.

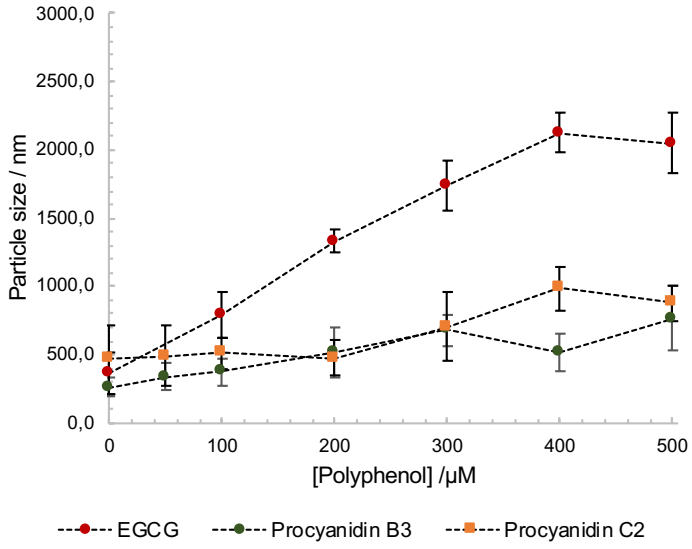

Fig. 34 - Changes in polyphenol-peptide aggregate size with increasing concentrations of EGCG, procyanidin B3 and the trimer C2 in PBS at 37 °C.

As it can be seen, EGCG produced the larger peptide aggregates that increased in size until reaching a plateau at a ligand-to-peptide ratio of 4:1. For procyanidin B3 and the trimer C2, however, there wasn't any significant variation in scattering intensity. Therefore, if an interaction occurred, it did not lead to the formation of detectable aggregates. Of note, the particle size distribution was different at 25 and 37 °C (*data not shown*). When procyanidin C2 was mixed with the 32-mer peptide at room temperature, the medium became immediately turbid as a result of the presence in solution of numerous aggregates or of large ones. Nevertheless, when the temperature was increased to 37 °C, the pre-existing supramolecular aggregates became solubilized and the suspensions turned metastable *i.e.* without any phase separation. For EGCG samples, the same behavior was not observed as the suspensions remained turbid at both temperatures. Overall, these light scattering results clearly show that the binding of both procyanidin oligomers and EGCG to the 32-mer peptide is kinetically different with EGCG being the most reactive polyphenol at both physiological pH and temperature. On an intestinal environment, procyanidin dimer B3 and trimer C2 behave as low-affinity

ligands towards the 32-mer peptide with a dissociation constant (K_D) higher than 310 μM, unlike EGCG that has a K_D around 25 μM (*Table 3*).

3.6. Transepithelial Transport Assays

Having characterized the interaction between the 32-mer peptide and EGCG, procyanidin B3 and procyanidin C2 on a molecular and thermodynamic perspective, we next wanted to study to which extent the complexation of the 32-mer peptide could influence its bioavailability in a transwell system composed of human intestinal Caco-2 cells. Despite its origin from a colon adenocarcinoma, this cell line still represents the best available *in vitro* model of absorptive enterocytes. These cells undergo a spontaneous differentiation for about two to three weeks leading to the formation of a polarized cell monolayer, hold together by tight junctions and expressing several morphological and functional features of small intestinal enterocytes. This cellular system has already been used in a CD context to study the mechanisms of epithelial translocation of many gliadin-derived peptides, including the 32/33-mer [65, 302-305].

A mixture containing both 32-mer peptide and EGCG in a 1:3 molar ratio was added to the apical compartment of Caco-2 cell monolayers grown on permeable transwell supports followed by an incubation period of 4h. After this, aliquots of the basolateral medium were collected, processed and analyzed by mass spectrometry (*Fig. 35*). At this peptide-to-EGCG molar ratio, *i.e.* 0.1 mM of 32-mer and 0.3 mM EGCG, there is an extensive complexation/aggregation of both species (*Fig. 34*), so that it constitutes an excellent starting point to see whether an EGCG-mediated scavenging of the 32-mer peptide can attenuate its transepithelial transport *in vitro*. It should be highlighted that the concentration of EGCG used in this study wasn't randomly selected. According to the USDA database for the flavonoid content of selected foods, it is within a physiologically relevant concentration range just by drinking one single cup of brewed green tea (240 mL) containing an average of 78 mg of EGCG *per* 100 mL (on the basis of 1 g leaf/100 mL infusion) [306]. Although this value may vary depending on the type of preparation, technique used, ethnicity and dosage form, the amount of EGCG at the intestinal level may reach concentrations as high as 1 mM or even more [307].

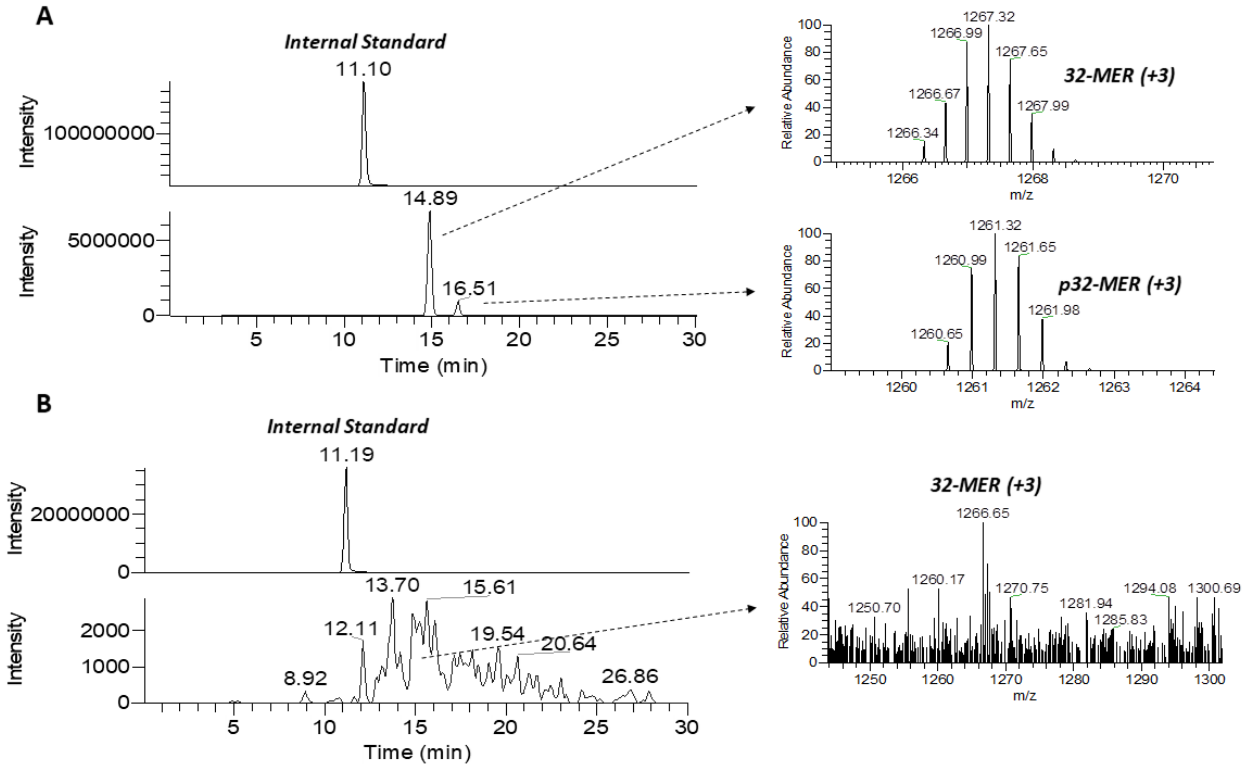

Fig. 35 - Extracted ion chromatograms and mass spectra amplifications of two representative basolateral samples corresponding to the incubation for 4h of Caco-2 cells monolayers with the 32-mer alone (A) or in the presence of EGCG at a molar ratio of 1:3 (B). The searched ions were the +1 (1043.53) and +2 (522.27) charges of the internal standard (top) along with the +3 and +4 charges of both 32-mer peptide and pyro-32-mer peptide (approximately 1267.32/950.50 and 1261.32/946.24 respectively) (bottom).

In all the assays without EGCG, around 2.5% of the apical 32-mer was shown to be able to cross the epithelial barrier in the apical-to-basal direction (*Fig. 35A*). However, in the assays containing EGCG, the 32-mer was nearly not detectable in the basolateral samples, being, when present, at the background noise level (*Fig. 35B*). Being mass spectrometry a highly sensitive technique, especially when there is a miniaturization of the LC system and its interface with MS, these results are quite impressive and demonstrate, for the first time and under near physiological conditions, the ability of EGCG to block, almost completely, the translocation of the 32-mer peptide through a simulated intestinal epithelial barrier. This decreased peptide absorption and availability, when transposed to an *in vivo* situation, may lead to a significant attenuation in subsequent cellular and molecular mechanisms inherent to CD including, for example, a lower activation and triggering of a gluten specific T cell-mediated immune response. This effect, however, needs to be demonstrated and is currently under investigation.

Having shown the ability of EGCG to modulate the translocation of the 32-mer peptide at relatively high concentrations, we questioned ourselves whether substoichiometric amounts of polyphenols could lead to a similar outcome. To do so, we incubated the 32-mer peptide with procyanidin B3 or procyanidin C2 (both at 0.08 mM) and quantified its passage using the same Caco-2 cell-based transepithelial transport assays (*Fig. 36*).

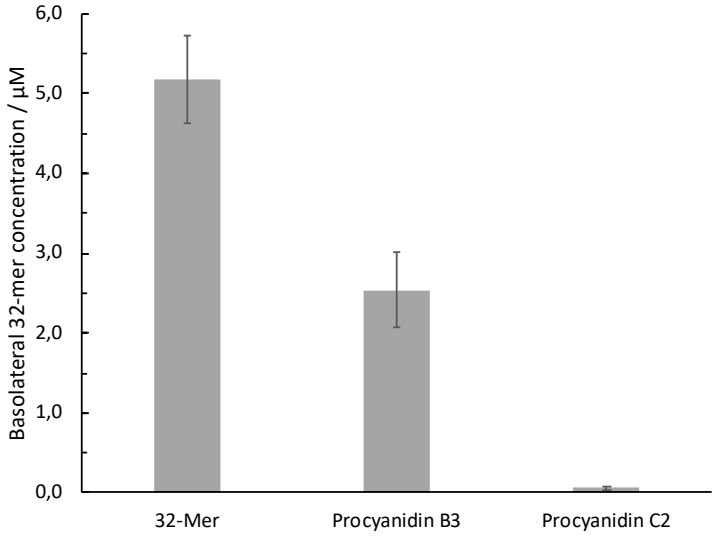

Fig. 36 - Apical-to-basolateral transport of the 32-mer peptide through Caco-2 cell monolayers incubated for 4h with procyanidin B3 and the trimer C2. Shown values are the arithmetic means (n = 3) ± standard error of mean (SEM).

Accordingly, in the absence of both procyanidins, the 32-mer achieved a basolateral concentration of 5.2 ± 0.6 µM. However, in the presence of procyanidin B3 and trimer C2, its apical-to-basolateral translocation was reduced to a final peptide concentration of 2.5 ± 0.5 µM and 0.06 ± 0.03 µM respectively. As such, it might be seen that co-incubation of the 32-mer peptide with procyanidin B3 and most importantly with trimer C2 lead to a remarkable attenuation of its transepithelial transport, a behavior that appears to be dependent on the tannin polymerization degree. Attending that both procyanidins had a similar association constant at physiological conditions, these results point out to the occurrence of other regulatory mechanisms of peptide transport mediated by procyanidins B3 and the trimer C2 in addition to a direct peptide binding, a feature that should not be overlooked. On a CD perspective, few studies are available concerning the transcytosis of the 32-mer peptide. Under healthy conditions, it is thought to enter the IEC and released basolaterally in the lamina propria by a transcellular pathway, without the involvement of a receptor (through fluid-phase endocytosis, *Fig. 37*), whereas under inflammatory conditions an IFN-γ-induced increase in the intestinal

permeability results in increased paracellular translocation of gliadin [308]. According to our data, we hypothesize that procyanidins could affect the 32-mer peptide translocation through competition for a membrane environment or by modifying the cell physiology. These mechanisms, however, need to be further explored both *in vitro* and *ex vivo*.

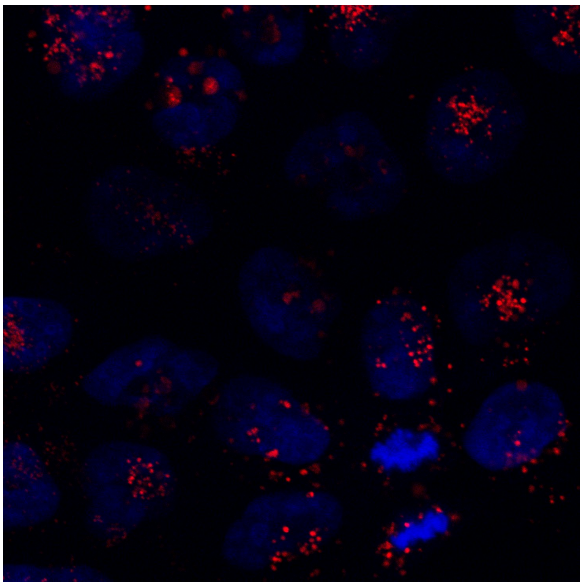

Fig. 37 - Cell imaging of Caco-2 cells (blue) incubated with rhodamine B-labelled 32-mer peptide (red) by laser confocal scanning microscopy. The 32-mer peptide was found to be located within intracellular endosomal vesicles. For these experiments, Caco-2 cells were seeded, at a density of 3 x 10^4 cells.mL^{-1}, in 35 mm imaging dishes with four compartments and an ibidi polymer coverslip bottom (Ibidi, Germany). After 24h, the complete medium was removed and the attached cells were washed with Balanced Salt Solution pH 7.4 before adding the 32-mer peptide at 100 μg.mL^{-1}. Cells were maintained at 37 °C in an atmosphere of 5% CO_2 and 90 % relative humidity. Following 3h of incubation with the 32-mer, Caco-2 cells were fixed with 4% paraformaldehyde solution (diluted in PBS) for 20 minutes at room temperature. To inhibit photobleaching of the fluorescent dye and to stain the cell's nuclei, fixed Caco-2 cells were subsequently treated with VECTASHIELD® mounting medium with DAPI (Vector Laboratories, California, USA). Cell imaging experiments were performed on a Leica TCS-SP8 inverted confocal microscope equipped with Diode 405, Ar (458, 476, 488, 496, 514), DPSS 561, HeNe 594 and HeNe 633 nm laser lines, a high-speed resonant plus conventional tandem scanner, 2 hybrid detector and 2 PMTs and an environmental chamber with temperature and CO_2 control. The excitation/emission pairs were 555/585 nm for the 32-mer peptide and 405/470 for DAPI. The objective was a 40x/1.10 CORR water. Images were obtained with the LAS AF software from Leica (Leica Microsystems, Germany) while the post-treatment was performed with Fiji (ImageJ). All the images, including controls and experiments, were treated with the same color, brightness and contrast parameters.

Recently, we have performed a transwell experiment in which fully differentiated Caco-2 cells were pre-treated for 24h with EGCG at three different physiological concentrations: 5, 10 and 25 μM. EGCG was prepared in *Hanks' Balanced Salt Solution* pH 7.4. Then, the wells were washed and added with 50 μM of 32-mer peptide, labeled with rhodamine B at its N-terminus. After 4h of incubation, aliquots were taken from the

basolateral compartment and analyzed by HPLC, coupled to a fluorescence detector (Dionex Ultimate™ 3000, ThermoFisher Scientific). The excitation wavelength was set to 555 nm while the emission was monitored at 585 nm (*Fig. 38*). In accordance with previous studies, the 32-mer peptide was found to cross the Caco-2 cell monolayer without any detectable degradation (*data not shown*). Nevertheless, when apical samples were analyzed by mass spectrometry, several peptide fragments were identified (*Table 4*). Their relative concentration, however, was very low when compared to the parent 32-mer peptide and were most probably the result of an enzymatic processing by exo- and endopeptidases anchored at the brush-border surface membrane (BBM) of Caco-2 cells. The latter include aminopeptidase N (APN), dipeptidyl peptidase IV (DPP IV) and peptidyl dipeptidase A (also known as dipeptidyl carboxypeptidase I, DCP I), all of which have already been shown to be involved in the BBM-mediated proteolysis of gliadin peptides into remarkably resistant immunodominant epitopes [302, 309]. The proline-processing dipeptidases DPP IV and DCP I, in particular, were identified as the rate-limiting enzymes in the overall destruction of immunodominant epitopes by rat and human BBM preparations [310]. Some deamidated peptides fragments were also detected; nevertheless, due to their low score values, they were excluded.

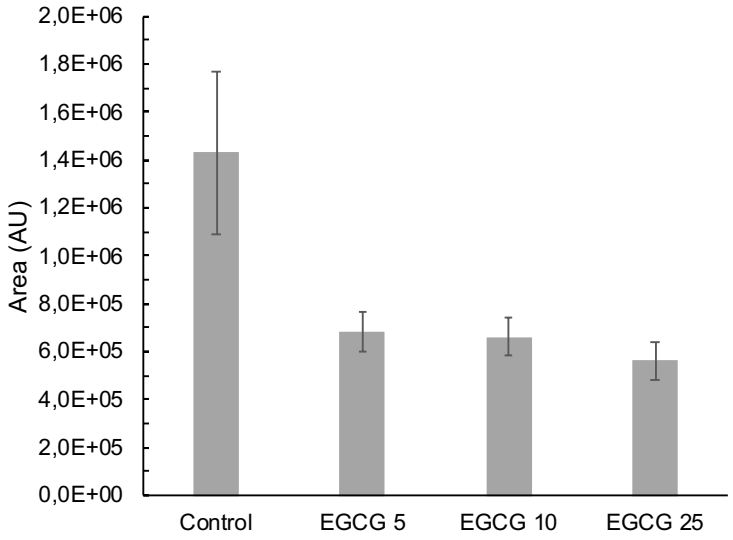

Fig. 38 - Apical-to-basolateral transport of the rhodamine B-labeled 32-mer peptide through Caco-2 cell monolayers pre-treated for 24h with EGCG at 5, 10 and 25 μM. Shown values are the arithmetic means (n = 5) ± standard error of mean (SEM).

Table 4 - Main peptide fragments, identified by nano-LC-MS/MS, upon incubation of the 32-mer peptide with differentiated Caco-2 cell monolayers. Their Identification was made by uploading the MS/MS data on the Proteome Discoverer 1.4 search engine (ThermoFisher Scientific, USA).

Sequence	Modifications	*XCorr*	MH^+ [Da]	RT [min]
QLQPFPQPQLPYPQPQLPYPQPQLPYPQPQPF	----	3,58	3797,0	22,5
(q)LQPFPQPQLPYPQPQLPYPQPQLPYPQPQPF	N-Term (Gln->pyro-Glu)	4,71	3780,0	21,2
LQPFPQPQLPYPQPQLPYPQPQLPYPQPQPF	----	3,76	3668,9	18,4
QLQPFPQPQLPYPQPQLPYPQPQLPYPQPQP -	----	5,71	3649,9	17,1
QLPYPQPQLPYPQPQLPYPQPQPF	----	2,05	2861,5	16,8
QLQPFPQPQLPYPQPQLPYPQPQL - - - - - - - - -	----	4,68	2842,5	17,0
PYPQPQLPYPQPQLPYPQPQPF	----	3,65	2620,3	16,4
PQPQLPYPQPQLPYPQPQPF	----	1,72	2360,2	16,2
PYPQPQLPYPQPQP -	----	1,58	1649,8	14,3
PQPQLPYPQPQPF	----	2,09	1536,8	15,0
QLQPFPQPQ- -	----	1,74	1082,6	13,5

As it can be seen from *Fig. 38*, pre-treatment of Caco-2 cells with EGCG resulted in a significant reduction of 32-mer peptide translocation from the apical to the basolateral compartment, without any statistical difference between treatments. The concentration of 32-mer peptide in the basolateral compartment has been determined in each experimental condition and corresponded to 4.3 ± 0.4, 1.9 ± 0.1, 1.9 ± 0.3 and 2.1 ± 0.6 $ng.mL^{-1}$, respectively. Interestingly, this attenuation of peptide transport was accompanied by a slight decrease on cell membrane permeability, according to the transepithelial electric resistance (TEER) values and lucifer yellow assay (*Fig. 39*). TEER is a widely accepted quantitative technique to measure the integrity of tight junction dynamics in several cell culture models and is based on measuring ohmic resistance across cellular monolayers, which in this case, was performed by using chopstick electrodes [311]. However, TEER values can be influenced by experimental variables such as composition of the culture medium and the type of measurement instrument. Accordingly, the total electrical resistance includes the ohmic resistance of the cell layer, the cell culture medium, the semipermeable membrane inserts and the electrode-medium interface. The lucifer yellow assay, on the other hand, is a robust marker to monitor the apparent paracellular permeability of confluent monolayers with functional tight junctions [312].

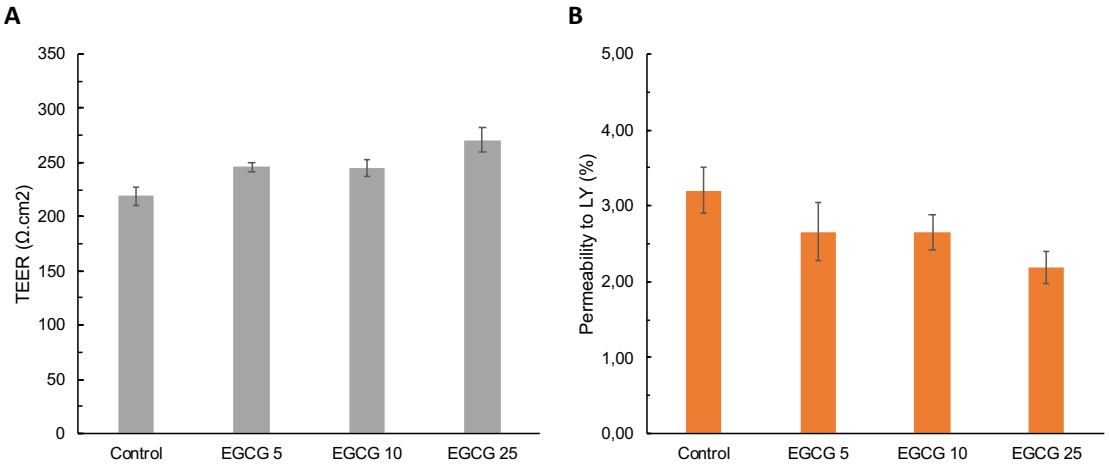

Fig. 39 - Permeability changes of Caco-2 cell monolayers upon treatment with different concentrations of EGCG for 24h. (A) Variation of transepithelial electric resistance (TEER) values after incubation of Caco-2 cells with EGCG; (B) Permeability of the Caco-2 cell barrier to lucifer yellow (LY) at the end of the transepithelial transport experiment.

In the last few years, specific research has been devoted to the evaluation of polyphenols as promising protective factors and regulators of epithelial homeostasis and intestinal barrier function [313]. Despite the advancements that have been made regarding the biological effects exerted by polyphenols at both intestinal and systemic levels, at present, the exact mechanisms by which these compounds modulate the intestinal barrier function remain unclear. The main experimental evidences linking polyphenols to regulatory pathways involved in intestinal permeability originate fundamentally from *in vitro* studies, most of which performed on the Caco-2 cell line as a model of the intestinal barrier. These studies have shown the ability of some polyphenols (*e.g.* berberine, quercetin, kaempferol, genistein, polyphenol-rich extracts, *etc.*) to increase the TEER across cellular monolayers, confirming the integrity and functional permeability of the membranes [313-318]. In addition, polyphenols were also found to increase the expression and cytoskeletal association of numerous tight junction proteins such as zonula occludens (ZO) proteins, occludin, and the family of claudins, to restore ZO-1/occludin assembly and to inhibit different kinases (PKC, MLCK) involved in phosphorylation of proteins controlling intestinal permeability [319-325]. These results are partially in line with the findings obtained from animal models, showing the capacity of polyphenols to improve intestinal permeability not only by increasing the expression of tight junction proteins but also by up- or downregulating key genes involved in the inflammatory process (*e.g.* AMPK, ERK and NF-κB) [313]. With regard to human studies, although scarce, recent literature suggests that polyphenols may modulate intestinal cell

function through a number of direct and indirect effects, including the impact on the gut microbial ecosystem and immune system [326]. From the data available, it seems that polyphenols activity is a consequence of multiple mechanisms, which may also depend upon the type and amount of compounds considered. Even though our findings are in line with previous experimental observations, which, as a whole, would explain the increase on TEER values and decreased LY permeability of Caco-2 cells pre-treated with EGCG (*Fig. 39*), it is difficult, based on these data, to come up with an explanation that rationalizes the decreased transepithelial translocation of the 32-mer peptide, taking into account that most studies appear to indicate that it is transported by transcytosis and not by a paracellular pathway. Therefore, it appears that EGCG is somehow able to modulate the basolateral delivery of the 32-mer peptide, by mechanisms, that so far, remain elusive. These may either involve the modulation of signal transduction pathways regulating intracellular vesicular trafficking or an enhanced lysosomal degradation of luminal antigens. Whatever be the case, further studies elucidating the detailed mechanisms by which EGCG and other polyphenols regulate cell metabolism under both normal and pathological conditions will shed light on these potentially novel roles for EGCG in promoting gut health and preventing the onset of CD through modulation of the epithelial transport of gluten reactive peptides into the lamina propria.

4. Conclusions

The world of polyphenols has fascinated researchers over the past decades, and *in* vitro, cell-based, animal and human studies have attempted to unravel the mechanisms underlaying their different bioactivities, which we now know that go far beyond their antioxidant potential. Indeed, there is an emerging acceptance that polyphenols, as well as their metabolites, exert modulatory actions through interaction with protein receptors or enzymes involved in signal transduction pathways, some of which directly implicated in human disease conditions. Herein, the interaction between some common food flavanols and oligomeric procyanidins towards the main bioactive CD peptide has been thoroughly characterized by means of different spectroscopic techniques and *in* silico simulations. These provided valuable insights on their binding affinity and specificity as well as the binding epitopes on both 32-mer peptide and polyphenol molecules. According to our findings, the overall reactivity of the 32-mer towards polyphenols can be explained by the combination of a set of structural and environmental factors, some

of which already explored throughout the manuscript. One of the factors that has not yet been addressed is the solvent pH (7.4). It is well known that the medium pH is directly involved in the interaction between tannins and proteins/peptides since it affects their degree of ionization [177]. In general, the degree of binding and precipitation is maximal close to the isoelectric point (in this case 5.9) where electrostatic repulsions between proteins or peptides are minimized. In fact, the 32-mer peptide net charge at pH 7.4 is zero and therefore, without repulsion, newly formed colloidal particles tend to aggregate together and precipitate. So, although in this system the initial polyphenol binding may have some kind of specificity, the subsequent aggregation process seems to be mainly due to superficial charge effects. Instead of two binding sets of interaction sites we can thus probably consider two entropy-driven interaction events. In general, the interactions observed in this study are similar to the interactions between polyphenols and proline-rich salivary proteins in that they are the result of cooperative binding mechanisms involving a combination of both enthalpic and entropic phenomena.

Additionally, it has been shown, for the first time and under near physiological conditions, that nutritional doses of EGCG and oligomeric procyanidins are able to reduce the transepithelial translocation of the 32-mer peptide *in vitro,* through mechanisms that could either involve their physical interaction or other regulatory pathways that are still unexplored. Taking into account the ever-growing demand for non-invasive strategies able to modulate critical regulatory functions in human health and disease, one may see that these findings clearly open unprecedented new perspectives towards the use of dietary polyphenols as an alternative, and safe, nutraceutical intervention able to mitigate the symptoms and immune responses associated with CD. Still, only the tip of the iceberg is hitherto understood so that further research needs to be done in order to fully understand the molecular and cellular mechanisms that underlie the pharmacological and CD-preventive properties of dietary polyphenols.

CHAPTER II

In vivo efficacy of polyphenols in a transgenic mouse model of CD enteropathy

1. Introduction

Over the last century, animal models have been used to address a variety of scientific questions, from the study of human physiology and pathology to the development and assessment of novel therapies (*e.g.* drugs, vaccines, antibodies, hormones, surgical procedures, etc.) to enhance and promote human health [327]. The use of animals is not only based on the vast commonalities in the biology of most mammals, but also on the fact that some human diseases also affect other animal species [328]. It is particularly the case for most infectious diseases and for a variety of common conditions such as type I diabetes, hypertension, allergies, cancer, epilepsy, myopathies and so on [329]. Unsurprisingly, a large number of innovations in basic science and medical research have been possible thanks to the observations and testing on animal models, many of which led to Nobel Prize awards.

Recently, large efforts have been devoted to the development of pertinent mouse models harboring the risk factors for human CD in order to explore pathogenic hypotheses, and also with the goal to design pre-therapeutic models that could be used to test innovative therapies and nutritional approaches [330]. Despite the advances that have been made in the past few years and the valuable insights they provided regarding the complex immunological jigsaw of CD pathophysiology, modeling this complex multifactorial disease has proven to be a very challenging task, particularly when it comes to the remarkable resistance of mice to develop a celiac-like enteropathy [331-334]. Accordingly, although humanized mice expressing the HLA-DQ2.5 and HLA-DQ8 heterodimers showed a gliadin-specific Th1 cell-mediated response similar to CD, the induced immunophenotype wasn't sufficient to switch off the oral tolerance to gluten and trigger a CD enteropathy, even when amplified with TG2 activation by *S. typhimurium* coinfection [335]. For this reason, additional mechanisms are necessary to break tolerance, stimulate the expansion and activation of cytotoxic IELs, and ultimately induce intestinal tissue damage and pathology [336].

One of the first *in vivo* studies attempting to reproduce CD was performed by *Black* and colleagues (2002) who studied $CD4^+$ T-cell responses to gluten and gliadin peptides in a double transgenic mouse model expressing the HLA-DQ8 and human CD4 genes [337]. Although hCD4/ DQ8 mice immunized in the footpad with crude gluten and complete Freund's adjuvant exhibited a strong proliferative T-cell response in the

draining lymph nodes, they failed to develop enteropathy *i.e.* there wasn't any villous flattening, crypt hyperplasia, and IEL infiltration of the proximal intestine. This issue was later addressed by *D'Arienzo et al.* (2009) who developed a mouse model of gliadin-specific enteropathy based on the synergistic action of DQ8 expression, gliadin sensitization and inhibition of intestinal COXs using indomethacin [338]. COXs are enzymes involved in the synthesis of prostaglandins from arachidonic acid [339]. Prostaglandin E2 (PGE_2), in particular, plays a critical role in guiding and governing various aspects of the inflammatory response. This prostaglandin is endowed with both pro-inflammatory and immunosuppressive properties, the latter of which contribute to the resolution phase of acute inflammation, facilitating tissue regeneration and the return to homeostasis [340, 341]. The downregulatory effects of PGE_2 are normally operative at the intestinal level but not in the systemic immune system, as evidenced by the high levels of PGE_2 produced by mononuclear cells in the lamina propria [342]. In this enteropathy model of CD, indomethacin-treated DQ8 mice showed a Th1-like gliadin-specific immune response, associated to a significant reduction of villus height without any crypt hyperplasia and expansion of IEL. Additionally, biochemical assessment of the intestinal lesion revealed increased mRNA levels for two extracellular matrix proteins, Lamb3 and Adamts2, and enhanced activities of metalloproteinases MMP-1, -2 and -7, involved in lamina propria remodeling [338]. More recently, it has been found that gliadin intake, in combination with COX inhibition and in the absence of mucosal immunization, was sufficient to cause a basal inflammatory status and an oxidative stress condition in the small intestine of DQ8 mice, characterized by a reduction of villus height, increased crypt depth, increased number of lamina propria-activated macrophages, and high basal interferon-γ secretion in mesenteric lymph nodes [343]. These architectural changes were followed by the development of a humoral response towards gliadins and tissue transglutaminase at the end of 30 days. No significant differences were observed among mice treated with the albumin and globulin fraction, which failed to generate any kind of mucosal damage or adaptive response.

In this study, we took advantage of the robustness of this long-term enteropathic CD model to exploit the health-promoting properties and applicability of dietary polyphenols as an alternative strategy to block gluten toxicity, something that is much needed to alleviate the burden of a life-long GFD or to treat severe cases that have become refractory to this regimen. Indeed, if one takes into account that in CD, oxidative stress mediates most of the cytotoxic effects induced by gliadin peptides on intestinal epithelial cells including apoptosis, impaired cell proliferation and tight junction disassembly and that polyphenols are well-known inducers of the Keap1/Nrf2 system-mediated

antioxidant and detoxifying enzymes, it is undeniable that their employment on a CD context could potentially provide clear health benefits and as such it deserves further research [344, 345]. In this particular case, in addition to the renowned epigallocatechin gallate (EGCG), we have also extracted and used two different polyphenol rich-extracts: one obtained from the green tea leaves of *Camellia Sinensis* cultivated in Portugal and the other one from the seeds of a common grape vine, *Vitis vinifera*. Taken together, this work constitutes a highly relevant breakthrough as it provides the fundamental basis concerning the significance and nutritional potential of natural polyphenols to be used in the development of innovative functional food formulations aimed at CD individuals who's a GFD is not indicative of a better quality of life.

2. Material and methods

2.1. Reagents

EGCG was purchased from Biopurify Phytochemicals *Ltd.* (Chengdu, Sichuan, China) while catechin, the Folin-Ciocalteu´s phenol reagent, 5,5'-dithio-bis (2-nitrobenzoic acid) (DTNB), reduced nicotinamide adenine dinucleotide phosphate (NADPH) and chlorodinitrobenzene (CDNB) were purchased from Sigma-Aldrich.

2.2. Extraction of Green Tea Catechins

Twenty grams of dried green tea leaves of *Camellia Sinensis* from Portuguese origin (Gorreana, Portugal) were grinded and extracted three times with 500 mL of 80% (v/v) ethanol for 1 hour at room temperature and under argon atmosphere. Between extractions, the slurry mixtures were centrifuged at 12.000 g for 20 min at 4°C and the resulting supernatants combined. The organic solvent was then removed using a rotary evaporator under reduced pressure resulting in a highly dense green residue. This residue was subsequently extracted three times with an equal volume of chloroform to remove methylxanthines and chlorophylls. Then, ethyl acetate was added in the same proportion of aqueous solution to extract green tea catechins, being this step repeated three additional times. After ethyl acetate evaporation, the resulting catechin-rich residue was loaded into an *Oasis HLB 35 cc Vac* cartridge from Waters and washed with 5%

acetonitrile/1% acetic acid to remove sugars, organic acids, and other polar compounds. The phenolic fraction was subsequently recovered by eluting the cartridge with an acetonitrile/methanol mixture (50:50, v/v). Later, the organic solvent was evaporated and the resulting green tea extract (GTE) freeze-dried.

2.3. Fractionation of Grape Seed Procyanidins

Oligomeric procyanidins were fractionated from a commercial grape seed extract of *Vitis vinifera* (*Vitisol™*, Berkem) through a TSK-Toyopearl HW-40(s) gel column (100 mm x 10 mm inner diameter) at 0.8 mL.min^{-1} using methanol as eluent. The first five fractions were obtained after elution with pure methanol for 15 min (1st), another 15 min (2nd) and 45 min (3rd). Deionized water was added to each of these fractions after which the organic solvent was eliminated in a rotary evaporator under reduced pressure at 30 °C and freeze-dried. Upon LC-ESI-MS/MS analysis (see below), the first two fractions were discarded as they contained only catechins and phenolic acids.

2.4. LC-ESI-MS/MS and HPLC Analysis

Green tea catechins and the oligomeric procyanidin fractions were analyzed by LC-MS/MS on an LTQ-Orbitrap XL mass spectrometer coupled to an Accela HPLC system (ThermoFisher Scientific). Separations were performed on a Hypersil BDS C18 column (150 mm length, 4.6 mm inner diameter, 3 µm particle size) (ThermoFisher Scientific). The mobile phases consisted of (A) water/0.1% formic acid (v/v) and (B) acetonitrile/0.1% formic acid (v/v). The program for gradient elution started at 95% solvent A and 5% solvent B and increased linearly to 85 % solvent A and 15% solvent B in 15 min. In the following 45 min, the percentage of solvent B increased from 15% to 30%, after which the column was washed and re-equilibrated. In these analyses, the column was kept at 35°C, the flow rate was 250 µL/min and the injection volume 25 µL (previously filtered through 0.45 µm *Millipore* filters). All mass spectra were acquired in a negative ionization and data-dependent mode; the instrument executed one MS scan followed by an MS/MS scan for each of the four most intense peaks in a mass-to-charge ratio (*m/z*) range from 120 to 2000. The relative collision energy was set to 45% in collision-induced dissociation mode. The electrospray conditions were as follows: ion

source voltage of 3.10 kV, source current of 100 μA, capillary temperature of 275 °C, capillary voltage of 50 V, sheath gas flow of 30 arbitrary units and the auxiliary gas flow of 10 arbitrary units. *Xcalibur* software (ThermoFisher Scientific) was used for the collection and data analysis.

The green tea extract was additionally analyzed by HPLC in order to quantify its EGCG content. These analyses were performed on Dionex UltiMate™ 3000 (ThermoFisher Scientific) using the same column, chromatographic method and mobile phases as in the LC-ESI-MS/MS analysis. The absorbance was monitored at 280 nm on an UltiMate™ diode array detector (DAD).

2.5. Total Phenolic Content

The total phenolic content of green tea and procyanidin extracts was determined following the *Folin-Ciocalteu* method adjusted to a microscale [346]. In an *eppendorf* tube, 610 μL of distilled water, 15 μL of sample extract dissolved in methanol, and 75 μL of *Folin-Ciocalteu* reagent were mixed. After 30 s, 0.3 mL of aqueous 20% Na_2CO_3 and 0.3 mL of distilled water were added. The mixture was mixed for 30 s and allowed to stand at room temperature in the dark for 30 min. The absorbance was read at 750 nm, and the total polyphenol concentration was calculated from a calibration curve, using gallic acid as standard. The results were expressed as gallic acid equivalents (GAE) *per* 100 g of extract.

2.6. *In vivo* Studies

2.6.1. Protein Preparation

Flour from wheat cultivar *Sagittario* was defatted twice with petroleum ether for 30 min. Albumins and globulins were extracted by resuspending the defatted flour in 0.4 M NaCl in 0.067 NaH_2PO_4 buffer at pH 7.6. The suspension was shaken for 10 min and centrifuged at 15,000 g for 15 min. The supernatant containing Alb/Glob was discarded. Gliadin was extracted from the pellet by adding a water/ethanol mixture to a final concentration of 70% (v/v) ethanol. The suspension was shaken for 45 min and centrifuged at 15,000 g for 10 min. The supernatant was freeze dried and stored at -

80°C. For in vivo experiments, wheat proteins were suspended at 1 mg.mL^{-1} in 200 mM acetic acid.

2.6.2. Experimental Design

Transgenic DQ8 mice, expressing the HLA-DQ8 molecule in the absence of endogenous mouse class II genes, were maintained in pathogen-free conditions on an accredited animal facility (Accreditation No. DM.161/99). Animals (*n* = 45) were reared on a GFD for several generations and used at the age of 6-12 weeks. All experiments were approved by the Italian Institutional Review Committee and performed in accordance with European regulations (EU Directive 2010/63/EU).

Herein, two sets of experiments were designed: a short-term and long-term treatment with both gliadins and polyphenols. For the short-term treatment, 25 animals were divided into 6 different groups: the first group (*n* = 5) was left untreated and served as negative control; the other ones (*n* = 4 each) were intragastrically administered with 25 mg.kg^{-1} doses of wheat gliadins on days 0, 3, 5, and 7. A previously established sub-enteropathic dose of indomethacin (1.5 mg/100 mL, Sigma-Aldrich) was given in the drinking water (changed every 3-4 days) for 10 days, after which they were euthanized. The effects produced by dietary supplementation with EGCG was studied in 4 of these 5 groups (one of them was used as a positive control): the first 3 groups received (*per os*) 25, 50 or 100 mg.kg^{-1}.day^{-1} of EGCG, two weeks before being separately treated with both gliadins and EGCG at their corresponding doses; the remaining group, on the other hand, was co-administrated, by intragastric gavage, with a mixture containing wheat gliadins and EGCG at 50 mg.kg^{-1}.day^{-1}, without any pre-treatment. With this slightly different protocol, it was intended to evaluate whether the complexation of EGCG with gliadin proteins would attenuate the development of a gluten-mediated enteropathy, when compared to the pre-conditioning of animals for 2 weeks.

Regarding the long-term treatment, a total of 20 DQ8 animals were divided into 4 different groups (*n* = 5). Three of these groups were pre-treated with EGCG, green tea catechins (GTE) or oligomeric procyanidins (PRC) at 50 mg.kg^{-1}.day^{-1}, two weeks before they were given gliadins three times a week for 30 days. The administration of polyphenols continued during this time period after which the animals were sacrificed. As for the short-term treatment, indomethacin was given in the drinking water (0.75 mg/100 mL) and changed every 3-4 days. The remaining group was used as a positive control for the long-term administration of gliadins. Of note, it must be underlined that the dose of green tea catechins used in this study was within the average dietary intake

values reported for humans. Accordingly, when expressed in a human equivalent dose, 50 $mg.kg^{-1}.day^{-1}$ in mice (20 mg) corresponds to approximately 244 $mg.day^{-1}$ in humans (60 Kg) or alternatively, to less than 200 mL of brewed green tea (assuming that each 240 mL serving provide an estimated 304 mg total catechins) [347]. The average daily intake of EGCG through green tea consumption, on the other hand, can reach approximately 560 $mg.day^{-1}$ for individuals consuming an average of three 8 oz. cups of green tea *per* day [306].

Recently it has been estimated that the mean dietary intake of proanthocyanidins (comprising both oligomers and polymers) in Mediterranean countries was 160 $mg.day^{-1}$ [348]. In contrast to Europe, adults in the USA consume lower amounts of total flavonoids, flavanols and proanthocyanidins, respectively. Accordingly, latest data from a 24 h food recall in a cohort of 5420 people above 20 years old indicated a mean total flavonoid intake of 251 $mg.day^{-1}$ of which 81% comprised flavanols mainly derived from tea [349]. The intake of oligomeric proanthocyanidins was estimated to range between 60 and 95 $mg.day^{-1}$ with apples, chocolate products, grapes, tea, legumes and wine as the major food sources [208, 350]. Therefore, according to these data, it may be seen that the dose of oligomeric procyanidins used in this study exceed the one that is normally achieved through food consumption but still realistic in a context of dietary supplementation.

2.6.3. Morphometry and Immunohistochemistry Analysis

Tissue fragments of the small intestine were collected and placed on black filter paper covered with normal saline. Their mucosal surfaces were immediately examined under a stereomicroscope. Tissue was then embedded in OCT compound, snap frozen in liquid nitrogen, and prepared for histological and immunohistochemical evaluation. Cryostat sections (5 μm) were air dried at room temperature, fixed in acetone, and tested with rat anti-mouse CD3 antibody (Bio-Rad AbD Serotec). Sections were then incubated with rabbit anti-rat serum (Agilent Dako) and finally with rat peroxidase anti-peroxidase complex (Rockland Immunochemicals). Slides were developed with 2-amino-9-ethyl-carbazole (Sigma-Aldrich). Nonspecific binding was monitored by omitting the primary antibody. Sections were finally stained with Mayer's hematoxylin and mounted. Villus height and crypt depth were measured with an ocular micrometer associated to a light microscope (Zeiss). Twenty to thirty individual measurements were made on each slide, and average crypt depths and villus heights were calculated. The density of

intraepithelial cells expressing CD3 was determined by counting the number of stained cells per millimeter of epithelium.

2.6.4. Real-Time PCR Analysis

RNA was extracted from the small intestinal samples using the TRIzol reagent (Invitrogen). cDNA was prepared by reverse transcription. Real-time PCR was performed on a CFX96 Touch Real-Time PCR Detection System (Bio-Rad Laboratories) using a total of 100 ng of cDNA, 300 nM of gene specific primers, *iTaq™ Universal SYBR Green Supermix* (Bio-Rad) and the following reaction conditions for 39 cycles: 95°C for 30 s, 54.6°C (L-32), x for 30 s, and 72°C for 40 s. Gene expression levels were calculated using the $\Delta\Delta$Ct method (where Ct is threshold cycle) and presented as fold changes after normalization to the L-32 housekeeping gene [351].

2.6.5. Duodenum Collection and Protein Extraction

Upon animal killing, 2 cm of proximal duodenum was flushed with ice-cold buffer (50 mM Tris-HCl pH 7.6, 150 mM NaCl; TBS) to remove fecal material, cut longitudinally and opened flat. Tissue samples were cut into pieces, snap frozen in liquid nitrogen and stored at −80 °C. Protein extracts were prepared in TBS supplemented with 0.01 % Triton X-100 and protease inhibitors after which they were used for biochemical (GSH) and enzymatic (glutathione S-transferases, GST; glutathione reductase, GSR, NAD(P)H quinone dehydrogenase 1, NQO1, glucose-6-phosphate dehydrogenase, G6PD) analysis.

2.6.6. RedOx Status Assessment

Total thiols (GSH_{tot} = GSH + GSSG), were quantified through enzymatic recycling of glutathione (GSH) from glutathione disulfide (GSSG) by GSR in the presence of NADPH [352]. In this assay, GSH reacts with DTNB [5,5'-dithio-bis (2-nitrobenzoic acid)] to produce the TNB (5-thio-2-nitrobenzoic acid) chromophore, which has a maximal absorbance at 412 nm, and GS-TNB (glutathione adducts of GSH). The disulfide product (GS-TNB) is then reduced by GR in the presence of NADPH, recycling GSH back into the reaction. The rate of change in absorbance (ΔA_{412} $nm.min^{-1}$) was linearly proportional to the total concentration of GSH. Upon normalization to the protein content, the concentration of GSH in tissue samples was expressed as $nmoles.mg^{-1}.min^{-1}$.

The activities of phase 2 enzymes (GST, GSR, NQO1) and G6PD were spectrophotometrically assayed in intestinal extracts by using standard protocols [353-356]. In particular, NQO1 and GSR activities were expressed as nmoles of NADPH $mg^{-1}.min^{-1}$ while GST and G6PD activities were expressed as nmoles of chlorodinitrobenzene (CDNB) $mg^{-1}.min^{-1}$ and nmoles of $NADP^+$ $mg^{-1}.min^{-1}$, respectively.

2.6.7. Statistical Analysis

All data, obtained from triplicate analyses, were presented as mean ± standard deviation. Groups were compared by the Student's *t* test, and $P < 0.05$ was considered as significant.

3. Results and Discussion

3.1. Identification of Green Tea Catechins and Grape Seed Procyanidins

The total ion chromatogram obtained by mass spectrometry analysis of the green tea extract (GTE) is displayed in *Fig. 40*. Its main phenolic compounds, listed in *Table 5*, were identified based on their mass-to-charge ratio values (*m/z*), retention time, fragmentation pattern, and comparison to previous reports [357-360].

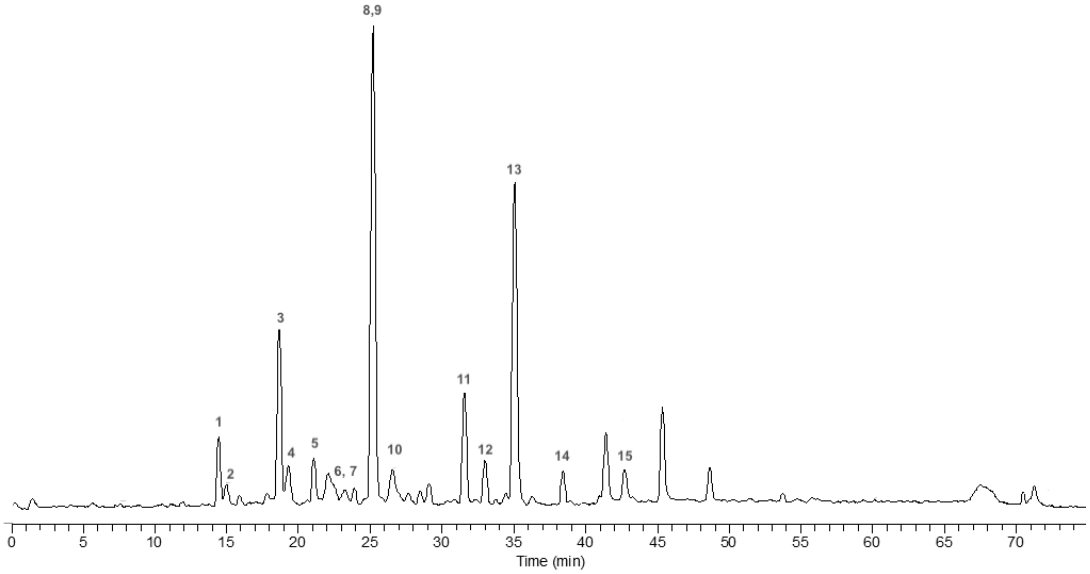

Fig. 40 - Total ion chromatogram (TIC) of GTE, acquired by LC-MS. Its main phenolic compounds were numbered and listed in *Table 5*.

Table 5 - Identification of the most important phenolic compounds of GTE, as revealed by LC-ESI-MS/MS analysis.

Compound	Name	$[M-H]^-$ (m/z)	MS^2 (m/z)
1	Gallocatechin	305	179, 219, 221, 261
2	Prodelphinidin B4	609	305, 423, 441, 483
3	Epigallocatechin	305	179, 219, 221, 261
4	(E)GC-(E)C dimer	593	289, 407, 425, 451
5	Catechin	289	203, 205, 245
6	(E)C-(E)C dimer	577	289, 407, 425, 451
7	(E)C-(E)GC-O-gallate	745	423, 575, 593
8	Epigallocatechin-3-O-gallate	457	169, 305, 331
9	Epicatechin	289	203, 205, 245
10	Gallocatechin-3-O-gallate	457	169, 305
11	Epigallocatechin-3-O-(3- or 4-O-methyl) gallate	471	183, 305
12	Quercetin-3-O-rutinoside	609	255, 271,301
13	Epicatechin-3-O-gallate	441	169, 289
14	Kaempferol-3-O-rutinoside	593	285, 447
15	Epicatechin-3-O-(4-O-methyl) gallate	455	183, 289

As it can be seen from *Table 5*, the obtained GTE was particularly rich in catechins and gallocatechins, some of which occurring in a galloylated and/or acylated form. Of these, epigallocatechin-*3*-*O*-gallate (EGCG), epigallocatechin-*3*-*O*-(*3- or 4*-*O*-methyl) gallate

and epicatechin-*3*-*O*-gallate (ECG) were found to be the most abundant polyphenols, as revealed by HPLC analysis (*Fig. 41*). Using an external standard calibration curve, the concentration of EGCG has been determined and corresponded to approximately 490 milligrams of EGCG *per* gram of GTE (almost half of the total compounds) or, alternatively, to 3.7 grams of EGCG *per* 100 grams of dry weight tea leaves.

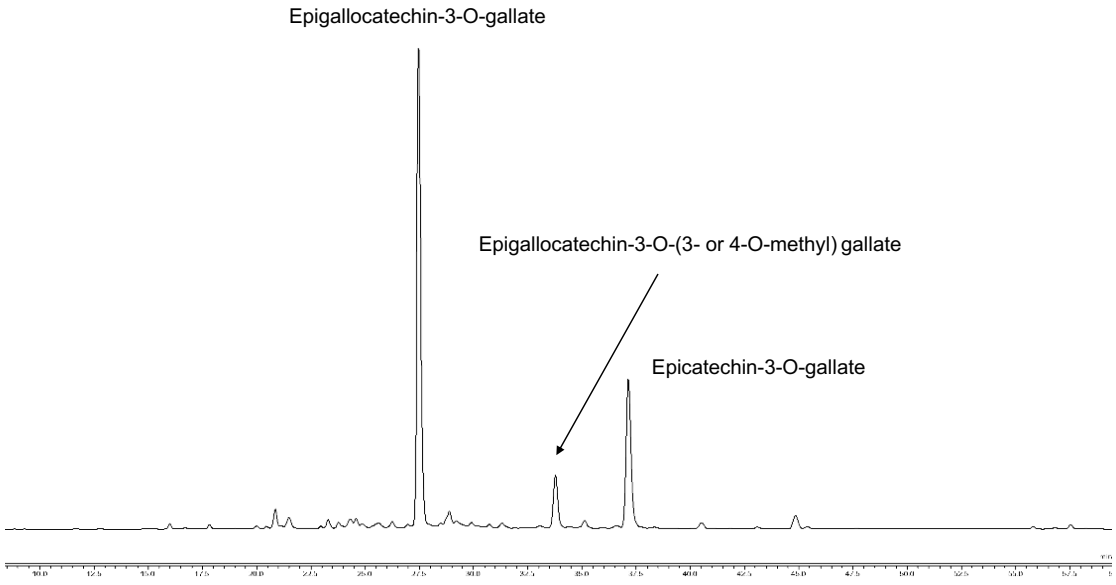

Fig. 41 - Chromatographic profile, acquired by HPLC detection at 280 nm, of the GTE.

Other minority compounds were also detected including prodelphinidin B2 (or B4) 3-O-gallate, myricetin derivatives and dimeric species (galloylated or not) between (epi)catechin and (epi)gallocatechin (*data not shown*). Their concentration, however, was residual and near the baseline level.

In general, green teas contain more catechins than most other teas, *i.e.* white, oolong and black teas, mainly because of the way they are processed after harvesting [361]. In fact, depending on numerous factors such as the genetic strain, climatic conditions, soil properties, plucking season, position of the leaf, processing and storage, the catechin content between green tea varieties and brands can be significantly different [362]. In this case, we have used a *Hysson* green tea from Gorreana (Azores, Portugal), which, according to its label, was produced by harvesting the top three leaves of the tea plant *Camellia Sinensis* in July and August. Among the literature, many studies have already demonstrated the relationship between green tea quality and its content in caffeine,

theanine and essential minerals [363, 364]. Nevertheless, because polyphenols are the most abundant and nutritionally significant group of bioactive compounds in green tea, they have been seen as the main determinants of tea quality and price. Accordingly, and even though it has not been established yet to what extent the quality of green teas is different according to their specific catechin content, some of the currently available studies appear to indicate that high quality green teas have high levels of EGCG and ECG and low levels of epigallocatechin (EGC) and epicatechin (EC) [365, 366]. Therefore, based on these observations, the predominant presence of both EGCG and ECG on the GTE provides indication that the starting plant material used in this study was of good quality and had a high antioxidant potential [367, 368].

Regarding the oligomeric procyanidins, these were obtained by column fractionation of a commercial grape seed extract, yielding three fractions containing procyanidins with increasing polymerization degrees [369]. The chromatographic profile and polyphenol composition of the procyanidin fraction (PRC) used in this study is displayed in *Fig. 42* and *Table 6*, respectively. This extract was mainly composed by C_4-C_8 and C_4-C_6 dimeric procyanidins as well as some of its galloylated derivatives and trimers.

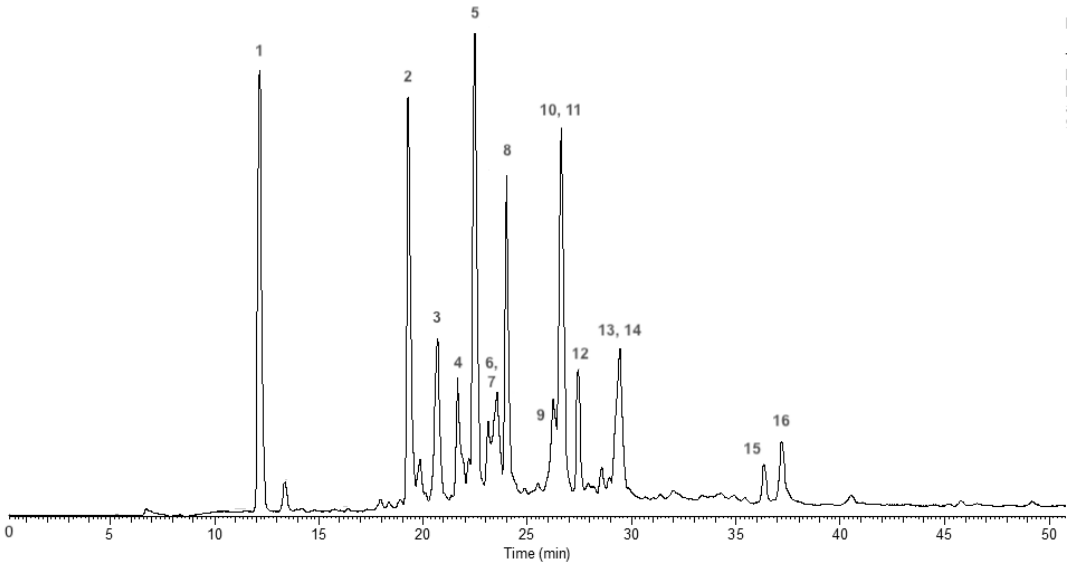

Fig. 42 - Total ion chromatogram (TIC) of PRC, acquired by LC-MS. Its main phenolic compounds were numbered and listed in *Table 6*.

Table 6 - Identification of the most important phenolic compounds of PRC, as revealed by LC-ESI-MS/MS analysis.

Compound	Name	$[M-H]^-$ (m/z)	MS^2 (m/z)
1	Gallic acid	169	-----
2	Procyanidin B1	577	289, 407, 425, 451
3	Procyanidin B3	577	289, 407, 425, 451
4	Procyanidin trimer	865	289, 407, 695
5	Catechin	289	203, 205, 245
6	Procyanidin B6	577	289, 407, 425, 451
7	Procyanidin B4	577	289, 407, 425, 451
8	Procyanidin B2	577	289, 407, 425, 451
9	Procyanidin B8	577	289, 407, 425, 451
10	Epicatechin	289	203, 205, 245
11	Galloylated procyandin dimer	729	528, 544, 580, 589, 697, 741
12	Procyanidin C1	865	289, 407, 577, 695
13	Procyanidin B7	577	289, 407, 425, 451
14	Procyanidin B2 gallate	729	289, 407, 451, 559, 577
15	Procyanidin B8	577	289, 407, 425, 451
16	Epicatechin-3-O-gallate	441	169, 289

The total phenolic content of both GTE and PRC was determined by using the Folin-Ciocalteu reagent [370]. This assay relies on the transfer of electrons in alkaline medium from phenolic compounds to phosphomolybdic/phosphotungstic acid complexes, that are determined spectroscopically at approximately 750 nm. Although the electron transfer reaction is not specific for phenolic compounds, this standardized method has been widely used as a measure of the antioxidant capacity of polyphenol-rich extracts and supplements using gallic acid as a standard compound [371]. Accordingly, the total phenolics of the GTE and PRC was 665 ± 50 and 597 ± 42 mg of GAE *per* 100 mg of extract, respectively. The difference between these two preparations is probably related to the high concentration of EGCG in GTE, which, by having a gallate group esterified at C_3 and an ortho-trihydroxylated B ring, makes it one of the most powerful antioxidants found in nature.

3.2. EGCG intake prevents small intestinal architectural changes in gliadin-treated DQ8 mice

The effects produced by EGCG intake on the small intestinal morphology of DQ8 mice challenged with indomethacin and wheat gliadins for 10 days was evaluated by

administering, *per os*, 25, 50 and 100 mg.Kg^{-1}.day^{-1} of EGCG when on a pre-treatment regimen or, alternatively, 50 mg.Kg^{-1}.day^{-1} when co-administered with gliadin proteins (*Fig. 43*).

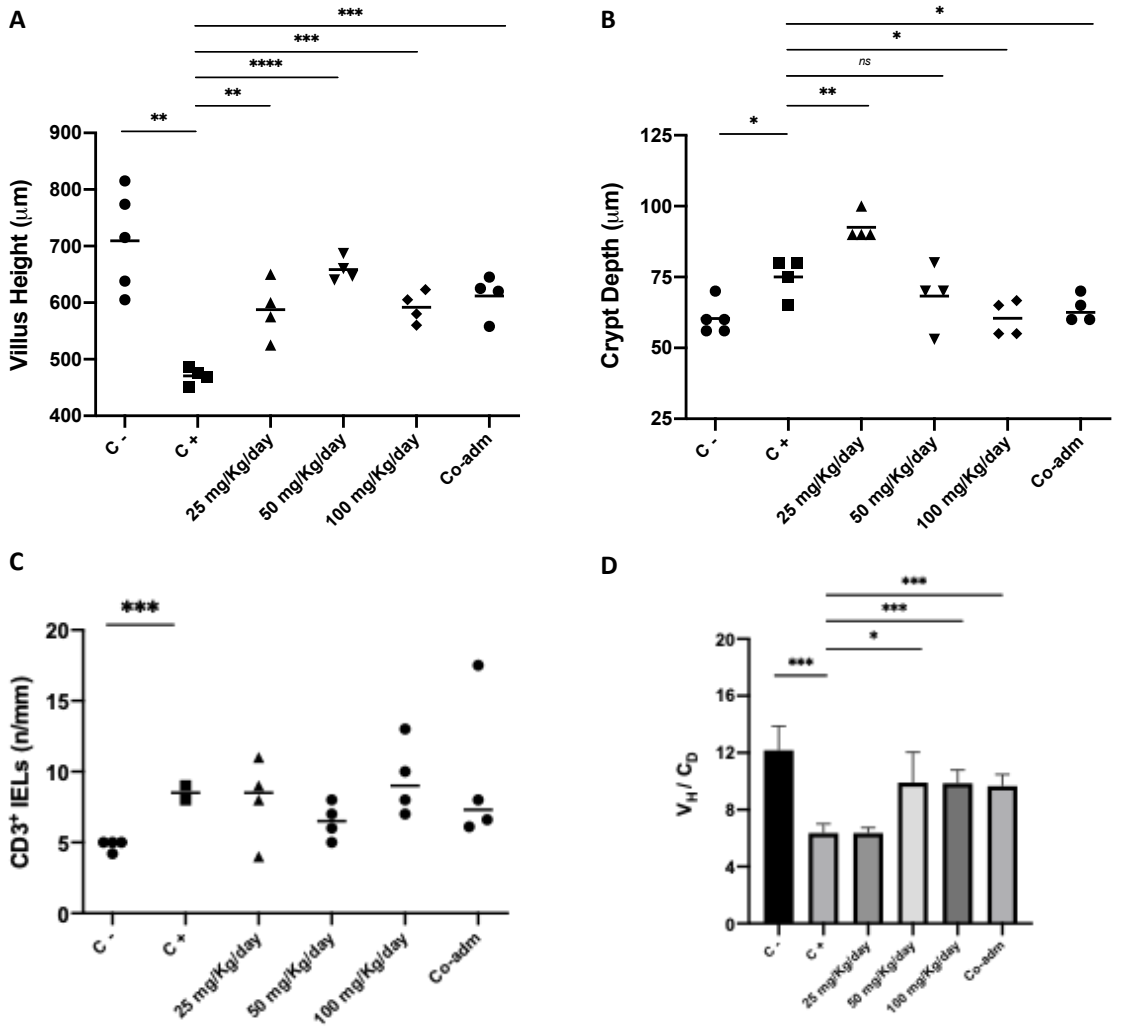

Fig. 43 - Morphometric assessment of villus height (A), crypt depth (B), number of IEL (C) and villus-to-crypt depth ratio (D) among the different experimental animal groups. The bars on (A), (B) and (C) represent mean values; in (D) the results were expressed as mean values ± standard deviation (SD). **p*<0.05, ***p*<0.01, ****p*<0.001, *****p*<0.0001. C$^-$, untreated controls; C$^+$, positive controls *i.e.* mice treated with indomethacin and wheat gliadins for 10 days.

Histological examination of the intestinal biopsy specimens from mice receiving only gliadin and indomethacin (C$^+$) revealed that their villi was significantly shorter in comparison to the untreated control group (C$^-$, *Fig.* 43A) whereas the crypt depth and number of intraepithelial lymphocytes (IEL) was significantly increased (*Fig. 43B* and *C*). These results are in line with previous observations showing that in the absence of COX

activity, the intake of gliadins by DQ8 mice triggers the development of a mucosal lesion similar to the one observed in CD [343]. Nevertheless, and differently to what happens on a CD background, the transcript levels of IFN-γ at the intestinal level remained unchanged (*data not shown*), thus suggesting that, in this model, the observed mucosal damage was not mediated by an exacerbated gliadin-specific Th1 response. As for the effects provided by dietary supplementation with EGCG, it was found that when given on a regular basis, EGCG was able to attenuate some of the morphological changes induced by subenteropathic doses of indomethacin and gliadins (*Fig. 43*).

According to *Fig 43A*, all the three doses of EGCG were capable of partially restoring the villi height of DQ8 mice, with almost no statistical difference between treatments. By lengthening the villi, one may expect the intake of EGCG to increase the total absorptive area at the villus surface, thus resulting in more satisfactory enzyme action, nutrient transport and growth efficiency [372]. Of these treatments, the pre-administration of 50 $mg.Kg^{-1}.day^{-1}$ of EGCG ended up being the most effective dose as it increased the intestinal villi from 66% to nearly 93% of their normal size, without any apparent change on crypt depth. This last observation contrasts, for example, to what happened when mice were fed with 25 $mg.Kg^{-1}.day^{-1}$ of EGCG. Indeed, in this particular case, the intestinal crypts became deeper which means that the host's intestine is still trying to compensate the villus atrophy elicited by gliadin proteins by expanding the proliferative compartment [373, 374]. Interestingly, even though the intake of 100 $mg.Kg^{-1}.day^{-1}$ of EGCG or its co-administration with wheat gliadins wasn't as effective as 50 $mg.Kg^{-1}.day^{-1}$ on the reestablishment of the villi length (*Fig. 43A*), the mice belonging to these two experimental groups had smaller crypts (*Fig. 43B*) and quite similar villus-to-crypt depth ratio values (*Fig. 43D*). The villus-to-crypt depth ratio is one of the most important histomorphometric parameters of the small intestine because it reflects the turnover rate of the intestinal mucosa *i.e* the metabolic cost associated to its renewal [375]. Under physiological conditions, this is a highly dynamic process, ensured by a complex interplay between proliferation, differentiation and apoptotic events occurring as the IEC migrate from the proliferative zone within the crypts up to the luminal surface and villous tips of the small intestine [376]. Based on the results displayed on *Fig. 43D*, one may see that when DQ8 mice were administrated with 50 or 100 $mg.Kg^{-1}.day^{-1}$ of EGCG, the villus-to-crypt depth ratio was significantly increased, meaning that the turnover rate, and consequent maintenance requirement of the intestinal epithelium was smaller. It thus seems that, in these cases, EGCG supplementation was able to counteract the toxic effects of gliadins by partially restoring the homeostatic equilibrium between cell proliferation at the crypt level and cell apoptosis at the tip of the villus, features that are

essential for the intestine to maintain its integrity and absorptive capacity. Curiously, the co-administration of gliadin proteins with 50 $mg.Kg^{-1}.day^{-1}$ of EGCG in just four days was as effective on the recovery of villi height, crypt depth and villi-to-crypt depth ratio as when it was pre-administrated for a period of 4 weeks, 2 of which coincided with the intragastric administration of gliadins (*Fig. 43*). To the best of our knowledge, this is the first time that it has been shown that, on a CD background, the health benefits provided by dietary supplementation with polyphenols do not exclusively depend on the frequency they are consumed but also on the timing and purpose by which they are introduced *i.e.* as prophylactic agents aiming to increase the intestine's antioxidant and anti-inflammatory defense mechanisms against inadvertent gluten exposure and/or as gliadin-scavenging compounds capable of neutralizing the digestibility and availability of CD-reactive peptides. Indeed, according to our observations, when EGCG was mixed with wheat gliadins before being given to mice by intragastric gavage (at a ratio of 2:1 *i.e.* 1 mg of EGCG + 0.5 mg of protein *per* mice), the solution became immediately turbid as a result of an extensive aggregation between both species. Therefore, it is expected that the bioaccessibility of gliadin proteins to digestive enzymes (whose activity is itself modulated by polyphenols) and subsequent bioavailability at the intestinal level should be limited, an aspect that has been recently demonstrated *in vitro* [238].

3.3. Short-term gliadin intake triggers a compensatory antioxidant response in the small intestine of indomethacin-treated DQ8 mice

Previous studies on this animal model have shown that the intake of gliadins for 10 days was associated to a substantial decline in the intestinal content of GSH and to a downregulation of both the expression and activity of cytoprotective enzymes including GST, HO-1, NQO1 and APEH (acylpeptide hydrolase) [377]. Therefore, on the basis of these results, the effects produced by EGCG on the intestinal redox status of gliadin-treated mice were evaluated in order to dissect the molecular mechanisms behind its protective effect against the gliadin-induced mucosal damage. First, the concentration of total tiols (GSH_{tot}) and GSR activity in intestinal tissue samples of mice receiving the different treatments was measured (*Fig. 44*).

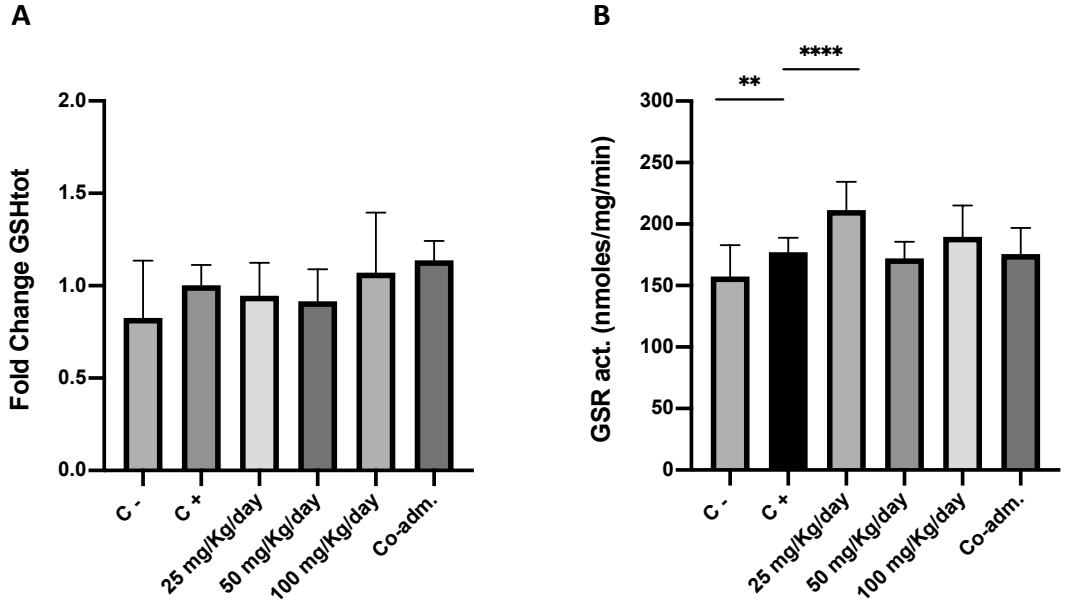

Fig. 44 - Effects of EGCG treatment on the total GSH content (A) and GSR activity (B) in the small intestine of DQ8 mice treated with gliadins and indomethacin for 10 days. The GSH content between experimental groups were normalized to the positive controls and expressed as fold change. Bars represent mean values ± SD from triplicate analyses. **p*<0.05, ***p*<0.01, ****p*<0.001, *****p*<0.0001. C^-, untreated controls; C^+, positive controls.

Surprisingly, there wasn´t any statistically significant change on GSH content among the different experimental groups so that the effect of EGCG ended up being meaningless on this parameter; more importantly, and contrary to what was previously described, it has been found that, in this case, the intragastric administration of gliadins elicited, by itself, a slight increase on GSR activity (P = 0.0018) rather than the expected decrease (a situation that would reflect an impairment of intestinal antioxidant and detoxifying defenses). At this point, the *in vivo* toxicity of this gliadin protein batch was reassessed by determining the activity of some specific cytoprotective enzymes (NQO1, GST, GSR and G6PD) in the small intestine of indomethacin-treated mice (*Fig. 45*).

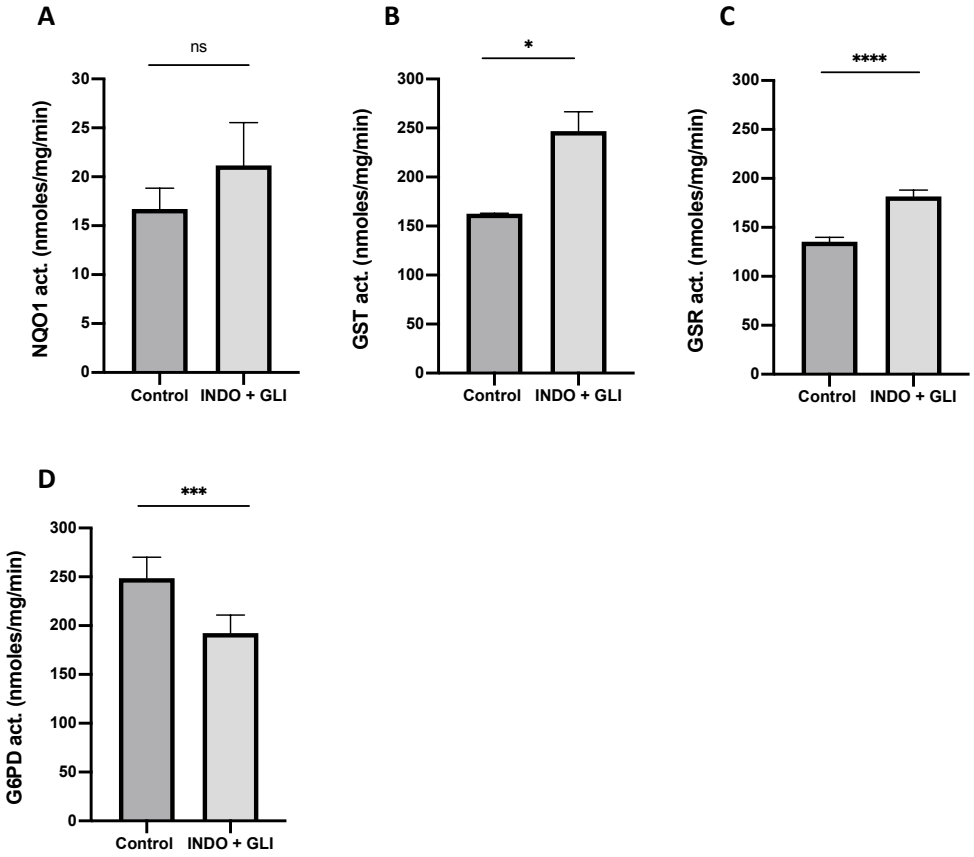

Fig. 45 - Modulatory effects of gliadins intake on the activity of cytoprotective intestinal enzymes including NQO1 (A), GST (B), GSR (C) and G6PD (D). Bars represent mean values ± SD from triplicate analyzes. *p<0.05, **p<0.01, ***p<0.001, ****p<0.0001.

As is can be seen from *Fig 45*, the intake of gliadin proteins, along with the inhibition of COXs, was accompanied by an upregulation of both GST (*Fig. 45B*) and GSR activities (*Fig. 45C*) and a small, yet non-significant, increase on NQO1 activity (*Fig. 45A*). Although unexpected, these results may be interpreted as an attempt of the intestinal mucosa of DQ8 mice to preserve its cellular integrity and tissue homeostasis by orchestrating a compensatory antioxidant response capable of improving its resilience towards the pro-oxidative effects of gliadins. Under these circumstances, enzymes such as GST, GSR or NQO1 are classical examples of some of the antioxidant and detoxifying defense mechanisms that intestinal cells have at their disposal to adapt themselves and respond to stress conditions. GST, for example, is well-known for its the high-capacity metabolic inactivation of electrophilic compounds and toxic substrates [378]. NQO1, on the other hand, is involved, for example, in the reduction of ubiquinone and vitamin E derivatives to their antioxidant forms, protection of proteins from 20S proteasomal degradation and in modulation of NAD(P)H/NAD(P)$^+$ intracellular pools [379].

Interestingly, it was found that upon gliadin treatment, the activity of G6PD went significantly down (*Fig. 45D*). G6PD is the first and rate-limiting enzyme of the pentose phosphate pathway; it catalyzes the conversion of glucose-6-phosphate to 6-phosphogluconolactone and the formation of NADPH from $NADP^+$ [380]. Therefore, G6PD activity is a key determinant of the cytosolic $NADP^+$/NADPH ratio and consequently it contributes to a variety of metabolic pathways that use NADPH as a cofactor [381]. These include, for instance, the glutathione and thioredoxin antioxidant defense systems, both of which rely heavily on NADPH to sustain their activity and respond to oxidative insults [382]. Intriguingly, according to our findings, the activity of GSR at the intestinal level was upregulated (*Fig. 45C*), meaning that gliadins were stimulating the reduction of oxidized glutathione (GSSG) to reduced glutathione (GSH), even though the regeneration of NADPH by G6PD was compromised. Although contradictory, these results could be easily explained if we consider that, within cells, there are other enzymatic sources of NADPH such as the isocitrate dehydrogenase, an enzyme that catalyzes the conversion of isocitrate to α-ketoglutarate and $NADP^+$ to NADPH [383, 384]. On the other hand, it must be taken into account that this is only a snapshot of what was happening at the intestine of DQ8 mice at the tenth day of treatment with both gliadins and indomethacin and that an oxidative stress isn't a condition, it is a highly dynamic process that is continuously changing in response to many environmental and nutritional stimuli and whose result will depend on the cells' ability to overcome these perturbations through up-regulation of a network of responsive proteins, typically activated downstream of the NF-κB or Nrf2 pathways [385]. Supporting this idea are the findings of Bergamo *et al.* (2016), showing that the expression of both NQO1 and HO-1 in the small intestine of gliadin-treated DQ8 mice varies considerably over time *i.e.* they increase during the first 7 days of treatment and then suddenly decrease in the last 3 days [377].

3.4. Animal pre-treatment with EGCG and polyphenol-rich extracts counteract gliadin-induced long-term enteropathy in DQ8 mice

After seeing the effects promoted by EGCG intake on the gliadin-induced short-term enteropathy, a question arose. Would EGCG, among other polyphenols, be able to

produce similar outcomes in DQ8 mice chronically administered with both gliadins and indomethacin for 30 days? This would be particularly interesting since it has been previously shown that, when on this regimen, these DQ8 mice not only become enteropathic but also develop anti-gliadin and anti-tTG antibodies, both of which constitute a hallmark of the HLA-restricted adaptive immune response in CD [343]. Therefore, based on the robustness of this model at the end of 30 days of treatment, the protective effects provided by PRC, EGCG and GTE supplementation on the intestinal mucosa of these enteropathic mice were explored by administering, *per os*, 50 $mg.Kg^{-1}.day^{-1}$ of polyphenols for approximately 6 weeks (2 weeks of pre-treatment plus 30 days of co-treatment). These results were then compared to those found in animals treated with only gliadins (positive controls) or not treated at all (negative control) (*Fig. 46*). As it can be seen from *Fig. 47*, on day 30, the DQ8 mice showed a significant reduction of intestinal villi height (*Fig. 47A*), increased crypt depths (*Fig. 47B*) and higher numbers of IEL (*Fig. 47C*). As before, these findings are consistent with the morphological changes observed in duodenal biopsy specimens from CD patients thus suggesting that, once more, the intrinsic toxicity of gliadins, in the absence of COXs activity, is sufficient to trigger several typical pathological signs of CD. To complete the whole picture, the villus-to-crypt depth ratio was also significantly reduced when compared to the negative controls (4.62 vs 12.12, respectively, *Fig. 47D*).

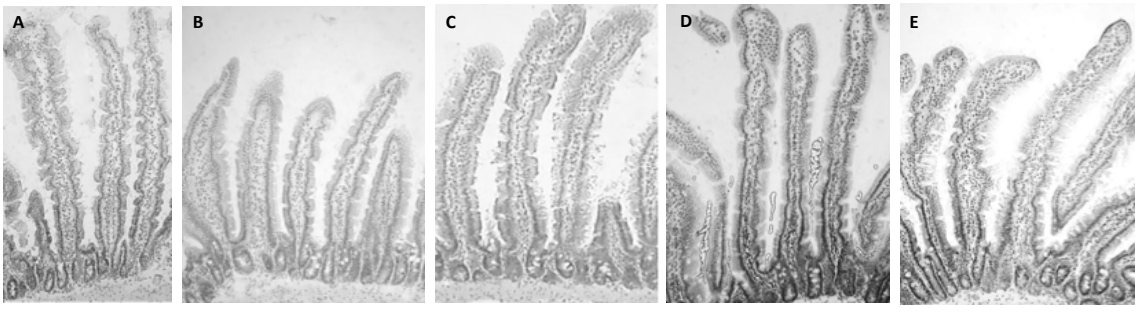

Fig. 46 - Small intestinal morphology of DQ8 mice left untreated (A), intragastrically administered with gliadin proteins for 30 days (B), or pre-treated for 6 weeks with PRC (C), EGCG (D) or GTE (E) at 50 $mg.Kg^{-1}.day^{-1}$; original magnification: ×20.

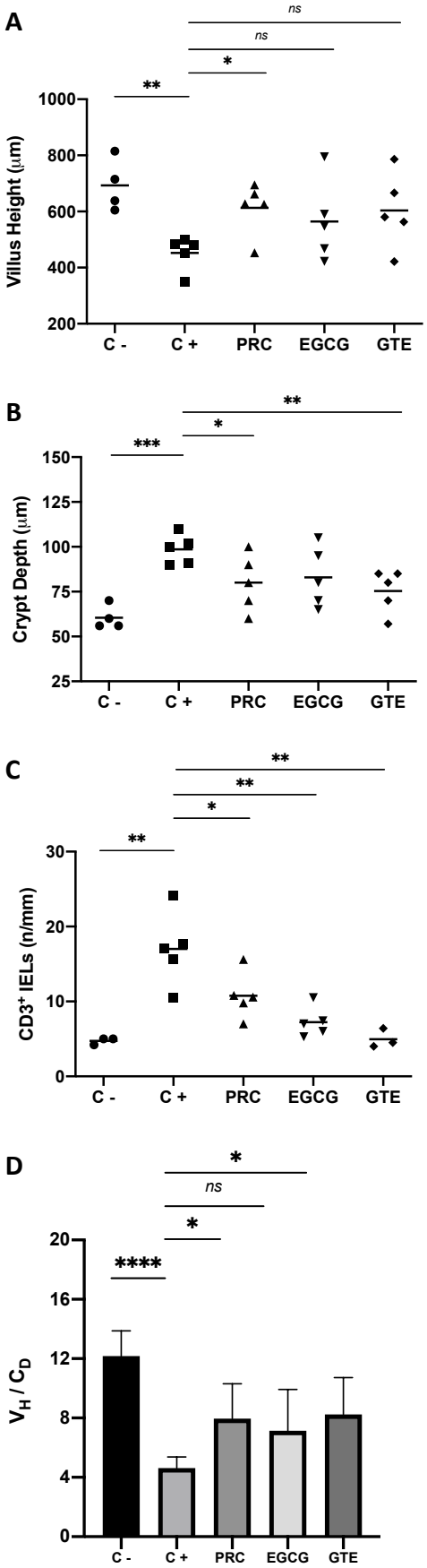

Fig. 47 - Morphometric assessment of villus height (A), crypt depth (B), number of IEL (C) and villus-to-crypt depth ratio (D) among the different experimental animal groups. The bars on (A), (B) and (C) represent mean values; in (D) the results were expressed as mean ± standard deviation. *p<0.05, **p<0.01, ***p<0.001, ****p<0.0001. C^-, untreated controls; C^+, positive controls *i.e.* mice treated with indomethacin and wheat gliadins for 30 days.

Notably, most of the histological changes caused by repeated gliadin exposure were, in a more or less significant fashion, considerably alleviated by polyphenol(s) (*Fig. 46* and *Fig. 47*). In this scenario, the PRC and GTE extracts were found to be the most effective ones, particularly when it comes to the recovery of the villus-to-crypt depth ratio (*Fig. 47D*). Moreover, the regular intake of polyphenols led to a remarkable decrease in the number of IEL (*Fig. 47C* and *Fig. 48*) as either the result of a reduced proliferation of pre-existent IELs or, alternatively, to their lower migration from the periphery into the intestinal epithelia. Whatever be the case, the fact is that, at the moment, there is a very limited number of *in vivo* studies exploring the modulatory effects of dietary polyphenols on IEL populations, especially in the framework of autoimmune responses to food allergens. There are, however, some few exceptions. For instance, it has been recently shown that female Lewis rats fed with a cocoa-containing diet had a higher number of TCRγδ$^+$ and NK cells in their small intestinal epithelium and a smaller TCRαβ$^+$ cell proportion that couldn't be attributed to any of the Th (CD4$^+$), Tc (CD8$^+$) and NKT subsets considered [386]. These results were in line with those of Akiyama et *al.* (2005), who reported that unripe apple polyphenols inhibited the development of an oral sensitization to ovalbumin by increasing the population of TCRγδ$^+$ IEL [387]. On another report, hesperidin intake was shown to increase the percentage of TCRγδ+ cells in IEL (140%) when compared to ovalbumin sensitized mice due to an increase in both TCRγδ$^+$ CD8αα$^+$ and TCRγδ$^+$ CD8αβ$^+$ subsets; in this compartment, hesperidin did not significantly modify other important lymphocytes such as TCRαβ$^+$ [388]. Despite promising, none of these studies were performed on CD-susceptible animal models and most of them relied on the strong adjuvant properties of cholera toxin. For this reason, the reduced IEL infiltration found in this study is probably the consequence of an efficient regression of the small intestinal mucosa to a basal homeostatic state that ended up being less vulnerable the gliadin toxic effects. Taken together, this data clearly strengthens the preventive potential of dietary polyphenols as natural molecules capable of delaying the onset of some of most characteristic structural abnormalities found in CD.

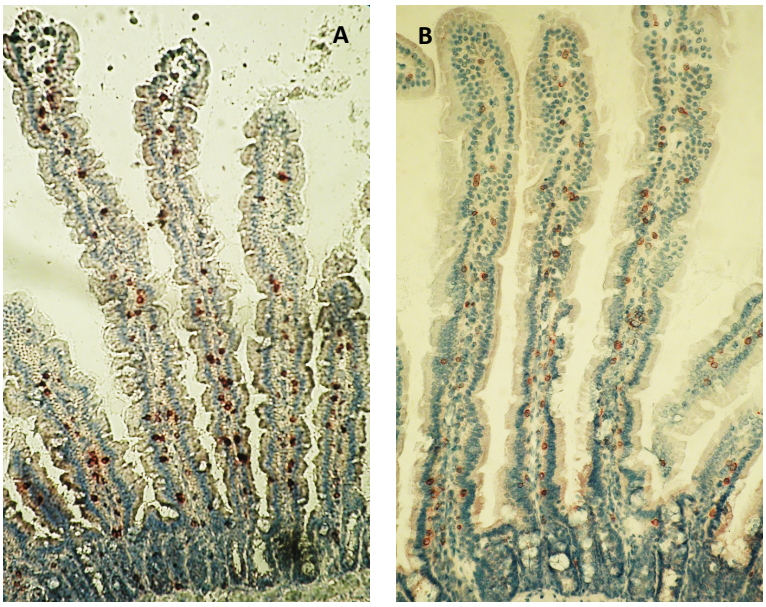

Fig. 48 - Immunohistochemical staining for the CD3 marker in the intestinal mucosa of mice treated with gliadins and indomethacin for 30 days (A) when supplemented with 50 $mg.Kg^{-1}.day^{-1}$ of EGCG (B). CD3 is a protein complex and T cell co-receptor that is involved in activating both the cytotoxic T cells and T helper cells. Original magnification: ×20.

3.5. Duodenal cytoprotections are improved by long-term polyphenol supplementation

The toxic effects induced by prolonged gliadin intake on the intestinal redox status and cytoprotective mechanisms were next examined (*Fig. 49*). Contrary to what was seen on the short-term treatment (*Fig. 44*), the chronic administration of gliadins was associated with a significant decline of both intracellular GSH content (*Fig. 49A*) and GSR activity (*Fig. 49B*), thus indicating that, when combined with indomethacin in a longer timeframe, gliadins triggered a redox status alteration in the small intestine of enteropathic DQ8 mice similar to the one observed in CD patients. Interestingly, these alterations were accompanied by an unusual G6PD enzyme activity (*Fig. 49C*). As mentioned, G6PD is a major source of reductive power in the form of NADPH, required by essential cellular systems including GSR. Therefore, this increase may be the result of an adaptive response aimed at compensating the previous alterations of the intestinal redox status produced by gliadins intake (where in animals treated with indomethacin and gliadin alone was not sufficient to restore GSH and GSR levels).

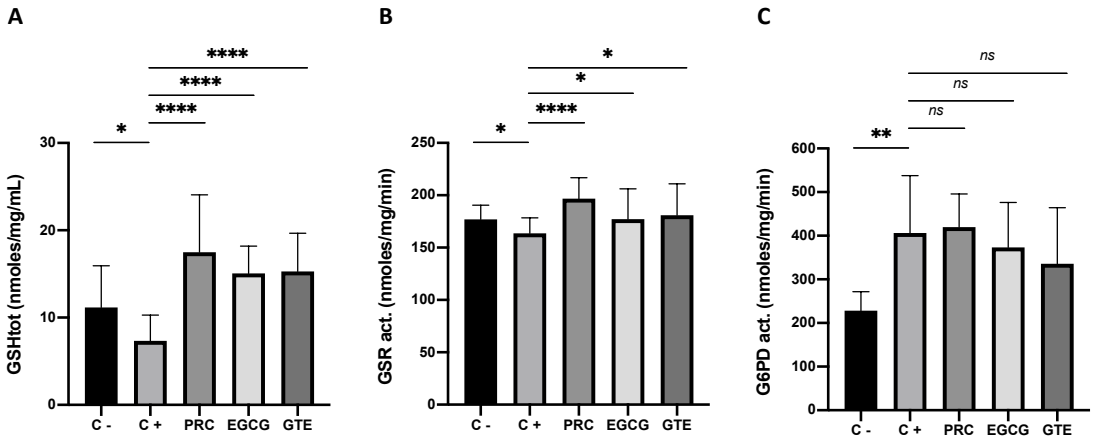

Fig. 49 - Effects of polyphenols pre-treatment on the total GSH content (A) GSR (B) and G6PD (C) enzyme activities in the small intestine of DQ8 mice treated with gliadins and indomethacin for 30 days. Bars represent mean values ± SD from triplicate analyses. *p<0.05, **p<0.01, ***p<0.001, ****p<0.0001.

Outstandingly, dietary supplementation with either PRC, EGCG and GTE polyphenols inhibited the gliadin-mediated toxic effects by significantly increasing the total GSH content and GSR activity in the small intestine of indomethacin-treated DQ8 mice (*Fig. 49*). It thus appears that, as nutritional electrophilic compounds, polyphenols helped to maintain a redox homeostasis at the intestinal level by restoring it nucleophilic tone before the inability of the mice's endogenous feedback mechanisms to deal with the persistent tissue damage brought by gliadin and indomethacin challenge [389]. Therefore, by protecting the small intestine against an oxidative aggression by gliadin proteins, these results may help explaining the architectural recovery observed on the intestinal mucosa of mice pre-administered with PRC, EGCG and GTE polyphenols. Interestingly, in addition to these redox status markers, biochemical assessment of the small intestine of polyphenol-treated DQ8 mice revealed a significant increase in the transcript levels of IL-15 relative to controls or to both IFN-γ and IL-10 mRNAs (*Fig. 50*).

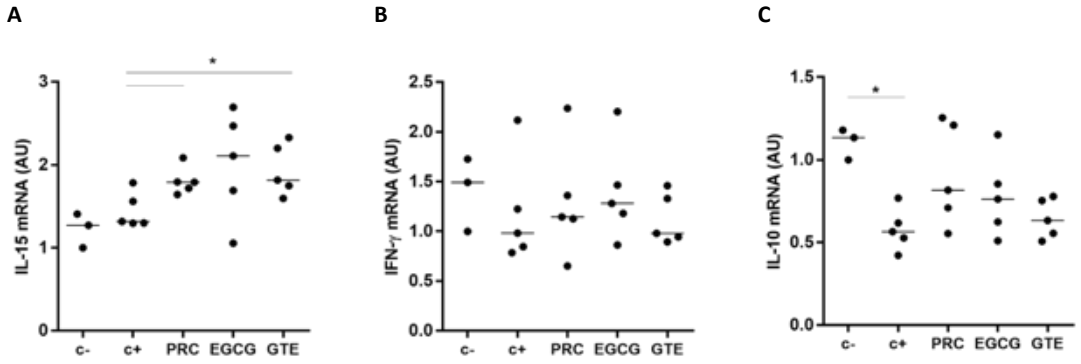

Fig. 50 - IL-15 (A), IFN-γ (B) and IL-10 (C) mRNA levels evaluated by real-time PCR in the five different experimental groups

Constitutively expressed by a broad array of cell types, including macrophages and epithelial cells, IL-15 is a cytokine that preferentially stimulates $CD8^+$ T cell and NK cell activation, proliferation, and cytolytic activity and whose upregulation has been implicated in many organ-specific autoimmune disorders where it impacts distinct immune components and pathways to disrupt intestinal immune homeostasis [94, 390]. Even though, at first sight, this pro-inflammatory role of IL-15 seems a contradiction to our findings, these could be easily explained if we consider the work of *Obermeier et al.* (2006) showing that IL-15 had a strong protective, anti-apoptotic effect on IEC that outweighed its negative pro-inflammatory effect in a dextran sulphate sodium (DSS)-induced model of chronic experimental colitis in which epithelial damage plays a dominant pathogenic role [391]. On another report, performed on an intestinal epithelial cell line, IL-15 was shown to regulate the expression and subcellular distribution of tight junction-associated proteins [392]. Therefore, based on these observations, the upregulation of IL-15 transcription on long-term enteropathic DQ8 mice may well constitute a novel and alternative pathway behind the protective effects of dietary polyphenols towards gliadin toxicity, instrumental to rescue the mucosal architecture. Noteworthy, no signs of gliadin-specific Th1 or Th2 immune responses were seen in DQ8 mice on day 30 (*Fig. 50B* and *C*), a result that agrees with a previous study showing that indomethacin downregulates these T-cell subsets in mice [393].

4. Conclusions

Nowadays, the growing consumer interest in the relationship between diet, good health and disease prevention has led up to a greater attention on informed dietary choices for high-quality foodstuffs. For the food industry, for instance, the health-promoting properties of functional foods represent an opportunity for product differentiation as well as a strategic competitive advantage [394]. In the past, many economic and technological limitations have interfered with the appropriate use and recycling of the high antioxidant potential of vegetable materials and industrial wastes [395]. These include, among many others, grape seeds and skins resulting from the winemaking process whose disposal represents a double loss for the food industry due to the costs associated to their disposal and for the loss of profits deriving from their recycling and exploitation [396]. Fortunately, management, recovery and conversion of food wastes and processing by-products into functional food ingredients is becoming a healthy trend in the current days as the market for functional foods has seen a tremendous demand in the recent years. Within the niche of functional food ingredients, polyphenols constitute one of the biggest classes of natural bioactive compounds whose increasing benefits on human health had prompted several researches focusing on their potential use in the formulation of functional foods with specific compositions to target specific health effects. Interestingly, up to now, none of these studies were performed on a CD background, so that the significance of polyphenols in this field were nothing more than *in vitro*- based speculations regarding their antioxidant and anti-inflammatory properties, some of which would be useful in preserving the intestinal barrier integrity and play a protective role against the toxicity of gluten peptides in CD subjects. Here, we have shown, for the first time and in an *in vivo* model of CD, that the intake of green tea catechins and grape seed procyanidins contributed to the maintenance of a metabolic and redox homeostasis in the small intestine of long-term enteropathic DQ8 mice. Concomitantly with the reestablishment of the nucleophilic tone at the intestinal level, these polyphenols attenuated some of the most characteristic histological changes associated to the consumption of gliadins including villus flattening, crypt hyperplasia and infiltration of IEL. Interestingly, when administered for a shorter period of time (10 days), gliadins induced a compensatory stress response in the small intestine of indomethacin-treated DQ8 which was associated to an upregulation of both GST and GSR activities and a small, yet non-significant, increase on NQO1 activity. Viewed as an attempt of the intestinal mucosa to preserve its integrity in the presence of gliadins, this functional adaptation ended up being useless as these gliadin-treated control mice showed a significant reduction of villi height, increased crypt depth and reduced villus-to-crypt depth ratios, all of which were partially reversed by nutritional doses of EGCG. Also, it has been shown

that the health benefits provided by EGCG supplementation on a CD context don't merely depend on the dose but also on the timing and administration protocol. Indeed, the co-administration of EGCG with gliadin proteins in just four days was as effective on the alleviation of a gliadin-induced intestinal damage as when it was pre-administered for 2 weeks. For this reason, we speculate that the preventive potential of polyphenols against a gliadin-induced cytotoxicity relies not only on a parahormesis effect but also on their ability to physically interact and reduce the bioaccessibility and intestinal bioavailability of gliadin proteins and derived peptides. Overall, this study provides the first *in vivo* evidences regarding the immunomodulatory role of polyphenols in the onset of CD and opens up new horizons concerning the applicability and valorization of polyphenol-rich functional foods and supplements as an effective nutritional strategy to manage and prevent CD.

ONGOING WORK & FUTURE PERSPECTIVES

The results presented and discussed throughout the previous chapters provide only a glimpse of the what was done during my PhD. Indeed, a lot more work has been developed in the past 2 years, which, due to their preliminary nature, won't fit into an independent chapter of their own. Still their relevance prevents me from leaving them in the drawer so that I will make a brief presentation of them, highlighting those who will probably be the next years of research in the area of polyphenols and their implication in CD.

Apart from the immunological - cellular and molecular - mechanisms associated to the pathogenesis of CD, a topic that has been widely studied and dissected in the past years, researchers are now keen to understand the upstream mechanisms that lead to the dysregulated production of IL-15 and the activation of the innate immune response. Distinct candidates have been proposed, including gluten itself. Nevertheless, as previously mentioned, there is a lot of controversy and conflicting data regarding the innate-stimulating properties of gluten so that, so far, there isn't any consensus concerning its cytotoxic effects among the literature. According to recent evidences, obtained mainly from cultured epithelial cells, some gliadin peptides (*e.g.* p31-43) have been shown to induce an intracellular pro-oxidative environment, rearrangement of actin cytoskeleton, impairment of epithelial tight-junction assembly and cell proliferation by interfering with endocytic vesicle maturation, which in turn prolongs EGFR activation and trans presentation of IL-15/IL-15-Rα in enterocytes [104, 106, 108, 109, 397-399].

In 2013, *Capozzi* and colleagues found out that a peptic-tryptic gliadin digestion was able to elicit an IRAK1, ERK1/2 and p38 MAPK phosphorylation, NF-kB activation and enhanced COX-2 enzyme expression and activity in confluent Caco-2 cells [400]. Also, the same gliadin digestion stimulated the production of two key pro-inflammatory cytokines, namely IL-6 and IL-8. In another study, published in 2015, it has been demonstrated that a similar gliadin peptide digestion triggered the synthesis of IL-1β and TNF-α in Caco-2 cells, an outcome that was in line with earlier findings [401, 402]. Interestingly, in 2013, a systematic genome-wide expression study on Caco-2 cells has

been conducted to see whether gliadin peptides had any direct effect on intestinal epithelial cell gene transcription, also suggestive of potential cell surface receptor-dependent signaling pathways [403]. At the end of the day, the authors were unable to replicate previously reported direct effects of gliadin peptides on enterocytes; the results rather suggested that certain epitopes from pepsin and trypsin may also affect gene transcription. Therefore, the authors conceived that the gliadin effects on IEC are secondary to oxidative stress, NF-kB activation and IL-15 up-regulation. Additionally, several mechanisms (paracellular and transcellular) of gliadin transport across the intestinal epithelial barrier have been suggested [80, 108, 115, 302, 404]. As such, despite the multitude of effects that have been attributed to cytotoxic gliadin peptides, the molecular mechanisms through which they are brought about still obscure. These include not only the mechanisms behind gliadin transport at the intestinal level, but also its potential cell surface receptors and gliadin-activated downstream signaling pathways [130]. Also, it is important to emphasize that most of these *in vitro* studies have been performed using undifferentiated Caco-2 cells so that they are, at least, questionable when transposed to a physiological situation. The Caco-2 cell line is derived from colonic epithelial adenocarcinoma cells. When grown under normal cell culture conditions, and after reaching confluence, they differentiate into small intestine enterocytes and become polarized, expressing many of the characteristics of these enterocytes (e.g. tight junctions, microvilli and membrane transporters) [405]. Without phenotypic differentiation Caco-2 cells still resemble human colonic cancer cells in a wide range of their gene expression patterns so that the differences in both cell models might lead to differential cellular responses towards food antigens and polyphenols [406].

A fundamental function of the intestinal epithelium is to act as a barrier that regulates the interaction between luminal contents, including the microbiota, the underlying immune system, and the remainder of the body, while supporting the transport of nutrients, water, and other products. As the first line of defense against several environmental stimuli, whose integrity must be maintained for optimal health, deciphering the exact mechanisms by which gliadin peptides affect the structure and function of IEC is crucial in order to fully understand the early stages of CD onset and to unravel novel biomarkers for improved diagnostics and therapeutic targets. Indeed, the T cell activation and mucosal inflammation persists only as long as gluten is present in the lamina propria beneath the epithelial layer so that the presence of gluten in the intestinal mucosa is a prerequisite for the activation of gluten-reactive T cells. Therefore, since the activation of IEC plays a pivotal role in CD, an alternative therapeutic option to a GFD would rely, for example, in reducing the pro-inflammatory response mediated by gliadin peptides in IEC

by taking advantage of the antioxidant, anti-inflammatory and/or peptide-binding properties of polyphenols. For this reason, we have decided to embrace this quest for an alternative supportive approach capable on improving the daily life of CD patients by exploring the immunomodulatory role of polyphenols in gliadin-challenged IEC.

As a starting point, and for comparison purposes, we have started by working with undifferentiated, yet confluent, Caco-2 cells using the 2',7'-dichlorofluorescin-diacetate (DCFDA) assay to detect ROS activity within cells treated with different concentrations of gliadin peptides ranging from 10 $\mu g.mL^{-1}$ to 2 $mg.mL^{-1}$ (*Fig. 51*). The protocol followed to obtain this peptide preparation was quite simple. First, gliadin proteins were extracted from a commercial crude extract (Sigma-Aldrich) according to the procedure described by *Wieser et al.* (1998) [407]. Then, its digestion was made following a simplified method with only proteolytic enzymes. Briefly, to simulate a gastric digestion, 100 mg of gliadins were weighed and dissolved in 0.01 M hydrochloridric acid followed by incubation in a 37 °C water bath with pepsin (1:100 protease to protein w/w ratio) at pH 2.0 for 45 min. The reaction mixture was then pH adjusted to 7.0 in 50 mM phosphate buffer and added with pancreatin (1:100 w/w), chymotrypsin (1:100 w/w) and trypsin (1:100 w/w) at 37 °C for 4 h. After this, the enzymes were inactivated by heating at 85 °C for 15 minutes. This peptide digest has been already characterized by nano-LC-MS/MS in previous works [236]. Prior to be used in cells, the samples were filter sterilized by passing them through 0.22 mm pore filters.

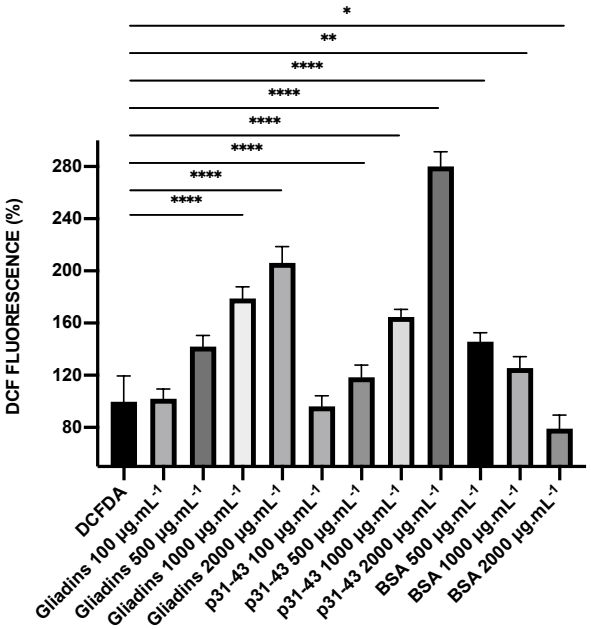

Fig. 51 - Intracellular ROS levels measured using the DCFDA assay in Caco-2 cells treated with different concentrations of gliadin peptides, p31-43 and BSA digest for 4h at 37 °C. Cells were seeded at a density of 7.4 x 10^4 $cells.cm^{-2}$ and allowed to grow for 5 days. Bars represent mean values ± SD from *n* = 6-12 analyses, performed on two independent days. *p<0.05, **p<0.01, ***p<0.001, ****p<0.0001.

As it can be seen from *Fig. 51*, the gliadin digest and the p31-43 peptide induced a dose- and time-dependent (*data not shown*) increase on intracellular ROS levels. According to previous findings, this exacerbated ROS production emerges as a result of a prolonged persistence of gliadin peptides in lysosomal associated membrane protein-1 (LAMP-1)-positive vesicles which subsequently activate different stress sensitive signaling pathways, including the Erk1/2 MAPK [109]. Remarkably, the peptide digest obtained from a purified bovine serum albumin (BSA, Sigma-Aldrich) had the exactly opposite behavior, that is, the ROS levels decreased with increasing BSA concentrations and were always significantly below to the corresponding gliadin counterparts. Taken together, these results underscore the peculiarity of gliadins as unusual dietary proteins capable of eliciting a deleterious pro-oxidant response in confluent Caco-2 cells, linked to an increased secretion of IL-8 into the culture medium when at a concentration of 1 $mg.mL^{-1}$ (*Fig. 52*). Under the same experimental conditions, we weren't able to detect any IL-1β production or NF-κB p65 phosphorylation on Caco-2 cells stimulated with different gliadin peptide concentrations for 24 h at 37 °C (*data not shown*). IL-8, also known as a neutrophil chemotactic factor, is a pro-inflammatory chemokine produced by many cell types, whose main function is to attract and activate neutrophils in inflamed tissues [408]. Interestingly, together with IL-2, this cytokine was shown to be one of the first cytokines to become significantly elevated as early as 2 hours after intradermal injection of gluten peptides to CD patients on a GFD [409]. On another study, which analyzed the cytokine mRNA profile in duodenal biopsy specimens from CD patients orally challenged with gluten, it was found that the mRNA of IL-8 was considerably elevated at the mucosal level, so that this cytokine must be implicated in the early immunological events associated to CD [410]. Of note, IL-8 is one of the genes that are kept under the control of NF-κB, being itself capable of activating NF-κB in a TRAF6-dependent pathway [411].

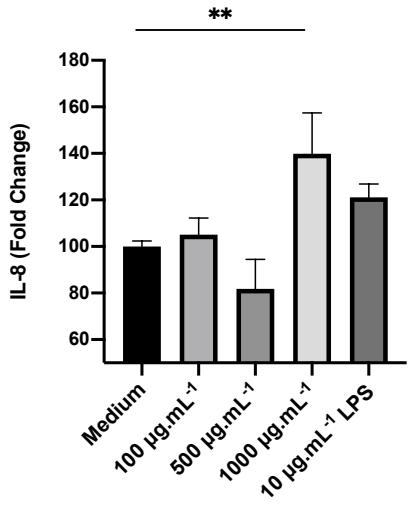

Fig. 52 - Fold change variation of IL-8 release by Caco-2 cells incubated with different concentrations of gliadin peptides and 10 μg.mL^{-1} of LPS (positive control) for 24h at 37 °C. Cells were seeded at a density of 7.4 x 10^4 cells.cm^{-2} and allowed to grow for 5 days. Bars represent mean values ± SD from *n* = 2-4 analyses, performed on two independent days. **p<0.01.

Next, in order to bring light into the likely mechanisms and signaling pathways behind these gliadin-mediated effects, we have decided to study the gene expression pattern of Caco-2 cells exposed to gliadin peptides for 24 h by determining the relative change in expression of twelve different transcripts including three transcription factors (NF-κB1, CREB-1 and c-Jun), two protein kinases (ERK-2 and JNK-1), two cytokines (IL-6 and IL-8) and three tight-junction proteins/regulators (occludin, claudin-1 and zonula occludens-1). In the case of the NF-κB, we have analyzed the gene expression of both p105 (which can undergo proteasomal processing to p50), RelA (or p65), and its inhibitor I-κB. These results are summarized in *Fig. 53*, with the exception of IL-6 and IL-8 whose mRNA levels were residual.

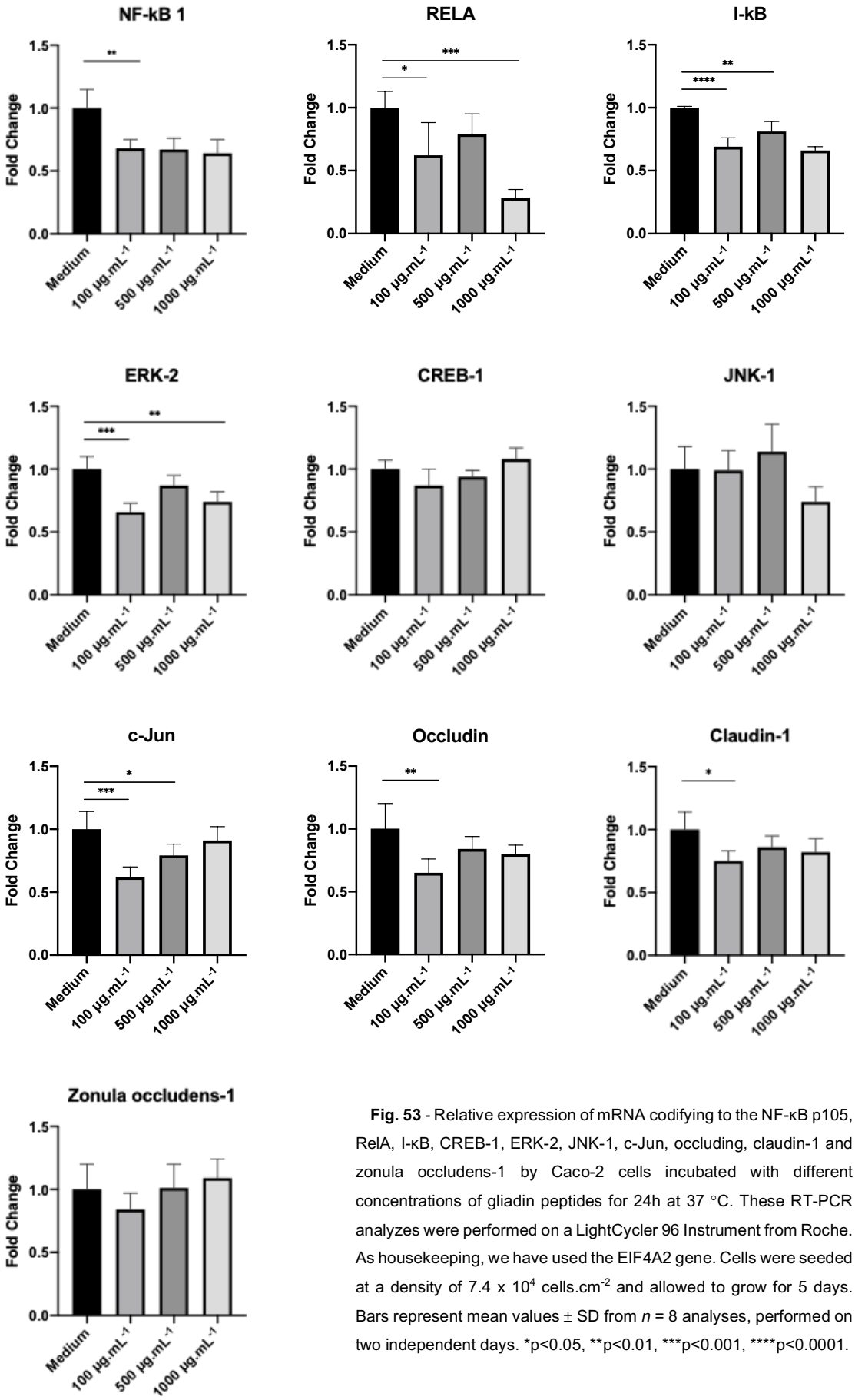

Fig. 53 - Relative expression of mRNA codifying to the NF-κB p105, RelA, I-κB, CREB-1, ERK-2, JNK-1, c-Jun, occluding, claudin-1 and zonula occludens-1 by Caco-2 cells incubated with different concentrations of gliadin peptides for 24h at 37 °C. These RT-PCR analyzes were performed on a LightCycler 96 Instrument from Roche. As housekeeping, we have used the EIF4A2 gene. Cells were seeded at a density of 7.4 x 10^4 cells.cm^{-2} and allowed to grow for 5 days. Bars represent mean values ± SD from *n* = 8 analyses, performed on two independent days. *p<0.05, **p<0.01, ***p<0.001, ****p<0.0001.

According to *Fig. 53*, one can see that the treatment with gliadin peptides induced either a downregulation of gene expression or didn't affect them at all, as was the case of CREB-1, JNK-1 and zonula occludens-1. CREB-1, also known as cyclic AMP responsive element binding protein 1, is a transcription factor regulating a remarkable spectrum of cellular responses involved in proliferation, differentiation and cell survival [412]. Multiple external stimuli induce CREB activation via several kinase pathways such as protein kinase A (PKA), calmodulin-dependent protein kinase (CaMK), mitogen-activated protein kinases (MAPK), including ERK1/2, among many others [413]. These signaling pathways lead to the phosphorylation of CREB at a conserved serine residue (Ser133) and triggers the interaction with its co-activators including CREB-binding protein (CBP) or p300 and subsequent binding to the cAMP response element (CRE) of CREB-responsive genes. Several immune-related genes possess this cAMP-responsive element, including IL-2, IL-6, IL-10, and TNF-α [414]. In addition, phosphorylated CREB has been proposed to directly inhibit NF-κB activation by blocking the binding of CREB binding protein to the NF-κB complex, thereby limiting pro-inflammatory responses [415]. Notably, the mRNA transcript level of one of the inducers of CREB activity, the extracellular signal-related kinase (ERK), was negatively affected by gliadins (*Fig. 53*). The ERK1/2 pathway for CREB phosphorylation occurs in part through an indirect way, mediated by pp90 ribosomal S6 kinase (RSK), mitogen- and stress-activated protein kinase (MSK)1/2, MAPKAP kinase 2 phosphorylation [416]. Oxidative stress is known to induce apoptosis in a variety of cell types by activating intracellular cell death signaling cascades. However, cells are constantly exposed to a myriad of potentially oxidative stimuli so that, in order to survive, they have to deal with these challenges by activating a complex series of defensive mechanisms. For instance, treatment of human SH-SY5Y neuroblastoma cells with H_2O_2 to generate ROS activates members of the MAPK family (ERK1/2 and JNK but not p38 MAPKs) and Akt/PKB [417]. Usually, the ERK1/2 and Akt/PKB activation promotes cell survival by activating antiapoptotic signaling pathways, whereas activation of JNK and p38 MAPK are frequently associated with cell death [418]. Of note, some studies have also suggested an apoptotic function for mitogen-activated protein kinase kinase (MEK)/ERK in H_2O_2-mediated signals [419]. Based on our findings *i.e.* the observed downregulation of ERK-2 without any significant change on JNK-1, it appears that rather than cell death, the prolonged exposure of Caco-2 cells to these gliadin peptides led to a growth arrest, as previously described [420]. Interestingly, with increasing gliadin concentrations, the mRNA level of c-Jun tended to increase gradually (*Fig. 53*). The c-Jun protein, when combined with c-Fos, forms the AP-1 early response transcription factor which is a key player in cell survival or death as well as an essential

regulator of cell metabolism and proliferation [421]. Unlike ERKs, JNKs are activated most potently by inflammatory cytokines and a variety of chemical and radiant stresses (that why they are commonly referred to as stress-activated kinases), several lines of evidence indicate that c-Jun is a specific target of JNK and not ERK [422].

Using a human colorectal carcinoma cell line (HCT116), it has been shown that the strong ROS-inducer 1,3-dibutyl-2-thiooxo-imidazolidine-4,5-dione triggers a robust activation of JNK by phosphorylation as early as 30 minutes after exposure, which persisted throughout the time course of 24 hours [423]. The total c-Jun levels and its phosphorylation product at Ser73 exhibited the same trend. Therefore, according to these observations, it seems that in this particular case, the increase on intracellular ROS triggered by gliadin challenge wasn't strong enough to activate these apoptotic signaling pathways so that the Caco-2 cells were still capable of dealing with this pro-oxidative environment without dying. Taken together, these results appear to indicate that gliadin stimulation provides nothing more than a mild oxidative stimulus, and not a pro-inflammatory one, an argument that is supported by the repression of both NF-κB p105, p65, IL-6 and IL-8 mRNAs. Surprisingly, the I-κB gene was also significantly downregulated by gliadin peptides. As previously mentioned, the I-κBs bind to NF-κB dimers and sterically block the function of their nuclear localization sequence, thereby causing their cytoplasmic retention [424]. In order to get NF-κB into the nucleus, its site of action, the cytoplasmic NF-κB:IkB complex needs to be disrupted by phosphorylation *via* I-κB kinase (IKK) [425]. Importantly, it has to be highlighted that these intracellular processes are highly dynamic. Therefore, in order to have a better overview regarding the intracellular signal transduction pathways activated by gliadins, it would be interesting the follow the time-course changes of these exactly same genes, instead of just measuring their changes at the end of 24 h (*Fig. 53*). Accordingly, if we consider the outcomes provided by previous reports, it is possible that as soon as the Caco-2 cells became exposed to gliadin peptides, they immediately activated a transient antioxidant stress response, which can be even mediated by NF-κB, so that at the end of 24 h the cells are still trying to recover from this stimulus and deciding whether they should live or die [400]. This behavior would explain the increased IL-8 concentration in the culture medium when its transcript levels were down (*data not shown*). Probably, for longer exposures, we would see a completely different picture as a result of an uncontrolled and persistent redox unbalance and the incapacity of cells to deal with it. Indeed, it has been recently demonstrated that at the end of 48 h, gliadin peptides (obtained following a similar digestion protocol) affected the viability of undifferentiated Caco-2 cells as confirmed by cytofluorimetric and apoptotic assays and through the analysis of

micronuclei induction [426]. Curiously, in that study, it has also been shown that Caco-2 cells were not only capable of up taking gliadin peptides and segregate them into early endosomal compartments, but also that these peptides were latter addressed to defective autophagosome vesicles that were incapable of degrading them. Moreover, upon exocytosis, these same peptides could be internalized by neighboring cells thus perpetuating the toxic effect of gliadins to the surroundings. In our case, after 24 h of gliadin treatment, the cells were still viable as assessed by MTT analysis (*Fig. 54*).

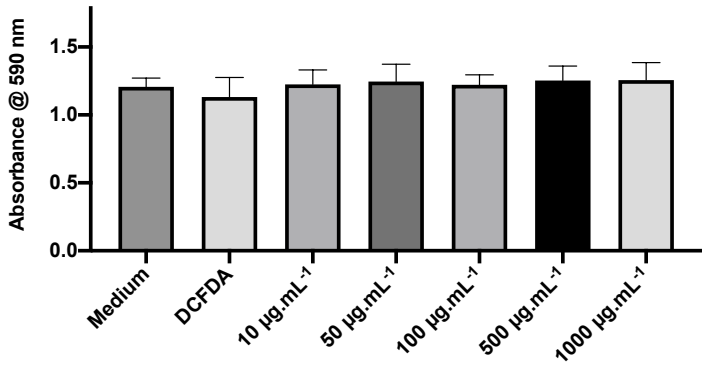

Fig. 54 - MTT assay in confluent Caco-2 cells incubated with different concentrations of gliadin peptides for 24h at 37 °C. Cells were seeded at a density of 7.4 x 10^4 cells.cm^{-2} and allowed to grow for 5 days. Bars represent mean values ± SD from *n* = 12 analyses, performed on two independent days.

As it can be seen by *Fig. 53*, incubation of Caco-2 cells with gliadin peptides induced a downregulation of both occludin and claudin-1. On the other hand, the transcription of zonula occludens-1 remained unaffected. In general, CD is characterized by an increased intestinal permeability and disassembly of epithelial tight junctions between cells, leading to a compromised barrier function [427]. This increased permeability favors the diffusion of gliadin peptides into the lamina propria where they trigger an adaptive immune response *via* gluten-specific T cells. CD individuals have fewer tight junction protein strands and less of the cytoplasmic scaffolding protein, zonula occludens-1, pointing to structural alterations at the tight junctions [428-430]. Proteins at the adherens junctions have also been shown to be altered in CD. For instance, the E-cadherin protein, required for tight junction formation, is reduced in the duodenum of children with CD [431]. In 2005, *Sanders* and coworkers found out that a peptic-tryptic digest of gliadins caused a reorganization of actin filaments and altered expression of the tight junction proteins occludin, claudin-3, claudin-4, zonula occludens-1 and E-cadherin in

differentiated Caco-2 cells [432]. Later, in 2008, it has been discovered that some of these gliadin peptides have the ability to bind to the chemokine receptor CXCR3 on the surface of IEC, leading to a MyD88-dependent zonulin release and subsequent activation of the EGFR through proteinase activated receptor-2 (PAR2) [115, 433]. This complex thus initiates an intracellular signaling pathway that results in a PCK-α dependent tight junctions disassembly and increased intestinal permeability. Even though the cells used herein weren't fully differentiated, the downregulation of both occludin and claudin-1 may reflect, or at least provide clues, regarding the antiproliferative and cytotoxic properties of gliadins. Overall, though we were unable to dissect the molecular mechanisms by which gliadins exert their cytotoxic effects, one thing became clear: gliadins by themselves aren't pro-inflammatory, at least, in a reasonable timeframe. For this reason, we prospect that the biological activity of these proteins on a CD context is the culmination of a sequence of pro-oxidative events, coupled to a genetic susceptibility, that results in an inflammatory cascade and further disruption of tight junction assembly and in which bacteria or bacterial products have certainly a role [434]. These effects, however, remain to be determined and will be scope of future works.

Next, and as it was done before, we have decided to evaluate the pro-oxidative effects of gliadin peptides in differentiated Caco-2 cells by measuring, again, the intracellular ROS content using the DFCDA assay (*Fig. 55*).

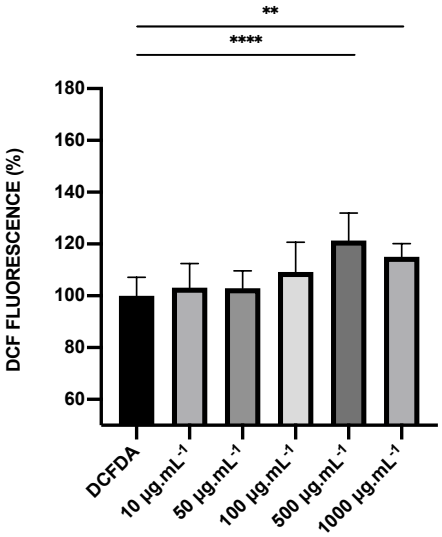

Fig. 55 - Intracellular ROS levels measured using the DCFDA assay in differentiated Caco-2 cells treated with different concentrations of gliadin peptides for 4h at 37 °C. Cells were seeded at a density of 7.4 x 10^4 cells.cm^{-2} and allowed to grow for 21 days. Bars represent mean values ± SD from *n* = 6-12 analyses, performed on two independent days. *p<0.05, **p<0.01, ***p<0.001, ****p<0.0001.

According to *Fig. 55*, and by comparison with the results of *Fig. 51*, one may see that when differentiated, the Caco-2 cells were more resistant to the pro-oxidative properties of gliadins. These findings are in line with previous studies confirming that IEC do become less sensitive to inflammatory stimulation upon differentiation and that mature adult as compared to young proliferating cells could contribute differentially to the inflammatory response in the gut [435]. This is most probably the result of a differential expression of receptors and modified intracellular signaling pathways occurring with cell differentiation [436]. Concerning the antioxidant defense mechanisms of Caco-2 cells, it has been found that over time (after confluence), with the exception of GPx, enzymes such catalase, SOD and GSR have a small, but statistically significant increase in their activity [437]. Additionally, the gene and protein expression levels of GST also increase during differentiation [438]. Therefore, it would be expected these cells to be much more resilient to the toxic effects of gliadins peptides *via* ROS, as shown not only by their slight increase with gliadin concentration (*Fig. 55*) but also by the absence of a statistically significant change on IL-8 production (*data not shown*) and cell viability (*Fig. 56*).

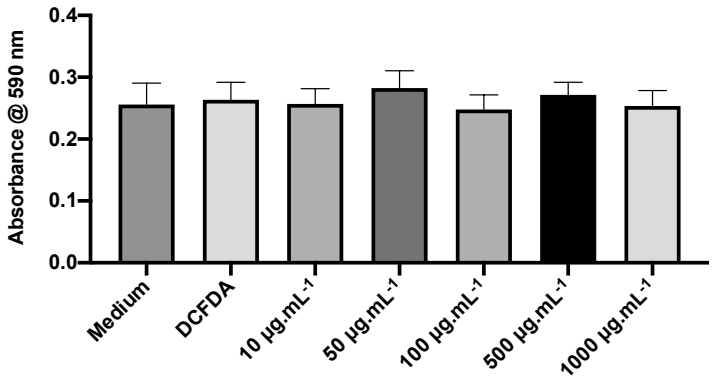

Fig. 56 - MTT assay in differentiated Caco-2 cells incubated with different concentrations of gliadin peptides for 24h at 37 °C. Cells were seeded at a density of 7.4 x 10^4 cells.cm^{-2} and allowed to grow for 21 days. Bars represent mean values ± SD from *n* = 8 analyses.

To complement the previous data, we have also analyzed the activation status of ERK1/2 (*Fig. 57*) at the end of 4h of treatment with 1 mg.mL^{-1} of gliadin peptides, incubated either alone or in combination with a cocktail of pro-inflammatory mediators containing 25 ng.mL^{-1} of IL-1β, 10 µg.mL^{-1} of LPS, 50 ng.mL^{-1} of TNF-α and 50 ng.mL^{-1} of IFN-γ.

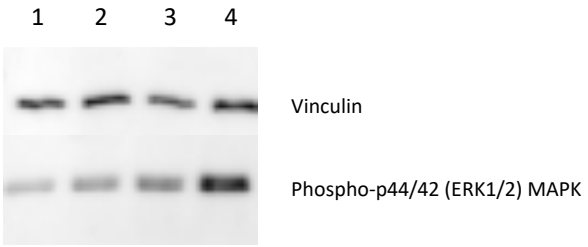

Fig. 57 - Western Blot analysis for ERK1/2 phosphorylation in Caco-2 cells incubated with 1 mg.mL^{-1} of gliadin peptides either alone or in combination with a pro-inflammatory cytokine and endotoxin cocktail for 4 h at 37 °C. 1- untreated cells, 2- gliadin-treated cells, 3- cytokine-treated cell control, 4- gliadin + cytokine-treated cells. All antibodies, including the secondary one, were purchased to Cell Signaling Technologies.

According to *Fig. 57*, it was found that the gliadin peptides induced an early activation of ERK1/2 by phosphorylation, without any significant change on NF-κB activation (*data not shown*). The same trend was also evidenced, although more prominently, when the peptides were incubated together with the cytokine and LPS cocktail (lane 2 and 4), used so that we could simulate an acute phase of intestinal inflammation [435]. As expected, in comparison to the negative control (lane 1), treatment of Caco-2 cells with IL-1β, TNF-α, IFN-γ and LPS (lane 3) enhanced the phosphorylation of ERK1/2 MAPKs, whose activation by TNF-α has been implicated in the disruption of the intestinal epithelial barrier and increased permeability, in a mechanism that appears to dependent on the phosphorylation and activation of the ETS domain-containing transcription factor Elk-1 and subsequent binding to its motif on the myosin light chain kinase (MLCK) promoter region [439]. Once activated, the MLCK induces the contraction of peri-junctional actomyosin filaments, leading to a mechanical tension–induced opening of the TJ barrier. IL-1β has also been shown to produce a similar outcome through another pathway, the p38/ATF-2/MLCK one [440].

As far as the gliadin peptides are concerned, it has been found that they promote cell proliferation and actin rearrangements in various cell lines, mimicking the effect of EGF. Gliadin peptides enhance the EGF pathway by increasing EGFR and ERK phosphorylation with consequent actin remodeling and proliferation. Constitutive activation of the EGF receptor/ligand system is also present in CD enterocytes. Indeed, increases in EGFR protein levels, EGF mRNA, the downstream effector molecule ERK and proliferation, which is ERK-dependent, have all been found in enterocytes from

normal biopsies of CD patients following a GFD [108]. Here, we haven't seen any difference on cell proliferation, regardless of the differentiation stage of Caco-2 cells (*Fig. 54* and *Fig. 55*). Likewise, the molecular mechanisms and cellular outcomes driven by this ERK1/2 activation appear to be much more complex than what initially thought. In any case, the co-treatment of gliadins with the pro-inflammatory cocktail exacerbated ERK1/2 phosphorylation, thus prospecting that, within a pro-inflammatory microenvironment, the cytotoxic effects of gliadin peptides could become much more amplified, with direct implications on cell growth, differentiation, stress and survival.

Having established the differences on Caco-2 cells susceptibility to the pro-oxidative effects of gliadin peptides (*Fig. 51* and *Fig. 55*), we wondered ourselves whether polyphenols would be able attenuate these nefarious responses *in vitro* as they did *in vivo*. As before, we have designed two sets of experiments using both confluent and differentiated Caco-2 cells: a pre-incubation and co-incubation protocol with EGCG for 90 min and 4 h, respectively (*Fig. 58A* and *B*).

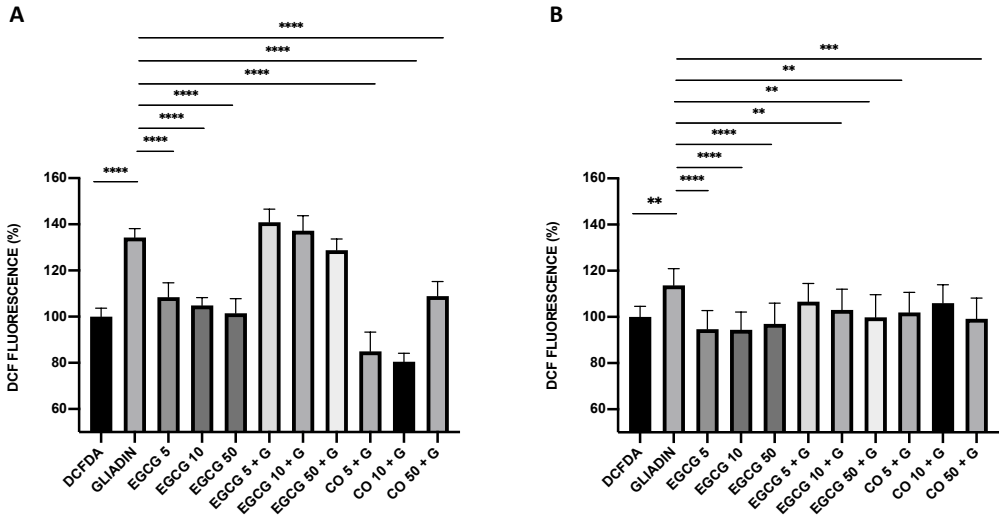

Fig. 58 - Intracellular ROS levels, measured using the DCFDA assay, in confluent (A) and differentiated (B) Caco-2 cells treated with 1 mg.mL^{-1} of gliadin peptides when pre-incubated (for 90 min) or co-incubated with EGCG at 5, 10 or 50 μM for 4 h at 37 °C.. Cells were seeded at a density of 7.4 x 10^4 cells.cm^{-2} and allowed to grow for 5 (A) and 21 days (B). Bars represent mean values ± SD from *n* = 6-14 analyses, performed on two independent days. *p<0.05, **p<0.01, ***p<0.001, ****p<0.0001.

As it can be observed from *Fig. 58*, EGCG reduced the intracellular ROS levels in Caco-2 cells challenged with 1 mg.mL^{-1} of gliadin peptides in quite different ways. Accordingly, while on differentiated Caco-2, both pre- and co-treatment induced, in a more or less significant manner, an attenuation of DCF fluorescence at the end of 4 hours of

incubation, on confluent cells, the same effect has only been observed when the latter were co-treated with gliadins. This result, by itself, its quite curious because even though the Caco-2 cells were responsive to EGCG on both differentiation stages (by comparing the second to the fifth bar of *Fig. 58*), when immature, the cells were unable to fight the pro-oxidative effects of gliadin peptides. The same effect has also been observed when confluent Caco-2 were incubated with 300 $\mu g.mL^{-1}$ of p31-43, immediately after or upon co-treatment with malvidin-3-glucoside (Mv-3-glc), EGCG, B2 and B2 gallate (B2g) (*Fig. 59*). Therefore, it thus seems that the functional consequences and amplitude of these polyphenol's antioxidant effects depend not only on the enterocyte differentiation stage but also on the time lag between treatments. The mechanisms underlying these differences, however, remain to be determined and will be the goal of future investigations.

Last but not least, it has been previously shown that the matrix and proteolytic system used in different *in vitro* digestion models of gluten proteins has a strong influence in the type of peptides produced, both qualitatively as quantitatively [441]. Indeed, even though the simplified peptic-tryptic/chymotryptic method can still be used for a varietal screening, at the end, it is not representative of the peptides that are trully generated at the gastrointestinal tract after physiological human digestion. Therefore, depending on the protocol followed, the content of proteolytic resistant peptides could be significantly different which could have dramatic implications on their pathogenicity on a CD context and the cause of conflicting results in many CD-related studies. For this reason, we have performed some preliminary experiments on differentiated Caco-2 cells in which gliadin proteins were digested based on a recently standardized protocol making use of artificial fluids simulating the exact composition of digestive juices [442]. This digestion has been thoroughly characterized by mass spectrometry, revealing the presence of thousands of proline and glutamine-rich peptides corresponding mainly to α- and γ-gliadins (*Table 7*).

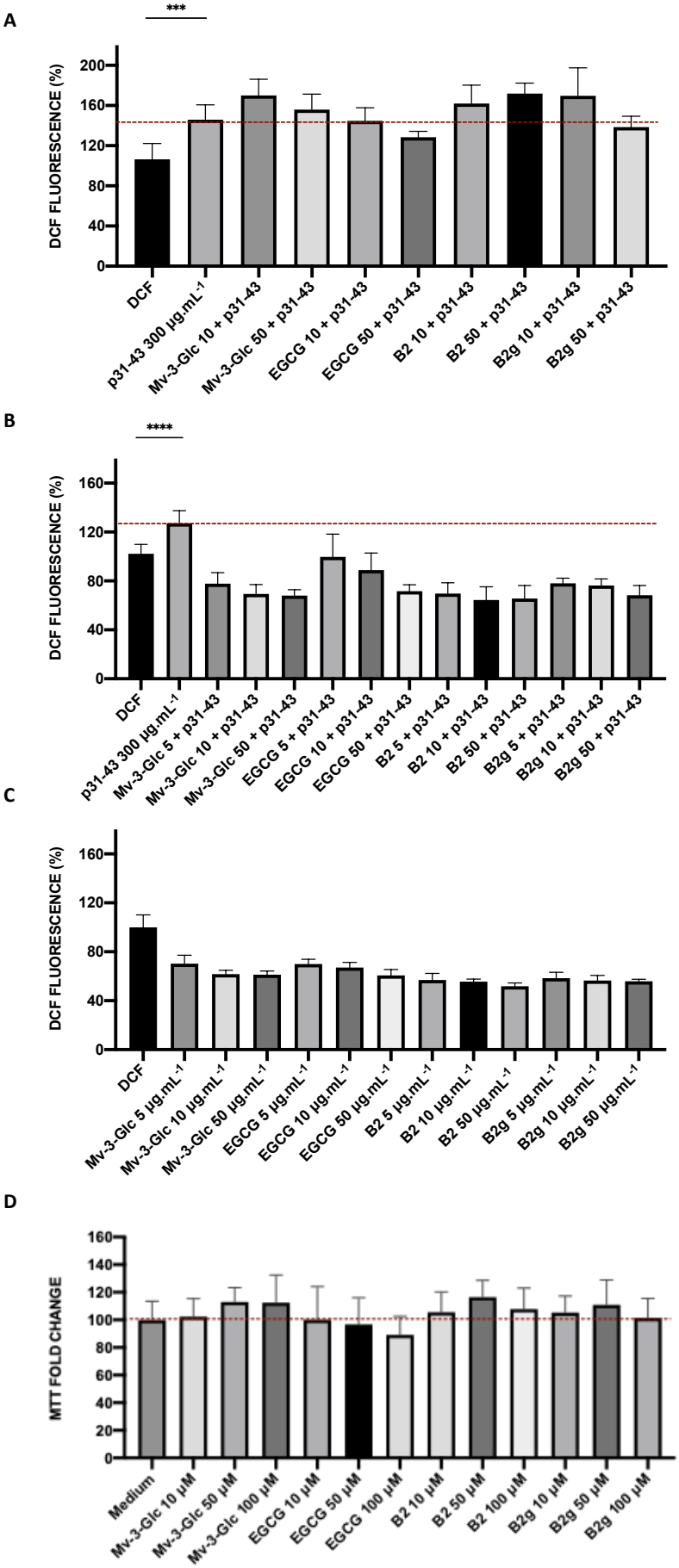
A
***
DCF FLUORESCENCE (%)
200
160
120
80
40
0
DCF
p31-43 300 µg.mL-1
Mv-3-Glc 10 + p31-43
Mv-3-Glc 50 + p31-43
EGCG 10 + p31-43
EGCG 50 + p31-43
B2 10 + p31-43
B2 50 + p31-43
B2g 10 + p31-43
B2g 50 + p31-43
B
****
DCF FLUORESCENCE (%)
160
120
80
40
0
DCF
p31-43 300 µg.mL-1
Mv-3-Glc 5 + p31-43
Mv-3-Glc 10 + p31-43
Mv-3-Glc 50 + p31-43
EGCG 5 + p31-43
EGCG 10 + p31-43
EGCG 50 + p31-43
B2 5 + p31-43
B2 10 + p31-43
B2 50 + p31-43
B2g 5 + p31-43
B2g 10 + p31-43
B2g 50 + p31-43
C
DCF FLUORESCENCE (%)
160
120
80
40
0
DCF
Mv-3-Glc 5 µg.mL-1
Mv-3-Glc 10 µg.mL-1
Mv-3-Glc 50 µg.mL-1
EGCG 5 µg.mL-1
EGCG 10 µg.mL-1
EGCG 50 µg.mL-1
B2 5 µg.mL-1
B2 10 µg.mL-1
B2 50 µg.mL-1
B2g 5 µg.mL-1
B2g 10 µg.mL-1
B2g 50 µg.mL-1
D
MTT FOLD CHANGE
160
140
120
100
80
60
40
20
0
Medium
Mv-3-Glc 10 µM
Mv-3-Glc 50 µM
Mv-3-Glc 100 µM
EGCG 10 µM
EGCG 50 µM
EGCG 100 µM
B2 10 µM
B2 50 µM
B2 100 µM
B2g 10 µM
B2g 50 µM
B2g 100 µM

Fig. 59 - Intracellular ROS levels, measured using the DCFDA assay, in confluent Caco-2 cells treated with 0.3 $mg.mL^{-1}$ of p31-43 when pre-incubated (for 90 min, A) or co-incubated with Mv-3-Glc, EGCG, B2 and B2g at 5, 10 or 50 μM for 4 h at 37 °C (B). In (C) it is represented the polyphenol control experiment of (B) and in (D) their MTT analysis in a concentration range from 10 to 100 μM. Cells were seeded at a density of 7.4 x 10^4 $cells.cm^{-2}$ and allowed to grow for 5. Bars represent mean values ± SD from *n* = 6-12 analyses, performed on two independent days. *p<0.05, **p<0.01, ***p<0.001, ****p<0.0001.

Table 7 - Identification, by nano-ESI-MS/MS, of the main gliadin proteins extracted from a commercial wheat flour and subsequently digested using a newly static digestion method that uses constant ratios of protein to digestive fluids and a constant pH for each step of digestion. This data was extracted from the Proteome Discoverer 1.4 software from ThermoFisher Scientific, used to interrogate protein databases for protein(s) identification through the SEQUEST search algorithm, after limiting the search to the *Triticum aestivum* gluten proteome (UniProtKB database). # PSM- number of peptide-spectrum matches, # AA- number of aminoacids, MW- molecular weight.

Accession	Protein	Score	Coverage (%)	# Peptides	# PSMs	# AAs	MW [kDa]	Calc. pI
A0A0E3Z506	Alpha-gliadin	457,57	97,08	291	552	308	35,4	7,71
A0A1K0IT13	Alpha-gliadin	430,46	97,08	310	555	308	35,5	8,25
K7WV37	Alpha-gliadin	377,20	97,40	297	525	308	35,4	8,18
R9XSV1	Alpha-gliadin	361,24	99,65	289	470	286	32,8	7,77
A5JSA9	Alpha-gliadin	338,71	99,36	278	461	312	35,9	7,77
A0A0E3UQU0	Alpha-gliadin	310,10	97,56	288	515	287	32,8	7,44
A0A1K0ISY9	Alpha-gliadin	303,12	97,76	272	447	312	35,9	7,30
A0A1W6C2K0	Alpha-gliadin	295,44	99,32	279	427	292	33,6	7,71
A5JSB3	Alpha-gliadin	258,71	97,21	240	406	287	33,0	7,40
A0A023WGX2	Alpha-gliadin	237,57	97,55	218	368	204	23,2	6,33
K7XR67	Alpha-gliadin	221,70	97,20	281	429	286	32,7	7,36
Q9M4L5	Gamma-gliadin	189,55	100,00	275	455	277	31,7	8,34
Q9M4L8	Alpha-gliadin	130,34	94,58	184	267	277	32,4	7,77

Differentiated Caco-2 cells were challenged with either 0.5 and 1.0 $mg.mL^{-1}$ of this new gliadin peptide digest for 6 and 24 h at 37 °C after which the activity of extracellular lactate dehydrogenase (LDH) and intracellular GSR and G6PD were measured (*Fig. 60*). The LDH assay is a colorimetric method that provides simple and reliable insights regarding cellular viability and cytotoxicity. Being a stable cytoplasmic enzyme, the LDH is rapidly released into the cell culture supernatant when the plasma membrane is damaged, a key feature of cells undergoing apoptosis, necrosis, and other forms of cellular damage [443]. In this case, the LDH activity was quantified by using the NADH produced during the conversion of lactate to pyruvate to reduce a tetrazolium salt, phenazine methosulfate (PMS), into a formazan dye that absorbed at 490 nm. The

amount of formazan generated was directly proportional to the amount of LDH in the culture medium, which was, in turn, directly proportional to the number of dead or damaged cells.

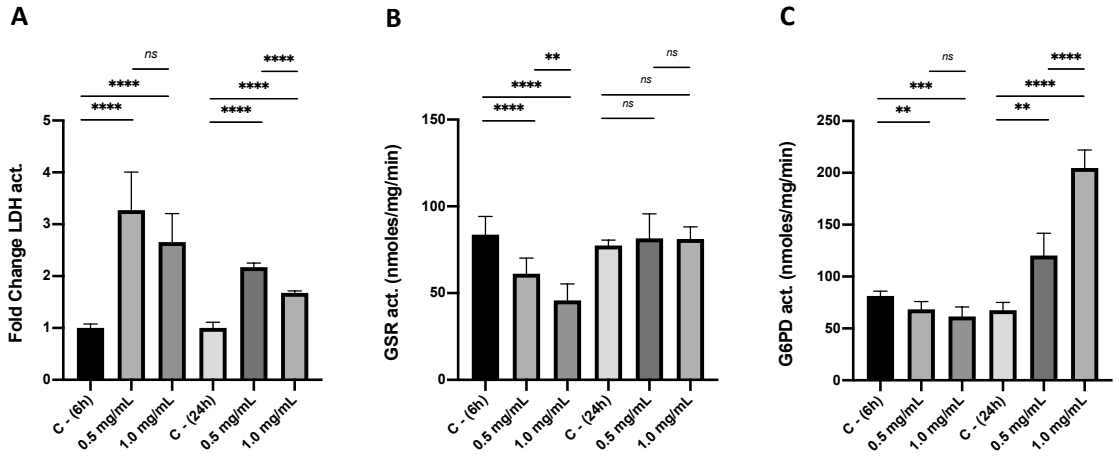

Fig. 60 - LDH (A), GSR (B) and G6PD (C) activity in differentiated Caco-2 cells treated with 0.5 and 1.0 mg.mL^{-1} of gliadin peptides for 6 and 24 h at 37 °C. Cells were seeded at a density of 7.4 x 10^4 cells.cm^{-2} and allowed to grow for 21 days. Bars represent mean values ± SD from *n* = 6 analyses. *p<0.05, **p<0.01, ***p<0.001, ****p<0.0001.

As it can be seen from *Fig. 60*, the results obtained with this new batch of gliadin peptides were astonishing, at least on a cytotoxicity basis, as they induced a highly significant release of LDH to the culture medium coupled to a downregulation of both GSR and G6PD activity in the first 6 h of incubation. In most cases there was a clear destabilization of the monolayer integrity, characterized by the presence of small holes along its surface, something that did not happen with the previous gliadin peptide preparation. At the end of 24 h, the activity of LDH was still above the negative control (C^-), but still, there was a normalization on GSR activity and an upregulation of G6PD. This could mean that by prolonging the exposure of differentiated Caco-2 to these gliadin peptides, the cells reacted by triggering an antioxidant stress response capable of counteracting the pro-oxidative properties of gliadins in an attempt to restore their nucleophilic tone and reductive power (in the form of NADPH). Taken together, these results support the idea that indeed, depending on the protocol followed during the *in vitro* gastrointestinal digestion of gluten proteins, their biological activity at the intestinal level could be significantly affected and that this could be the main source of conflicting results between and within research groups. As such it would be important to standardize this protocol as a physiologically accurate model for simulating human gastrointestinal

digestion of gluten proteins, so that there could be a meaningful comparison of results among the literature, accompanying that which has been the trend of the last few years and the growing data that have been acquired concerning the physiology of the human gastrointestinal tract. Future fine-tuning of these experimental conditions together with a reliable *in vitro* modeling and understanding of (i) the sequential and time-dependent release of inflammatory mediators and interacting signaling pathways that are involved in the early inflammatory reaction to gluten peptides; (ii) the anti-oxidant and anti-inflammatory mechanisms by which polyphenols, among other food bioactives, counteract these effects; and (iii) the involvement of additional cellular partners such as macrophages, dendritic cells or lymphocytes, will provide supplementary insights regarding the applicability of polyphenols as nutritional modulators of CD at the intestinal level, the first line of defense against the detrimental effects of gluten.

CONCLUDING REMARKS

Currently, the mainstay of treatment for CD depends on a strict life-long adherence to a GFD. However, even though for most patients a GFD results in full clinical and histological remission and is associated with improvements in symptoms and quality-of-life, a decrease in long term health risks and health gains for problems associated with CD, this diet is restrictive and can be difficult for some patients to follow. Unsurprisingly, the most common cause of persistent symptoms is nothing less than gluten consumption itself. According to a recent study coming from the UK, more than 70% of diagnosed CD patients consume gluten either intentionally or inadvertently [444]. Furthermore, in a substantial fraction of CD patients, a GFD is not enough to suppress the disease or completely alleviate symptoms. For this reason, there has been an increasing demand in developing new therapies capable of supplementing or supplanting a GFD, ideally combining efficiency to safety.

Over the past decades, dietary polyphenols have been a focus of intensive research in the context of prevention and treatment of several oxidative stress and inflammatory-related diseases. Initially seen as regular anti-oxidant compounds, more recently, and mainly because of their poor gastrointestinal bioavailability, alternative pathways have been unraveled and increasing evidence strongly supports that the health benefits of dietary polyphenols are also mediated by their ability to modulate key signaling pathways and gene transcription events. Considering that the gastrointestinal tract is the compartment where the concentration of polyphenols might achieve their higher concentrations in the human body and that CD primarily affects the small intestinal mucosa, we aimed to determine whether polyphenols would be able to scavenge and/or counteract the cytotoxicity of CD-bioactive peptides. As one of the first studies exploring the dietary polyphenols role in CD onset, this work lays the foundations for future investigations by providing a set of innovative *in vitro* and *in vivo* experimental evidences regarding the immunomodulatory role of polyphenols against the detrimental effects of gluten peptide. Starting from a fundamental base that so far remained completely unexplored, this thesis is the result of a multidisciplinary work, transversal to the fields of organic chemistry, analytical chemistry, physical chemistry and biochemistry of biological systems with direct implications in a priority area of today's society. Nonetheless, this is

only the beginning of a history that stills in its infancy so that further researches are needed to thoroughly understand the mechanisms underlying the health promoting properties of polyphenols in a CD framework.

REFERENCES

1. Lindfors, K., et al., *Coeliac disease.* Nature Reviews Disease Primers, 2019. **5**(1): p. 3.
2. Lebwohl, B., D.S. Sanders, and P.H.R. Green, *Coeliac disease.* The Lancet, 2018. **391**(10115): p. 70-81.
3. Biagi, F. and G.R. Corazza, *Mortality in celiac disease.* Nature Reviews Gastroenterology & Hepatology, 2010. **7**(3): p. 158-162.
4. Abadie, V., et al., *Integration of Genetic and Immunological Insights into a Model of Celiac Disease Pathogenesis.* Annual Review of Immunology, 2011. **29**(1): p. 493-525.
5. Jabri, B. and L.M. Sollid, *Tissue-mediated control of immunopathology in coeliac disease.* Nature Reviews Immunology, 2009. **9**(12): p. 858-870.
6. Singh, P., et al., *Global prevalence of celiac disease: systematic review and meta-analysis.* Clinical Gastroenterology and Hepatology, 2018. **16**(6): p. 823-836. e2.
7. Tuire, I., et al., *Persistent duodenal intraepithelial lymphocytosis despite a long-term strict gluten-free diet in celiac disease.* American Journal of Gastroenterology, 2012. **107**(10): p. 1563-1569.
8. Lohi, S., et al., *Increasing prevalence of coeliac disease over time.* Alimentary pharmacology & therapeutics, 2007. **26**(9): p. 1217-1225.
9. Rubio–Tapia, A., et al., *Increased prevalence and mortality in undiagnosed celiac disease.* Gastroenterology, 2009. **137**(1): p. 88-93.
10. Catassi, C., et al., *Natural history of celiac disease autoimmunity in a USA cohort followed since 1974.* Annals of medicine, 2010. **42**(7): p. 530-538.
11. Fasano, A., et al., *Prevalence of celiac disease in at-risk and not-at-risk groups in the United States: a large multicenter study.* Archives of internal medicine, 2003. **163**(3): p. 286-292.
12. Choung, R.S., et al., *Prevalence and Morbidity of Undiagnosed Celiac Disease From a Community-Based Study.* Gastroenterology, 2017. **152**(4): p. 830-839.e5.
13. Downey, L., et al., *Recognition, assessment, and management of coeliac disease: summary of updated NICE guidance.* Bmj, 2015. **351**: p. h4513.
14. Volta, U., et al., *The changing clinical profile of celiac disease: a 15-year experience (1998-2012) in an Italian referral center.* BMC gastroenterology, 2014. **14**(1): p. 194.

15. Jericho, H., N. Sansotta, and S. Guandalini, *Extraintestinal manifestations of celiac disease: effectiveness of the gluten-free diet.* Journal of pediatric gastroenterology and nutrition, 2017. **65**(1): p. 75-79.
16. Reunala, T., et al., *Dermatitis herpetiformis: a common extraintestinal manifestation of coeliac disease.* Nutrients, 2018. **10**(5): p. 602.
17. Fuchs, V., et al., *Delayed celiac disease diagnosis predisposes to reduced quality of life and incremental use of health care services and medicines: A prospective nationwide study.* United European gastroenterology journal, 2018. **6**(4): p. 567-575.
18. Singh, P., et al., *Risk of celiac disease in the first-and second-degree relatives of patients with celiac disease: a systematic review and meta-analysis.* American Journal of Gastroenterology, 2015. **110**(11): p. 1539-1548.
19. Tosi, R., et al., *Evidence that celiac disease is primarily associated with a DC locus allelic specificity.* Clinical immunology and immunopathology, 1983. **28**(3): p. 395-404.
20. Karell, K., et al., *HLA types in celiac disease patients not carrying the DQA1* 05-DQB1* 02 (DQ2) heterodimer: results from the European Genetics Cluster on Celiac Disease.* Human immunology, 2003. **64**(4): p. 469-477.
21. Sollid, L.M., *The roles of MHC class II genes and post-translational modification in celiac disease.* Immunogenetics, 2017. **69**(8-9): p. 605-616.
22. Abadie, V., et al., *Integration of genetic and immunological insights into a model of celiac disease pathogenesis.* Annual review of immunology, 2011. **29**: p. 493-525.
23. Trynka, G., et al., *Dense genotyping identifies and localizes multiple common and rare variant association signals in celiac disease.* Nature genetics, 2011. **43**(12): p. 1193-1201.
24. Withoff, S., et al., *Understanding celiac disease by genomics.* Trends in Genetics, 2016. **32**(5): p. 295-308.
25. Jabri, B. and L.M. Sollid, *T Cells in Celiac Disease.* Journal of immunology (Baltimore, Md. : 1950), 2017. **198**(8): p. 3005-3014.
26. Smyth, D.J., et al., *Shared and distinct genetic variants in type 1 diabetes and celiac disease.* New England Journal of Medicine, 2008. **359**(26): p. 2767-2777.
27. Zhernakova, A., et al., *Meta-analysis of genome-wide association studies in celiac disease and rheumatoid arthritis identifies fourteen non-HLA shared loci.* Annals of the Rheumatic Diseases, 2011. **70**(Suppl 2): p. A21-A21.

28. Sollid, L.M. and B. Jabri, *Triggers and drivers of autoimmunity: lessons from coeliac disease.* Nature Reviews Immunology, 2013. **13**(4): p. 294-302.
29. Wieser, H., *Chemistry of gluten proteins.* Food Microbiology, 2007. **24**(2): p. 115-119.
30. Biesiekierski, J.R., *What is gluten?* Journal of Gastroenterology and Hepatology, 2017. **32**(S1): p. 78-81.
31. Koehler, P. and H. Wieser, *Chemistry of Cereal Grains*, in *Handbook on Sourdough Biotechnology*, M. Gobbetti and M. Gänzle, Editors. 2013, Springer US. p. 11-45.
32. Shewry, P., *What Is Gluten—Why Is It Special?* Frontiers in Nutrition, 2019. **6**(101).
33. Veraverbeke, W.S. and J.A. Delcour, *Wheat protein composition and properties of wheat glutenin in relation to breadmaking functionality.* Critical reviews in food science and nutrition, 2002. **42**(3): p. 179-208.
34. Delcour, J.A., et al., *Wheat gluten functionality as a quality determinant in cereal-based food products.* Annual review of food science and technology, 2012. **3**: p. 469-492.
35. Kucek, L.K., et al., *A grounded guide to gluten: how modern genotypes and processing impact wheat sensitivity.* Comprehensive Reviews in Food Science and Food Safety, 2015. **14**(3): p. 285-302.
36. Uil-Dieterman, I., et al., *The daily gluten intake in relatives of patients with coeliac disease compared with that of the general Dutch population.* European journal of gastroenterology & hepatology, 1997. **9**(11): p. 1097-1099.
37. Ooms, N. and J.A. Delcour, *How to impact gluten protein network formation during wheat flour dough making.* Current opinion in food science, 2019.
38. Wieser, H., *Relation between gliadin structure and coeliac toxicity.* Acta Paediatrica, 1996. **85**: p. 3-9.
39. Wieser, H. and R. Kieffer, *Correlations of the amount of gluten protein types to the technological properties of wheat flours determined on a micro-scale.* Journal of Cereal Science, 2001. **34**(1): p. 19-27.
40. Hamer, R. and T.v. Vliet. *Understanding the structure and properties of gluten: an overview*. in *Wheat gluten. Proceedings of the 7th International Workshop Gluten 2000, Bristol, UK, 2-6 April 2000*. 2000. Royal Society of Chemistry.
41. Grosch, W. and H. Wieser, *Redox reactions in wheat dough as affected by ascorbic acid.* Journal of cereal science, 1999. **29**(1): p. 1-16.

42. Müller, S. and H. Wieser, *The location of disulphide bonds in α-type gliadins.* Journal of cereal Science, 1995. **22**(1): p. 21-27.
43. Keck, B., P. Köhler, and H. Wieser, *Disulphide bonds in wheat gluten: cystine peptides derived from gluten proteins following peptic and thermolytic digestion.* Zeitschrift für Lebensmittel-Untersuchung und Forschung, 1995. **200**(6): p. 432-439.
44. Muller, S. and H. Wieser, *location of disulphide bonds in monomeric gamma-type gliadins.* Journal of cereal science, 1997.
45. Tatham, A.S. and P.R. Shewry, *The conformation of wheat gluten proteins. The secondary structures and thermal stabilities of α-, β-, γ-and ω-gliadins.* Journal of Cereal Science, 1985. **3**(2): p. 103-113.
46. Banc, A., et al., *Structure and Orientation Changes of ω- and γ-Gliadins at the Air−Water Interface: A PM−IRRAS Spectroscopy and Brewster Angle Microscopy Study.* Langmuir, 2007. **23**(26): p. 13066-13075.
47. Anderson, O.D., et al., *A New Class of Wheat Gliadin Genes and Proteins.* PLOS ONE, 2012. **7**(12): p. e52139.
48. Wieser, H., W. Bushuk, and F. MacRitchie, *The polymeric glutenins.* Gliadin and Glutenin: The Unique Balance of Wheat Quality, 2006: p. 213-240.
49. Wellner, N., et al., *Changes in protein secondary structure during gluten deformation studied by dynamic Fourier transform infrared spectroscopy.* Biomacromolecules, 2005. **6**(1): p. 255-261.
50. Lawrence, G. and K. Shepherd, *Chromosomal location of genes controlling seed proteins in species related to wheat.* Theoretical and Applied Genetics, 1981. **59**(1): p. 25-31.
51. Shewry, P.R., et al., *The high molecular weightsubunitsofwheatgluteninandtheirroleindetermining wheat processing properties.* Adv Food Nutr Res, 2003. **45**: p. 219-302.
52. Shewry, P.R. and N.G. Halford, *Cereal seed storage proteins: structures, properties and role in grain utilization.* Journal of experimental botany, 2002. **53**(370): p. 947-958.
53. Shewry, P., N. Halford, and A. Tatham, *High molecular weight subunits of wheat glutenin.* Journal of cereal science, 1992. **15**(2): p. 105-120.
54. Urade, R., N. Sato, and M. Sugiyama, *Gliadins from wheat grain: an overview, from primary structure to nanostructures of aggregates.* Biophysical reviews, 2018. **10**(2): p. 435-443.

55. Shewry, P.R. and A.S. Tatham, *Disulphide Bonds in Wheat Gluten Proteins.* Journal of Cereal Science, 1997. **25**(3): p. 207-227.
56. Koehler, P. and H. Wieser. *Structure and functionality of gluten proteins: an overview*. in *Proc. of the 10th Int. Gluten Workshop, Clermont-Ferrand, France*. 2009.
57. Peña, E., et al., *Do tyrosine crosslinks contribute to the formation of the gluten network in common wheat (Triticum aestivum L.) dough?* Journal of Cereal Science, 2006. **44**(2): p. 144-153.
58. Erickson, R.H. and Y.S. Kim, *Digestion and absorption of dietary protein.* Annual review of medicine, 1990. **41**(1): p. 133-139.
59. Gray, G.M., *Dietary protein processing: intraluminal and enterocyte surface events.* Comprehensive physiology, 2010: p. 411-420.
60. Shan, L., et al., *Structural basis for gluten intolerance in Celiac sprue.* Science, 2002. **297**(5590): p. 2275-2279.
61. Sollid, L.M., *Coeliac disease: Dissecting a complex inflammatory disorder.* Nature Reviews Immunology, 2002. **2**(9): p. 647-655.
62. Shan, L., et al., *Identification and analysis of multivalent proteolytically resistant peptides from gluten: implications for celiac sprue.* J Proteome Res, 2005. **4**(5): p. 1732-41.
63. Mamone, G., et al., *Identification of a peptide from α-gliadin resistant to digestive enzymes: Implications for celiac disease.* Journal of Chromatography B, 2007. **855**(2): p. 236-241.
64. Ferretti, G., et al., *Celiac Disease, Inflammation and Oxidative Damage: A Nutrigenetic Approach.* Nutrients, 2012. **4**(4): p. 243-257.
65. Zimmermann, C., et al., *Epithelial transport of immunogenic and toxic gliadin peptides in vitro.* PloS one, 2014. **9**(11): p. e113932.
66. Molberg, Ø., et al., *Tissue transglutaminase selectively modifies gliadin peptides that are recognized by gut-derived T cells in celiac disease.* Nature medicine, 1998. **4**(6): p. 713-717.
67. van de Wal, Y., et al., *Cutting edge: selective deamidation by tissue transglutaminase strongly enhances gliadin-specific T cell reactivity.* The Journal of Immunology, 1998. **161**(4): p. 1585-1588.
68. Molberg, Ø., et al., *T cells from celiac disease lesions recognize gliadin epitopes deamidated in situ by endogenous tissue transglutaminase.* European journal of immunology, 2001. **31**(5): p. 1317-1323.

69. Fleckenstein, B., et al., *Gliadin T cell epitope selection by tissue transglutaminase in celiac disease. Role of enzyme specificity and pH influence on the transamidation versus deamidation process.* J Biol Chem, 2002. **277**(37): p. 34109-16.
70. Vader, L.W., et al., *Specificity of tissue transglutaminase explains cereal toxicity in celiac disease.* The Journal of experimental medicine, 2002. **195**(5): p. 643-649.
71. Gundemir, S., et al., *Transglutaminase 2: a molecular Swiss army knife.* Biochimica et Biophysica Acta (BBA)-Molecular Cell Research, 2012. **1823**(2): p. 406-419.
72. Strnad, P. and M.B. Omary, *Transglutaminase cross-links Sp1-mediated transcription to ethanol-induced liver injury.* Gastroenterology, 2009. **136**(5): p. 1502-1505.
73. Tollefsen, S., et al., *HLA-DQ2 and-DQ8 signatures of gluten T cell epitopes in celiac disease.* The Journal of clinical investigation, 2006. **116**(8): p. 2226-2236.
74. Sollid, L.M., et al., *Nomenclature and listing of celiac disease relevant gluten T-cell epitopes restricted by HLA-DQ molecules.* Immunogenetics, 2012. **64**(6): p. 455-460.
75. Camarca, A., A. Del Mastro, and C. Gianfrani, *Repertoire of gluten peptides active in celiac disease patients: perspectives for translational therapeutic applications.* Endocrine, metabolic & immune disorders drug targets, 2012. **12**(2): p. 207-19.
76. Nilsen, E., et al., *Gluten specific, HLA-DQ restricted T cells from coeliac mucosa produce cytokines with Th1 or Th0 profile dominated by interferon gamma.* Gut, 1995. **37**(6): p. 766-776.
77. Bodd, M., et al., *HLA-DQ2-restricted gluten-reactive T cells produce IL-21 but not IL-17 or IL-22.* Mucosal immunology, 2010. **3**(6): p. 594-601.
78. Stamnaes, J. and L. Sollid. *Celiac disease: autoimmunity in response to food antigen*. in *Seminars in immunology*. 2015. Elsevier.
79. Yu, X.B., et al., *Autoantibodies in the extraintestinal manifestations of celiac disease.* Nutrients, 2018. **10**(8): p. 1123.
80. Matysiak-Budnik, T., et al., *Secretory IgA mediates retrotranscytosis of intact gliadin peptides via the transferrin receptor in celiac disease.* The Journal of experimental medicine, 2008. **205**(1): p. 143-154.

81. Lebreton, C., et al., *Interactions among secretory immunoglobulin A, CD71, and transglutaminase-2 affect permeability of intestinal epithelial cells to gliadin peptides.* Gastroenterology, 2012. **143**(3): p. 698-707. e4.
82. Rauhavirta, T., et al., *Transglutaminase 2 and transglutaminase 2 autoantibodies in celiac disease: a review.* Clinical reviews in allergy & immunology, 2016: p. 1-16.
83. Meresse, B., et al., *Coordinated induction by IL15 of a TCR-independent NKG2D signaling pathway converts CTL into lymphokine-activated killer cells in celiac disease.* Immunity, 2004. **21**(3): p. 357-366.
84. Meresse, B., et al., *Reprogramming of CTLs into natural killer–like cells in celiac disease.* The Journal of experimental medicine, 2006. **203**(5): p. 1343-1355.
85. Braud, V.M., et al., *HLA-E binds to natural killer cell receptors CD94/NKG2A, B and C.* Nature, 1998. **391**(6669): p. 795-799.
86. Bauer, S., et al., *Activation of NK cells and T cells by NKG2D, a receptor for stress-inducible MICA.* Science, 1999. **285**(5428): p. 727-729.
87. Hüe, S., et al., *A direct role for NKG2D/MICA interaction in villous atrophy during celiac disease.* Immunity, 2004. **21**(3): p. 367-377.
88. Liu, R.B., et al., *IL-15 in tumor microenvironment causes rejection of large established tumors by T cells in a noncognate T cell receptor-dependent manner.* Proceedings of the National Academy of Sciences, 2013. **110**(20): p. 8158-8163.
89. Rosen, D.B., et al., *A structural basis for the association of DAP12 with mouse, but not human, NKG2D.* The Journal of Immunology, 2004. **173**(4): p. 2470-2478.
90. Setty, M., et al., *Distinct and Synergistic Contributions of Epithelial Stress and Adaptive Immunity to Functions of Intraepithelial Killer Cells and Active Celiac Disease.* Gastroenterology, 2015. **149**(3): p. 681-91.e10.
91. de Wit, T.R., et al., *Differential expression of the HLA class I multigene family by human embryonal carcinoma and choriocarcinoma cell lines.* The Journal of Immunology, 1990. **144**(3): p. 1080-1087.
92. Sarra, M., et al., *Targeting interleukin-21 in immune-mediated pathologies.* Current drug targets, 2010. **11**(5): p. 645-649.
93. Mention, J.-J., et al., *Interleukin 15: a key to disrupted intraepithelial lymphocyte homeostasis and lymphomagenesis in celiac disease.* Gastroenterology, 2003. **125**(3): p. 730-745.
94. Abadie, V. and B. Jabri, *IL-15: a central regulator of celiac disease immunopathology.* Immunological reviews, 2014. **260**(1): p. 221-234.

95. Benahmed, M., et al., *Inhibition of TGF-beta signaling by IL-15: a new role for IL-15 in the loss of immune homeostasis in celiac disease.* Gastroenterology, 2007. **132**(3): p. 994-1008.
96. Ahmed, M.B., et al., *IL-15 Renders Conventional Lymphocytes Resistant to Suppressive Functions of Regulatory T Cells through Activation of the Phosphatidylinositol 3-Kinase Pathway.* The Journal of Immunology, 2009. **182**(11): p. 6763.
97. Tang, F., et al., *Cytosolic PLA2 is required for CTL-mediated immunopathology of celiac disease via NKG2D and IL-15.* Journal of Experimental Medicine, 2009. **206**(3): p. 707-719.
98. Tang, F., et al., *Cysteinyl leukotrienes mediate lymphokine killer activity induced by NKG2D and IL-15 in cytotoxic T cells during celiac disease.* Journal of Experimental Medicine, 2015. **212**(10): p. 1487-1495.
99. Maiuri, L., et al., *Association between innate response to gliadin and activation of pathogenic T cells in coeliac disease.* The Lancet, 2003. **362**(9377): p. 30-37.
100. Barone, M.V., R. Troncone, and S. Auricchio, *Gliadin peptides as triggers of the proliferative and stress/innate immune response of the celiac small intestinal mucosa.* International journal of molecular sciences, 2014. **15**(11): p. 20518-20537.
101. Maiuri, L., et al., *In vitro Activities of A-Gliadin-Related Synthetic Peptides Damaging Effect on the Atrophic Coeliac Mucosa and Activation of Mucosal Immune Response in the Treated Coeliac Mucosa.* Scandinavian journal of gastroenterology, 1996. **31**(3): p. 247-253.
102. Gómez Castro, M.F., et al., *p31-43 Gliadin peptide forms oligomers and induces NLRP3 inflammasome/caspase 1-dependent mucosal damage in small intestine.* Frontiers in immunology, 2019. **10**: p. 31.
103. Zimmer, K.-P., et al., *Endocytotic segregation of gliadin peptide 31–49 in enterocytes.* Gut, 2010. **59**(3): p. 300-310.
104. Barone, M.V., et al., *Gliadin-mediated proliferation and innate immune activation in celiac disease are due to alterations in vesicular trafficking.* PLoS One, 2011. **6**(2).
105. Clemente, M.G., et al., *Early effects of gliadin on enterocyte intracellular signalling involved in intestinal barrier function.* Gut, 2003. **52**(2): p. 218-223.
106. Barone, M.V., et al., *Growth factor-like activity of gliadin, an alimentary protein: implications for coeliac disease.* Gut, 2007. **56**(4): p. 480-488.

107. Juuti-Uusitalo, K., et al., *Gluten affects epithelial differentiation-associated genes in small intestinal mucosa of coeliac patients.* Clinical & Experimental Immunology, 2007. **150**(2): p. 294-305.
108. Barone, M.V., et al., *Gliadin peptide P31-43 localises to endocytic vesicles and interferes with their maturation.* PloS one, 2010. **5**(8).
109. Luciani, A., et al., *Lysosomal accumulation of gliadin p31–43 peptide induces oxidative stress and tissue transglutaminase-mediated PPARγ downregulation in intestinal epithelial cells and coeliac mucosa.* Gut, 2010. **59**(3): p. 311-319.
110. Caputo, I., et al., *Gliadin peptides induce tissue transglutaminase activation and ER-stress through Ca2+ mobilization in Caco-2 cells.* PLoS One, 2012. **7**(9).
111. Maiuri, M.C., et al., *Nuclear factor κB is activated in small intestinal mucosa of celiac patients.* Journal of molecular medicine, 2003. **81**(6): p. 373-379.
112. Liu, T., et al., *NF-κB signaling in inflammation.* Signal transduction and targeted therapy, 2017. **2**: p. 17023.
113. Lee, J., et al., *Transglutaminase 2 induces nuclear factor-κB activation via a novel pathway in BV-2 microglia.* Journal of Biological Chemistry, 2004. **279**(51): p. 53725-53735.
114. Verma, A. and K. Mehta, *Transglutaminase-mediated activation of nuclear transcription factor-κB in cancer cells: a new therapeutic opportunity.* Current cancer drug targets, 2007. **7**(6): p. 559-565.
115. Lammers, K.M., et al., *Gliadin induces an increase in intestinal permeability and zonulin release by binding to the chemokine receptor CXCR3.* Gastroenterology, 2008. **135**(1): p. 194-204. e3.
116. Luciani, A., et al., *Defective CFTR induces aggresome formation and lung inflammation in cystic fibrosis through ROS-mediated autophagy inhibition.* Nature cell biology, 2010. **12**(9): p. 863-875.
117. Villella, V., et al., *Disease-relevant proteostasis regulation of cystic fibrosis transmembrane conductance regulator.* Cell Death & Differentiation, 2013. **20**(8): p. 1101-1115.
118. Cutting, G.R., *Cystic fibrosis genetics: from molecular understanding to clinical application.* Nature Reviews Genetics, 2015. **16**(1): p. 45-56.
119. Ferrari, E., et al., *Cysteamine re-establishes the clearance of Pseudomonas aeruginosa by macrophages bearing the cystic fibrosis-relevant F508del-CFTR mutation.* Cell death & disease, 2018. **8**(1): p. e2544-e2544.
120. Villella, V.R., et al., *A pathogenic role for cystic fibrosis transmembrane conductance regulator in celiac disease.* The EMBO journal, 2019. **38**(2).

121. Araya, R.E., et al., *Intraluminal administration of poly I: C causes an enteropathy that is exacerbated by administration of oral dietary antigen.* PloS one, 2014. **9**(6).
122. Kim, S.M., T. Mayassi, and B. Jabri, *Innate immunity: actuating the gears of celiac disease pathogenesis.* Best Practice & Research Clinical Gastroenterology, 2015. **29**(3): p. 425-435.
123. Stene, L.C., et al., *Rotavirus infection frequency and risk of celiac disease autoimmunity in early childhood: a longitudinal study.* American Journal of Gastroenterology, 2006. **101**(10): p. 2333-2340.
124. Verdu, E., et al., *Clinical onset of celiac disease after an episode of Campylobacter jejuni enteritis.* Canadian Journal of Gastroenterology and Hepatology, 2007. **21**(7): p. 453-455.
125. Marshall, J.K., et al., *Postinfectious irritable bowel syndrome after a food-borne outbreak of acute gastroenteritis attributed to a viral pathogen.* Clinical Gastroenterology and Hepatology, 2007. **5**(4): p. 457-460.
126. Iacomino, G., et al., *Celiac disease: role of intestinal compartments in the mucosal immune response.* Molecular and cellular biochemistry, 2016. **411**(1-2): p. 341-349.
127. Bouziat, R., et al., *Reovirus infection triggers inflammatory responses to dietary antigens and development of celiac disease.* Science, 2017. **356**(6333): p. 44-50.
128. Araya, R.E., et al., *Mechanisms of innate immune activation by gluten peptide p31-43 in mice.* American Journal of Physiology-Gastrointestinal and Liver Physiology, 2016. **311**(1): p. G40-G49.
129. Nanayakkara, M., et al., *P31–43, an undigested gliadin peptide, mimics and enhances the innate immune response to viruses and interferes with endocytic trafficking: a role in celiac disease.* Scientific reports, 2018. **8**(1): p. 1-12.
130. Paolella, G., et al., *The toxic alpha-gliadin peptide 31–43 enters cells without a surface membrane receptor.* Cell biology international, 2018. **42**(1): p. 112-120.
131. Forsberg, G., et al., *Presence of bacteria and innate immunity of intestinal epithelium in childhood celiac disease.* American Journal of Gastroenterology, 2004. **99**(5): p. 894-904.
132. Ou, G., et al., *Proximal small intestinal microbiota and identification of rod-shaped bacteria associated with childhood celiac disease.* American Journal of Gastroenterology, 2009. **104**(12): p. 3058-3067.

133. Sánchez, E., et al., *Duodenal-mucosal bacteria associated with celiac disease in children.* Appl. Environ. Microbiol., 2013. **79**(18): p. 5472-5479.
134. Wacklin, P., et al., *Altered duodenal microbiota composition in celiac disease patients suffering from persistent symptoms on a long-term gluten-free diet.* American Journal of Gastroenterology, 2014. **109**(12): p. 1933-1941.
135. D'argenio, V., et al., *Metagenomics reveals dysbiosis and a potentially pathogenic N. flavescens strain in duodenum of adult celiac patients.* The American journal of gastroenterology, 2016. **111**(6): p. 879.
136. Husby, S., J.A. Murray, and D.A. Katzka, *AGA Clinical Practice Update on Diagnosis and Monitoring of Celiac Disease-Changing Utility of Serology and Histologic Measures: Expert Review.* Gastroenterology, 2019. **156**(4): p. 885-889.
137. Werkstetter, K.J., et al., *Accuracy in diagnosis of celiac disease without biopsies in clinical practice.* Gastroenterology, 2017. **153**(4): p. 924-935.
138. Bibbins-Domingo, K., et al., *Screening for celiac disease: US Preventive Services Task Force recommendation statement.* Jama, 2017. **317**(12): p. 1252-1257.
139. James, M.W. and B.B. Scott, *Endomysial antibody in the diagnosis and management of coeliac disease.* Postgraduate Medical Journal, 2000. **76**(898): p. 466.
140. Kaswala, D.H., et al., *Celiac Disease: Diagnostic Standards and Dilemmas.* Diseases (Basel, Switzerland), 2015. **3**(2): p. 86-101.
141. Korponay-Szabó, I.R., et al., *Elevation of IgG antibodies against tissue transglutaminase as a diagnostic tool for coeliac disease in selective IgA deficiency.* Gut, 2003. **52**(11): p. 1567-1571.
142. Hoerter, N.A., et al., *Diagnostic yield of isolated deamidated gliadin peptide antibody elevation for celiac disease.* Digestive diseases and sciences, 2017. **62**(5): p. 1272-1276.
143. Caio, G., et al., *Celiac disease: a comprehensive current review.* BMC Medicine, 2019. **17**(1): p. 142.
144. Husby, S., et al., *European Society for Pediatric Gastroenterology, Hepatology, and Nutrition guidelines for the diagnosis of coeliac disease.* Journal of pediatric gastroenterology and nutrition, 2012. **54**(1): p. 136-160.
145. Salmi, T., et al., *Diagnostic methods beyond conventional histology in coeliac disease diagnosis.* Digestive and Liver Disease, 2010. **42**(1): p. 28-32.
146. Pallav, K., et al., *Clinical utility of celiac disease-associated HLA testing.* Digestive diseases and sciences, 2014. **59**(9): p. 2199-2206.

147. See, J.A., et al., *Practical insights into gluten-free diets.* Nature reviews Gastroenterology & hepatology, 2015. **12**(10): p. 580.
148. Newnham, E.D., et al., *Adherence to the gluten-free diet can achieve the therapeutic goals in almost all patients with coeliac disease: A 5-year longitudinal study from diagnosis.* Journal of gastroenterology and hepatology, 2016. **31**(2): p. 342-349.
149. Hære, P., et al., *Long-term mucosal recovery and healing in celiac disease is the rule–not the exception.* Scandinavian journal of gastroenterology, 2016. **51**(12): p. 1439-1446.
150. Aziz, I., et al., *Are patients with coeliac disease seeking alternative therapies to a gluten-free diet.* J Gastrointestin Liver Dis, 2011. **20**(1): p. 27-31.
151. Branchi, F., et al., *Celiac disease and drug-based therapies: inquiry into patients demands.* Digestion, 2016. **93**(2): p. 160-166.
152. Lee, A., et al., *Economic burden of a gluten-free diet.* Journal of human Nutrition and Dietetics, 2007. **20**(5): p. 423-430.
153. Syage, J.A., et al., *Determination of gluten consumption in celiac disease patients on a gluten-free diet.* The American journal of clinical nutrition, 2018. **107**(2): p. 201-207.
154. Farage, P. and R. Zandonadi, *The gluten-free diet: difficulties celiac disease patients have to face daily.* Austin J Nutri Food Sci, 2014. **2**(5): p. 1027.
155. Ciacci, C. and F. Zingone, *The Perceived Social Burden in Celiac Disease.* Diseases, 2015. **3**(2): p. 102-110.
156. Villafuerte-Galvez, J., et al., *Factors governing long-term adherence to a gluten-free diet in adult patients with coeliac disease.* Alimentary pharmacology & therapeutics, 2015. **42**(6): p. 753-760.
157. Ilus, T., et al., *Refractory coeliac disease in a country with a high prevalence of clinically-diagnosed coeliac disease.* Alimentary pharmacology & therapeutics, 2014. **39**(4): p. 418-425.
158. Rubio-Tapia, A. and J.A. Murray, *Classification and management of refractory coeliac disease.* Gut, 2010. **59**(4): p. 547-557.
159. Plugis, N.M. and C. Khosla, *Therapeutic approaches for celiac disease.* Best practice & research Clinical gastroenterology, 2015. **29**(3): p. 503-521.
160. Yoosuf, S. and G.K. Makharia, *Evolving Therapy for Celiac Disease.* Frontiers in pediatrics, 2019. **7**: p. 193-193.
161. Gotsis, E., et al., *Health benefits of the Mediterranean diet: an update of research over the last 5 years.* Angiology, 2015. **66**(4): p. 304-318.

162. Wallace, T.C., et al., *Fruits, vegetables, and health: A comprehensive narrative, umbrella review of the science and recommendations for enhanced public policy to improve intake.* Critical Reviews in Food Science and Nutrition, 2019: p. 1-38.
163. Manach, C., et al., *Addressing the inter-individual variation in response to consumption of plant food bioactives: towards a better understanding of their role in healthy aging and cardiometabolic risk reduction.* Molecular nutrition & food research, 2017. **61**(6): p. 1600557.
164. Pandey, K.B. and S.I. Rizvi, *Plant polyphenols as dietary antioxidants in human health and disease.* Oxidative medicine and cellular longevity, 2009. **2**(5): p. 270-278.
165. Vauzour, D., et al., *Polyphenols and human health: prevention of disease and mechanisms of action.* Nutrients, 2010. **2**(11): p. 1106-1131.
166. Li, A.-N., et al., *Resources and biological activities of natural polyphenols.* Nutrients, 2014. **6**(12): p. 6020-6047.
167. Figueira, I., et al., *Polyphenols Beyond Barriers: A Glimpse into the Brain.* Current neuropharmacology, 2017. **15**(4): p. 562-594.
168. Potì, F., et al., *Polyphenol Health Effects on Cardiovascular and Neurodegenerative Disorders: A Review and Meta-Analysis.* International journal of molecular sciences, 2019. **20**(2): p. 351.
169. Williamson, G., *The role of polyphenols in modern nutrition.* Nutrition bulletin, 2017. **42**(3): p. 226-235.
170. Yang, G., et al., *Regulation of the intestinal tight junction by natural polyphenols: A mechanistic perspective.* Critical reviews in food science and nutrition, 2017. **57**(18): p. 3830-3839.
171. Chaplin, A., C. Carpéné, and J. Mercader, *Resveratrol, Metabolic Syndrome, and Gut Microbiota.* Nutrients, 2018. **10**(11): p. 1651.
172. Fraga, C.G., et al., *The effects of polyphenols and other bioactives on human health.* Food & function, 2019. **10**(2): p. 514-528.
173. Yoshida, K., V. Cheynier, and S. Quideau, *Recent Advances in Polyphenol Research*. 2017: Wiley.
174. Tsao, R., *Chemistry and biochemistry of dietary polyphenols.* Nutrients, 2010. **2**(12): p. 1231-1246.
175. Lattanzio, V., et al., *Plant Phenolics – Secondary Metabolites with Diverse Functions*, in *Recent Advances in Polyphenol Research*. 2009, Wiley-Blackwell. p. 1-35.

176. Del Rio, D., et al., *Dietary (poly)phenolics in human health: structures, bioavailability, and evidence of protective effects against chronic diseases.* Antioxidants & redox signaling, 2013. **18**(14): p. 1818-1892.
177. de Freitas, V. and N. Mateus, *Protein/Polyphenol Interactions: Past and Present Contributions. Mechanisms of Astringency Perception.* Current Organic Chemistry, 2012. **16**(6): p. 724-746.
178. Cory, H., et al., *The Role of Polyphenols in Human Health and Food Systems: A Mini-Review.* Frontiers in nutrition, 2018. **5**: p. 87-87.
179. Cutrim, C.S. and M.A.S. Cortez, *A review on polyphenols: Classification, beneficial effects and their application in dairy products.* International Journal of Dairy Technology, 2018. **71**(3): p. 564-578.
180. Serafini, M., A. Ghiselli, and A. Ferro-Luzzi, *Red wine, tea, and antioxidants.* Lancet (London, England), 1994. **344**(8922): p. 626-626.
181. Cherrak, S.A., et al., *In vitro antioxidant versus metal ion chelating properties of flavonoids: A structure-activity investigation.* PloS one, 2016. **11**(10).
182. Han, X., T. Shen, and H. Lou, *Dietary polyphenols and their biological significance.* International Journal of Molecular Sciences, 2007. **8**(9): p. 950-988.
183. Kim, H.-S., M.J. Quon, and J.-A. Kim, *New insights into the mechanisms of polyphenols beyond antioxidant properties; lessons from the green tea polyphenol, epigallocatechin 3-gallate.* Redox biology, 2014. **2**: p. 187-195.
184. Zhang, H. and R. Tsao, *Dietary polyphenols, oxidative stress and antioxidant and anti-inflammatory effects.* Current Opinion in Food Science, 2016. **8**: p. 33-42.
185. Silva, R.F. and L. Pogačnik, *Polyphenols from Food and Natural Products: Neuroprotection and Safety.* Antioxidants, 2020. **9**(1): p. 61.
186. Hussain, T., et al., *Oxidative stress and inflammation: what polyphenols can do for us?* Oxidative medicine and cellular longevity, 2016. **2016**.
187. Yahfoufi, N., et al., *The immunomodulatory and anti-inflammatory role of polyphenols.* Nutrients, 2018. **10**(11): p. 1618.
188. Zhai, X., et al., *Dietary flavonoid genistein induces Nrf2 and phase II detoxification gene expression via ERKs and PKC pathways and protects against oxidative stress in Caco-2 cells.* Molecular nutrition & food research, 2013. **57**(2): p. 249-259.
189. Upadhyay, S. and M. Dixit, *Role of polyphenols and other phytochemicals on molecular signaling.* Oxidative medicine and cellular longevity, 2015. **2015**.

190. Forman, H.J., K.J. Davies, and F. Ursini, *How do nutritional antioxidants really work: nucleophilic tone and para-hormesis versus free radical scavenging in vivo.* Free Radical Biology and Medicine, 2014. **66**: p. 24-35.
191. D'Archivio, M., et al., *Bioavailability of the polyphenols: status and controversies.* International journal of molecular sciences, 2010. **11**(4): p. 1321-1342.
192. Spencer, J.P., et al., *Biomarkers of the intake of dietary polyphenols: strengths, limitations and application in nutrition research.* British Journal of Nutrition, 2008. **99**(1): p. 12-22.
193. Pinto, P. and C.N. Santos, *Worldwide (poly) phenol intake: assessment methods and identified gaps.* European journal of nutrition, 2017. **56**(4): p. 1393-1408.
194. Panche, A., A. Diwan, and S. Chandra, *Flavonoids: an overview.* Journal of nutritional science, 2016. **5**.
195. Nishihara, M. and T. Nakatsuka, *Genetic engineering of flavonoid pigments to modify flower color in floricultural plants.* Biotechnology letters, 2011. **33**(3): p. 433-441.
196. Kumar, S. and A.K. Pandey, *Chemistry and biological activities of flavonoids: an overview.* The Scientific World Journal, 2013. **2013**.
197. Howes, M.-J.R., *Chapter 28 - Phytochemicals as Anti-inflammatory Nutraceuticals and Phytopharmaceuticals*, in *Immunity and Inflammation in Health and Disease*, S. Chatterjee, W. Jungraithmayr, and D. Bagchi, Editors. 2018, Academic Press. p. 363-388.
198. Del Rio, D., et al., *Dietary (poly) phenolics in human health: structures, bioavailability, and evidence of protective effects against chronic diseases.* Antioxidants & redox signaling, 2013. **18**(14): p. 1818-1892.
199. Manach, C., et al., *Polyphenols: food sources and bioavailability.* The American journal of clinical nutrition, 2004. **79**(5): p. 727-747.
200. Pérez-Jiménez, J., et al., *Identification of the 100 richest dietary sources of polyphenols: an application of the Phenol-Explorer database.* European journal of clinical nutrition, 2010. **64**(3): p. S112-S120.
201. Cheynier, V., *Polyphenols in foods are more complex than often thought.* The American journal of clinical nutrition, 2005. **81**(1): p. 223S-229S.
202. Wink, M., *Compartmentation of secondary metabolites and xenobiotics in plant vacuoles*, in *Advances in botanical research*. 1997, Elsevier. p. 141-169.
203. Aron, P.M. and J.A. Kennedy, *Flavan-3-ols: Nature, occurrence and biological activity.* Molecular nutrition & food research, 2008. **52**(1): p. 79-104.

204. Crozier, A., I.B. Jaganath, and M.N. Clifford, *Dietary phenolics: chemistry, bioavailability and effects on health.* Natural product reports, 2009. **26**(8): p. 1001-1043.
205. Serrano, J., et al., *Tannins: current knowledge of food sources, intake, bioavailability and biological effects.* Molecular nutrition & food research, 2009. **53**(S2): p. S310-S329.
206. Clifford, M.N. and A. Crozier, *Phytochemicals in teas and tisanes and their bioavailability.* Teas, Cocoa and Coffee: Plant Secondary Metabolites and Health, 2011. **1**: p. 45-98.
207. Renard, C.M.G.C., N. Dupont, and P. Guillermin, *Concentrations and characteristics of procyanidins and other phenolics in apples during fruit growth.* Phytochemistry, 2007. **68**(8): p. 1128-1138.
208. Gu, L.W., et al., *Concentrations of proanthocyanidins in common foods and estimations of normal consumption.* Journal of Nutrition, 2004. **134**(3): p. 613-617.
209. Saura-Calixto, F., J. Serrano, and I. Goni, *Intake and bioaccessibility of total polyphenols in a whole diet.* Food Chemistry, 2007. **101**(2): p. 492-501.
210. Bohn, T., *Dietary factors affecting polyphenol bioavailability.* Nutrition reviews, 2014. **72**(7): p. 429-452.
211. Del Bo, C., et al., *Systematic review on polyphenol intake and health outcomes: is there sufficient evidence to define a health-promoting polyphenol-rich dietary pattern?* Nutrients, 2019. **11**(6): p. 1355.
212. Doo, T. and G. Maskarinec, *Polyphenols and breast cancer prevention: A summary of the epidemiologic evidence*, in *Polyphenols in human health and disease*. 2014, Elsevier. p. 1331-1340.
213. Visioli, F., et al., *Polyphenols and human health: a prospectus.* Critical reviews in food science and nutrition, 2011. **51**(6): p. 524-546.
214. Palafox-Carlos, H., J.F. Ayala-Zavala, and G.A. González-Aguilar, *The role of dietary fiber in the bioaccessibility and bioavailability of fruit and vegetable antioxidants.* Journal of food science, 2011. **76**(1): p. R6-R15.
215. Day, A.J., et al., *Dietary flavonoid and isoflavone glycosides are hydrolysed by the lactase site of lactase phlorizin hydrolase.* FEBS letters, 2000. **468**(2-3): p. 166-170.
216. Gee, J.M., et al., *Intestinal transport of quercetin glycosides in rats involves both deglycosylation and interaction with the hexose transport pathway.* The Journal of nutrition, 2000. **130**(11): p. 2765-2771.

217. Donovan, J.L., et al., *Absorption and metabolism of dietary plant secondary metabolites.* Plant secondary metabolites: occurrence, structure and role in the human diet, 2006: p. 303-51.
218. Marín, L., et al., *Bioavailability of dietary polyphenols and gut microbiota metabolism: antimicrobial properties.* BioMed research international, 2015. **2015**.
219. Teng, H. and L. Chen, *Polyphenols and bioavailability: an update.* Critical Reviews in Food Science and Nutrition, 2019. **59**(13): p. 2040-2051.
220. Williamson, G. and M.N. Clifford, *Role of the small intestine, colon and microbiota in determining the metabolic fate of polyphenols.* Biochemical Pharmacology, 2017. **139**: p. 24-39.
221. Kay, C.D., P.A. Kroon, and A. Cassidy, *The bioactivity of dietary anthocyanins is likely to be mediated by their degradation products.* Molecular nutrition & food research, 2009. **53**(S1): p. S92-S101.
222. Kahle, K., et al., *Polyphenols are intensively metabolized in the human gastrointestinal tract after apple juice consumption.* Journal of agricultural and food chemistry, 2007. **55**(26): p. 10605-10614.
223. Manach, C., et al., *Bioavailability and bioefficacy of polyphenols in humans. I. Review of 97 bioavailability studies.* The American journal of clinical nutrition, 2005. **81**(1): p. 230S-242S.
224. Appeldoorn, M.M., et al., *Procyanidin dimers are metabolized by human microbiota with 2-(3, 4-dihydroxyphenyl) acetic acid and 5-(3, 4-dihydroxyphenyl)-γ-valerolactone as the major metabolites.* Journal of Agricultural and Food Chemistry, 2009. **57**(3): p. 1084-1092.
225. Stoupi, S., et al., *In Vivo Bioavailability, Absorption, Excretion, and Pharmacokinetics of [¹⁴C]Procyanidin B2 in Male Rats.* Drug Metabolism and Disposition, 2010. **38**(2): p. 287.
226. Saura-Calixto, F., J. Serrano, and I. Goñi, *Intake and bioaccessibility of total polyphenols in a whole diet.* Food Chemistry, 2007. **101**(2): p. 492-501.
227. Gonthier, M.-P., et al., *Metabolism of dietary procyanidins in rats.* Free Radical Biology and Medicine, 2003. **35**(8): p. 837-844.
228. Martins, N., et al., *The increasing demand for functional foods.* Wild Plants, Mushrooms and Nuts: Functional Food Properties and Applications, 2017.
229. Wildman, R.E. and R.S. Bruno, *Handbook of nutraceuticals and functional foods*. 2019: CRC press.
230. Shi, J., G. Mazza, and M. Le Maguer, *Functional foods: biochemical and processing aspects*. Vol. 2. 2016: CRC Press.

231. Liang, L., et al., *Interaction of α-gliadin with poly (HEMA-co-SS): Structural characterization and biological implication.* Biopolymers: Original Research on Biomolecules, 2009. **91**(2): p. 169-178.
232. Pinier, M., et al., *Polymeric binders suppress gliadin-induced toxicity in the intestinal epithelium.* Gastroenterology, 2009. **136**(1): p. 288-298.
233. Pinier, M., et al., *The copolymer P (HEMA-co-SS) binds gluten and reduces immune response in gluten-sensitized mice and human tissues.* Gastroenterology, 2012. **142**(2): p. 316-325. e12.
234. Sample, D.A., et al., *AGY, a Novel egg yolk-derived anti-gliadin antibody, is safe for patients with celiac disease.* Digestive diseases and sciences, 2017. **62**(5): p. 1277-1285.
235. Eggenreich, B., et al., *The production of a recombinant tandem single chain fragment variable capable of binding prolamins triggering celiac disease.* BMC biotechnology, 2018. **18**(1): p. 30.
236. Dias, R., et al., *Interaction study between wheat-derived peptides and procyanidin B3 by mass spectrometry.* Food chemistry, 2016. **194**: p. 1304-1312.
237. Dias, R., et al., *The interaction between tannins and gliadin derived peptides in a celiac disease perspective.* RSC Advances, 2015. **5**(41): p. 32151-32158.
238. Van Buiten, C.B., J.D. Lambert, and R.J. Elias, *Green Tea Polyphenols Mitigate Gliadin-Mediated Inflammation and Permeability in Vitro.* Molecular nutrition & food research, 2018. **62**(12): p. 1700879.
239. Tye-Din, J.A., et al., *Comprehensive, Quantitative Mapping of T Cell Epitopes in Gluten in Celiac Disease.* Science Translational Medicine, 2010. **2**(41).
240. Schalk, K., et al., *Quantitation of the immunodominant 33-mer peptide from α-gliadin in wheat flours by liquid chromatography tandem mass spectrometry.* Scientific Reports, 2017. **7**(1): p. 45092.
241. Dias, R., et al., *Molecular insights on the interaction and preventive potential of epigallocatechin-3-gallate in Celiac Disease.* Int J Biol Macromol, 2018. **112**: p. 1029-1037.
242. Dias, R., et al., *A multi-spectroscopic study on the interaction of food polyphenols with a bioactive gluten peptide: From chemistry to biological implications.* Food Chem, 2019. **299**: p. 125051.
243. Jakobek, L., *Interactions of polyphenols with carbohydrates, lipids and proteins.* Food chemistry, 2015. **175**: p. 556-567.
244. Soares, S., et al., *Sensorial properties of red wine polyphenols: Astringency and bitterness.* Critical reviews in food science and nutrition, 2017. **57**(5): p. 937-948.

245. García-Estévez, I., A.M. Ramos-Pineda, and M.T. Escribano-Bailón, *Interactions between wine phenolic compounds and human saliva in astringency perception.* Food & function, 2018. **9**(3): p. 1294-1309.
246. Ferrer-Gallego, R., et al., *Effect of flavonols on wine astringency and their interaction with human saliva.* Food chemistry, 2016. **209**: p. 358-364.
247. García-Estévez, I., et al., *First evidences of interaction between pyranoanthocyanins and salivary proline-rich proteins.* Food chemistry, 2017. **228**: p. 574-581.
248. Soares, S., et al., *Study of human salivary proline-rich proteins interaction with food tannins.* Food Chemistry, 2018. **243**: p. 175-185.
249. Gibbins, H.L. and G.H. Carpenter, *Alternative Mechanisms of Astringency – What is the Role of Saliva?* Journal of Texture Studies, 2013. **44**(5): p. 364-375.
250. Bennick, A., *Interaction of plant polyphenols with salivary proteins.* Critical Reviews in Oral Biology & Medicine, 2002. **13**(2): p. 184-196.
251. Boze, H., et al., *Proline-rich salivary proteins have extended conformations.* Biophysical journal, 2010. **99**(2): p. 656-665.
252. Soares, S., et al., *Interaction between Ellagitannins and Salivary Proline-Rich Proteins.* Journal of agricultural and food chemistry, 2019. **67**(34): p. 9579-9590.
253. Lamkin, M.S. and F.G. Oppenheim, *Structural features of salivary function.* Critical Reviews in Oral Biology & Medicine, 1993. **4**(3): p. 251-259.
254. Mennen, L.I., et al., *Risks and safety of polyphenol consumption.* The American Journal of Clinical Nutrition, 2005. **81**(1): p. 326S-329S.
255. Cirkovic Velickovic, T.D. and D.J. Stanic-Vucinic, *The Role of Dietary Phenolic Compounds in Protein Digestion and Processing Technologies to Improve Their Antinutritive Properties.* Comprehensive Reviews in Food Science and Food Safety, 2018. **17**(1): p. 82-103.
256. Lambert, J.D., et al., *Metabolism of dietary polyphenols and possible interactions with drugs.* Current drug metabolism, 2007. **8**(5): p. 499-507.
257. Delimont, N.M., M.D. Haub, and B.L. Lindshield, *The Impact of Tannin Consumption on Iron Bioavailability and Status: A Narrative Review.* Current developments in nutrition, 2017. **1**(2): p. 1-12.
258. Williamson, M.P., et al., *Epigallocatechin gallate, the main polyphenol in green tea, binds to the T-cell receptor, CD4: Potential for HIV-1 therapy.* Journal of allergy and clinical immunology, 2006. **118**(6): p. 1369-1374.

259. Ueda, K., et al., *Inactivation of Pathogenic Viruses by Plant-Derived Tannins: Strong Effects of Extracts from Persimmon (Diospyros kaki) on a Broad Range of Viruses.* PLoS ONE, 2013. **8**(1): p. e55343.
260. Zhang, T., et al., *Molecular Mechanism of the Inhibition of EGCG on the Alzheimer Aβ1–42 Dimer.* The Journal of Physical Chemistry B, 2013. **117**(15): p. 3993-4002.
261. Ferreira, N., M.J. Saraiva, and M.R. Almeida, *Epigallocatechin-3-gallate as a potential therapeutic drug for TTR-related amyloidosis: "in vivo" evidence from FAP mice models.* PloS one, 2012. **7**(1): p. e29933-e29933.
262. Hong, J., et al., *Stability, cellular uptake, biotransformation, and efflux of tea polyphenol (−)-epigallocatechin-3-gallate in HT-29 human colon adenocarcinoma cells.* Cancer Research, 2002. **62**(24): p. 7241-7246.
263. Tsukamoto, S., et al., *Green tea polyphenol EGCG induces lipid-raft clustering and apoptotic cell death by activating protein kinase Cδ and acid sphingomyelinase through a 67 kDa laminin receptor in multiple myeloma cells.* The Biochemical journal, 2012. **443**(2): p. 525-534.
264. Tachibana, H., et al., *A receptor for green tea polyphenol EGCG.* Nature structural & molecular biology, 2004. **11**(4): p. 380-381.
265. Melgarejo, E., et al., *Targeting of histamine producing cells by EGCG: a green dart against inflammation?* Journal of physiology and biochemistry, 2010. **66**(3): p. 265-270.
266. Melgarejo, E., et al., *(—)-Epigallocatechin-3-gallate interferes with mast cell adhesiveness, migration and its potential to recruit monocytes.* Cellular and molecular life sciences, 2007. **64**(19-20): p. 2690.
267. Singh, A., et al., *Identification of epicatechin as one of the key bioactive constituents of polyphenol-enriched extracts that demonstrate an anti-allergic effect in a murine model of food allergy.* British journal of nutrition, 2014. **112**(3): p. 358-368.
268. Abril-Gil, M., et al., *Effect of a cocoa-enriched diet on immune response and anaphylaxis in a food allergy model in Brown Norway rats.* The Journal of nutritional biochemistry, 2016. **27**: p. 317-326.
269. Singh, A., S. Holvoet, and A. Mercenier, *Dietary polyphenols in the prevention and treatment of allergic diseases.* Clinical and experimental allergy : journal of the British Society for Allergy and Clinical Immunology, 2011. **41**: p. 1346-59.

270. Plundrich, N.J., et al., *Novel strategy to create hypoallergenic peanut protein-polyphenol edible matrices for oral immunotherapy.* Journal of agricultural and food chemistry, 2014. **62**(29): p. 7010-7021.
271. Plundrich, N.J., et al., *Protein-bound Vaccinium fruit polyphenols decrease IgE binding to peanut allergens and RBL-2H3 mast cell degranulation in vitro.* Food & function, 2017. **8**(4): p. 1611-1621.
272. Ognjenović, J., et al., *Interactions of epigallo-catechin 3-gallate and ovalbumin, the major allergen of egg white.* Food chemistry, 2014. **164**: p. 36-43.
273. Perot, M., et al., *Polyphenol interactions mitigate the immunogenicity and allergenicity of gliadins.* Journal of Agricultural and Food Chemistry, 2017.
274. Smeriglio, A., et al., *Proanthocyanidins and hydrolysable tannins: occurrence, dietary intake and pharmacological effects.* British journal of pharmacology, 2017. **174**(11): p. 1244-1262.
275. Scalbert, A., et al., *Proanthocyanidins and human health: systemic effects and local effects in the gut.* Biofactors, 2000. **13**(1-4): p. 115-120.
276. Delcour, J.A., D. Ferreira, and D.G. Roux, *SYNTHESIS OF CONDENSED TANNINS .9. THE CONDENSATION SEQUENCE OF LEUCOCYANIDIN WITH (+)-CATECHIN AND WITH THE RESULTANT PROCYANIDINS.* Journal of the Chemical Society-Perkin Transactions 1, 1983(8): p. 1711-1717.
277. Geissman, T.A. and Yoshimur.Nn, *SYNTHETIC PROANTHOCYANIDIN.* Tetrahedron Letters, 1966(24): p. 2669-&.
278. Viegas, A., et al., *Saturation-transfer difference (STD) NMR: a simple and fast method for ligand screening and characterization of protein binding.* Journal of chemical Education, 2011. **88**(7): p. 990-994.
279. Wishart, D.S., et al., *1H, 13C and 15N random coil NMR chemical shifts of the common amino acids. I. Investigations of nearest-neighbor effects.* Journal of biomolecular NMR, 1995. **5**(1): p. 67-81.
280. Parrot, I., P.C. Huang, and C. Khosla, *Circular dichroism and nuclear magnetic resonance spectroscopic analysis of immunogenic gluten peptides and their analogs.* Journal of Biological Chemistry, 2002. **277**(47): p. 45572-45578.
281. Herrera, M.G., et al., *Circular dichroism and electron microscopy studies in vitro of 33-mer gliadin peptide revealed secondary structure transition and supramolecular organization.* Biopolymers, 2014. **101**(1): p. 96-106.
282. Arentz–Hansen, H., et al., *Celiac lesion T cells recognize epitopes that cluster in regions of gliadins rich in proline residues.* Gastroenterology, 2002. **123**(3): p. 803-809.

283. Williamson, M.P., *Using chemical shift perturbation to characterise ligand binding.* Progress in nuclear magnetic resonance spectroscopy, 2013. **73**: p. 1-16.
284. Kyte, J. and R.F. Doolittle, *A simple method for displaying the hydropathic character of a protein.* Journal of molecular biology, 1982. **157**(1): p. 105-132.
285. Chothia, C., *The nature of the accessible and buried surfaces in proteins.* Journal of molecular biology, 1976. **105**(1): p. 1-12.
286. Cala, O., et al., *NMR and molecular modeling of wine tannins binding to saliva proteins: revisiting astringency from molecular and colloidal prospects.* The FASEB Journal, 2010. **24**(11): p. 4281-4290.
287. Tarascou, I., et al., *Structural and conformational analysis of two native procyanidin trimers.* Magnetic Resonance in Chemistry, 2007. **45**(2): p. 157-166.
288. Mayer, M. and B. Meyer, *Group epitope mapping by saturation transfer difference NMR to identify segments of a ligand in direct contact with a protein receptor.* Journal of the American Chemical Society, 2001. **123**(25): p. 6108-6117.
289. Goldflam, M., et al., *NMR studies of protein–ligand interactions*, in *Protein NMR techniques*. 2012, Springer. p. 233-259.
290. Williamson, M.P., *The transferred NOE*, in *Modern magnetic resonance*. 2008, Springer. p. 1357-1362.
291. Charlton, A.J., E. Haslam, and M.P. Williamson, *Multiple conformations of the proline-rich protein/epigallocatechin gallate complex determined by time-averaged nuclear Overhauser effects.* Journal of the American Chemical Society, 2002. **124**(33): p. 9899-9905.
292. Murray, N.J., et al., *Study of the interaction between salivary proline-rich proteins and a polyphenol by 1H-NMR spectroscopy.* European journal of biochemistry, 1994. **219**(3): p. 923-935.
293. Fernandez, J. and T.H. Lilley, *Aqueous solutions containing amino acids and peptides. Part 28.—Enthalpy of interaction of some amides with glycine and α-alanine: interactions of the zwitterionic group of α-amino acids with hydrophobic groups and peptide groups.* Journal of the Chemical Society, Faraday Transactions, 1992. **88**(17): p. 2503-2509.
294. Pianet, I., et al., *Modeling procyanidin self-association processes and understanding their micellar organization: a study by diffusion NMR and molecular mechanics.* Langmuir, 2008. **24**(19): p. 11027-11035.
295. Du, X., et al., *Insights into protein–ligand interactions: mechanisms, models, and methods.* International journal of molecular sciences, 2016. **17**(2): p. 144.

296. Jung, H.I., et al., *Thermodynamic analysis of the binding of component enzymes in the assembly of the pyruvate dehydrogenase multienzyme complex of Bacillus stearothermophilus.* Protein science, 2002. **11**(5): p. 1091-1100.
297. Cooper, A., *Heat capacity effects in protein folding and ligand binding: a re-evaluation of the role of water in biomolecular thermodynamics.* Biophysical chemistry, 2005. **115**(2-3): p. 89-97.
298. Perozzo, R., G. Folkers, and L. Scapozza, *Thermodynamics of protein–ligand interactions: history, presence, and future aspects.* Journal of Receptors and Signal Transduction, 2004. **24**(1-2): p. 1-52.
299. Jöbstl, E., et al., *Molecular Model for Astringency Produced by Polyphenol/Protein Interactions.* Biomacromolecules, 2004. **5**(3): p. 942-949.
300. Canon, F., et al., *Folding of a Salivary Intrinsically Disordered Protein upon Binding to Tannins.* Journal of the American Chemical Society, 2011. **133**(20): p. 7847-7852.
301. Xiong, X., et al., *Investigation on the interaction of antibacterial drug moxifloxacin hydrochloride with human serum albumin using multi-spectroscopic approaches, molecular docking and dynamical simulation.* Rsc Advances, 2017. **7**(77): p. 48942-48951.
302. Schumann, M., et al., *Mechanisms of epithelial translocation of the alpha-gliadin-33mer in coeliac sprue.* Gut, 2008. **57**(6): p. 747.
303. Iacomino, G., et al., *Structural analysis and Caco-2 cell permeability of the celiac-toxic A-gliadin peptide 31–55.* Journal of agricultural and food chemistry, 2013. **61**(5): p. 1088-1096.
304. Rauhavirta, T., et al., *Epithelial transport and deamidation of gliadin peptides: a role for coeliac disease patient immunoglobulin A.* Clinical & Experimental Immunology, 2011. **164**(1): p. 127-136.
305. Caputo, I., et al., *Celiac anti-tissue transglutaminase antibodies interfere with the uptake of alpha gliadin peptide 31–43 but not of peptide 57–68 by epithelial cells.* Biochimica et Biophysica Acta (BBA)-Molecular Basis of Disease, 2010. **1802**(9): p. 717-727.
306. Hu, J., et al., *The safety of green tea and green tea extract consumption in adults–results of a systematic review.* Regulatory toxicology and pharmacology, 2018. **95**: p. 412-433.
307. Mudie, D.M., et al., *Quantification of gastrointestinal liquid volumes and distribution following a 240 mL dose of water in the fasted state.* Molecular pharmaceutics, 2014. **11**(9): p. 3039-3047.

308. Lammers, K.M., M.G. Herrera, and V.I. Dodero, *Translational Chemistry Meets Gluten-Related Disorders.* ChemistryOpen, 2018. **7**(3): p. 217-232.
309. Howell, S., A.J. Kenny, and A.J. Turner, *A survey of membrane peptidases in two human colonic cell lines, Caco-2 and HT-29.* Biochemical Journal, 1992. **284**(2): p. 595-601.
310. Hausch, F., et al., *Intestinal digestive resistance of immunodominant gliadin peptides.* American Journal of Physiology-Gastrointestinal and Liver Physiology, 2002. **283**(4): p. G996-G1003.
311. Srinivasan, B., et al., *TEER measurement techniques for in vitro barrier model systems.* Journal of laboratory automation, 2015. **20**(2): p. 107-126.
312. Zhao, W., et al., *Lucifer Yellow - A Robust Paracellular Permeability Marker in a Cell Model of the Human Blood-brain Barrier.* Journal of visualized experiments : JoVE, 2019(150): p. 10.3791/58900.
313. Bernardi, S., et al., *Polyphenols and intestinal permeability: rationale and future perspectives.* Journal of agricultural and food chemistry, 2019.
314. Wang, K., et al., *Polyphenol-rich propolis extracts strengthen intestinal barrier function by activating AMPK and ERK signaling.* Nutrients, 2016. **8**(5): p. 272.
315. Valenzano, M.C., et al., *Remodeling of tight junctions and enhancement of barrier integrity of the CACO-2 intestinal epithelial cell layer by micronutrients.* PloS one, 2015. **10**(7).
316. Cremonini, E., et al., *Anthocyanins inhibit tumor necrosis alpha-induced loss of Caco-2 cell barrier integrity.* Food & function, 2017. **8**(8): p. 2915-2923.
317. Cremonini, E., et al., *(-)-Epicatechin protects the intestinal barrier from high fat diet-induced permeabilization: Implications for steatosis and insulin resistance.* Redox biology, 2018. **14**: p. 588-599.
318. Ling, K.-H., et al., *Protective capacity of resveratrol, a natural polyphenolic compound, against deoxynivalenol-induced intestinal barrier dysfunction and bacterial translocation.* Chemical Research in Toxicology, 2016. **29**(5): p. 823-833.
319. Kaulmann, A. and T. Bohn, *Bioactivity of polyphenols: Preventive and adjuvant strategies toward reducing inflammatory bowel diseases—promises, perspectives, and pitfalls.* Oxidative medicine and cellular longevity, 2016. **2016**.
320. Das, J., R. Ramani, and M.O. Suraju, *Polyphenol compounds and PKC signaling.* Biochimica et Biophysica Acta (BBA)-General Subjects, 2016. **1860**(10): p. 2107-2121.

321. Park, H.-Y., et al., *Theaflavins enhance intestinal barrier of Caco-2 Cell monolayers through the expression of AMP-activated protein kinase-mediated Occludin, Claudin-1, and ZO-1.* Bioscience, biotechnology, and biochemistry, 2015. **79**(1): p. 130-137.
322. Contreras, T.C., et al., *(−)-Epicatechin in the prevention of tumor necrosis alpha-induced loss of Caco-2 cell barrier integrity.* Archives of biochemistry and biophysics, 2015. **573**: p. 84-91.
323. Suzuki, T., S. Tanabe, and H. Hara, *Kaempferol enhances intestinal barrier function through the cytoskeletal association and expression of tight junction proteins in Caco-2 cells.* The Journal of nutrition, 2011. **141**(1): p. 87-94.
324. Noda, S., S. Tanabe, and T. Suzuki, *Naringenin enhances intestinal barrier function through the expression and cytoskeletal association of tight junction proteins in C aco-2 cells.* Molecular nutrition & food research, 2013. **57**(11): p. 2019-2028.
325. Nunes, C., et al., *Red wine extract preserves tight junctions in intestinal epithelial cells under inflammatory conditions: Implications for intestinal inflammation.* Food & function, 2019. **10**(3): p. 1364-1374.
326. Kumar Singh, A., et al., *Beneficial Effects of Dietary Polyphenols on Gut Microbiota and Strategies to Improve Delivery Efficiency.* Nutrients, 2019. **11**(9): p. 2216.
327. Barré-Sinoussi, F. and X. Montagutelli, *Animal models are essential to biological research: issues and perspectives.* Future science OA, 2015. **1**(4).
328. Perlman, R.L., *Mouse models of human disease: An evolutionary perspective.* Evolution, medicine, and public health, 2016. **2016**(1): p. 170-176.
329. Conn, P.M., *Animal models for the study of human disease*. 2017: Academic Press.
330. Korneychuk, N., B. Meresse, and N. Cerf-Bensussan, *Lessons from rodent models in celiac disease.* Mucosal immunology, 2015. **8**(1): p. 18-28.
331. Troncone, R. and A. Ferguson, *Animal model of gluten induced enteropathy in mice.* Gut, 1991. **32**(8): p. 871-875.
332. Galipeau, H.J., et al., *Sensitization to gliadin induces moderate enteropathy and insulitis in nonobese diabetic-DQ8 mice.* The Journal of Immunology, 2011. **187**(8): p. 4338-4346.
333. Verdu, E.F., et al., *Gliadin-dependent neuromuscular and epithelial secretory responses in gluten-sensitive HLA-DQ8 transgenic mice.* American Journal of Physiology-Gastrointestinal and Liver Physiology, 2008. **294**(1): p. G217-G225.

334. D'arienzo, R., et al., *Immunomodulatory Effects of Lactobacillus casei Administration in a Mouse Model of Gliadin-Sensitive Enteropathy.* Scandinavian journal of immunology, 2011. **74**(4): p. 335-341.
335. de Kauwe, A.L., et al., *Resistance to celiac disease in humanized HLA-DR3-DQ2-transgenic mice expressing specific anti-gliadin CD4+ T cells.* The Journal of Immunology, 2009. **182**(12): p. 7440-7450.
336. Tye-Din, J.A., H.J. Galipeau, and D. Agardh, *Celiac disease: a review of current concepts in pathogenesis, prevention, and novel therapies.* Frontiers in pediatrics, 2018. **6**: p. 350.
337. Black, K.E., J.A. Murray, and C.S. David, *HLA-DQ determines the response to exogenous wheat proteins: a model of gluten sensitivity in transgenic knockout mice.* The Journal of Immunology, 2002. **169**(10): p. 5595-5600.
338. D'Arienzo, R., et al., *A deregulated immune response to gliadin causes a decreased villus height in DQ8 transgenic mice.* European journal of immunology, 2009. **39**(12): p. 3552-3561.
339. Fitzpatrick, F., *Cyclooxygenase enzymes: regulation and function.* Current pharmaceutical design, 2004. **10**(6): p. 577-588.
340. Nakanishi, M. and D.W. Rosenberg, *Multifaceted roles of PGE2 in inflammation and cancer.* Seminars in immunopathology, 2013. **35**(2): p. 123-137.
341. Miyoshi, H., et al., *Prostaglandin E2 promotes intestinal repair through an adaptive cellular response of the epithelium.* The EMBO journal, 2017. **36**(1): p. 5-24.
342. Newberry, R.D., W.F. Stenson, and R.G. Lorenz, *Cyclooxygenase-2-dependent arachidonic acid metabolites are essential modulators of the intestinal immune response to dietary antigen.* Nature medicine, 1999. **5**(8): p. 900-906.
343. Mazzarella, G., et al., *Gliadin intake alters the small intestinal mucosa in indomethacin-treated HLA-DQ8 transgenic mice.* American Journal of Physiology-Gastrointestinal and Liver Physiology, 2014. **307**(3): p. G302-G312.
344. Qin, S. and D.X. Hou, *Multiple regulations of Keap1/Nrf2 system by dietary phytochemicals.* Mol Nutr Food Res, 2016. **60**(8): p. 1731-55.
345. Pérez, S., et al., *Redox signaling in the gastrointestinal tract.* Free Radical Biology and Medicine, 2017. **104**: p. 75-103.
346. Arnous, A., D.P. Makris, and P. Kefalas, *Effect of principal polyphenolic components in relation to antioxidant characteristics of aged red wines.* Journal of agricultural and food chemistry, 2001. **49**(12): p. 5736-5742.

347. Reagan-Shaw, S., M. Nihal, and N. Ahmad, *Dose translation from animal to human studies revisited.* The FASEB journal, 2008. **22**(3): p. 659-661.
348. Weseler, A.R. and A. Bast, *Masquelier's grape seed extract: from basic flavonoid research to a well-characterized food supplement with health benefits.* Nutrition journal, 2017. **16**(1): p. 5.
349. Sebastian, R.S., et al., *A new database facilitates characterization of flavonoid intake, sources, and positive associations with diet quality among US adults.* The Journal of nutrition, 2015. **145**(6): p. 1239-1248.
350. Wang, Y., et al., *Estimation of daily proanthocyanidin intake and major food sources in the US diet.* The Journal of nutrition, 2011. **141**(3): p. 447-452.
351. Livak, K.J. and T.D. Schmittgen, *Analysis of relative gene expression data using real-time quantitative PCR and the 2− ΔΔCT method.* methods, 2001. **25**(4): p. 402-408.
352. Rahman, I., A. Kode, and S.K. Biswas, *Assay for quantitative determination of glutathione and glutathione disulfide levels using enzymatic recycling method.* Nat Protoc, 2006. **1**(6): p. 3159-65.
353. Benson, A.M., M.J. Hunkeler, and P. Talalay, *Increase of NAD (P) H: quinone reductase by dietary antioxidants: possible role in protection against carcinogenesis and toxicity.* Proceedings of the National Academy of Sciences, 1980. **77**(9): p. 5216-5220.
354. Habig, W.H. and W.B. Jakoby, *[51] Assays for differentiation of glutathione S-Transferases*, in *Methods in enzymology*. 1981, Elsevier. p. 398-405.
355. Mavis, R.D. and E. Stellwagen, *Purification and subunit structure of glutathione reductase from bakers' yeast.* Journal of Biological Chemistry, 1968. **243**(4): p. 809-814.
356. Glock, G.E. and L.P. Mc, *Further studies on the properties and assay of glucose 6-phosphate dehydrogenase and 6-phosphogluconate dehydrogenase of rat liver.* Biochem J, 1953. **55**(3): p. 400-8.
357. Dou, J., et al., *Identification and comparison of phenolic compounds in the preparation of oolong tea manufactured by semifermentation and drying processes.* Journal of Agricultural and Food Chemistry, 2007. **55**(18): p. 7462-7468.
358. Baptista, J.A., J.F. da P Tavares, and R.C. Carvalho, *Comparative study and partial characterization of Azorean green tea polyphenols.* Journal of Food Composition and Analysis, 1999. **12**(4): p. 273-287.

359. Bastos, D.H., et al., *Phenolic antioxidants identified by ESI-MS from yerba mate (Ilex paraguariensis) and green tea (Camelia sinensis) extracts.* Molecules, 2007. **12**(3): p. 423-432.
360. Lin, L.-Z., P. Chen, and J.M. Harnly, *New phenolic components and chromatographic profiles of green and fermented teas.* Journal of Agricultural and food chemistry, 2008. **56**(17): p. 8130-8140.
361. Reygaert, W.C., *Green Tea Catechins: Their Use in Treating and Preventing Infectious Diseases.* BioMed research international, 2018. **2018**: p. 9105261-9105261.
362. Yuan, Y., et al., *Simultaneous determination of caffeine, gallic acid, theanine,(−)-epigallocatechin and (−)-epigallocatechin-3-gallate in green tea using quantitative 1 H-NMR spectroscopy.* Analytical Methods, 2014. **6**(3): p. 907-914.
363. Yamamoto, T., L.R. Juneja, and M. Kim, *Chemistry and applications of green tea*. 1997: CRC press.
364. Koch, W., et al., *Green Tea Quality Evaluation Based on Its Catechins and Metals Composition in Combination with Chemometric Analysis.* Molecules (Basel, Switzerland), 2018. **23**(7): p. 1689.
365. Le Gall, G., I.J. Colquhoun, and M. Defernez, *Metabolite profiling using 1H NMR spectroscopy for quality assessment of green tea, Camellia sinensis (L.).* Journal of Agricultural and Food Chemistry, 2004. **52**(4): p. 692-700.
366. Tarachiwin, L., et al., *1H NMR based metabolic profiling in the evaluation of Japanese green tea quality.* Journal of Agricultural and Food Chemistry, 2007. **55**(23): p. 9330-9336.
367. Lee, L.-S., et al., *Quantitative analysis of major constituents in green tea with different plucking periods and their antioxidant activity.* Molecules, 2014. **19**(7): p. 9173-9186.
368. Additives, E.P.o.F., et al., *Scientific opinion on the safety of green tea catechins.* EFSA Journal, 2018. **16**(4): p. e05239.
369. de Freitas, V.A.P., et al., *Characterisation of oligomeric and polymeric procyanidins from grape seeds by liquid secondary ion mass spectrometry.* Phytochemistry, 1998. **49**(5): p. 1435-1441.
370. Ainsworth, E.A. and K.M. Gillespie, *Estimation of total phenolic content and other oxidation substrates in plant tissues using Folin-Ciocalteu reagent.* Nat Protoc, 2007. **2**(4): p. 875-7.

371. Singleton, V.L., R. Orthofer, and R.M. Lamuela-Raventós, *[14] Analysis of total phenols and other oxidation substrates and antioxidants by means of folin-ciocalteu reagent*, in *Methods in enzymology*. 1999, Elsevier. p. 152-178.
372. Seyyedin, S. and M.N. Nazem, *Histomorphometric study of the effect of methionine on small intestine parameters in rat: an applied histologic study.* Folia morphologica, 2017. **76**(4): p. 620-629.
373. Savidge, T., et al., *Intestinal proliferation in coeliac disease: looking into the crypt.* Gut, 1995. **36**(3): p. 321.
374. Ducatelle, R., et al., *Biomarkers for monitoring intestinal health in poultry: present status and future perspectives.* Veterinary research, 2018. **49**(1): p. 43.
375. van Nevel, C.J., et al., *Incorporation of galactomannans in the diet of newly weaned piglets: effect on bacteriological and some morphological characteristics of the small intestine.* Archives of animal nutrition, 2005. **59**(2): p. 123-138.
376. Jaladanki, R.N. and J.-Y. Wang. *Regulation of gastrointestinal mucosal growth*. in *Colloquium series on integrated systems physiology: from molecule to function*. 2011. Morgan & Claypool Life Sciences.
377. Bergamo, P., et al., *Adaptive response activated by dietary cis9, trans11 conjugated linoleic acid prevents distinct signs of gliadin-induced enteropathy in mice.* European journal of nutrition, 2016. **55**(2): p. 729-740.
378. Allocati, N., et al., *Glutathione transferases: substrates, inihibitors and pro-drugs in cancer and neurodegenerative diseases.* Oncogenesis, 2018. **7**(1): p. 1-15.
379. Ross, D. and D. Siegel, *Functions of NQO1 in cellular protection and CoQ10 metabolism and its potential role as a redox sensitive molecular switch.* Frontiers in physiology, 2017. **8**: p. 595.
380. Kruger, N.J. and A. von Schaewen, *The oxidative pentose phosphate pathway: structure and organisation.* Current opinion in plant biology, 2003. **6**(3): p. 236-246.
381. Park, Y.J., et al., *The role of glucose-6-phosphate dehydrogenase in adipose tissue inflammation in obesity.* Adipocyte, 2017. **6**(2): p. 147-153.
382. Ren, X., et al., *Redox Signaling Mediated by Thioredoxin and Glutathione Systems in the Central Nervous System.* Antioxidants & redox signaling, 2017. **27**(13): p. 989-1010.
383. Corpas, F.J. and J.B. Barroso, *NADPH-generating dehydrogenases: their role in the mechanism of protection against nitro-oxidative stress induced by adverse environmental conditions.* Frontiers in Environmental Science, 2014. **2**: p. 55.

384. White, K., et al., *G6pd deficiency does not affect the cytosolic glutathione or thioredoxin antioxidant defense in mouse cochlea.* Journal of Neuroscience, 2017. **37**(23): p. 5770-5781.
385. Wardyn, J.D., A.H. Ponsford, and C.M. Sanderson, *Dissecting molecular cross-talk between Nrf2 and NF-κB response pathways.* Biochemical society transactions, 2015. **43**(4): p. 621-626.
386. Camps-Bossacoma, M., et al., *Effect of a cocoa diet on the small intestine and gut-associated lymphoid tissue composition in an oral sensitization model in rats.* The Journal of nutritional biochemistry, 2017. **42**: p. 182-193.
387. Akiyama, H., et al., *Dietary unripe apple polyphenol inhibits the development of food allergies in murine models.* FEBS Lett, 2005. **579**(20): p. 4485-91.
388. Camps-Bossacoma, M., et al., *Influence of hesperidin on the systemic and intestinal rat immune response.* Nutrients, 2017. **9**(6): p. 580.
389. Ursini, F., M. Maiorino, and H.J. Forman, *Redox homeostasis: The Golden Mean of healthy living.* Redox biology, 2016. **8**: p. 205-215.
390. Perera, P.-Y., et al., *The role of interleukin-15 in inflammation and immune responses to infection: implications for its therapeutic use.* Microbes and infection, 2012. **14**(3): p. 247-261.
391. Obermeier, F., et al., *IL-15 protects intestinal epithelial cells.* European journal of immunology, 2006. **36**(10): p. 2691-2699.
392. Nishiyama, R., et al., *Interleukin-2 receptor β subunit-dependent and-independent regulation of intestinal epithelial tight junctions.* Journal of Biological Chemistry, 2001. **276**(38): p. 35571-35580.
393. Yamaki, K., et al., *Effect of the nonsteroidal anti-inflammatory drug indomethacin on Th1 and Th2 immune responses in mice.* Journal of pharmaceutical sciences, 2003. **92**(8): p. 1723-1729.
394. Bigliardi, B. and F. Galati, *Innovation trends in the food industry: the case of functional foods.* Trends in Food Science & Technology, 2013. **31**(2): p. 118-129.
395. Gupta, C. and D. Prakash, *Phytonutrients as therapeutic agents.* Journal of Complementary and Integrative Medicine, 2014. **11**(3): p. 151-169.
396. Lucarini, M., et al., *Bio-Based Compounds from Grape Seeds: A Biorefinery Approach.* Molecules (Basel, Switzerland), 2018. **23**(8): p. 1888.
397. Schumann, M., et al., *Cell polarity-determining proteins Par-3 and PP-1 are involved in epithelial tight junction defects in coeliac disease.* Gut, 2012. **61**(2): p. 220-228.

398. Ciccocioppo, R., et al., *Altered expression, localization, and phosphorylation of epithelial junctional proteins in celiac disease.* American Journal of Clinical Pathology, 2006. **125**(4): p. 502-511.
399. Reinke, Y., et al., *Impairment of protein trafficking by direct interaction of gliadin peptides with actin.* Experimental cell research, 2011. **317**(15): p. 2124-2135.
400. Capozzi, A., et al., *Modulatory effect of gliadin peptide 10-mer on epithelial intestinal CACO-2 cell inflammatory response.* PloS one, 2013. **8**(6).
401. Laparra, J.M. and Y. Sanz, *Bifidobacteria inhibit the inflammatory response induced by gliadins in intestinal epithelial cells via modifications of toxic peptide generation during digestion.* Journal of cellular biochemistry, 2010. **109**(4): p. 801-807.
402. Gujral, N., J.W. Suh, and H.H. Sunwoo, *Effect of anti-gliadin IgY antibody on epithelial intestinal integrity and inflammatory response induced by gliadin.* BMC immunology, 2015. **16**: p. 41-41.
403. Parmar, A., et al., *Gene expression profiling of gliadin effects on intestinal epithelial cells suggests novel non-enzymatic functions of pepsin and trypsin.* PLoS One, 2013. **8**(6).
404. Heyman, M. and S. Menard, *Pathways of gliadin transport in celiac disease.* Annals of the New York Academy of Sciences, 2009. **1165**(1): p. 274.
405. Lea, T., *Caco-2 cell line*, in *The impact of food bioactives on health*. 2015, Springer, Cham. p. 103-111.
406. Sääf, A.M., et al., *Parallels between global transcriptional programs of polarizing Caco-2 intestinal epithelial cells in vitro and gene expression programs in normal colon and colon cancer.* Molecular biology of the cell, 2007. **18**(11): p. 4245-4260.
407. Wieser, H., S. Antes, and W. Seilmeier, *Quantitative determination of gluten protein types in wheat flour by reversed-phase high-performance liquid chromatography.* Cereal chemistry, 1998. **75**(5): p. 644-650.
408. Bickel, M., *The role of interleukin-8 in inflammation and mechanisms of regulation.* Journal of periodontology, 1993. **64**(5 Suppl): p. 456-460.
409. Goel, G., et al., *Cytokine release and gastrointestinal symptoms after gluten challenge in celiac disease.* Science advances, 2019. **5**(8): p. eaaw7756.
410. Brottveit, M., et al., *Mucosal cytokine response after short-term gluten challenge in celiac disease and non-celiac gluten sensitivity.* American Journal of Gastroenterology, 2013. **108**(5): p. 842-850.

411. Manna, S.K. and G.T. Ramesh, *Interleukin-8 induces nuclear transcription factor-κB through a TRAF6-dependent pathway.* Journal of Biological Chemistry, 2005. **280**(8): p. 7010-7021.
412. Mayr, B. and M. Montminy, *Transcriptional regulation by the phosphorylation-dependent factor CREB.* Nature reviews Molecular cell biology, 2001. **2**(8): p. 599-609.
413. Wang, H., et al., *cAMP response element-binding protein (CREB): a possible signaling molecule link in the pathophysiology of schizophrenia.* Frontiers in molecular neuroscience, 2018. **11**: p. 255.
414. Wen, A.Y., K.M. Sakamoto, and L.S. Miller, *The role of the transcription factor CREB in immune function.* The Journal of Immunology, 2010. **185**(11): p. 6413-6419.
415. Ghosh, S. and M.S. Hayden, *New regulators of NF-κB in inflammation.* Nature Reviews Immunology, 2008. **8**(11): p. 837-848.
416. Koga, Y., et al., *Roles of cyclic AMP response element binding activation in the ERK1/2 and p38 MAPK signalling pathway in central nervous system, cardiovascular system, osteoclast differentiation and mucin and cytokine production.* International journal of molecular sciences, 2019. **20**(6): p. 1346.
417. Ruffels, J., M. Griffin, and J.M. Dickenson, *Activation of ERK1/2, JNK and PKB by hydrogen peroxide in human SH-SY5Y neuroblastoma cells: role of ERK1/2 in H2O2-induced cell death.* European journal of pharmacology, 2004. **483**(2-3): p. 163-173.
418. Zhou, Y., et al., *Signal transduction pathways involved in oxidative stress-induced intestinal epithelial cell apoptosis.* Pediatric research, 2005. **58**(6): p. 1192-1197.
419. Bhat, N.R. and P. Zhang, *Hydrogen peroxide activation of multiple mitogen-activated protein kinases in an oligodendrocyte cell line: role of extracellular signal-regulated kinase in hydrogen peroxide-induced cell death.* Journal of neurochemistry, 1999. **72**(1): p. 112-119.
420. Rivabene, R., E. Mancini, and M. De Vincenzi, *In vitro cytotoxic effect of wheat gliadin-derived peptides on the Caco-2 intestinal cell line is associated with intracellular oxidative imbalance: implications for coeliac disease.* Biochimica et Biophysica Acta (BBA)-Molecular Basis of Disease, 1999. **1453**(1): p. 152-160.
421. Meng, Q. and Y. Xia, *c-Jun, at the crossroad of the signaling network.* Protein & cell, 2011. **2**(11): p. 889-898.

422. Dunn, C., et al., *Molecular mechanism and biological functions of c-Jun N-terminal kinase signalling via the c-Jun transcription factor.* Cellular signalling, 2002. **14**(7): p. 585-593.
423. Wong, C.H., et al., *Simultaneous induction of non-canonical autophagy and apoptosis in cancer cells by ROS-dependent ERK and JNK activation.* PloS one, 2010. **5**(4).
424. Nelson, D., et al., *Oscillations in NF-κB signaling control the dynamics of gene expression.* Science, 2004. **306**(5696): p. 704-708.
425. Morgan, M.J. and Z.-g. Liu, *Crosstalk of reactive oxygen species and NF-κB signaling.* Cell research, 2011. **21**(1): p. 103-115.
426. Manai, F., et al., *The in vitro effects of enzymatic digested gliadin on the functionality of the autophagy process.* International journal of molecular sciences, 2018. **19**(2): p. 635.
427. Khaleghi, S., et al., *The potential utility of tight junction regulation in celiac disease: focus on larazotide acetate.* Therapeutic advances in gastroenterology, 2016. **9**(1): p. 37-49.
428. Schulzke, J.-D., et al., *Epithelial tight junction structure in the jejunum of children with acute and treated celiac sprue.* Pediatric research, 1998. **43**(4): p. 435-441.
429. Montalto, M., et al., *Immunohistochemical analysis of ZO-1 in the duodenal mucosa of patients with untreated and treated celiac disease.* Digestion, 2002. **65**(4): p. 227-233.
430. Pizzuti, D., et al., *Transcriptional downregulation of tight junction protein ZO-1 in active coeliac disease is reversed after a gluten-free diet.* Digestive and liver disease, 2004. **36**(5): p. 337-341.
431. Barshack, I., et al., *Immunohistochemical analysis of candidate gene product expression in the duodenal epithelium of children with coeliac sprue.* Journal of clinical pathology, 2001. **54**(9): p. 684-688.
432. Sander, G.R., A.G. Cummins, and B.C. Powell, *Rapid disruption of intestinal barrier function by gliadin involves altered expression of apical junctional proteins.* FEBS letters, 2005. **579**(21): p. 4851-4855.
433. Sturgeon, C. and A. Fasano, *Zonulin, a regulator of epithelial and endothelial barrier functions, and its involvement in chronic inflammatory diseases.* Tissue barriers, 2016. **4**(4): p. e1251384-e1251384.
434. Freire, R., et al., *Human gut derived-organoids provide model to study gluten response and effects of microbiota-derived molecules in celiac disease.* Scientific reports, 2019. **9**(1): p. 7029.

435. Van De Walle, J., et al., *Inflammatory parameters in Caco-2 cells: effect of stimuli nature, concentration, combination and cell differentiation.* Toxicology in Vitro, 2010. **24**(5): p. 1441-1449.
436. Buhrke, T., I. Lengler, and A. Lampen, *Analysis of proteomic changes induced upon cellular differentiation of the human intestinal cell line Caco-2.* Development, growth & differentiation, 2011. **53**(3): p. 411-426.
437. Baker, S.S. and R.D. Baker, *Antioxidant enzymes in the differentiated Caco-2 cell line.* In Vitro Cellular & Developmental Biology-Animal, 1992. **28**(9-10): p. 643-647.
438. Scharmach, E., et al., *Glutathione S-transferase expression and isoenzyme composition during cell differentiation of Caco-2 cells.* Toxicology, 2009. **265**(3): p. 122-6.
439. Al-Sadi, R., et al., *TNF-alpha modulation of intestinal epithelial tight junction barrier is regulated by ERK1/2 activation of Elk-1.* Am J Pathol, 2013. **183**(6): p. 1871-1884.
440. Al-Sadi, R., et al., *Mechanism of IL-1β modulation of intestinal epithelial barrier involves p38 kinase and activating transcription factor-2 activation.* The Journal of Immunology, 2013. **190**(12): p. 6596-6606.
441. Prandi, B., et al., *Qualitative and quantitative determination of peptides related to celiac disease in mixtures derived from different methods of simulated gastrointestinal digestion of wheat products.* Analytical and bioanalytical chemistry, 2014. **406**(19): p. 4765-4775.
442. Brodkorb, A., et al., *INFOGEST static in vitro simulation of gastrointestinal food digestion.* Nature protocols, 2019. **14**(4): p. 991-1014.
443. Kumar, P., A. Nagarajan, and P.D. Uchil, *Analysis of cell viability by the lactate dehydrogenase assay.* Cold Spring Harbor Protocols, 2018. **2018**(6): p. pdb. prot095497.
444. Hall, N.J., G.P. Rubin, and A. Charnock, *Intentional and inadvertent non-adherence in adult coeliac disease. A cross-sectional survey.* Appetite, 2013. **68**: p. 56-62.

SUPPORTING INFORMATION

Supplementary table 1 - Hydrogen bonds present during more than 5% of each MD simulation. Distances are in Angstrom.

MD	Atom 1	Atom 2	Frequency (%)	Average Distance
1	PHE_32@OXT	OH-B ring of EGCG	25	2.64
	PRO_29@O	OH-B ring of EGCG	15	2.73
	LEU_24@O	OH-B ring of EGCG	12	2.74
	GLN_23@O	OH-A ring of EGCG	12	2.71
	PRO_29@O	OH-B ring of EGCG	10	2.74
	GLN_16@O	OH-B ring of EGCG	7	2.83
	GLN_28@O	OH-B ring of EGCG	5	2.81
	PHE_32@O	OH-A ring of EGCG	5	2.62
2	PRO_4@O	OH-A ring of EGCG	43	2.72
	PRO_31@O	OH-A ring of EGCG	15	2.66
	GLN_23@O	OH-B ring of EGCG	13	2.77
	PRO_20@O	OH-B ring of EGCG	13	2.82
	GLN_14@OE1	OH-A ring of EGCG	8	2.73
	PRO_4@O	OH-A ring of EGCG	5	2.69
3	LEU_10@O	OH-B ring of EGCG	72	2.70
	GLN_14@OE1	OH-B ring of EGCG	72	2.72
	PHE_32@OXT	OH-A ring of EGCG	24	2.63
	LEU_24@O	OH-A ring of EGCG	14	2.72
	GLN_9@OE1	OH-galloyl ring of EGCG	12	2.75
	GLN_28@OE1	OH-galloyl ring of EGCG	10	2.80
	PRO_29@O	OH-galloyl ring of EGCG	10	2.71
	LEU_17@O	OH-A ring of EGCG	10	2.70
	PHE_32@O	OH-A ring of EGCG	10	2.66
	PHE_32@OXT	OH-B ring of EGCG	9	2.67
	PHE_32@OXT	OH-B ring of EGCG	9	2.66
	PRO_6@O	OH-galloyl ring of EGCG	6	2.80
	GLN_30@O	OH-B ring of EGCG	6	2.85
	GLN_28@OE1	OH-A ring of EGCG	5	2.72
	GLN_28@OE1	OH-A ring of EGCG	5	2.79
	GLN_3@O	OH-galloyl ring of EGCG	5	2.80
	PHE_5@O	OH-galloyl ring of EGCG	5	2.81

Supplementary table 2 - Hydrophobic and hydrophilic interactions between the B3 molecules and the peptide that are present during more than 5% of MD-1 simulation. CO = carbonyl group, SC = sidechain.

Type of interaction	Residue	B3	Time of binding / ns	Frequency / %
Hydrophobic	F5	1	27.8	12
		2	2.9	10
	P8	2	3.0	9
	Y2	1	13.9	45
	P3	1	26.4	45
	P15	1	9.3	79
	L17	3	27.4	39
	P18	3	29.4	24
	Y19	1	9.4	76
	P20	1	9.2	82
	L24	1	7.6	46
	P25	1	7.3	10
	Y26	3	21.4	53
	P27	3	21.1	44
	P29	3	21.2	50
	P31	1	7.8	30
	F32	1	7.0	83
Hydrophilic (H-bonds)	Y12 (CO)	1	18.9	38
	Q21 (SC)	3	9.6	19
	Q23 (SC)	1	5.4	11
	Y26 (SC)	3	4.0	8
	Q28 (SC)	3	20.8	42
	P29 (CO)	3	3.0	6
	F32 (CO)	1	36.0	72

Supplementary table 3 - Hydrophobic and hydrophilic interactions between the B3 molecules and the peptide that are present during more than 5% of MD-2 simulation. CO = carbonyl group, SC = sidechain.

Type of interaction	Residue	B3	Time of binding / ns	Frequency / %
Hydrophobic	L2	1	21.2	7
	P4	1	19.6	7
	F5	1	19.3	39
	P6	1	18.8	30
	L10	1	18.6	46
	Y12	1	18.7	57
	P13	1	18.6	62
	Y19	1	28.5	8
	P20	1	18.7	48
	P22	1	12.4	14
	L24	1	12.4	75
	P25	1	12.2	67
	Y26	1	11.6	12
Hydrophilic (H-bonds)	Q9 (CO)	1	18.6	37
	Q9 (SC)	1	8.5	17
	P22 (CO)	1	4.9	10
	Q23 (CO)	1	4.9	10

Supplementary table 4 - Hydrophobic and hydrophilic interactions between the B3 molecules and the peptide that are present during more than 5% of MD-3 simulation. CO = carbonyl group, NH = amine group, SC = sidechain.

Type of interaction	Residue	B3	Time of binding / ns	Frequency / %
Hydrophobic	L2	2	25.5	48
	P4	1	9.9	16
		2	25.8	43
	F5	1	9.5	29
		2	25.5	46
	P6	1	7.6	35
		2	25.5	48
	P8	1	6.6	46
	L10	1	6.6	49
		2	26.2	31
	P11	1	6.6	47
	Y12	1	7.0	16
		2	27.3	33
		3	19.3	18
	P13	2	26.4	35
		3	19.6	16
	P15	3	19.0	22
	P18	3	19.1	6
	Y19	3	19.0	12
	P22	3	29.8	29
	L24	3	35.4	29
	P25	3	31.6	30
	Y26	3	29.8	39
	P27	3	31.5	7
	P29	1	44.9	10
	P31	2	28.1	18
	F32	1	20.4	6
		2	25.8	47
Hydrophilic (H-bonds)	Q3 (CO)	2	5.1	10
	Q9 (SC)	2	3.6	7
	Y12 (CO)	3	5.6	11
	Q21 (CO)	3	10.6	21
	P22 (CO)	3	4.6	9
	P31 (CO)	2	4.1	8
	F32 (CO)	2	20.7	41
	Q16 (SC)	2	4.4	9
	Q21 (CO)	1	4.4	9

	L24 (CO)	1	7.4	15
	P25 (CO)	1	17.1	34
	Q28 (NH)	1	16.0	32
	Q30 (CO)	2	10.6	21
	F32 (CO)	2	14.3	29

Supplementary table 5 - Hydrophobic and hydrophilic interactions between the C2 molecules and the peptide that are present during more than 5% of MD-1 simulation. CO = carbonyl group, SC = sidechain.

Type of interaction	Residue	C2	Time of binding / ns	Frequency / %
Hydrophobic	L2	1	3.0	19
		2	15.2	69
	P4	1	3.4	17
		2	15.6	67
	F5	1	3.1	65
		2	17.4	12
	P8	1	5.2	85
	L10	1	12.7	16
		2	21.8	26
	P11	1	7.5	76
	Y12	1	5.0	79
	P13	1	18.2	51
	P15	1	12.1	19
	L17	2	24.9	29
		3	11.8	12
	P18	3	12.6	61
	Y19	3	9.4	76
	P20	3	9.8	80
	L24	3	9.3	62
	P25	3	10.0	80
	Y26	3	10.2	76
	P27	3	11.0	8
	P29	2	24.5	51
	P31	2	24.6	50
	F32	1	1.4	23
		2	21.0	44
Hydrophilic (H-bonds)	Q1 (SC)	2	2.6	5
	L2 (CO)	2	8.7	17
	L2 (CO)	1	7.0	14
	P8 (CO)	1	12.1	24
	Q9 (CO)	1	5.0	10
	Q14 (SC)	2	7.3	15
	P18 (CO)	3	18.6	37
	P20 (CO)	3	17.0	34
	Q21 (SC)	3	2.8	6
	P25 (CO)	3	4.2	8
	Y26 (CO)	3	3.8	8

Supplementary table 6 - Hydrophobic and hydrophilic interactions between the C2 molecules and the peptide that are present during more than 5% of MD-2 simulation. CO = carbonyl group, SC = sidechain.

Type of interaction	Residue	C2	Time of binding / ns	Frequency / %
Hydrophobic	L2	2	7.8	76
	P4	2	7.8	79
	F5	2	26.3	16
	P6	3	8.7	17
	P8	2	8.5	19
	L10	3	10.2	9
	P11	2	7.1	80
	Y12	2	7.1	86
	P13	2	8.2	37
	P15	2	7.1	70
	L17	2	40.6	6
	Y19	2	34.6	24
		3	2.5	63
	P20	2	34.5	20
		3	1.9	61
	P22	3	7.8	15
	L24	3	6.6	55
	P25	1	16.7	9
		3	5.1	90
	Y26	3	4.2	91
	P27	3	2.0	95
	P29	3	2.9	94
	P31	3	1.8	96
	F32	2	7.4	49
		3	2.0	15
Hydrophilic (H-bonds)	Q1 (SC)	2	5.2	10
	L2 (CO)	2	17.4	35
	P11 (CO)	2	4.6	9
	Y12 (CO)	2	11.8	24
	Q16 (SC)	2	2.9	6
	Q23 (CO)	3	5.3	11
	Y26 (CO)	3	37.2	74
	P27 (CO)	3	18.3	37
	P29 (CO)	3	41.5	83

Supplementary table 7 - Hydrophobic and hydrophilic interactions between the C2 molecules and the peptide that are present during more than 5% of MD-3 simulation. CO = carbonyl group, NH = amine group, SC = sidechain.

Type of interaction	Residue	C2	Time of binding / ns	Frequency (%)
Hydrophobic	L2	2	29.8	38
	P4	1	6.8	87
		2	30.9	19
	F5	1	2.1	95
		2	29.8	40
	P6	2	31.4	15
		3	12.1	21
	P8	3	2.0	87
	L10	1	2.0	96
		3	1.9	84
	P11	1	6.4	10
		3	1.4	87
	Y12	2	29.1	32
		3	1.8	17
	P13	1	4.2	82
		2	31.3	28
	P15	3	1.4	8
	L17	1	1.7	95
	P20	1	1.8	6
	P22	1	11.8	9
	L24	1	1.8	95
	P25	1	1.4	83
	Y26	1	0.3	99
	P27	1	0.5	98
		2	32.1	21
	P29	1	0.8	98
		2	33.5	33
	P31	2	33.2	34
	F32	2	28.8	42
Hydrophilic (H-bonds)	Q3 (CO)	2	6.1	12
	F5 (NH)	1	5.3	11
	Q7 (CO)	3	9.2	18
	P8 (CO)	3	3.8	8
	Q9 (SC)	2	2.6	5
	Q14 (SC)	3	6.5	13
	Q16 (SC)	2	4.4	9
	Q21 (CO)	1	4.4	9

	L24 (CO)	1	7.4	15
	P25 (CO)	1	17.1	34
	Q28 (NH)	1	16.0	32
	Q30 (CO)	2	10.6	21
	F32 (CO)	2	14.3	29